RESEARCH ADVANCES IN DENGUE VIRUS

EDITED BY: Qiangming Sun, Gong Cheng, James Drew Brien, Jianfeng Dai and Penghua Wang

PUBLISHED IN: Frontiers in Cellular and Infection Microbiology

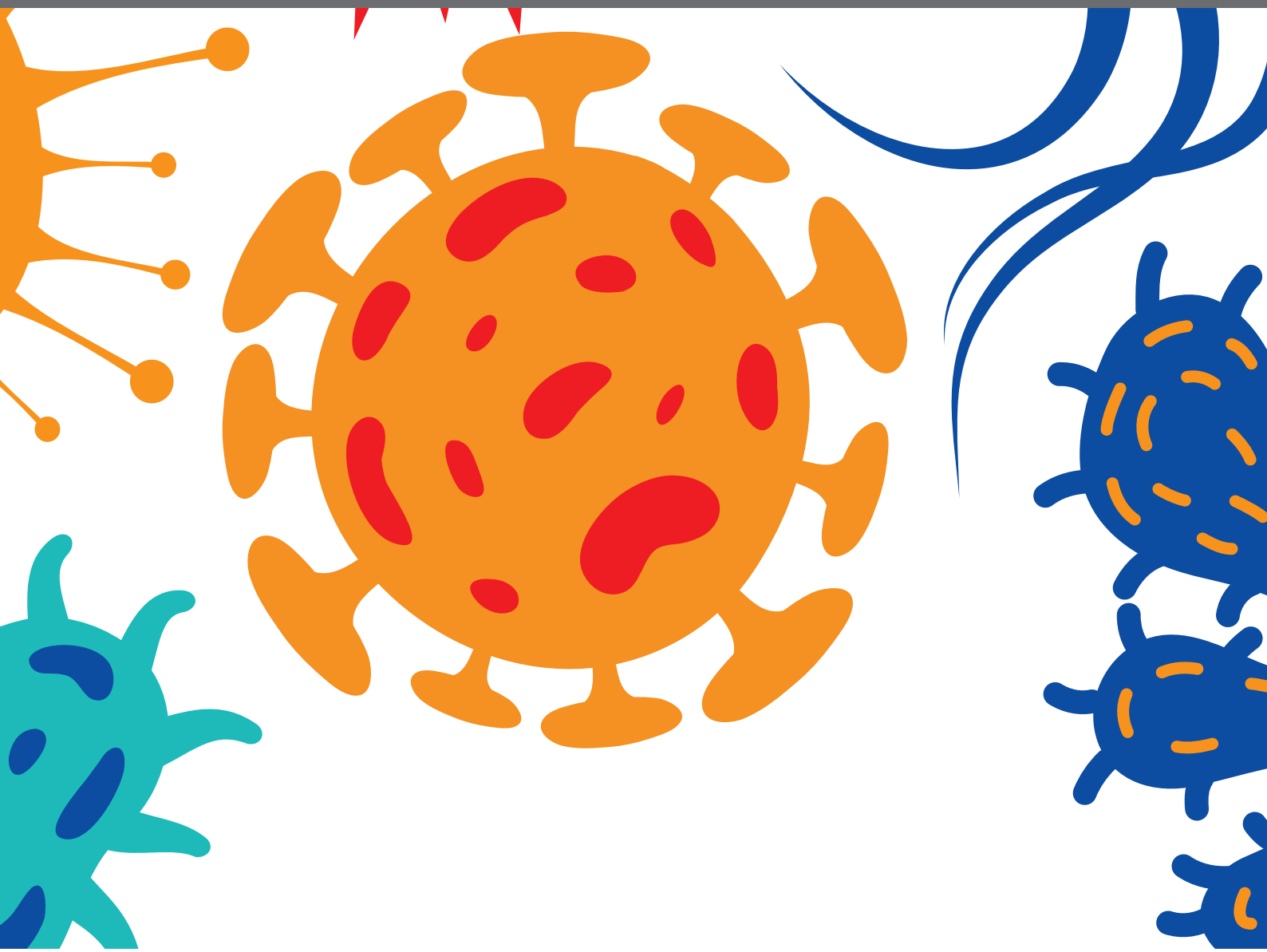

frontiers Research Topics

frontiers

ISSN 1664-8714
ISBN 978-2-88966-002-5
DOI 10.3389/978-2-88966-002-5

About Frontiers

Frontiers is more than just an open-access publisher of scholarly articles: it is a pioneering approach to the world of academia, radically improving the way scholarly research is managed. The grand vision of Frontiers is a world where all people have an equal opportunity to seek, share and generate knowledge. Frontiers provides immediate and permanent online open access to all its publications, but this alone is not enough to realize our grand goals.

Frontiers Journal Series

The Frontiers Journal Series is a multi-tier and interdisciplinary set of open-access, online journals, promising a paradigm shift from the current review, selection and dissemination processes in academic publishing. All Frontiers journals are driven by researchers for researchers; therefore, they constitute a service to the scholarly community. At the same time, the Frontiers Journal Series operates on a revolutionary invention, the tiered publishing system, initially addressing specific communities of scholars, and gradually climbing up to broader public understanding, thus serving the interests of the lay society, too.

Dedication to Quality

Each Frontiers article is a landmark of the highest quality, thanks to genuinely collaborative interactions between authors and review editors, who include some of the world's best academicians. Research must be certified by peers before entering a stream of knowledge that may eventually reach the public - and shape society; therefore, Frontiers only applies the most rigorous and unbiased reviews.
Frontiers revolutionizes research publishing by freely delivering the most outstanding research, evaluated with no bias from both the academic and social point of view. By applying the most advanced information technologies, Frontiers is catapulting scholarly publishing into a new generation.

What are Frontiers Research Topics?

Frontiers Research Topics are very popular trademarks of the Frontiers Journals Series: they are collections of at least ten articles, all centered on a particular subject. With their unique mix of varied contributions from Original Research to Review Articles, Frontiers Research Topics unify the most influential researchers, the latest key findings and historical advances in a hot research area! Find out more on how to host your own Frontiers Research Topic or contribute to one as an author by contacting the Frontiers Editorial Office: researchtopics@frontiersin.org

RESEARCH ADVANCES IN DENGUE VIRUS

Topic Editors:
Qiangming Sun, Institute of Medical Biology, China
Gong Cheng, Tsinghua University, China
James Drew Brien, Saint Louis University, United States
Jianfeng Dai, Soochow University, China
Penghua Wang, University of Connecticut Health Center, United States

Citation: Sun, Q., Cheng, G., Brien, J. D., Dai, J., Wang, P., eds. (2020). Research Advances in Dengue Virus. Lausanne: Frontiers Media SA.
doi: 10.3389/978-2-88966-002-5

Table of Contents

frontiers in Cellular and Infection Microbiology

ORIGINAL RESEARCH
published: 09 May 2017
doi: 10.3389/fcimb.2017.00157

Anti-Idiotypic Antibodies Specific to prM Monoantibody Prevent Antibody Dependent Enhancement of Dengue Virus Infection

*Miao Wang[1,2], Fan Yang[2], Dana Huang[2], Yalan Huang[2], Xiaomin Zhang[2], Chao Wang[2], Shaohua Zhang[2] and Renli Zhang[1,2]**

[1] College of Life Science and Oceanography, Shenzhen University, Shenzhen, China, [2] Shenzhen Center for Disease Control and Prevention, Shenzhen, China

Dengue virus (DENV) co-circulates as four serotypes (DENV1-4). Primary infection only leads to self-limited dengue fever. But secondary infection with another serotype carries a higher risk of increased disease severity, causing life-threatening dengue hemorrhagic fever/dengue shock syndrome (DHF/DSS). Serotype cross-reactive antibodies facilitate DENV infection in Fc-receptor-bearing cells by promoting virus entry via Fcγ receptors (FcγR), a process known as antibody dependent enhancement (ADE). Most studies suggested that enhancing antibodies were mainly specific to the structural premembrane protein (prM) of DENV. However, there is still no effective drugs or vaccines to prevent ADE. In this study, we firstly confirmed that both DENV-2 infected human sera (anti-DENV-2) and DENV-2 prM monoclonal antibody (prM mAb) could significantly enhance DENV-1 infection in K562 cells. Then we developed anti-idiotypic antibodies (prM-AIDs) specific to prM mAb by immunizing of Balb/c mice. Results showed that these polyclonal antibodies can dramatically reduce ADE phenomenon of DENV-1 infection in K562 cells. To further confirm the anti-ADE effect of prM-AIDs *in vivo*, interferon-α and γ receptor-deficient mice (AG6) were used as the mouse model for DENV infection. We found that administration of DENV-2 prM mAb indeed caused a higher DENV-1 titer as well as interleukin-10 (IL-10) and alaninea minotransferase (ALT) in mice infected with DENV-1, similar to clinical ADE symptoms. But when we supplemented prM-AIDs to DENV-1 challenged AG6 mice, the viral titer, IL-10 and ALT were obviously decreased to the negative control level. Of note, the number of platelets in peripheral blood of prM-AIDs group were significantly increased at day 3 post infection with DENV-1 compared that of prM-mAb group. These results confirmed that our prM-AIDs could prevent ADE not only *in vitro* but also *in vivo*, suggested that anti-idiotypic antibodies might be a new choice to be considered to treat DENV infection.

Keywords: dengue virus, prM antibody, antibody-dependent enhancement, anti-idiotypic antibodies, *in vitro and in vivo*

OPEN ACCESS

Edited by:
Gong Cheng,
Tsinghua University, China

Reviewed by:
Long Yang,
New York Medical College, USA
Qiangming Sun,
Chinese Academy of Medical Sciences, China

***Correspondence:**
Renli Zhang
renlizhangszcdc@aliyun.com

Received: *18 February 2017*
Accepted: *12 April 2017*
Published: *09 May 2017*

Citation:
Wang M, Yang F, Huang D, Huang Y, Zhang X, Wang C, Zhang S and Zhang R (2017) Anti-Idiotypic Antibodies Specific to prM Monoantibody Prevent Antibody Dependent Enhancement of Dengue Virus Infection. Front. Cell. Infect. Microbiol. 7:157. doi: 10.3389/fcimb.2017.00157

INTRODUCTION

Dengue virus (DENV) is a mosquito-borne virus circulating with four distinct, but closely related serotypes (DENV1-4). The virus is transmitted to humans through bites of infected *Aedes albopictus* or *Aedes aegypti*. The incidence of dengue has grown dramatically around the world in recent decades. One estimate indicates 390 million dengue infections per year, of which 96 million clinically apparent cases and 3.9 billion people are at risk of infection in 128 countries (Brady et al., 2012; Bhatt et al., 2013).

Most people who are infected with DENV only show symptoms of mild dengue fever, but some may progress to severe dengue hemorrhagic fever (DHF) or dengue shock syndrome (DSS). Infection by one serotype provides lifelong immunity against that particular serotype (Reich et al., 2013; Forshey et al., 2016). However, subsequent infection by another serotype may increase the risk of developing severe dengue (Sangkawibha et al., 1984; Guzman et al., 2000; Screaton et al., 2015). It has been proven that infants born to dengue immunized mothers have higher risk of DHF during primary infection with DENV (Chau et al., 2008; Clapham et al., 2015). One explanation of severe DENV infections is the theory of antibody dependent enhancement (ADE) raised by Halstead in 1977 (Halstead and O'Rourke, 1977). The enhancing antibodies facilitate virus entry into susceptible myeloid cell types via FcR pathway and trigger the massive release of inflammatory and vasoactive mediators, which contribute to the disease severity (Halstead and O'Rourke, 1977; Flipse et al., 2013). High viral load, liver injury and vascular leakage are the cardinal features of severe dengue (Wichmann et al., 2004). Both sera interleukin 10 (IL-10) and alanine aminotransferase (ALT) levels were higher in those with severe dengue compared to those with mild dengue (Malavige et al., 2013; Liao et al., 2015). And high levels of IL-10 and ALT were found to associate with liver failure in dengue infections (Ferreira et al., 2015; Fernando et al., 2016). Therefore, IL-10 and ALT can be taken as the biomarkers of sever dengue disease (John et al., 2015).

Dengue virus (DENV) contains 180 copies of envelop (E) and membrane (M) protein. The premembrane (prM) protein, which consists of two moieties of the pr and M domins, is the precursor of M protein. During virus maturation, furin protein cleaves prM protein to M protein in the trans-Golgi compartment. However, about 30% immature virions are released from infected cells (Zybert et al., 2008). A study reported that prM antibodies of DENV-2 facilitate efficient binding and cell entry of the immature type 2 viral particles into Fc-receptor-expressing cells (Rodenhuis-Zybert et al., 2010). The immune response in human to DENV is mainly caused by prM antibodies, which are highly cross-reactive among the four DENV serotypes (Beltramello et al., 2010; Dejnirattisai et al., 2010; Flipse and Smit, 2015). They do not neutralize infection but potently promote ADE even at high concentrations (Beltramello et al., 2010; Dejnirattisai et al., 2010). Therefore, it is the major challenge to design effective vaccine without triggering ADE activities because most current vaccines containing naive dengue prM protein (Ramakrishnan et al., 2015).

The lack of suitable animal models hinders the development of anti-dengue drugs. Currently, there is no specific treatment for severe dengue disease. It is urgent to search novel therapeutic strategies to block ADE. Anti-idiotypic antibodies (Anti-ids) are antibodies against the antigen binding sites of another antibody. Anti-ids have been studied and used in a variety of situations including therapeutic agents (Pan et al., 1995). Thus, we firstly developed mouse polyclonal anti-ids (prM-AIDs) targeting the antigen binding sites of DENV-2 prM monoclonal antibody (prM mAb). Then we displayed the anti-ADE effects of the prM-AIDs in both K562 cells and a recently reported IFN-α and -γ receptors deficient mouse model (C57BL/6 strain, AG6 strain) for DENV infection (Liu et al., 2016). Our results suggested that anti-ids specific to prM antibody might be considered as a potential candidate to reduce ADE in DENV infection.

RESULT

ADE of DENV Infection Mediated by Human Anti-Denv-2 Sera in K562 Cells

To confirm whether anti-DENV-2 antibodies could induce ADE to DENV-1 infection, we collected six DENV-2 infected human sera (α-DENV-2). Dengue IgG in the sera was detected by ELISA. Results showed five of them were considered positive of dengue IgG. The average optical density values (O.D.) of DENV IgG in α-DENV-2 and control group were 0.439 ± 0.278 and 0.137 ± 0.056, respectively (**Figure 1A**). To confirm whether proteins of DENV-1 cross-reactive with human anti-DENV-2 sera and a commercial mouse DENV-2 prM mAb, we used DENV-1 as antigens and the mixed sera of six patients or prM mAb as the first antibody for western blot. Results showed human anti-DENV-2 sera contained corresponding anbodies for prM, M, NS1 and E protein of DENV-1. Anti-DENV-2 prM mAb could react with DENV-1 prM protein (**Figure 1B**).

Dengue virus (DENV) mainly infected monocytes, macrophages and dendritic cells in patients (Jessie et al., 2004). Human monocyte cell line K562 (Fc receptor-bearing) was a common cell type to demonstrate the ADE of DENV *in vitro*. To confirm whether the human anti-DENV-2 sera could induce ADE, we infected K562 cells with DENV-1, then determined the viral load in the supernatant by qRT-PCR and detected infected cell number by flow cytometry. PCR results showed 10–100 fold enhancement of infection in four human anti-DENV-2 sera (**Figure 1C**). Similarly, anti-DENV-2 sera also led to a significant increase of infected cells (**Figure 1D**).

ADE of DENV Infection Mediated by prM mAb in K562 Cells

Next, to determine ADE effect of mouse prM mAb, we incubated K562 cells with DENV-1 (MOI = 1) and a series of diluted prM mAb for 72 h. Results showed that prM mAb had strong enhancement effect for DENV-1 infection in a concentration-dependent manner. A 100-fold enhancement of DENV replication was detected with 0.1, 0.25 and 0.5 μg/ml prM mAb when analyzed by qRT-PCR (**Figure 2A**). Less than one percent of monocytes were infected with DENV-1 without

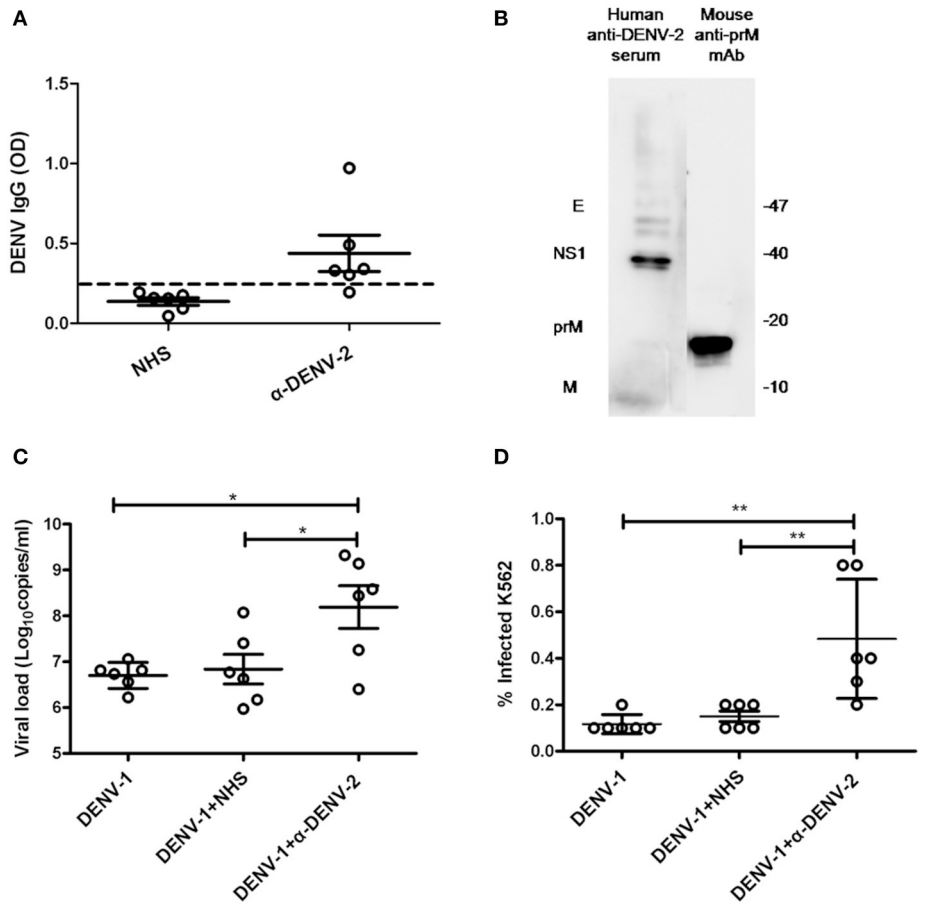

FIGURE 1 | Cross-reactivity and enhancing properties of human anti-DENV-2 sera. (A) The OD of DENV IgG in the naive human sera (NHS) and human anti-DENV-2 sera (α-DENV-2) was determined by ELISA ($n = 6$). **(B)** Western blot of DENV-1 showing reactivity with antibodies of dengue E, NS1, prM and M in human anti-DENV-2 sera. **(C)** Human anti-DENV-2 sera was incubated with DENV-1 for 1 h at 25°C, then they were transferred to K562 cells at MOI of 1 and kept incubation for 72 h. Viral RNA copies of infected supernatant were quantified by qRT-PCR. **(D)** Infected cells were determined by flow cytometry. Error bars show the means ± SEM and pairwise comparisons were performed by unpaired test (*$p < 0.05$, **$p < 0.01$). Dotted line presents the limit value to be considered positive.

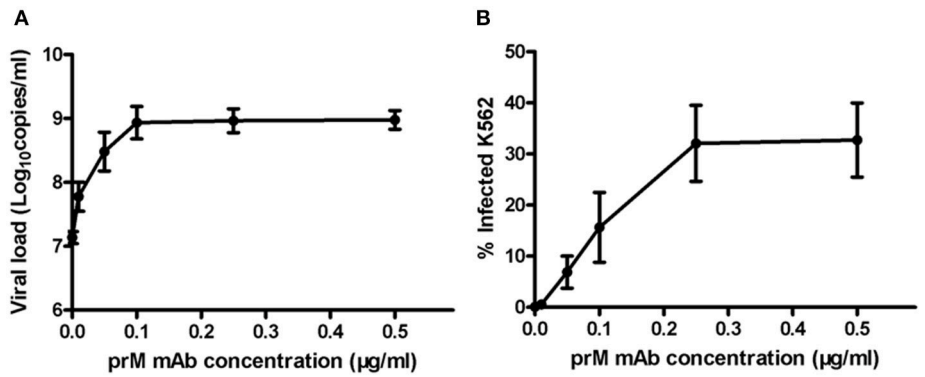

FIGURE 2 | ADE of DENV replication in K562 cells mediated by prM mAb. prM mAb was diluted to a series of different concentrations, then they were incubated with DENV-1 for 1 h at 25°C and transferred to K562 cells at MOI of 1. Infected cells were incubated for 72 h at 37°C. **(A)** Viral RNA copies in infected supernatant were quantified by qRT-PCR. **(B)** Infected cells were determined by flow cytometry. Data are expressed as means of three independent experiments. Error bars show the means ± SEM.

prM mAb. However, the percent of infected cells displayed an increased trend along with higher prM mAb concentration. The largest DENV-1 infected cell percentage was detected when the added prM mAb concentration was increased to 0.25 μg/mL(**Figure 2B**). These results illustrated that prM mAb could enhance the infection of heterotypic virus and might played a vital role in dengue disease.

Characterization of prM-AIDs

Then, to prevent ADE induced by prM mAb, we developed anti-idiotypic antibodies (prM-AIDs) specific to prM mAb by immunizing balb/c mice. prM-AIDs in immunized mice were detected by ELISA and the titer was increased continually from day 7 after mouse immunization (**Figure 3A**). When the titer of anti-sera reached 1:40000 at day 35 (**Figure 3A**), mice were sacrificed to collect blood. prM-AIDs in the sera and naive mouse antibodies (NM-Abs) were purified by Protein-G column. The quantity and quality of purified prM-AIDs was determined by SDS-PAGE and ELISA. Results showed the purified antibody's heavy chain (about 55KDa) and light chain (about 25KDa) (**Figure 3B**). The optical density values of prM-AIDs in the naive mouse antibodies (NM-Abs) or immunized mouse antibodies (IM-Abs) and 0.093 ± 0.014 and 0.28 ± 0.073, respectively (**Figure 3C**). These data demonstrated balb/c mice immunized with prM mAb produced a high level of prM-AIDs.

prM-AIDs Inhibited ADE of DENV Infection in K562 Cells

To determine whether our purified prM-AIDs could inhibit ADE of DENV infection, K562 cells were infected with DENV-1 virus and prM antibody and various concentrations of prM-AIDs. prM mAb was added instead of prM-AIDs as a control group. The results showed that if only adding prM mAb and DENV-1, viral load in supernatant was significantly higher than the DENV-1 alone group. But when we added prM-AIDs, the viral load was decreased in a dose-dependent manner. Compared with the prM mAb group ($8.2 \pm 2.8 \times 10^8$ copies/mL), the viral load in the supernatant with prM-AIDs (25 μg/mL) was dramatically decreased to $7.8 \pm 3.4 \times 10^7$ copies/mL (**Figure 4A**). Therefore, prM-AIDs significantly diminished ADE induced by prM mAb through decreasing 90% viral replication (**Figure 4B**).

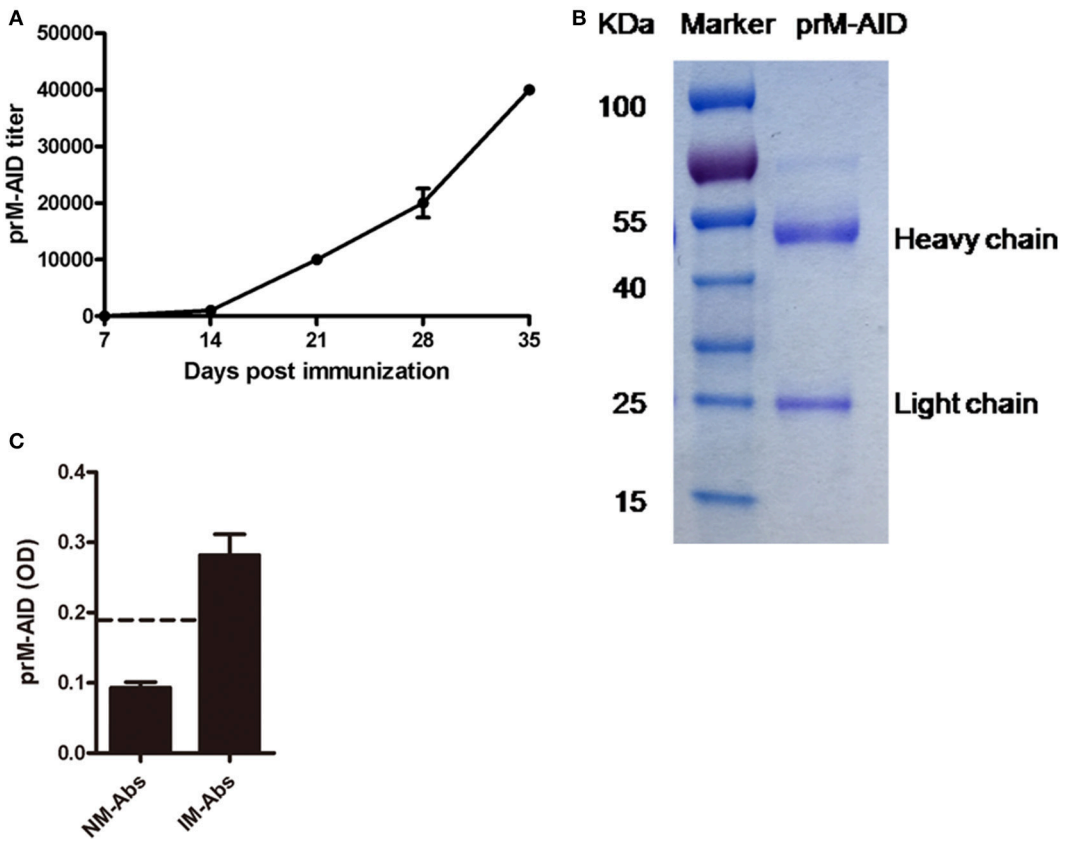

FIGURE 3 | Characterization of prM-AIDs. (A) The titer of prM-AIDs in immunizzed sera were determined by ELISA every 2 weeks ($n = 6$). Dilution of immunized or naive mouse sera were coated in 96-well plates. Biotinylated prM mAb were added. Bound prM mAb was detected by addition of streptavidin-HRP. **(B)** Purified prM-AIDs was identified by SDS-PAGE. **(C)** The specificity of prM-AIDs was analyzed by ELISA. Diluted naive mouse antibodies (NM-Abs), or immunized mouse antibodies (IM-Abs) were coated in 96-well plates. Biotinylated prM mAb were added. Bound prM mAb was detected by addition of streptavidin-HRP. Dotted line shows samples were considered positive if Positive/Native ration>2.1.

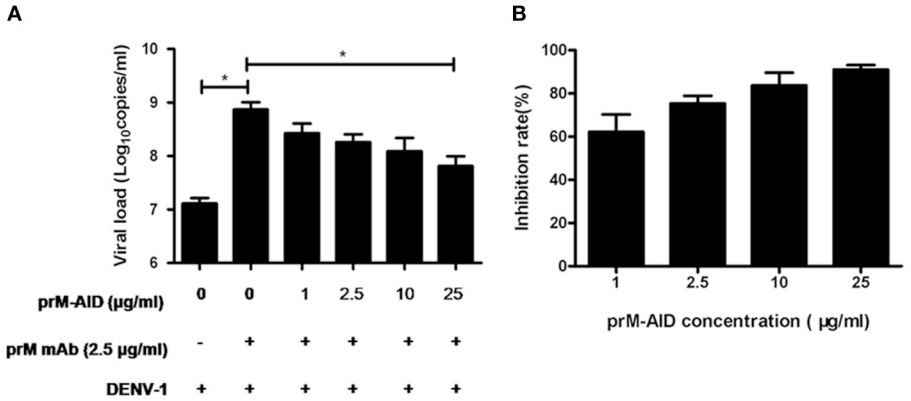

FIGURE 4 | ADE of DENV infection blocked by prM-AIDs in K562 cells. (A,B) prM-AIDs was incubated for 1 h at 25°C with DENV-1 and 0.25 μg prM mAb at an MOI of 1. The mixtures infected K562 cell for 72 h. The virus in the supernatant was determined by qRT-PCR. Data are expressed as means of three independent experiments. Error bars show the means ± SEM and paired comparisons were performed by unpaired test (*$p < 0.05$).

ADE of DENV Infection Mediated by prM mAb in AG6 Mice

To assess the ability of prM-AIDs to block ADE *in vivo*, we utilized a recently described AG6 mouse model (interferon-α and γ receptor deficient mice) for ADE of dengue infection. (**Figure 5A**) prM mAb with or without prM-AIDs were transferred into AG6 mice by i.v. prior to infection with DENV-1. Antibodies from naive mouse sera were purified as control antibodies (NM-Abs). Viral RNA load in blood cells was detected by qRT-PCR (**Figure 5B**), while infective viral particles in plasma was detected by plaque assay (**Figure 5C**). QA peak viremia titer in blood cells was detected at day 3 post infection (**Figure 5B**). Compared with the NM-Abs group, the viremia titer was 1-fold higher in the prM mAb group (**Figure 5B**). At day 3 after inoculation, the platelet counts in DENV-1 injected mice were significantly lower than that of uninfected mice. Challenging with prM mAbs significantly reduced platelets (**Figure 5D**).

To further explore the inflammation response and liver damage of ADE infection, we also detected ALT (**Figure 5E**) and IL-10 (**Figure 5F**) in the plasma of mice at days 3 post infection by ELISA assay. Compared with the uninfected groups, a significant higher level of ALT and IL-10 were observed in the DENV infected groups (**Figures 5E,F**). Compared to the pure DENV-1 infected mice group, the level of ALT and IL-10 were increased in the prM mAb mice group. These data show that ADE of DENV-1 infection in AG6 mice by passive transfer prM antibody.

prM-AIDs Inhibited ADE of DENV Infection in AG6 Mice

However, by comparison, a significant difference in viral load of blood cell between the mice that received prM-AID and the mice that received prM mAb at day 3 post infection (**Figure 5B**). Similarly, the viral load in the plasma also showed a peak at day 3 post infection. Although the viral titer in the prM-AIDs group displayed the lowest trend, there was no statistically significant difference among all the groups. Compared with the prM mAb group, the mean viremia titer in the prM-AIDs group decreased about 1-fold (**Figure 5C**).

Interestingly, the number of the platelets in the prM-AIDs challenged mice was significantly higher than that of NM-Abs group at day 3 post infection (**Figure 5D**). Besides, challenged with prM-AIDs showed decreased trend of the level of ALT and IL-10 than the prM mAb mice group and naive mouse antibodies group (**Figures 5E,F**).

DISCUSSION

In this study, we firstly confirmed ADE to DENV-1 infection induced by human anti-DENV-2 sera and murine anti-DENV-2 prM mAb in K562 cells. Then we developed and characterized prM-AIDs targeting the antigen-binding site of prM mAb. We showed that prM-AIDs significantly inhibited ADE mediated by prM mAb *in vitro*. Importantly, administration of prM-AIDs to AG6 mice largely reduced the disease severity of DENV-1 infection.

Secondary infection with another DENV serotype carries an increased risk of severe disease (Soo et al., 2016). A high viral load in blood, severe thrombocytopenia, and platelet dysfunction may result in increased capillary fragility (Ojha et al., 2017), clinically manifested as petechiae, easy bruising, and gastrointestinal mucosal bleeding (Deshwal et al., 2016), which is characteristic of DHF/DSS. ADE has been proposed as an underlying pathogenic mechanism of DHF/DSS (Halstead, 1970). On one hand, enhancing antibodies can bind DENV through Fab fragments, on the other hand, virus-antibodies complex still could recognize Fc receptor-bearing cells via their Fc region, leading to increased virus uptake and replication (Gan et al., 2017). Many evidences showed viral premembrane protein prM mAbs broad cross-activity with the four DENV serotypes and showed poor neutralization function but potently promote ADE (Beltramello et al., 2010; Dejnirattisai et al., 2010). To confirm the ADE induced by prM mAb, we incubated DENV-1 infected K562 cells with either human anti-DNEV2 sera or

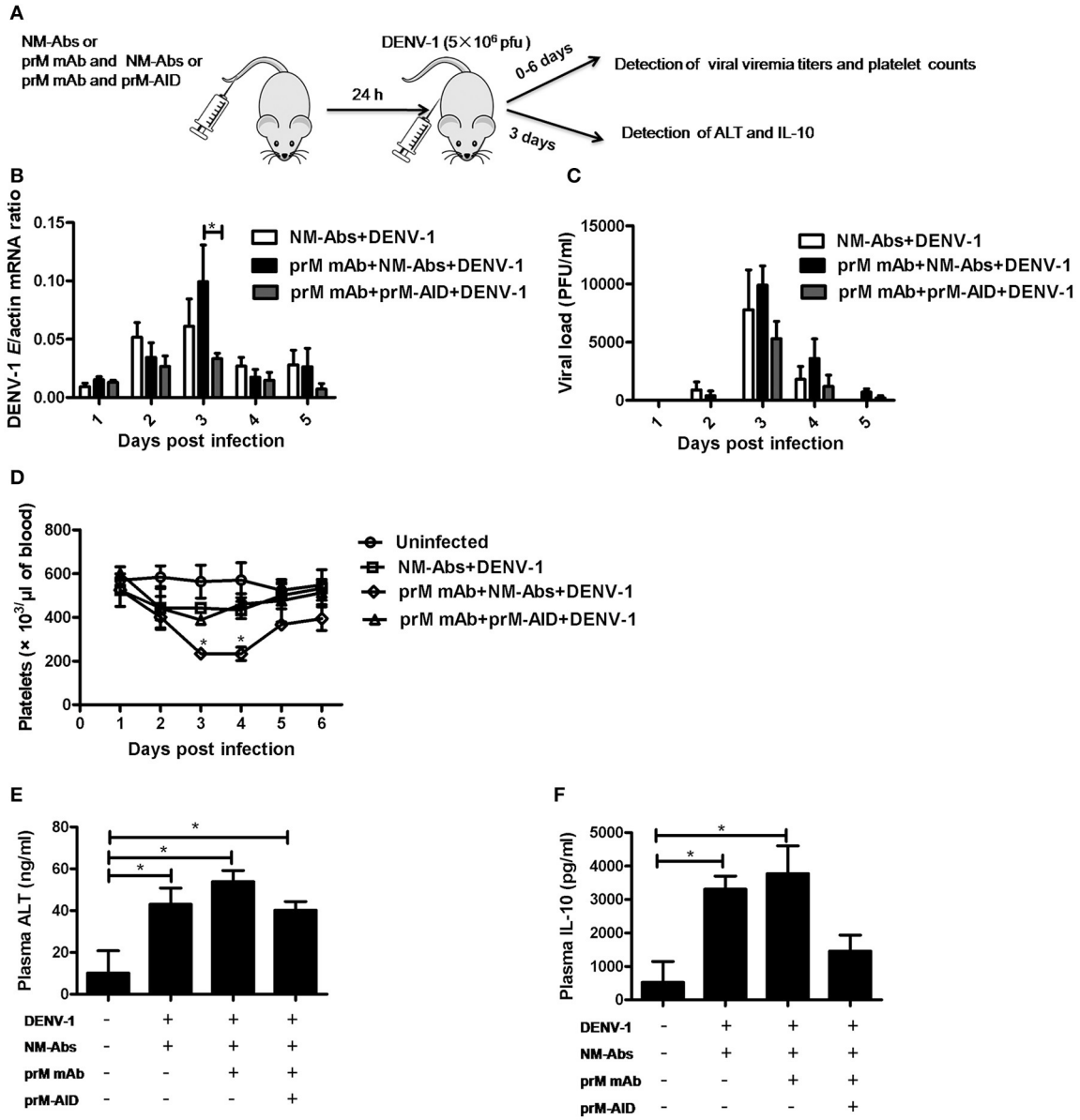

FIGURE 5 | prM-AIDs inhibited ADE of DENV infection *in vivo*. (A) Schematic representation of the study design. Mice were first administered with naive mouse antibodies (NM-Abs), prM mAb and prM-AIDs, then 24 h later they were challenged with DENV-1 by *i.p.*. Blood was collected from the vail veins from 0 to 5 days post-infection. **(B)** Viral copies in the blood cells were quantified by qRT-PCR. **(C)** Infectious viral particles in the plasma were assessed by plaque assay. **(D)** Platelets in blood were counted using a hemocytometer under a light microscope. **(E,F)** The levels of ALT and IL-10 in plasma were measured by ELISA at day 3 post-infection. $n = 4$–5 mice per group. Error bars show the means ± SEM and pairwise comparisons were performed by non-parametric Mann-Whitney test (*$p < 0.05$).

mouse prM mAb. The K562 cell line was chosen as a simple and easily interpretable model system for the *in vitro* study of ADE and ADE inhibition as it only expresses the Fcγ II receptor (Clark et al., 2016). ADE induced by patients' sera had once been reported in laboratory virus strains (Chaichana et al., 2014; de Alwis et al., 2014). Here, a clinical DENV-1 isolate was taken to perform ADE assay. We confirmed clinical isolate DV1 infection was enhanced by human anti-DV2 sera or murine anti-DV2 prM mAb in Fcγ receptor-bearing K562 cells. Besides, since the clinical isolated DENV-1 virus strain and the anti-DENV-2 sera were both derived from Guangdong local DENV infected patients. It indicates that people living in Guangdong who were primarily infected with DENV-2 have high risk of developing severe dengue disease once they are further attacked by DENV-1.

To date, no entirely successful attempt of active immunization or drug treatment in the field of DENV has been published. The only licensed tetravalent dengue vaccine Dengvaxia (CYD-TDV)

which was developed by Sanofi Pasteur and TAK-003 (Takeda) as a candidate vaccine both showed moderate efficacy against dengue infection (Osorio et al., 2014; Godoi et al., 2017). However, considering the ADE activities, current vaccines have a potential risk of aggravating disease (Aguiar et al., 2017). A recent report published on *science* suggested that vaccination of Dengvaxia in low-transmission settings might increase the incidence of more severe "secondary-like" infection and hospitalizations (Ferguson et al., 2016). Meanwhile, some anti-viral compounds have shown efficient ADE inhibition of DENV (Ayala-Nunez et al., 2013; Flingai et al., 2015). Anti-TNFα therapy totally protected the DENV-2 infected A129 mice (Martinez Gomez et al., 2016). Importantly, humanized anti-DENV antibodies engineered with mutations in Fc region were developed to prevent binding to FcR for the treatment of dengue disease in AG129 mice (Goncalvez et al., 2007; Balsitis et al., 2010; Beltramello et al., 2010; Ramadhany et al., 2015). A recent study reported plant-produced anti-dengue virus monoclonal antibodies exhibited reduced ADE activity in FcR expressing human cells (Dent et al., 2016). However, to our knowledge, no method mentioned above has been widely accepted. As a consequence, passive immune therapy of anti-idiotypic antibodies by blocking enhancing antibodies may provide an alternative strategy for the treatment of dengue, especially for patients who have already acquired primary infection or reside in endemic areas.

When one antibody binds to the variable region of another antibody, it is referred to as an anti-idiotypic antibody. Over the past years, anti-idiotypic antibodies have been studied and used in a variety of situations including attempts to use them as therapeutic agents (Denapoli et al., 2017). They are ideal for bioanalytical assays in preclinical research and clinical drug monitoring due to their high specificity and sensitivity (Bulashev et al., 2016). One research showed that anti-idiotypic antibodies could inhibit the binding between autoantibodies and autoantigens, resulting to prevent the development of autoimmune disease (Hampe, 2012). In this study we produced high titer of prM-AIDs by immunizing mice with prM mAbs. Results confirmed that prM-AIDs significantly inhibited DENV-1 replication in K562 cells in a dose-dependent manner. Although other modified antibodies could reduce their enhancing activity (Dent et al., 2016; Wang et al., 2017), they couldn't block the enhancing antibodies that already existed in primary infection. Polyclonal antibodies can be easily raised, as their production steps do not require any sophisticated laboratory facility. Therefore, anti-idiotypic antibody therapy represents a novel approach for dengue disease prevention and treatment. They have great potential to be used in combination with viral replication inhibitors that will decrease the emergence chance of resistant virus strains.

Many ADE-related studies were limited in *in vitro* assays (Dent et al., 2016; Wang et al., 2017). The evidence demonstrating ADE *in vivo* was first described by Healstead in rhesus monkeys (Halstead, 1979). Recently, a new animal model AG6 mice (interferon-α and γ receptor deficient mice) for dengue infection was reported to study the function of secreted DENV NS1 protein (Liu et al., 2016). In this model, DENV could lead to lethal disease characterized by reduced white blood cells and platelets as well as vascular leakage (Orozco et al., 2012; Liu et al., 2016), all features associated with severe dengue symptoms in humans (Halstead, 2007). Therefore, we chose AG6 mice as an animal model system for the study of ADE and ADE inhibition *in vivo*. ADE of DENV-1 replication in AG6 mice was demonstrated by passive antibody transfer. Increased virus titers, IL-10 and ALT in the blood were observed in the mice after prM antibody injection by i.v. Besides, the number of the platelets was 2-fold lower in mice challenged with prM antibody than that in the control mice. These results were similar to those in another ADE mice model-AG129 (IFN-α and β receptor deficient) (Balsitis et al., 2010; Martinez Gomez et al., 2016). Here, we first demonstrated ADE in AG6 mice by passively transfering prM mAb, although the enhancing effect was not very significant compared with other studies using different ADE mice models. We proposed that the different virus strains as well as viral challenging routes and doses might impact the disease progression and manifestations. For example, in this study, we challenged mice with DENV-1, which was believed to be weaker than DENV-2 used in other studies in pathogenesis.

Next, to confirm whether our prM-AIDs had the same inhibitory effect *in vivo* similar to that in cells, we challenged AG6 mice with both DENV-1 and prM-AIDs. Results showed prM-AIDs were capable to block the ADE effect and reducing the viral burden to an equivalent level to the DENV-1 control group in absence of prM mAb During the ADE and severe dengue symptoms, reduced platelets, platelet dysfunction as well as liver damages were common pathogenesis mechanisms. Therefore, in this study, besides the viral load in blood cells and the plasma, the levels of IL-10, ALT and platelet counts in the blood were also detected. We found the levels of IL-10 and ALT were decreased by prM-AIDs, suggesting that mice had reduced inflammatory responses and liver damages. The number of platelets in the peripheral blood of prM-AIDs group returned to normal level, which hinted that vascular damages and bleeding possibility were also reduced. These results demonstrated that the prM-AIDs could inhibit ADE induced by prM mAb *in vivo* at least from immune responses as well as liver functions and platelet counts. The mechanisms of anti-ADE by prM-AIDs might be that they specifically bound to the antigenic determinants of prM mAbs, resulting in inhibition of the binding between prM mAbs and viruses. Further studies needed to be done to confirm the detailed anti-ADE mechanisms of prM-AIDs.

Taken together, we successfully demonstrated the ADE in both cell level and in a recently reported AG6 mice model by challenging prM mAbs. Then, we developed prM-AIDs specific to this anti-dengue prM mAb. Furthermore, the prM-AIDs successfully inhibited ADE not only *in vitro* but also protected mice avoiding severe inflammatory responses as well as liver damages *in vivo*. It provided a new strategy to develop specific treatment for severe DENV infection.

MATERIALS AND METHODS

Ethics Statement

All patient samples and data were assigned institution-specific identification numbers to ensure patient anonymity.Balb/c mice were purchased from Guangdong medical Laboratory Animal

Center. The mice were bred and maintained under SPF animal house in Shenzhen Center for Disease Control and Prevention. C57BL/6 mice deficient in type I and type II interferon (IFN) receptors (AG6 mice) were purchased from Institute Pasteur of Shanghai, Chinese Academy of Science, which is bred and maintained under SPF animal house in Tsinghua University. All experiments procedures were approved and performed according to the guidelines of the Experimental Animal Welfare and Ethics Committee of Shenzhen Center for Disease Control and Prevention.

Cell Lines and Virus

The Aedesalbopictus cell line C6/36 and Baby Hamster Kidney-21 (BHK-21) cell line were cultured in Dulbecco's modification of Eagle's medium (DMEM). Human erythroleukaemic K562 cells were grown in Roswell Park Memorial Institute (RPMI) 1640 medium. All media were supplemented with 10% fetal bovine sera, 100 U/mL penicillin, and 100 μg/mL streptomycin. C6/36 cells were propagated at 28°C and BHK-21 and K562 cells were propagated at 37°C. All the materials used for cell culture were purchased from GIBOCO and cells were from China Center for Type Culture Collection.

DENV-1 was isolated in our laboratory from a patient during a DENV outbreak in Shenzhen, China in 2014. Virus was propagated in C6/36 cell line. After 3-4 days, the supernatant was harvested, and cell debrises were removed by centrifuge at 10000 rpm for 10 min at 4°C. DENV-1 was used after being passaged for 3 times in C6/36 cells. To increase the virus titer, the supernatant were concentrated by centrifuge at 4,000 g for 30 min at 4°C using filtration device (Millipore, Cat. No# UFC901008). Virus stocks were stored at −80°C.

Anti-DENV-2 Sera

Human anti-DENV-2 sera samples were obtained from patients during a DENV outbreak in Guangdong, China. Human anti-DENV-2 sera samples and native human sera samples were collected from Shenzhen Center for Disease Control and Prevention.

Anti-prM Monoclonal Antibody

Dengue virus (DENV) type 2 prM IgG1 monoclonal antibody, directed against pre-membrane glycoprotein of DENV serotype 2 was purchased from Thermo (Cat. No#, MA1-71252). To remove sodium azide in the supernatant, the antibody was further purified by the Montage Prosep-G kit (Millipore, Cat. No# P36491) and quantitated by the BCA Protein Quantitate Kit (Thermo Scientific, Cat.No# 23225) ccording to manufacturer's instructions.

Plaque Forming Assay

The titer of virus was determined by plaque assay in BHK-21 cells. BHK-21 cells were seeded in 6-well plate in DMEM with 10% FBS at 37°C. Next day, virus was serially diluted with DMEM medium and incubated with BHK cells for 1 h. Subsequently, the viral suspension was removed, and DMEM medium containing 2% FBS and 1% low-melting point agarose were added. After incubation at 37°C for 6 days, cells were fixed with 4% formaldehyde for 2 h. After the overlay was removed, cells were stained by crystal violet for a few minutes and washed carefully by water. Plaques were calculated by naked eyes.

Cross-Reactivity Analysis between DENV-1 and Human Anti-DENV Sera or prM mAb by Western Blot

The DENV-1 supernatant was electrophoresed through 12% SDS/polyacrylamide gels and then electrotransferred to nitrocellulose membrane (Millipore). The membrane was blocked with 5% BSA in TBST before incubation overnight with human anti-DENV sera (1:100 diluted) or prM mAb at 4°C. Wash the membrane with TBST four times. Peroxidase-Labeled Antibody to Human IgG (KPL, Cat. No# 04-10-20, 1:2,000 dilute) or Peroxidase-Labeled Antibody to mice IgG (Abcam,Cat. No#ab6789, 1:100,000 dilute) was added in TBST with 5% BSA for 2 h at room temperature. After washing the membrane, bands were detected by using SuperSignal West Pico chemiluminescent substrate (Thermo Scientific, Cat. No#HF104626).

Analysis of ADE Induced by Human Sera or prM mAb in K562 Cell

Human sera or prM mAb was incubated with DENV-1 at an MOI of 1 for 1 h at 25°C in shaking table at 80 rpm to form virus-antibody complexes. The mixtures infected K562 cells in 24-well plates (1×10^5 cells/well) at 37°C for 72 h. The number of infected cells was determined by flow cytometry. The virus in the supernatant was determined by qRT-PCR.

DENV-1 infected and mock K562 cells were harvested and washed with cold phosphate buffered saline (PBS). To block cell surface FcR, incubate cells with 0.5 μg Human BD Fc Block™(BD, Cat. No#564220) for 20 min at room temperature. Fixation, permeabilized and intracellular fluorescence labeling were performed by Fixation/Permeabilization solution (BD, Cat. No#554714) according to manufacturer's instructions. For labeling, cells were incubated with anti-dengue virus E glycoprotein antibody (abcam, Cat. No# ab41329, 1:20 dilute) and then labeled with Donkey F(ab')2 Anti-Mouse IgG H&L (Alexa Fluor® 488,abcam, Cat. No#ab181289). Finally, cells were suspended in PBS containing 1% FBS and subjected to flow cytometry.

RNA in the supernatant was extracted using Viral RNA kit (Roche, Cat. No#13438700). qRT-PCR was carried out with DENV General-type Real Time RT-PCR Kit (Shanghai ZJ, Cat. No#ER-0101-02). Amplification conditions were 45°C for 10 min, 95°C for 15 min and 40 cycles of 95°C for 15 s, 60°C for 1 min.

Preparation of prM-AIDs

To obtain prM-AID, six female Balb/c mice (6 weeks of age) were subcutaneously immunized with dengue prM mAb three times at 2-week intervals in Freund's complete(sigma, Cat. No#F5881) or incomplete adjuvant (sigma, Cat. No#F5506). Blood samples were collected from the tail

vein of immunized mice to determinate the titer of antibody. Seven days after the final immunization, mice were sacrificed to take the blood. The sera were separated from the blood by centrifuge at 2,500 g for 30 min at 4°C and the products was purified from sera using the Montage Prosep-G kit (Millipore Cat. No#P36491). The polyclonal antibodies were concentrated using centrifugal filter device (Millipore) and quantitated by the BCA Protein Quantitate Kit (Thermo, Cat. No#23225) according to manufacturer's instructions. The purity of polyclonal antibodies was identified by sodium dodecyl sulfate-poly-acrylamide gel electrophoresis (SDS-PAGE) on 12% polyacrylamide gels under denaturating and reducing conditions and evaluated by Coomassie blue staining.

Detection of prM-AIDs by ELISA

To dectect prM-AIDs titer in the immunized sera, serially diluted control and immunized sera were coated in 96-well plates at 4°C overnight. And to identify prM-AIDs in purify antibodies, antibodies purified from naive mice as negative control, and purify anti-idiotypic antibodies from immunized mice were coated in 96-well plates at 4°C overnight. The plates were blocked by 2% BSA in PBST for 1 h at room temperature. The prM mAb was biotinylated by using NH2-reactive biotin (Elabscience, Cat. No#EBLK0002). After washing with TBST, biotinylated prM mAb was added and incubated for 1 h at 37°C. Plates were washed four times with TBST. Streptavidin-HRP (1:10,000 diluted, Beyotime, Cat. No#A0303) were added and incubated for 30 h at 37°C. Wash the plates as above. TMB was added as the substrate, and the reaction was stopped by H_2SO_4 stop solution. The OD at 450 nm was measured with an iMarkTM Microplate Reader. Samples were considered positive if P/N ration>2.1.

ADE Inhibition Assay by prM-AID in K562 Cells

prM-AIDs was incubated for 1 h at 25°C in shaking table at 80 rpm with DENV-1 and prM mAb at an MOI of 1. The mixtures infected K562 cells in 24-well plates at 37°C with 5% CO_2 for 72 h. The virus in the supernatant was determined by qRT-PCR.

ADE Inhibition by prM-AID in AG6 Mice

Twenty six to eight week-old AG6 mice were randomly into four groups. Antibodies were purified from naive mouse sera (NM-Abs) as control antibodies. Mice were injected 100 μg NM-Abs, 20 μg prM mAb and 100 μg NM-Abs or 20 μg prM mAb and 100 μg prM-AID by intravenous injection (*i.v*) into the tail vein then intraperitoneal (*i.p*) infected 24 h later with 10^6 PFU of DENV-1. Blood samples from each mice were collected from the tail vein daily for the next 5 days. Viremia titers were detected from day 1 to day 5 post infection. Platelets were count from day 1 to day 5 post infection. The level of IL-10 and ALT were determined at day 3 post infection.

Quantitative Analysis of DENV-1 Viremia in AG6 Mice

10 μl whole blood was collected each day after viral challenge into tubes containing sodium citrate. Samples were centrifuged at 6,000 g and 4°C for 5 min to separate plasma and blood cells. Viral load in the plasma was determined by plaque. RNA was extracted from blood cells using an RNA Mini kit (Qiagen, Cat. No#154025157) and reverse transcripted into cDNA using an iScript cDNA kit (Bio-Rad, Cat. No#1708891). Viral genomes were quantified via TaqMan qPCR amplification. The DENV-1 primer pairs were GCTCCCACGTCGGAAATACA and TGT TCTAGGTGAGCAGTCCAATG. The probe was FAM 5′CTG ACTGACTACGGAGCC-3′ TAMRA. The sequence of mouse actin primer pairs were AGCCATGTACGTAGCCATCCA and TCTCCGGAGTCCATCACAATG. The probe was FAM 5′-TGTCCCTGTATGCCTCTGGTCGTACCAC-3′ TAMRA. Gene quantities were normalized against mouse actin.

Detection of IL-10 and ALT by ELISA

IL-10 (Abcam,Cat. No#ab46103) and ALT (Cloud-clone, Cat. No#SEA207Mu) in the infected and mock-infected mice was quantified using commercially available ELISA kits. The experiment was performed according to manufacturer's instructions.

Statistical Analysis

Unpaired *t*-test was used to comparison of viral road and percentage of infection in ADE and ADE inhibition assay. Non-parametric Mann-Whitney test were used for pairwise comparisons of viral road, IL-10, ALT and platelets in AG6 mice. All calculations were performed in GraphPad Prism 5.0 software.

AUTHOR CONTRIBUTIONS

RZ designed the experiments; RZ, MW, XZ, and YH wrote the manuscript and performed the majority of the experiments and analyzed data; FY, DH, CW, and SZ supplied material and performed a part of the experiments. All authors reviewed, critiqued, and provided comments to the text.

FUNDING

This work was financially supported by the National major science and technology research projects of China (No.2016YFC1202001) and science and technology research projects of Shenzhen (No. JCYJ20160427151920801).

ACKNOWLEDGMENTS

We are grateful to Prof. Gong Cheng from Tsinghua University for providing AG6 mice. We thank the supports of Shenzhen San-Ming project for prevention and Resaearch on Vector-borne Disease.

REFERENCES

Aguiar, M., Halstead, S. B., and Stollenwerk, N. (2017). Consider stopping dengvaxia administration without immunological screening. *Expert Rev. Vaccines* 16, 301–302. doi: 10.1080/14760584.2017.1276831

Ayala-Nunez, N. V., Jarupathirun, P., Kaptein, S. J., Neyts, J., and Smit, J. M. (2013). Antibody-dependent enhancement of dengue virus infection is inhibited by SA-17, a doxorubicin derivative. *Antiviral Res.* 100, 238–245. doi: 10.1016/j.antiviral.2013.08.013

Balsitis, S. J., Williams, K. L., Lachica, R., Flores, D., Kyle, J. L., Mehlhop, E., et al. (2010). Lethal antibody enhancement of dengue disease in mice is prevented by Fc modification. *PLoS Pathog.* 6:e1000790. doi: 10.1371/journal.ppat.1000790

Beltramello, M., Williams, K. L., Simmons, C. P., Macagno, A., Simonelli, L., Quyen, N. T., et al. (2010). The human immune response to Dengue virus is dominated by highly cross-reactive antibodies endowed with neutralizing and enhancing activity. *Cell Host Microbe* 8, 271–283. doi: 10.1016/j.chom.2010.08.007

Bhatt, S., Gething, P. W., Brady, O. J., Messina, J. P., Farlow, A. W., Moyes, C. L., et al. (2013). The global distribution and burden of dengue. *Nature* 496, 504–507. doi: 10.1038/nature12060

Brady, O. J., Gething, P. W., Bhatt, S., Messina, J. P., Brownstein, J. S., Hoen, A. G., et al. (2012). Refining the global spatial limits of dengue virus transmission by evidence-based consensus. *PLoS Negl. Trop. Dis.* 6:e1760. doi: 10.1371/journal.pntd.0001760

Bulashev, A. K., Borovikov, S. N., Serikova, S. S., Suranshiev, Z. A., Kiyan, V. S., and Eskendirova, S. Z. (2016). Development of an ELISA using anti-idiotypic antibody for diagnosis of opisthorchiasis. *Folia Parasitol.* 63:205. doi: 10.14411/fp.2016.025

Chaichana, P., Okabayashi, T., Puiprom, O., Sasayama, M., Sasaki, T., Yamashita, A., et al. (2014). Low levels of antibody-dependent enhancement *in vitro* using viruses and plasma from dengue patients. *PLoS ONE* 9:e92173. doi: 10.1371/journal.pone.0092173

Chau, T. N., Quyen, N. T., Thuy, T. T., Tuan, N. M., Hoang, D. M., Dung, N. T., et al. (2008). Dengue in Vietnamese infants–results of infection-enhancement assays correlate with age-related disease epidemiology, and cellular immune responses correlate with disease severity. *J. Infect. Dis.* 198, 516–524. doi: 10.1086/590117

Clapham, H., Cummings, D. A., Nisalak, A., Kalayanarooj, S., Thaisomboonsuk, B., Klungthong, C., et al. (2015). Epidemiology of infant dengue cases illuminates serotype-specificity in the interaction between immunity and disease, and changes in transmission dynamics. *PLoS Negl. Trop. Dis.* 9:e0004262. doi: 10.1371/journal.pntd.0004262

Clark, K. B., Hsiao, H. M., Bassit, L., Crowe, J. E. Jr., Schinazi, R. F., Perng, G. C., et al. (2016). Characterization of dengue virus 2 growth in megakaryocyte-erythrocyte progenitor cells. *Virology* 493, 162–172. doi: 10.1016/j.virol.2016.03.024

de Alwis, R., Williams, K. L., Schmid, M. A., Lai, C. Y., Patel, B., Smith, S. A., et al. (2014). Dengue viruses are enhanced by distinct populations of serotype cross-reactive antibodies in human immune sera. *PLoS Pathog.* 10:e1004386. doi: 10.1371/journal.ppat.1004386

Dejnirattisai, W., Jumnainsong, A., Onsirisakul, N., Fitton, P., Vasanawathana, S., Limpitikul, W., et al. (2010). Cross-reacting antibodies enhance dengue virus infection in humans. *Science* 328, 745–748. doi: 10.1126/science.1185181

Denapoli, P. M., Zanetti, B. F., Dos Santos, A. A., de Moraes, J. Z., and Han, S. W. (2017). Preventive DNA vaccination against CEA-expressing tumors with anti-idiotypic scFv6.C4 DNA in CEA-expressing transgenic mice. *Cancer Immunol. Immunother.* 66, 333–342. doi: 10.1007/s00262-016-1940-4

Dent, M., Hurtado, J., Paul, A. M., Sun, H., Lai, H., Yang, M., et al. (2016). Plant-produced anti-dengue virus monoclonal antibodies exhibit reduced antibody-dependent enhancement of infection activity. *J. Gen. Virol.* 97, 3280–3290. doi: 10.1099/jgv.0.000635

Deshwal, R., Qureshi M. I., and Singh, R. (2016). Clinical and laboratory profile of dengue fever patients: a clinical experience. *J. Assoc. Physicians India* 64:71.

Ferguson, N. M., Rodriguez-Barraquer, I., Dorigatti, I., Mier, Y. T.-R. L., Laydon, D. J., and Cummings, D. A. (2016). Benefits and risks of the Sanofi-Pasteur dengue vaccine: modeling optimal deployment. *Science* 353, 1033–1036. doi: 10.1126/science.aaf9590

Fernando, S., Wijewickrama, A., Gomes, L., Punchihewa, C. T., Madusanka, S. D., Dissanayake, H., et al. (2016). Patterns and causes of liver involvement in acute dengue infection. *BMC Infect. Dis.* 16:319. doi: 10.1186/s12879-016-1656-2

Ferreira, R. A., de Oliveira, S. A., Gandini, M., Ferreira Lda, C., Correa, G., Abiraude, F. M., et al. (2015). Circulating cytokines and chemokines associated with plasma leakage and hepatic dysfunction in Brazilian children with dengue fever. *Acta Trop.* 149, 138–147. doi: 10.1016/j.actatropica.2015.04.023

Flingai, S., Plummer, E. M., Patel, A., Shresta, S., Mendoza, J. M., Broderick, K. E., et al. (2015). Protection against dengue disease by synthetic nucleic acid antibody prophylaxis/immunotherapy. *Sci. Rep.* 5:12616. doi: 10.1038/srep12616

Flipse, J., and Smit, J. M. (2015). The Complexity of a Dengue vaccine: a review of the human antibody response. *PLoS Negl. Trop. Dis.* 9:e0003749. doi: 10.1371/journal.pntd.0003749

Flipse, J., Wilschut, J., and Smit, J. M. (2013). Molecular mechanisms involved in antibody-dependent enhancement of dengue virus infection in humans. *Traffic* 14, 25–35. doi: 10.1111/tra.12012

Forshey, B. M., Stoddard, S. T., and Morrison, A. C. (2016). Dengue viruses and lifelong immunity: reevaluating the conventional wisdom. *J. Infect. Dis.* 214, 979–981. doi: 10.1093/infdis/jiw102

Gan, E. S., Ting, D. H., and Chan, K. R. (2017). The mechanistic role of antibodies to dengue virus in protection and disease pathogenesis. *Expert Rev. Anti Infect. Ther.* 15, 111–119. doi: 10.1080/14787210.2017.1254550

Godoi, I. P., Lemos, L. L., de Araujo, V. E., Bonoto, B. C., Godman, B., and Guerra Junior, A. A. (2017). CYD-TDV dengue vaccine: systematic review and meta-analysis of efficacy, immunogenicity and safety. *J. Comp. Eff. Res.* 6, 165–180. doi: 10.2217/cer-2016-0045

Goncalvez, A. P., Engle, R. E., St Claire, M., Purcell, R. H., and Lai, C. J. (2007). Monoclonal antibody-mediated enhancement of dengue virus infection *in vitro* and *in vivo* and strategies for prevention. *Proc. Natl. Acad. Sci. U.S.A.* 104, 9422–9427. doi: 10.1073/pnas.0703498104

Guzman, M. G., Kouri, G., Valdes, L., Bravo, J., Alvarez, M., Vazques, S., et al. (2000). Epidemiologic studies on Dengue in Santiago de Cuba, 1997. *Am. J. Epidemiol.* 152, 793–799. doi: 10.1093/aje/152.9.793

Halstead, S. B. (1970). Observations related to pathogensis of dengue hemorrhagic fever. VI. Hypotheses and discussion. *Yale J. Biol. Med.* 42, 350–362.

Halstead, S. B. (1979). *In vivo* enhancement of dengue virus infection in rhesus monkeys by passively transferred antibody. *J. Infect. Dis.* 140, 527–533. doi: 10.1093/infdis/140.4.527

Halstead, S. B. (2007). Dengue. *Lancet* 370, 1644–1652. doi: 10.1016/S0140-6736(07)61687-0

Halstead, S. B., and O'Rourke, E. J. (1977). Dengue viruses and mononuclear phagocytes. I. Infection enhancement by non-neutralizing antibody. *J. Exp. Med.* 146, 201–217. doi: 10.1084/jem.146.1.201

Hampe, C. S. (2012). Protective role of anti-idiotypic antibodies in autoimmunity–lessons for type 1 diabetes. *Autoimmunity* 45, 320–331. doi: 10.3109/08916934.2012.659299

Jessie, K., Fong, M. Y., Devi, S., Lam, S. K., and Wong, K. T. (2004). Localization of dengue virus in naturally infected human tissues, by immunohistochemistry and *in situ* hybridization. *J. Infect. Dis.* 189, 1411–1418. doi: 10.1086/383043

John, D. V., Lin, Y. S., and Perng, G. C. (2015). Biomarkers of severe dengue disease - a review. *J. Biomed. Sci.* 22:83. doi: 10.1186/s12929-015-0191-6

Liao, B., Tang, Y., Hu, F., Zhou, W., Yao, X., Hong, W., et al. (2015). Serum levels of soluble vascular cell adhesion molecules may correlate with the severity of dengue virus-1 infection in adults. *Emerg. Microbes Infect.* 4:e24. doi: 10.1038/emi.2015.24

Liu, J., Liu, Y., Nie, K., Du, S., Qiu, J., Pang, X., et al. (2016). Flavivirus NS1 protein in infected host sera enhances viral acquisition by mosquitoes. *Nat. Microbiol.* 1:16087. doi: 10.1038/nmicrobiol.2016.87

Malavige, G. N., Gomes, L., Alles, L., Chang, T., Salimi, M., Fernando, S., et al. (2013). Serum IL-10 as a marker of severe dengue infection. *BMC Infect. Dis.* 13:341. doi: 10.1186/1471-2334-13-341

Martinez Gomez, J. M., Ong, L. C., Lam, J. H., Binte Aman, S. A., Libau, E. A., Lee, P. X., et al. (2016). Maternal antibody-mediated disease enhancement in type i interferon-deficient mice leads to lethal disease associated with liver damage. *PLoS Negl. Trop. Dis.* 10:e0004536. doi: 10.1371/journal.pntd.0004536

Ojha, A., Nandi, D., Batra, H., Singhal, R., Annarapu, G. K., Bhattacharyya, S., et al. (2017). Platelet activation determines the severity of thrombocytopenia in dengue infection. *Sci. Rep.* 7:41697. doi: 10.1038/srep41697

Orozco, S., Schmid, M. A., Parameswaran, P., Lachica, R., Henn, M. R., Beatty, R., et al. (2012). Characterization of a model of lethal dengue virus 2 infection in C57BL/6 mice deficient in the alpha/beta interferon receptor. *J. Gen. Virol.* 93(Pt 10), 2152–2157. doi: 10.1099/vir.0.045088-0

Osorio, J. E., Velez, I. D., Thomson, C., Lopez, L., Jimenez, A., Haller, A. A., et al. (2014). Safety and immunogenicity of a recombinant live attenuated tetravalent dengue vaccine (DENVax) in flavivirus-naive healthy adults in Colombia: a randomised, placebo-controlled, phase 1 study. *Lancet Infect. Dis.* 14, 830–838. doi: 10.1016/S1473-3099(14)70811-4

Pan, Y., Yuhasz, S. C., and Amzel, L. M. (1995). Anti-idiotypic antibodies: biological function and structural studies. *FASEB J.* 9, 43–49.

Ramadhany, R., Hirai, I., Sasaki, T., Ono, K., Ramasoota, P., Ikuta, K., et al. (2015). Antibody with an engineered Fc region as a therapeutic agent against dengue virus infection. *Antiviral Res.* 124, 61–68. doi: 10.1016/j.antiviral.2015.10.012

Ramakrishnan, L., Pillai, M. R., and Nair, R. R. (2015). Dengue vaccine development: strategies and challenges. *Viral Immunol.* 28, 76–84. doi: 10.1089/vim.2014.0093

Reich, N. G., Shrestha, S., King, A. A., Rohani, P., Lessler, J., Kalayanarooj, S., et al. (2013). Interactions between serotypes of dengue highlight epidemiological impact of cross-immunity. *J. R. Soc. Interface* 10:20130414. doi: 10.1098/rsif.2013.0414

Rodenhuis-Zybert, I. A., van der Schaar, H. M., da Silva Voorham, J. M., van der Ende-Metselaar, H., Lei, H.-Y., Wilschut, J., et al. (2010). Immature dengue virus: a veiled pathogen? *PLoS Pathog* 6:e1000718. doi: 10.1371/journal.ppat.1000718

Sangkawibha, N., Rojanasuphot, S., Ahandrik, S., Viriyapongse, S., Jatanasen, S., Salitul, V., et al. (1984). Risk factors in dengue shock syndrome: a prospective epidemiologic study in Rayong, Thailand. I. The 1980 outbreak. *Am. J. Epidemiol.* 120, 653–669. doi: 10.1093/oxfordjournals.aje.a113932

Screaton, G., Mongkolsapaya, J., Yacoub, S., and Roberts, C. (2015). New insights into the immunopathology and control of dengue virus infection. *Nat. Rev. Immunol.* 15, 745–759. doi: 10.1038/nri3916

Soo, K. M., Khalid, B., Ching, S. M., and Chee, H. Y. (2016). Meta-analysis of dengue severity during infection by different dengue virus serotypes in primary and secondary infections. *PLoS ONE* 11:e0154760. doi: 10.1371/journal.pone.0154760

Wang, Y., Si, L. L., Guo, X. L., Cui, G. H., Fang, D. Y., Zhou, J. M., et al. (2017). Substitution of the precursor peptide prevents anti-prM antibody-mediated antibody-dependent enhancement of dengue virus infection. *Virus Res.* 229, 57–64. doi: 10.1016/j.virusres.2016.12.003

Wichmann, O., Hongsiriwon, S., Bowonwatanuwong, C., Chotivanich, K., Sukthana, Y., and Pukrittayakamee, S. (2004). Risk factors and clinical features associated with severe dengue infection in adults and children during the 2001 epidemic in Chonburi, Thailand. *Trop. Med. Int. Health* 9, 1022–1029. doi: 10.1111/j.1365-3156.2004.01295.x

Zybert, I. A., van der Ende-Metselaar, H., Wilschut, J., and Smit, J. M. (2008). Functional importance of dengue virus maturation: infectious properties of immature virions. *J. Gen. Virol.* 89(Pt 12), 3047–3051. doi: 10.1099/vir.0.2008/002535-0

Conflict of Interest Statement: The authors declare that the research was conducted in the absence of any commercial or financial relationships that could be construed as a potential conflict of interest.

frontiers in Cellular and Infection Microbiology

ORIGINAL RESEARCH
published: 12 May 2017
doi: 10.3389/fcimb.2017.00175

Effective Protection Induced by a Monovalent DNA Vaccine against Dengue Virus (DV) Serotype 1 and a Bivalent DNA Vaccine against DV1 and DV2 in Mice

Xiaoyan Zheng[1,2†], *Hui Chen*[1†], *Ran Wang*[1], *Dongying Fan*[1], *Kaihao Feng*[1], *Na Gao*[1] and *Jing An*[1,3*]

[1] Department of Microbiology and Parasitology, School of Basic Medical Sciences, Capital Medical University, Beijing, China, [2] Beijing Tropical Medicine Research Institute, Beijing Friendship Hospital, Capital Medical University, Beijing, China, [3] Center of Epilepsy, Beijing Institute for Brain Disorders, Beijing, China

Dengue virus (DV) is the causal pathogen of dengue fever, which is one of the most rapidly spread mosquito-borne disease worldwide and has become a severe public health problem. Currently, there is no specific treatment for dengue; thus, a vaccine would be an effective countermeasure to reduce the morbidity and mortality. Although, the chimeric Yellow fever dengue tetravalent vaccine has been approved in some countries, it is still necessary to develop safer, more effective, and less costly vaccines. In this study, a DNA vaccine candidate pVAX1-D1ME expressing the prME protein of DV1 was inoculated in BALB/c mice via intramuscular injection or electroporation, and the immunogenicity and protection were evaluated. Compared with traditional intramuscular injection, administration with 50 μg pVAX1-D1ME via electroporation with three immunizations induced persistent humoral and cellular immune responses and effectively protected mice against lethal DV1 challenge. In addition, immunization with a bivalent vaccine consisting of pVAX1-D1ME and pVAX1-D2ME via electroporation generated a balanced IgG response and neutralizing antibodies against DV1 and DV2 and could protect mice from lethal challenge with DV1 and DV2. This study sheds new light on developing a dengue tetravalent DNA vaccine.

Keywords: dengue virus, DNA vaccine, monovalent vaccine, bivalent vaccine, electroporation, dengue

OPEN ACCESS

Edited by:
Gong Cheng,
Tsinghua University, China

Reviewed by:
Cheng-Feng Qin,
Beijing Institute of Microbiology and Epidemiology, China
Xia Jin,
Institute Pasteur of Shanghai (CAS), China

***Correspondence:**
Jing An
anjing@ccmu.edu.cn

[†] *These authors have contributed equally to this work.*

Received: *05 March 2017*
Accepted: *24 April 2017*
Published: *12 May 2017*

Citation:
Zheng X, Chen H, Wang R, Fan D, Feng K, Gao N and An J (2017) Effective Protection Induced by a Monovalent DNA Vaccine against Dengue Virus (DV) Serotype 1 and a Bivalent DNA Vaccine against DV1 and DV2 in Mice. Front. Cell. Infect. Microbiol. 7:175. doi: 10.3389/fcimb.2017.00175

INTRODUCTION

Dengue virus (DV) is a member of the family *Flaviviridae* and contains four distinct serotypes (DV1-4). DV infections cause either asymptomatic disease or some clinical illnesses ranging from self-limited dengue fever (DF) to severe dengue (sDF), including dengue hemorrhagic fever and dengue shock syndrome (Bhatt et al., 2013); dengue is the most important arbovirus disease in the world in terms of the highest morbidity and mortality (Porter and Raviprakash, 2015). It was reported that there were 58.4 million symptomatic DV infections with 13,586 fatal cases in 2013, and the global cost is 8.9 billion US dollars annually (Shepard et al., 2016). As a major public health problem, dengue is considered to be one of the fastest growing epidemics

by the World Health Organization (Arima et al., 2015; Rogers, 2015). In its global strategy for dengue control, the World Health Organization aims to reduce dengue mortality and morbidity by at least 50 and 25%, respectively, by 2020 (WHO, 2012).

Since the first outbreak in Guangdong province in 1978, dengue has broken out several times in the Hainan, Fujian, Guangxi, and Zhejiang provinces in mainland China in recent years (Wu et al., 2010; Lin et al., 2016). In these dengue outbreaks, all four dengue serotypes were found to be co-circulating in endemic areas, but DV1 is the predominant serotype. In 2014, the Guangdong province of China suffered from the most serious dengue outbreak in its history, and the total number of DF cases was more than 45,000 (Huang et al., 2016). In the outbreak, co-circulation of DV1 and DV2 was identified, and some isolates of DV1 or DV2 were closely related with Guangzhou isolates from previous years; the frequency of DV1 epidemics was still higher than that of DV2 (Zhang et al., 2014; Ren et al., 2015), indicating that dengue became endemic in Guangdong and is no longer an imported disease in China (Lin et al., 2016; Zhao et al., 2016). Therefore, controlling dengue is a long-term effort, and developing a vaccine is believed to be the most reliable approach to achieve this goal (Hermann et al., 2015).

Theoretically, a secondary DV infection of heterotypic serotype may increase the risk of sDF in patients and it is the major barrier for developing successful vaccine against DVs. The reason is not very clear currently, but the more accepted interpretation is the role of antibody dependent enhancement (ADE) (Cummings et al., 2005). Therefore, optimal dengue vaccines should induce a balanced immune response to all four DV serotypes. A DNA vaccine, as a simple and efficient technique with attractive advantages including inexpensiveness, ease of production, stability for storage and shipping, may overcome the obstacle of ADE through balanced and long-term expression of immunogens of all four DV serotypes.

The DV genome contains a single open reading frame and encodes three structural proteins: the capsid protein (C), the precursor of membrane protein (prM), and the envelope protein (E), followed by seven non-structural proteins. Among the structural proteins, the prM and E proteins are major target molecules for developing vaccines because the E protein contains the immunological epitopes for inducing humoral and cellular immune responses, and the prM protein is essential for the correct conformation of the E protein during the viral maturation (Bray and Lai, 1991). Therefore, the *prM* and *E* genes are the principal molecular candidates for developing flavivirus DNA vaccines.

In our previous studies, DNA vaccine candidates expressing the prM and E proteins of DV1 or DV2 with the eukaryotic expression vector pCAGGSP7 have been demonstrated to induce some immune protection at three doses (100 μg each) of DNA delivered by intramuscular (IM) injection (Zheng et al., 2011; Lu et al., 2013). Recently, to translate the DNA vaccine candidates for further clinical application, the plasmids were reconstructed using pVAX1, a unique US FDA-approved vector for developing DNA vaccines; it was confirmed that the DNA vaccine candidate pVAX1-D2ME containing the *prM* and *E* genes of DV2 could protect mice from lethal DV2 infection and induce an effective specific antibody response in rabbits (Chen et al., 2016). These findings establish an important foundation for further researching a DV1 vaccine.

In this study, another DNA vaccine candidate, pVAX1-D1ME, encoding the prM and E proteins of DV1 was constructed and vaccinated in mice via IM injection or *in vivo* electroporation (EP); immune responses and protection were determined. Based on this, the immunogenicity and immuno-protection of a bivalent vaccine candidate consisting of pVAX1-D1ME and pVAX1-D2ME was evaluated in mice to explore the possibility of a bivalent vaccine against DV1 and DV2 and simultaneously lay the foundation for the study of a tetravalent DNA vaccine against all DV serotypes. Our results showed that the immunization of pVAX1-D1ME via EP could induce persistent humoral and cellular immune responses and effectively protect mice against lethal DV1 challenge. The immunization of a bivalent vaccine consisting of pVAX1-D1ME and pVAX1-D2ME via EP could generate a balanced IgG response against DV1 and DV2 and protect mice from lethal challenge with DV1 and DV2. Moreover, no increased clinical signs were observed in the mice. This study encourages further development of a dengue tetravalent DNA vaccine.

MATERIALS AND METHODS

Animals and Ethics Statement

Six-week-old female BALB/c mice were purchased from Vital River Laboratories (Beijing, China) and were maintained in specific pathogen-free environments. Animal care and experimental procedures were approved by the Institutional Animal Care and Use Committee of Chinese Capital Medical University (approval number: AEEI-2015-066).

Cells and Viruses

Vero cells were grown at 37°C in minimal essential medium (MEM) supplemented with 5% fetal bovine serum (FBS). Baby hamster kidney (BHK) cells were grown at 37°C in MEM supplemented with 10% FBS. *Aedes albopictus* C6/36 cells were grown at 28°C in RPMI 1640 supplemented with 10% FBS. Mice fibroblast L929 cells were grown in RPMI 1640 supplemented with 10% FBS at 37°C.

The DV1 (Hawaii strain) and the DV2 (New Guinea C strain) used in challenge model were clinical isolates provided by Guangdong Center for Disease Control and Prevention. Viruses were propagated in C6/36 cells and their titers were determined by plaque assays on Vero cells.

Construction of Plasmids

The DNA vaccine candidate was constructed for the expression of DV1 prME using the eukaryotic expression vector pVAX1 (Invitrogen, USA). Briefly, the fragments of DV1 *prM* and *E* (GenBank accession number U88535.1, nucleotides 365 to 2419 bp) were amplified by polymerase chain reaction from a full-length infectious clone of DV1. The forward and reverse primers were as follows: 5′-GCGTTC**GCTAGC**ATGGCAATG TTGAACATAATGAAC-3′ and 5′-GGCACA**CTCGAG**TTA CGCCTGAACCATGACTCCTAG-3′. The gene of interest was

finally sub-cloned into pVAX1, and the recombinant plasmid was named as pVAX1-D1ME, which was further verified by enzyme digestion and DNA sequencing.

Indirect Immunofluorescence (IFA) Staining

To detect the expression of the recombinant plasmid in eukaryotic cells, BHK cells (0.5×10^5 per well) in a 24-well plate were transfected with the pVAX1-D1ME and served as the antigen. The transfection was performed with Lipofectamine 2000 (Invitrogen, USA) as specified by the supplier's instruction. Transfected BHK cells were fixed with 4% PFA, permeabilized with 0.2% Triton X-100 in PBS and then blocked with 1% bovine serum albumin in PBS. The DV1-infected mouse serum diluted 1:1,000 was used as the primary antibody. The secondary antibody was goat anti-mouse IgG conjugated with FITC (EarthOx, USA) diluted 1:500. DAPI (Sigma, USA) diluted 1:2500 was used to stain nucleus. After mounting with 40% glycerol, the cells were examined and photographed under a fluorescence microscope (Olympus BX61, Japan). Cells transfected with the vector pVAX1 served as the negative control.

Vaccination of pVAX1-D1ME

To evaluate the immunogenicity of pVAX1-D1ME with different dosage and delivery methods, female BALB/c mice were divided into four groups (EP50, EP5, IM50, and pVAX1 groups, **Table 1**). In the IM50 group, each mouse was immunized with 50 μg pVAX1-D1ME into the quadriceps muscle of the hind limb by a syringe. In the EP groups, two silver needles 6 mm apart were inserted over the injection site, 5 μg or 50 μg pVAX1-D1ME was injected into the muscle, and then six electric pulses (36 V, 10 ms) were applied using the gene delivery device (Terasa Healthcare Sci-Tech, China). Mice inoculated with 50 μg pVAX1 via EP served as the negative controls. The mice were immunized three times at two-week intervals.

To determine the appropriate immunization schedule, the mice were divided into four groups (once-EP50, twice-EP50, thrice-EP50, and pVAX1 groups, **Table 1**), and immunized with 50 μg pVAX1-D1ME via EP once, twice or three times at two-week intervals, respectively. Mice inoculated with 50 μg pVAX1 via EP three times served as the negative controls.

Immunization of the Bivalent Vaccine Consisting of pVAX1-D1ME and pVAX1-D2ME

To evaluate the immunogenicity of the bivalent vaccine consisting of pVAX1-D1ME and pVAX1-D2ME, BALB/c mice were divided into three groups (**Table 1**). In the B-IM group, mice were immunized with 50 μg pVAX1-D1ME and 50 μg pVAX1-D2ME into the quadriceps muscles of the left and right hind limbs via IM injection. In the B-EP group, mice were immunized via EP immediately after IM injection with 50 μg pVAX1-D1ME and 50 μg pVAX1-D2ME. In the B-pVAX1 group, mice were inoculated via EP immediately after IM injection with 100 μg pVAX1 (50 μg in each leg), and served as the negative controls. The immunization was performed three times with two-week intervals.

TABLE 1 | Mouse immunization groups and scheme.

Groups	Immunogen	Gene delivery	Dose (μg)	Vaccination times, interval (weeks)	EP Voltage (V)	EP Pulse length (ms)
EVALUATING THE IMMUNE RESPONSES OF pVAX1-D1ME (4 GROUPS)						
EP50	pVAX1-D1ME	EP	50	3, 2	36	10
EP5	pVAX1-D1ME	EP	5	3, 2	36	10
IM50	pVAX1-D1ME	IM	50	3, 2	–	–
pVAX1	pVAX1	EP	50	3, 2	36	10
DETECTING THE OPTIMAL IMMUNIZATION TIMES OF pVAX1-D1ME (4 GROUPS)						
Once-EP50	pVAX1-D1ME	EP	50	1, 0	36	10
Twice-EP50	pVAX1-D1ME	EP	50	2, 2	36	10
Thrice-EP50	pVAX1-D1ME	EP	50	3, 2	36	10
pVAX1	pVAX1	EP	50	3, 2	36	10
EVALUATING THE IMMUNE RESPONSES OF THE BIVALENT VACCINE (3 GROUPS)						
B-EP	pVAX1-D1ME pVAX1-D2ME	EP	50[a] 50[a]	3, 2	36	10
B-IM	pVAX1-D1ME pVAX1-D2ME	IM	50[b] 50[b]	3, 2	–	–
B-pVAX1	pVAX1	EP	50[c] 50[c]	3, 2	36	10

[a] The mice were immunized with 50 μg pVAX1-D1ME and 50 μg pVAX1-D2ME via IM into limbs bilaterally, then six electric pulses (36V, 10 ms) were applied using the gene delivery device. [b] The mice were immunized with 50 μg pVAX1-D1ME and 50 μg pVAX1-D2ME via IM into limbs bilaterally. [c] The mice were immunized with 50 μg pVAX1 via IM into bilateral limbs, then six electric pulses (36V, 10 ms) were applied using the gene delivery device.

Immunohistochemistry (IHC) Staining

IHC staining was conducted to detect the expression of the DV1 prME protein in the local injection site. Two weeks after the third immunization, the thigh muscles of mice were isolated and cut into 5-μm consecutive paraffin sections. Following the manufacturer's instructions, the sections were processed for IHC analyses using the PV6001 IHC detection reagent (ZSGB-BIO, China). Briefly, the slides were blocked in 1% bovine serum albumin at 37°C for 1 h. The DV1-infected mouse serum diluted 1:500 was used as the primary antibody and incubated at 4°C overnight. The secondary antibody was HRP-conjugated goat anti-mouse IgG (SANTA, USA) diluted 1:2,000 at 37°C for 1 h.

Enzyme-Linked Immunosorbent Assay (ELISA)

Serum samples were collected by tail bleeding, and specific IgG antibodies against DV1 or DV2 were determined by ELISA. Briefly, each well of the 96-well microtiter plate was coated with 2 μg of the concentrated DV1 or DV2 protein from the infected C6/36 cells, and followed by blocking with 2% bovine serum albumin. The plate was incubated with two-fold serial dilutions of the serum samples (started from 1:100), then antibody titers were detected with HRP-conjugated goat anti-mouse IgG (1:5,000, SANTA, USA), and substrate solution of orthophenylene diamine. The absorbance at 492 nm was

measured using a microplate reader (Thermo, USA). The highest dilution, yielding an optical density (OD) greater than that of the negative control at the same dilution, was recorded as the end-point titer.

To determine the IgG subclasses, two weeks after the third immunization, antibody isotype ELISA was performed using serum samples (1:100) as the first antibody, and goat anti-mouse IgG1-HRP or IgG2a-HRP (1:4,000, SouthernBiotech, USA) was used as the secondary antibody.

Plaque Reduction Neutralization Test (PRNT)

Two weeks after the third immunization, serum samples were collected to detect the levels of anti-DV1 neutralizing antibody (NAb) by PRNT. After heating at 56°C for 30 min to inactivate complement, sera were two-fold diluted (starting from 1:10) in MEM containing 2% FBS. Diluted sera were mixed 1:1 with DV1 suspension containing 100 plaque-forming units (PFU), and incubated at 37°C for 1 h. Then, the mixture was added to Vero cell in duplicate wells of a 24-well plate, and incubated at 37°C for another 1 h. The infected Vero cells were washed then layered with MEM containing 2% FBS and 1.1% methylcellulose. After incubation at 37°C for 8 days in 5% CO_2, the plaques were stained with crystal violet and counted. The maximum serum dilution that yielded a 50% plaque reduction ($PRNT_{50}$) compared to the average plaque number of the virus control wells was calculated as the NAb titer.

Enzyme-Linked Immunospot (ELISPOT) Assay

Two weeks after the third immunization, splenocytes were isolated aseptically from mice to measure the generation of interferon (IFN)-γ, interleukin (IL)-2, IL-4, and IL-10 using ELISPOT kits per the manufacturer's instructions (BD Biosciences, USA). Briefly, splenocytes (1×10^6 cells/well) were added into 96-well plates (Millipore, USA) pre-coated with 100 μl (1.0 mg/ml) of capture antibodies, and stimulated with 5 μg/well of concentrated DV1 proteins or concanavalin A (0.5 μg/well, positive control) or RPMI 1640 medium (negative control) at 37°C for 60 h. The cells were then incubated with secondary biotinylated detection antibodies, streptavidin-HRP (BD Biosciences, USA), and substrate (AEC Chromogen). The spot-forming units (SFU), which represented the positive single cells, were counted automatically using an ELISPOT reader (CTL, USA).

Cytotoxic T Lymphocyte (CTL) Activity

Two weeks after the third vaccination, freshly isolated mouse splenocytes were stimulated with concentrated DV1 proteins (2 μg/10^5 cells) for 72 h to prepare effector cells. L929 cells infected with DV1 (multiplicity of infection = 10) for 16–18 h were used as target cells. In U-bottom 96-well plates, the target cell suspension (5×10^3 cells/well) was dispensed with the effector cells at various effector: target (E:T) ratios of 100:1, 50:1, 25:1, and 5:1. After incubation for 5 h at 37°C and 5% CO_2, 50 μl/well of the supernatant was transferred to 96-well flat-bottom plates. The lactate dehydrogenase (LDH) activity was determined by the CytoTox non-radioactive cytotoxicity assay kit (Promega, USA) per the manufacturer's instructions. The absorbance at 490 nm was recorded on a microplate reader, and the percentage of specific lysis (% LDH release) was calculated using the following formula: % cytotoxicity = 100 × (experimental release – effector spontaneous release – target spontaneous release)/(target maximum release – target spontaneous release).

Lymphocyte Proliferation Ability

Two weeks after the third inoculation, 100 μl of freshly isolated mouse splenocytes (1×10^6 cells) were stimulated with concentrated DV1 proteins (100 μg/ml) or ConA (5 μg/ml, positive control) at 37°C for 72 h. Then, 10 μl of the CCK-8 solution (Dojindo, Japan) was added to each well, and incubated for 5 h. The OD at 450 nm was detected using a microplate reader. The stimulation index (SI) was calculated as $(OD_{stimulated} - OD_{blank}) / (OD_{unstimulated} - OD_{blank})$.

Protection Test

Two weeks after the last immunization, the mice were challenged with 50 LD_{50} of DV1 (2×10^7 PFU) or 30 LD_{50} of DV2 (600 PFU) intracerebrally (Chen et al., 2016). Body weight, clinical signs, and mortality were monitored daily for 30 days. Clinical symptoms were scored as follows: 0, healthy; 1, ruffled hair or hunchbacked appearance; 2, asthenia, wasting or bradykinesia; 3, forelimb or hindlimb weakness; 4, paralysis or moribundity; and 5, death.

Statistical Analysis

All data were analyzed using SPSS software (version 17.0). Kaplan-Meier survival curves and the log rank test were used for survival analysis. Weight changes and sign scores were analyzed by the repeated measures analysis of variance. Others were analyzed by one way analysis of variance. Differences were considered to be statistically significant and highly significant at $p < 0.05$ (∗) and $p < 0.01$ (∗∗), respectively.

RESULTS

Expression of the prME Protein in BHK Cells and the Injection Site of Immunized Mice

To determine the *in vitro* expression of the prME protein in eukaryotic cells by IFA, the BHK cells were transfected with the plasmids pVAX1-D1ME and pVAX1. As shown in **Figure 1A**, the BHK cells that received the pVAX1-D1ME exhibited intense fluorescence in the cytoplasm; while negative control cells received the pVAX1 vector failed to show any specific fluorescence. This result confirmed that the pVAX1-D1ME was successfully transfected into eukaryotic cells and worked effectively. Thus, this plasmid could be used for further experiments.

Furthermore, to determine the *in vivo* expression of the prME protein by IHC, the muscle tissues were sampled from mice sacrificed two weeks after the third immunization. As shown in **Figure 1B**, expression of the protein of interest was detected in

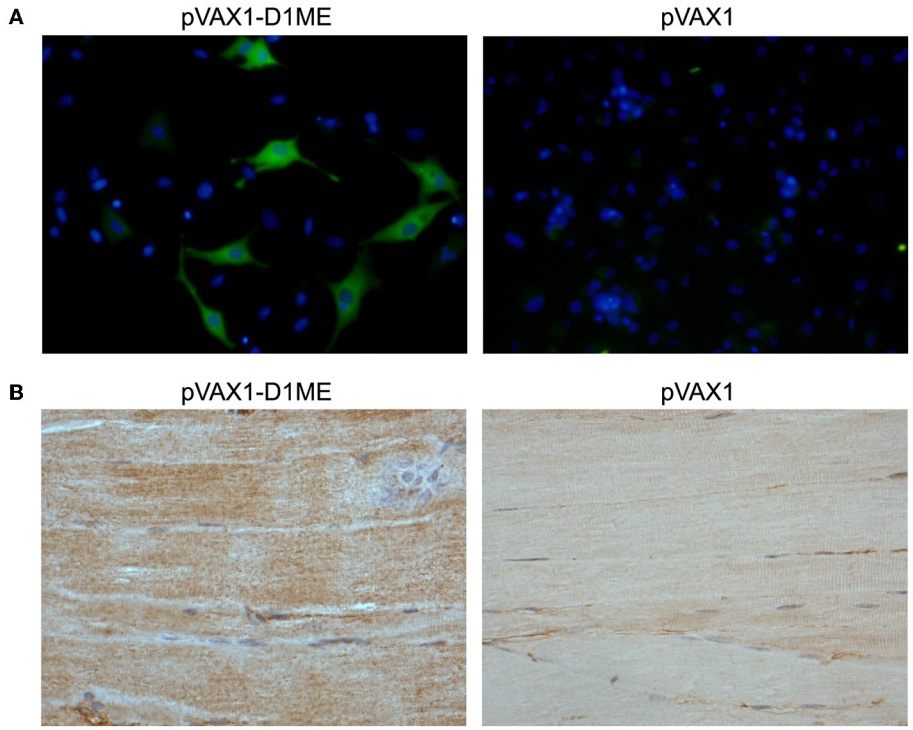

FIGURE 1 | Determination of prME protein expression. (A) *In vitro* expression of the prME protein in DNA-transfected BHK cells by IFA (fluorescence microscopy, × 400). **(B)** *In vivo* expression of the prME protein in tissues by IHC. The muscle tissues were collected from mice sacrificed two weeks after the third immunization with 50 μg DNA (light microscopy, × 200).

the muscle tissue of the mouse that received the pVAX1-D1ME but not the pVAX1 vector. This result confirmed that the pVAX1-D1ME was successfully transfected into muscle cells via EP and worked effectively. Thus, this plasmid could be used as the DNA vaccine candidate in further experiments.

Antibody Response to Immunization with the pVAX1-D1ME

The dynamic anti-DV1 IgG response at various time points was analyzed by ELISA. As shown in **Figure 2A**, the DV1-specific IgG level in the EP50 group showed an increased trend after the prime immunization, attained a significantly high level after the second immunization, and then maintained the highest level during the observed period. In the EP5 group, increased anti-DV1 IgG levels were observed, but the amplitude was limited compared with that in the EP50 group. However, the antibody response in the IM50 group showed no obvious change. After the third vaccination, the end-point geometric mean titer (GMT) of the IgG antibody in the EP50 group reached 1:2111 (**Figure 2B**), which was significantly different from that in the EP5 (1:606, $p < 0.01$) or the IM50 (1:400, $p < 0.01$) group. These results indicated that 50 μg pVAX1-D1ME delivered by EP could induce humoral immune response more effectively.

The levels of DV1-specific IgG subclasses were determined by ELISA. In general, the IgG1 and IgG2a isotypes are associated with the Th2 and Th1 immune responses, respectively. As shown in **Figure 2C**, the EP50 and EP5 groups elicited higher levels of IgG2a than IgG1 with mean IgG2a/IgG1 ratios of 3.90 and 3.39, respectively. The IM50 group induced almost equal levels of IgG1 and IgG2a, which was similar to the control group. IgG2a levels in mice inoculated via EP were significantly higher than those in the control and IM groups ($p < 0.01$), indicating that immunization with the pVAX1-D1ME via EP induced a bias toward the Th1 immune response, whereas vaccination via IM showed no obvious bias.

Two weeks after the third immunization, serum samples were collected to detect the anti-DV1 NAb level by $PRNT_{50}$. As shown in **Figure 2D**, the highest NAb level was observed in the EP50 group with a GMT of 1:349, while NAb levels in the EP5 and IM50 were 1:80 and 1:57, respectively. There were significant differences in NAb titers between the experimental groups (EP50, EP5 and IM) and the pVAX1 group ($p < 0.01$ or $p < 0.05$).

Cytokine Generation to Immunization with pVAX1-D1ME

Cytokines secreted by splenocytes upon stimulation with the DV1 antigen were detected by ELISPOT assay. As shown in **Figure 3**, levels of IFN-γ, IL-2, and IL-4 increased markedly in the EP50 group ($p < 0.01$ or $p < 0.05$) compared to the pVAX1 group. In the EP5 group, levels of IFN-γ and IL-4 increased significantly ($p < 0.01$ or $p < 0.05$) compared to the pVAX1 group. In the IM50 group, only the increased IFN-γ level was

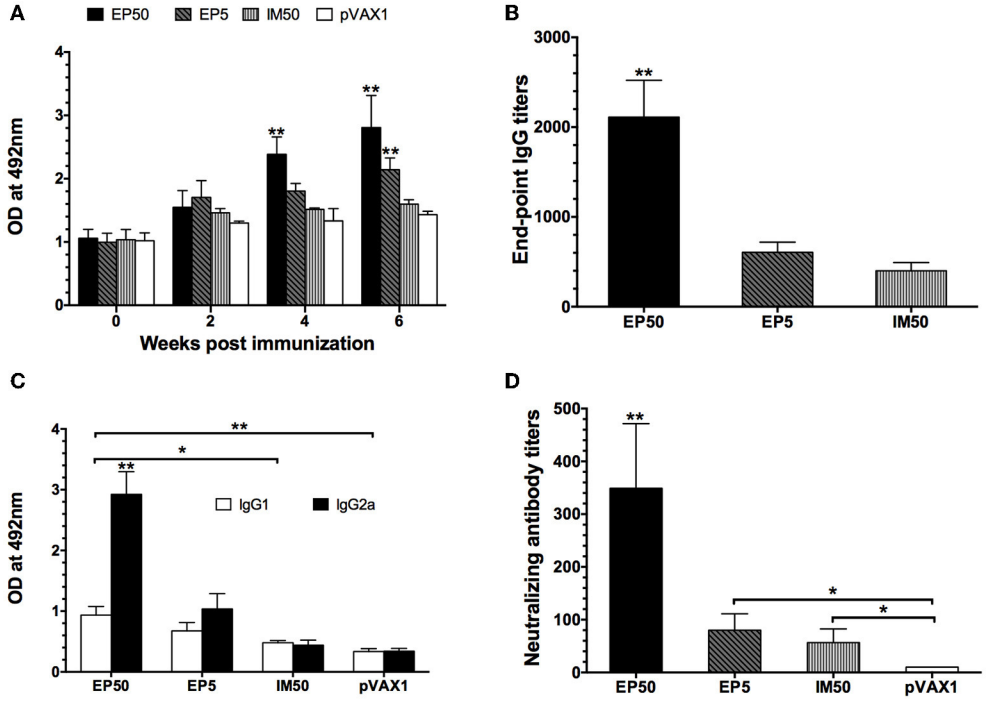

FIGURE 2 | DV1-specific antibody responses in mice sera. (A) Dynamics of the IgG responses detected by ELISA. The mice were immunized three times at two-week intervals. Sera were collected at weeks 0, 2, 4, and 6. All samples were diluted at 1:800 ($n = 6$). **(B)** End-point titers of anti-DV1 antibodies assayed by ELISA ($n = 6$). Sera were collected two weeks after the third immunization. The results were expressed as GMT + standard deviation (SD). **(C)** The anti-DV1 IgG subclasses in mice sera determined by ELISA. Sera were collected two weeks after the third immunization. Values of IgG2a and IgG1 were reported as the mean OD + SD at 492 nm at a serum dilution of 1:100 ($n = 8$). **(D)** Serum NAb responses assayed by $PRNT_{50}$ ($n = 8$). Sera were collected two weeks after the third immunization. NAb titers were recorded as GMT + SD. *$p < 0.05$, **$p < 0.01$.

observed ($p < 0.05$). There was no significant change in IL-10 levels in all groups. Generally, IFN-γ and IL-2 are defined as markers of the Th1 response and IL-4 is defined as a marker of the Th2 response; the above results suggested that both the Th1- and Th2-type immune responses were effectively evoked by 50 μg pVAX1-D1ME via EP administration.

Cell-Mediated Immune Response to Immunization with pVAX1-D1ME

Splenocytes isolated from immunized mice were stimulated with the DV1 antigen, and the specific CTL activity was determined. As shown in **Figure 4A**, increased CTL activity was observed in both the EP and IM groups, with an E:T ratio-dependent pattern, but not in the control group. The EP50 group showed significantly increased CTL activity based on E:T ratios ≥ 25:1 and then maintained the highest CTL activity among all groups. When the E:T ratio was 100:1, the CTL activity was 38.4% in the EP50 group, with a significant difference ($p < 0.01$) from the activities in the EP5 group (22.2%) and the IM50 group (22.6%).

The splenocytes stimulated with DV1 antigen were also used to examine lymphocyte proliferation. As shown in **Figure 4B**, no distinct lymphocyte proliferation was observed in the pVAX1 group (SI = 1.61 ± 0.22). However, SIs in the EP50, EP5, and IM50 groups showed an increased trend, with values at 3.37 ± 0.57, 2.53 ± 0.64, and 2.03 ± 0.47, respectively, when 100 μg/ml of DV1 antigen was used. Only the lymphocyte proliferation in the EP50 group showed a significant difference compared with that in the pVAX1 group ($p < 0.01$). Taken together, the above results indicated that immunization with pVAX1-D1ME induced not only humoral but also cellular immune responses.

Protective Immunity Elicited by pVAX1-D1ME

Two weeks after the third immunization, the mice were challenged with lethal doses of DV1, and the protective efficacy of the pVAX1-D1ME DNA vaccine was evaluated. All mice in the control group showed illness at day 7 post infection, and gradually became worse (**Figure 5A**) with obvious body weight loss (**Figure 5B**). At day 16, body weight in the control group decreased by more than 21%. Finally, a total of 60% of control mice died (**Figure 5C**), and some surviving mice showed sequelae such as paralysis of hind limbs. In comparison, the EP50 group showed a transient and mild illness at day 9, and completely recovered without obvious changes of body weight and any sequelae during the 30-day observation period (**Figures 5A,B**). All mice in the EP50 group survived the viral challenge (**Figure 5C**). Mice in the EP5 and IM50 groups also showed illness at day 7, and clinical symptoms were more serious than those in the EP 50 group but milder than those in the control group (**Figure 5A**). Survival rates of 100% and 90% were seen in

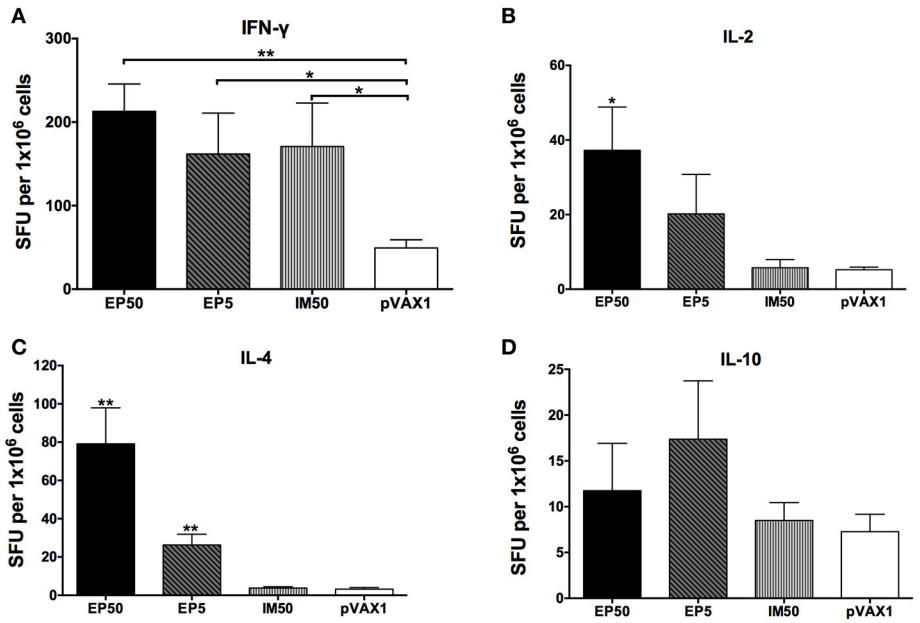

FIGURE 3 | The levels of splenocyte-secreted IFN-γ (A), IL-2 **(B)**, IL-4 **(C)**, and IL-10 **(D)** cytokines by ELISPOT assays ($n = 6$). Splenocytes were isolated two weeks after the third immunization. The numbers of cytokine-positive cells were recorded as the mean SFU/1 $\times$ 10^6 splenocytes + SD. *$p < 0.05$; **$p < 0.01$.

both the EP5 and IM50 groups with the same body weight loss of 16% (**Figures 5B,C**). The survival rate in all pVAX1-D1ME-vaccinated groups was remarkably different from that in the control group ($p < 0.01$, **Figure 5C**). The results suggested that the immunization with 50 μg pVAX1-D1ME via EP could induce significantly effective protection against the DV1 challenge with a 100% survival rate and only mild clinical symptoms.

Determination of Optimum Immunization Times of pVAX1-D1ME

The above results indicated that 50 μg pVAX1-D1ME via EP could induce effective immune responses and protection after immunization with three doses. To further evaluate the cost-effectiveness of vaccination, mice were immunized with 50 μg pVAX1-D1ME via EP once, twice, and three times. As shown in **Figure 6A**, the end-point GMT of anti-DV1 IgG was 1:2,016 in the thrice-EP50 group, which was the highest compared to that in the once-EP50 group (1:356, $p < 0.01$) and twice-EP50 group (1:635, $p < 0.01$).

After challenge with a lethal dose of DV1, the most serious symptom was observed in the pVAX1 group, but relatively mild clinical signs were observed in three pVAX1-D1ME-vaccinated groups (**Figure 6B**). In the pVAX1 group, mice showed illness beginning at day 7, some mice still showed sequelae within 30 days (**Figure 6B**), and the most notable body weight loss was 22% (**Figure 6C**), which was the highest among the four groups ($p < 0.01$). Meanwhile, all the vaccinated mice started to show illness at day 9, followed by differential duration of disease with various body weight losses. The symptoms of the mice in the thrice-EP50 group were the mildest; the mice completely recovered within 21 days (**Figure 6B**), and the most notable body weight loss was only 6.1% (**Figure 6C**). The mice in the once-EP50 group and twice-EP50 group gradually recovered within 28 days and 26 days (**Figure 6B**), and the most marked body weight losses were 11.3 and 7.3%, respectively (**Figure 6C**).

The aforementioned results demonstrated that three doses of pVAX1-D1ME via EP significantly ameliorated the immune response and protection and were necessary for vaccination.

Humoral Immune Response and Protection Induced by the Bivalent Vaccine

To investigate the humoral immune response elicited by the bivalent vaccine, serum samples from the immunized mice were collected to analyze the specific IgG titers and NAb titers. After the final vaccination, both the DV1-specific and DV2-specific IgG levels (**Figure 7A**) and neutralizing activity (**Figure 7B**) in the B-EP group were significantly higher than those in the B-IM group. In the B-EP group, the end-point GMTs of anti-DV1 and anti-DV2 IgG were 1:1,056 and 1:1,425, respectively, which were almost two times higher than those in the B-IM group. Meanwhile, the GMTs of anti-DV1 and anti-DV2 NAbs in the B-EP group were 1:160 and 1:279, respectively, which were 3-fold higher than those obtained from the mice immunized via IM. The DV1-specific and DV2-specific IgG levels as well as the neutralizing activities within B-EP group did not show significant differences ($p > 0.05$), indicating a balanced immune response to DV1 and DV2 induced by the bivalent vaccine.

To evaluate the protective efficacy of the bivalent DNA vaccine, two weeks after the third vaccination, mice were challenged with a lethal dose of DV1 or DV2. After challenge with DV1, the most severe symptom was observed in the B-pVAX1 group, which started at day 7 and became progressively

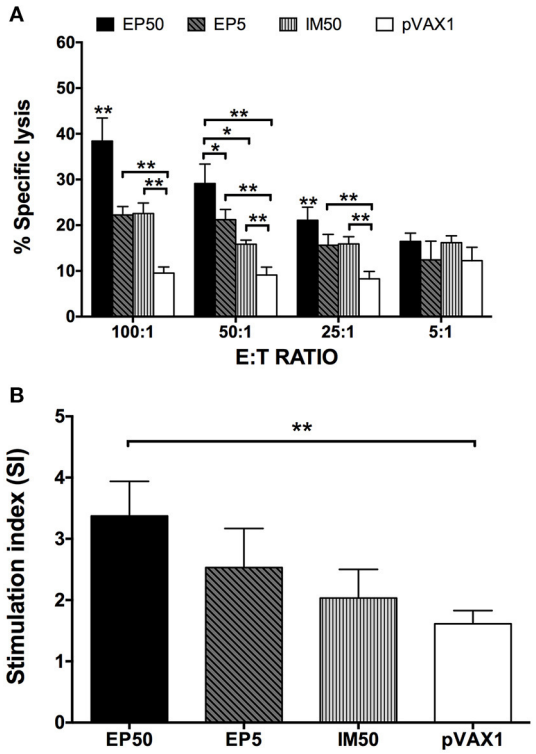

FIGURE 4 | DV1-specific cell-mediated immune responses in DNA-immunized mice. Splenocytes were isolated two weeks after the third immunization. **(A)** DV1-specific CTL response ($n = 6$). Percentages of specific lysis + SD were shown at different E:T ratios. **(B)** Lymphocyte proliferation measured with CCK-8 ($n = 6$). The results were recorded as the mean SI + SD. $^{*}p < 0.05$, $^{**}p < 0.01$.

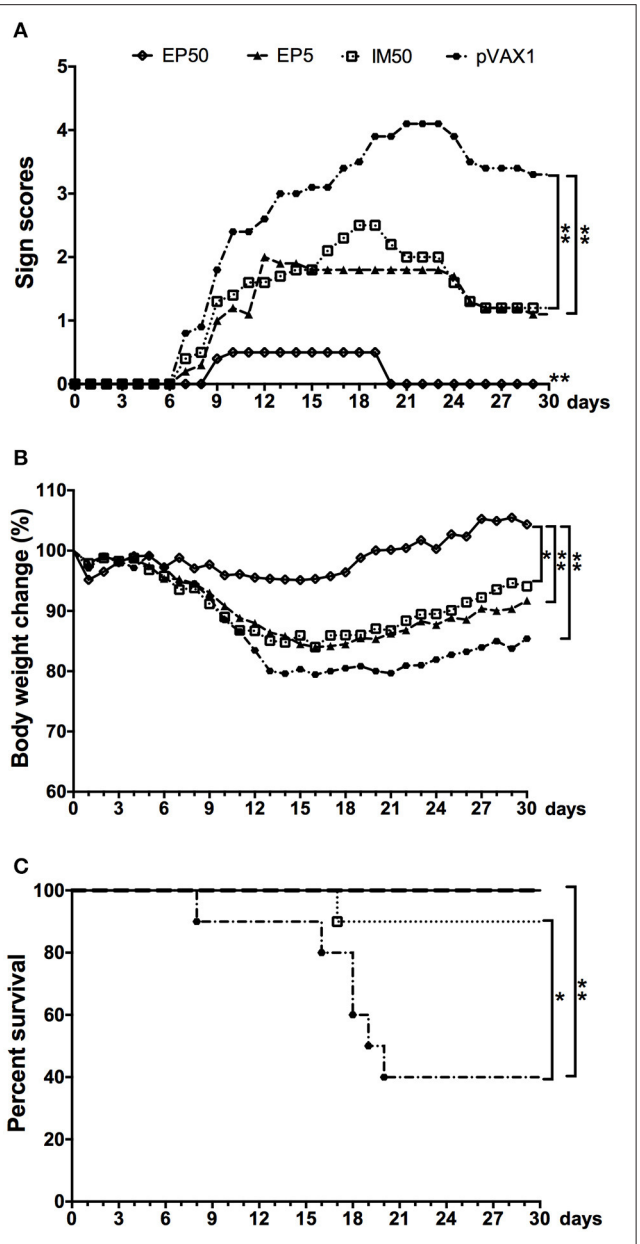

FIGURE 5 | Protective immunity elicited by the pVAX1-D1ME against DV1 infection ($n = 10$). (A) Pathological symptoms recorded as the mean sign scores. **(B)** The body weight reported as percentages compared to day 0. **(C)** The survival rate shown as the percentage of survivors. $^{*}p < 0.05$, $^{**}p < 0.01$.

worse (**Figure 8A**); the maximum body weight loss was 13.5% (**Figure 8B**). In the B-IM group, the symptoms started at day 10, and the mice completely recovered at day 22, with a maximum body weight loss of 8.4%. The mildest symptom was observed in the B-EP group, which began at day 11; all mice recovered absolutely at day 20 with only 5.3% maximum body weight loss. Similarly, after challenge with DV2, the B-pVAX1 group showed the most severe symptom, which began at day 7 and then became rapidly worse; all mice died till day 14 with a 33.4% body weight loss (**Figures 8C,D**). The mice in the B-IM group became sick at day 10; all mice died at day 18 with a 33.7% body weight loss. Meanwhile, the B-EP group showed the mildest symptom, which began at day 12; all mice survived, and the maximum body weight loss was only 5.4%. Importantly, there were no increased clinical signs observed in mice immunized with the bivalent vaccine after either DV1 or DV2 challenge, although there is theoretical risk of immune enhancement.

DISCUSSION

During the last 50 years, several groups have made concerted efforts in developing dengue vaccines, and significant progress has been made (Thomas and Endy, 2011; Guzman and Harris, 2015). The recombinant, live, attenuated, chimeric yellow-dengue tetravalent dengue vaccine (CYD-TDV, Dengvaxia) produced by Sanofi Pasteur is the most promising (Guy et al., 2015). CYD-TDV was structured using the backbone of the yellow fever 17D vaccine strain by replacing the *prM* and *E* genes with those of DV1-4 (Flipse and Smit, 2015). The most noticeable benefit of the vaccine was the large reduction in hospitalization of dengue by 67% to 80%, but vaccination-related side effects occur in children younger than 9 years old (Capeding et al.,

2014; Da Costa et al., 2014; Dorigatti et al., 2015; Villar et al., 2015). Although, the CYD-TDV has been recently registered in several countries, the United States still vigorously promoted the research of phase 3 clinical trials of the attenuated dengue vaccine developed by the NIH in Brazil (NIAID News Releases, 2016). Therefore, it is necessary to develop safer, more economical and effective DV vaccines.

DNA vaccines have been developed for decades with a number of potential advantages as mentioned above (Khan, 2013). However, as a novel methodology in the prevention of infectious diseases, DNA vaccination has not yet achieved much success in large animals, mainly due to the insufficient immunogenicity, and no licensed DNA vaccine is currently available in humans. Several technical improvements have been investigated, and EP is considered as one of the most promising delivery strategies and has been used in many non-human research and human clinical trials (Lu et al., 2008; Sardesai and Weiner, 2011). In Australia, a growth hormone-releasing hormone plasmid delivered by EP has been approved in the treatment of pigs (Person et al., 2008). In our recent studies, the DNA vaccine candidates inoculated using EP showed enhanced expression of the antigen in local sites, strong immune response and protective efficacy in mice, rabbits and pigs (Chen et al., 2016; Sheng et al., 2016). Thus, in the present study, we constructed the DNA vaccine candidate pVAX1-D1ME and explored *in vivo* EP for gene delivery in comparison with traditional IM injection in mice. Immunization with three doses of 50 μg pVAX1-D1ME via EP not only elicited a consistently higher IgG response and higher NAb titer but also generated higher specific CTL activity, a stronger lymphocyte proliferative response and higher levels of splenocyte-secreted IFN-γ, IL-2, and IL-4. Our results indicated that three doses of 50 μg pVAX1-D1ME via EP could induce both antibody- and cell-mediated immune responses in mice.

Although, there was no significant difference in survival rates among the EP50, EP5, and IM50 groups in the protection test (**Figure 5**), the severity of clinical signs was different. The EP50 group only had transient mild illness with unchanged body weight, while the EP5 and IM50 groups showed moderate illness with 16% of body weight loss. This result was much better than that observed in our previous study (Zheng et al., 2011). In the latter, although the same survival rate could be achieved by 100 μg of the DNA pCAG/DV1/E (expressing the prM and E proteins of DV1) inoculated by IM without EP, immunized mice showed obvious illness. EP delivery only requires one-tenth of the DNA dose used in IM injection but enhances plasmid delivery by 100–1,000-fold; gene expression then induces a more effective immune response (Wang et al., 2014). Therefore, in combination with humoral and cellular responses, the results suggests that *in vivo* EP with a suitable plasmid dose is a promising strategy for DV DNA vaccination, and three immunizations at 50 μg pVAX1-D1ME are necessary for inducing effective immune response and protection. A recent report by Prompetchara et al. demonstrated that a tetravalent prME DNA vaccine candidate administered by EP could induce high levels of NAb against all DV serotypes (Prompetchara et al., 2014), which supports our results and suggests that EP is an important method for further developing a tetravalent vaccine.

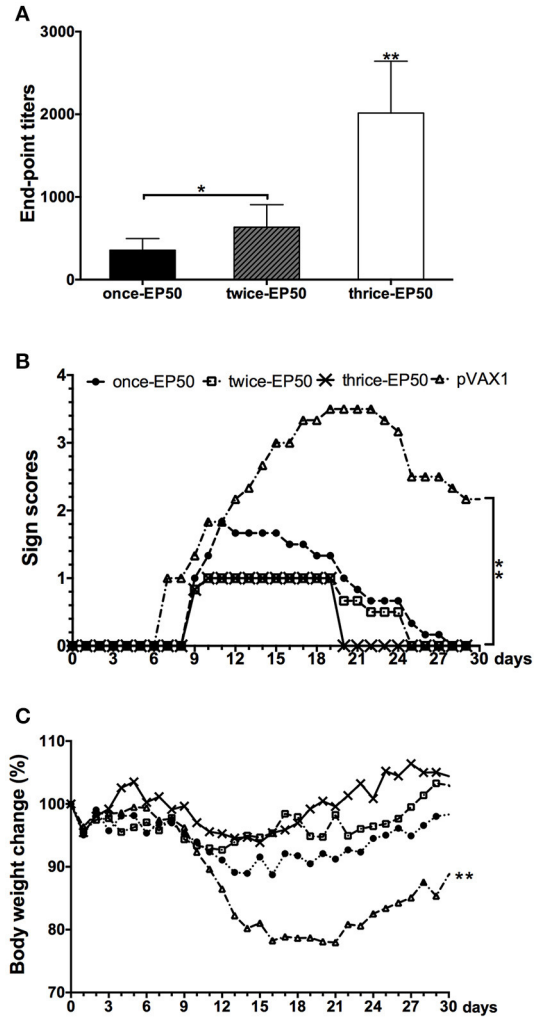

FIGURE 6 | End-point titers of anti-DV1 antibodies and protect immunity elicited by the pVAX1-D1ME under different times of vaccination ($n = 6$). (A) End-point titers of anti-DV1 antibodies. **(B)** Pathological symptoms recorded as the mean sign scores. **(C)** Body weight calculated as percentages compared with day 0. $^*p < 0.05$, $^{**}p < 0.01$.

Ideal multivalent dengue vaccines should induce a balanced immune response to all DV serotypes. In this study, the immune response and protection induced by the bivalent vaccine against DV1 and DV2 were preliminarily evaluated in mice. We found that immunization via EP could induce similar levels of anti-DV1 and anti-DV2 IgG antibodies as well as NAb titers, indicating balanced humoral immune responses to two serotypes. Notably, immunization with the bivalent vaccine could reduce illness severity and body weight loss, indicating a protective effect. However, the results against challenge with DV1 showed some differences from cases of challenge with DV2. The B-EP and B-IM groups showed similar results in reducing severity of illness and limiting body weight loss against DV1. After DV2 challenge, only the B-EP group exhibited protection compared with the B-IM and control groups. This result was consistent with our recent study, in which the pVAX1-D2ME via IM failed to provide

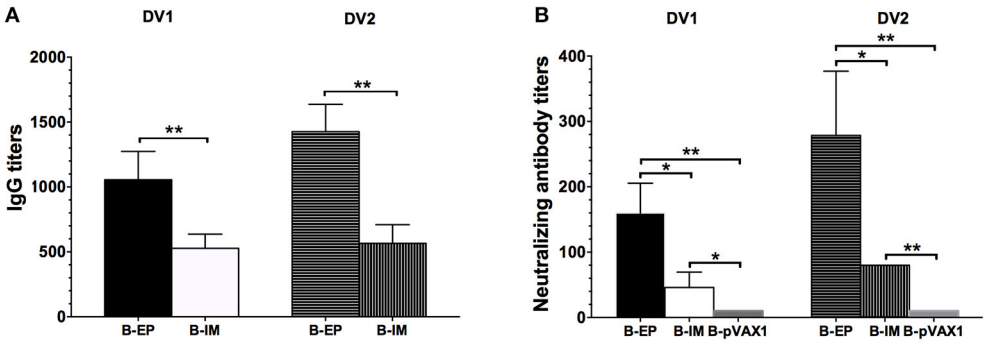

FIGURE 7 | DV1- and DV2-specific antibody responses in mice immunized with the bivalent vaccine ($n = 5$). Sera were collected two weeks after the third immunization. **(A)** End-point titers of anti-DV1 and anti-DV2 IgG assayed by ELISA. The results were recorded as GMT + SD. **(B)** End-point titers of anti-DV1 and anti-DV2 NAb assayed by $PRNT_{50}$. The results were recorded as GMT + SD. $^{*}p < 0.05$, $^{**}p < 0.01$.

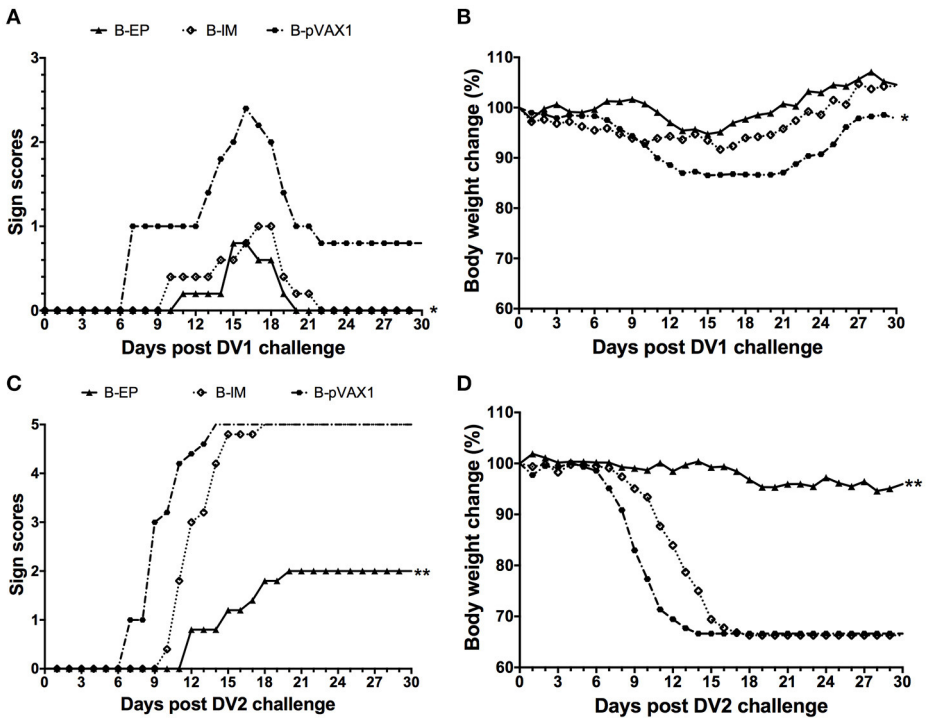

FIGURE 8 | Protective immunity elicited by the bivalent DNA vaccine against DV1 and DV2 infection ($n = 5$). (A,C) Pathological symptoms recorded as the mean sign scores. **(B,D)** The body weight reported as percentages compared to day 0. $^{*}p < 0.05$, $^{**}p < 0.01$.

full protection (Chen et al., 2016). The symptoms were not aggravated in the mice immunized with the bivalent vaccine via EP after challenge with DV1 or DV2, and 33% of body weight loss after DV2 challenge was similar with those in the monovalent DV2 vaccine-immunized mice (Chen et al., 2016), meaning no ADE occurred. In combination with the results in our previous study, the effectiveness of the pVAX1-D1ME vaccine candidate is mainly attributed to the suitable immunogen and EP delivery system. Meanwhile, it was noted that the end-point titers of anti-DV1 and anti-DV2 in the bivalent vaccine-immunized mice were lower than those in the monovalent vaccine-immunized mice, indicating interference between the DV1 and DV2 vaccine candidates. This evidence should be considered in further research on DV tetravalent vaccine. It has been reported that dose adjustment, multisite vaccination, and immunologic priming against DV and other flaviviruses might reduce interference in DV vaccines (Anderson et al., 2011).

In summary, this study demonstrated that administration with three doses of 50 μg pVAX1-D1ME via EP induced persistent humoral and cellular immune responses and effectively protected mice against lethal DV1 challenge. Immunization with the bivalent vaccine via EP generated

balanced antibody responses and protection against DV1 and DV2 without increased clinical signs. Our results suggest a promising method for developing a DV tetravalent DNA vaccine.

AUTHOR CONTRIBUTIONS

XZ: Performed research, analyzed data, and wrote paper. HC: Designed research, analyzed data, and revised paper. RW: Helped with experiment and analyzed data. DF, KF and NG: Helped with experiment. JA: Designed research and revised paper. All authors have read the manuscript and approved its submission. XZ and HC have equal contribution to this work (Co-first authors).

FUNDING

We acknowledge the financial support by the National Natural Science Foundation of China (81372935, 81271839, 81671971, 81471957, and U1602223).

REFERENCES

Anderson, K. B., Gibbons, R. V., Edelman, R., Eckels, K. H., Putnak, R. J., Innis, B. L., et al. (2011). Interference and facilitation between dengue serotypes in a tetravalent live dengue virus vaccine candidate. *J. Infect. Dis.* 204, 442–450. doi: 10.1093/infdis/jir279

Arima, Y., Chiew, M., and Matsui, T. (2015). Epidemiological update on the dengue situation in the Western Pacific Region, (2012). *West. Pac. Surveill. Response J.* 6, 82–89. doi: 10.5365/wpsar.2014.5.4.002

Bhatt, S., Gething, P. W., Brady, O. J., Messina, J. P., Farlow, A. W., Moyes, C. L., et al. (2013). The global distribution and burden of dengue. *Nature* 496, 504–507. doi: 10.1038/nature12060

Bray, M., and Lai, C.-J. (1991). Dengue virus premembrane and membrane proteins elicit a protective immune response. *Virology* 185, 505–508. doi: 10.1016/0042-6822(91)90809-P

Capeding, M. R., Tran, N. H., Hadinegoro, S. R., Ismail, H. I., Chotpitayasunondh, T., Chua, M. N., et al. (2014). Clinical efficacy and safety of a novel tetravalent dengue vaccine in healthy children in Asia: a phase 3, randomised, observer-masked, placebo-controlled trial. *Lancet* 384, 1358–1365. doi: 10.1016/S0140-6736(14)61060-6

Chen, H., Zheng, X., Wang, R., Gao, N., Sheng, Z., Fan, D., et al. (2016). Immunization with electroporation enhances the protective effect of a DNA vaccine candidate expressing prME antigen against dengue virus serotype 2 infection. *Clin. Immunol.* 171, 41–49. doi: 10.1016/j.clim.2016.08.021

Cummings, D. A., Schwartz, I. B., Billings, L., Shaw, L. B., and Burke, D. S. (2005). Dynamic effects of antibody-dependent enhancement on the fitness of viruses. *Proc. Natl. Acad. Sci. U.S.A.* 102, 15259–15264. doi: 10.1073/pnas.0507320102

Da Costa, V. G., Marques-Silva, A. C., Floriano, V. G., and Moreli, M. L. (2014). Safety, immunogenicity and efficacy of a recombinant tetravalent dengue vaccine: a meta-analysis of randomized trials. *Vaccine* 32, 4885–4892. doi: 10.1016/j.vaccine.2014.07.008

Dorigatti, I., Aguas, R., Donnelly, C. A., Guy, B., Coudeville, L., Jackson, N., et al. (2015). Modelling the immunological response to a tetravalent dengue vaccine from multiple phase-2 trials in Latin America and South East Asia. *Vaccine* 33, 3746–3751. doi: 10.1016/j.vaccine.2015.05.059

Flipse, J., and Smit, J. M. (2015). The complexity of a dengue vaccine: a review of the human antibody response. *PLoS Negl. Trop. Dis.* 9:e0003749. doi: 10.1371/journal.pntd.0003749

Guy, B., Briand, O., Lang, J., Saville, M., and Jackson, N. (2015). Development of the Sanofi Pasteur tetravalent dengue vaccine: one more step forward. *Vaccine* 33, 7100–7111. doi: 10.1016/j.vaccine.2015.09.108

Guzman, M. G., and Harris, E. (2015). Dengue. *Lancet* 385, 453–465. doi: 10.1016/S0140-6736(14)60572-9

Hermann, L. L., Gupta, S. B., Manoff, S. B., Kalayanarooj, S., Gibbons, R. V., and Coller, B. A. (2015). Advances in the understanding, management, and prevention of dengue. *J. Clin. Virol.* 64, 153–159. doi: 10.1016/j.jcv.2014.08.031

Huang, L., Luo, X., Shao, J., Yan, H., Qiu, Y., Ke, P., et al. (2016). Epidemiology and characteristics of the dengue outbreak in Guangdong, Southern China, in 2014. *Eur. J. Clin. Microbiol. Infect. Dis.* 35, 269–277. doi: 10.1007/s10096-015-2540-5

Khan, K. H. (2013). DNA vaccines: roles against diseases. *Germs* 3, 26–35. doi: 10.11599/germs.2013.1034

Lin, Y. P., Luo, Y., Chen, Y., Lamers, M. M., Zhou, Q., Yang, X. H., et al. (2016). Clinical and epidemiological features of the 2014 large-scale dengue outbreak in Guangzhou city, China. *BMC Infect. Dis.* 16:102. doi: 10.1186/s12879-016-1379-4

Lu, S., Wang, S., and Grimes-Serrano, J. M. (2008). Current progress of DNA vaccine studies in humans. *Expert Rev. Vaccines* 7, 175–191. doi: 10.1586/14760584.7.2.175

Lu, H., Xu, X. F., Gao, N., Fan, D. Y., Wang, J., and An, J. (2013). Preliminary evaluation of DNA vaccine candidates encoding dengue-2 prM/E and NS1: their immunity and protective efficacy in mice. *Mol. Immunol.* 54, 109–114. doi: 10.1016/j.molimm.2012.11.007

NIAID News Releases (2016). *Dengue Vaccine Enters Phase 3 Trial in Brazil.* Available online at: https://www.nih.gov/news-events/news-releases/dengue-vaccine-enters-phase-3-trial-brazil

Person, R., Bodles-Brakhop, A. M., Pope, M. A., Brown, P. A., Khan, A. S., and Draghia-Akli, R. (2008). Growth hormone-releasing hormone plasmid treatment by electroporation decreases offspring mortality over three pregnancies. *Mol. Ther.* 16, 1891–1897. doi: 10.1038/mt.2008.178

Porter, K. R., and Raviprakash, K. (2015). Nucleic acid (DNA) immunization as a platform for dengue vaccine development. *Vaccine* 33, 7135–7140. doi: 10.1016/j.vaccine.2015.09.102

Prompetchara, E., Ketloy, C., Keelapang, P., Sittisombut, N., and Ruxrungtham, K. (2014). Induction of neutralizing antibody response against four dengue viruses in mice by intramuscular electroporation of tetravalent DNA vaccines. *PLoS ONE* 9:e92643. doi: 10.1371/journal.pone.0092643

Ren, H., Ning, W., Lu, L., Zhuang, D., and Liu, Q. (2015). Characterization of dengue epidemics in mainland China over the past decade. *J. Infect. Dev. Ctries.* 9, 970–976. doi: 10.3855/jidc.5998

Rogers, D. J. (2015). Dengue: recent past and future threats. *Philos. Trans. R. Soc. Lond. B. Biol. Sci.* 370:20130562. doi: 10.1098/rstb.2013.0562

Sardesai, N. Y., and Weiner, D. B. (2011). Electroporation delivery of DNA vaccines: prospects for success. *Curr. Opin. Immunol.* 23, 421–429. doi: 10.1016/j.coi.2011.03.008

Sheng, Z., Gao, N., Cui, X., Fan, D., Chen, H., Wu, N., et al. (2016). Electroporation enhances protective immune response of a DNA vaccine against Japanese encephalitis in mice and pigs. *Vaccine* 34, 5751–5757. doi: 10.1016/j.vaccine.2016.10.001

Shepard, D. S., Undurraga, E. A., Halasa, Y. A., and Stanaway, J. D. (2016). The global economic burden of dengue: a systematic analysis. *Lancet Infect. Dis.* 16, 935–941. doi: 10.1016/S1473-3099(16)00146-8

Thomas, S. J., and Endy, T. P. (2011). Critical issues in dengue vaccine development. *Curr. Opin. Infect. Dis.* 24, 442–450. doi: 10.1097/QCO.0b013e32834a1b0b

Villar, L., Dayan, G. H., Arredondo-Garcia, J. L., Rivera, D. M., Cunha, R., Deseda, C., et al. (2015). Efficacy of a tetravalent dengue vaccine in children in Latin America. *N. Engl. J. Med.* 372, 113–123. doi: 10.1056/NEJMoa1411037

Wang, Q., Jiang, W., Chen, Y., Liu, P., Sheng, C., Chen, S., et al. (2014). *In vivo* electroporation of minicircle DNA as a novel method of vaccine delivery to enhance HIV-1-specific immune responses. *J. Virol.* 88, 1924–1934. doi: 10.1128/JVI.02757-13

WHO (2012). *Global Strategy for Dengue Prevention and Control, 2012–2020*. Geneva: World Health Organization.

Wu, J. Y., Lun, Z. R., James, A. A., and Chen, X. G. (2010). Dengue fever in mainland China. *Am. J. Trop. Med. Hyg.* 83, 664–671. doi: 10.4269/ajtmh.2010.09-0755

Zhang, H., Zhang, Y., Hamoudi, R., Yan, G., Chen, X., and Zhou, Y. (2014). Spatiotemporal characterizations of dengue virus in mainland China: insights into the whole genome from 1978 to 2011. *PLoS ONE* 9:e87630. doi: 10.1371/journal.pone.0087630

Zhao, H., Zhang, F. C., Zhu, Q., Wang, J., Hong, W. X., Zhao, L. Z., et al. (2016). Epidemiological and virological characterizations of the 2014 dengue outbreak in Guangzhou, China. *PLoS ONE* 11:e0156548. doi: 10.1371/journal.pone.0156548

Zheng, Q., Fan, D., Gao, N., Chen, H., Wang, J., Ming, Y., et al. (2011). Evaluation of a DNA vaccine candidate expressing prM-E-NS1 antigens of dengue virus serotype 1 with or without granulocyte-macrophage colony-stimulating factor (GM-CSF) in immunogenicity and protection. *Vaccine* 29, 763–771. doi: 10.1016/j.vaccine.2010.11.014

Conflict of Interest Statement: The authors declare that the research was conducted in the absence of any commercial or financial relationships that could be construed as a potential conflict of interest.

frontiers in Cellular and Infection Microbiology

ORIGINAL RESEARCH
published: 12 July 2017
doi: 10.3389/fcimb.2017.00317

Global Epidemiology of Dengue Outbreaks in 1990–2015: A Systematic Review and Meta-Analysis

Congcong Guo[1], Zixing Zhou[1], Zihao Wen[1], Yumei Liu[1,2], Chengli Zeng[1], Di Xiao[1], Meiling Ou[1,2], Yajing Han[1,2], Shiqi Huang[1], Dandan Liu[1], Xiaohong Ye[1,2], Xiaoqian Zou[1,2], Jing Wu[1,2], Huanyu Wang[3,4], Eddy Y. Zeng[5], Chunxia Jing[1,5] and Guang Yang[2,5]**

[1] Department of Epidemiology, School of Medicine, Jinan University, Guangzhou, China, [2] Department of Parasitology, School of Medicine, Jinan University, Guangzhou, China, [3] Department of Viral Encephalitis, Chinese Center for Disease Control and Prevention, Institute for Viral Disease Control and Prevention, National Institute for Viral Disease Control and Prevention, Beijing, China, [4] State Key Laboratory for Infectious Disease Prevention and Control, Chinese Center for Disease Control and Prevention, Beijing, China, [5] Guangzhou Key Laboratory of Environmental Exposure and Health, Guangdong Key Laboratory of Environmental Pollution and Health, School of Environment, Jinan University, Guangzhou, China

OPEN ACCESS

Edited by:
Penghua Wang,
New York Medical College,
United States

Reviewed by:
Jianfeng Dai,
Soochow University, China
Fengwei Bai,
University of Southern Mississippi,
United States
Manoj N. Krishnan,
National University of Singapore,
Singapore

***Correspondence:**
Chunxia Jing
jcxphd@gmail.com
Guang Yang
guangyangphd@gmail.com

Received: 25 April 2017
Accepted: 27 June 2017
Published: 12 July 2017

Citation:
Guo C, Zhou Z, Wen Z, Liu Y, Zeng C, Xiao D, Ou M, Han Y, Huang S, Liu D, Ye X, Zou X, Wu J, Wang H, Zeng EY, Jing C and Yang G (2017) Global Epidemiology of Dengue Outbreaks in 1990–2015: A Systematic Review and Meta-Analysis.
Front. Cell. Infect. Microbiol. 7:317.
doi: 10.3389/fcimb.2017.00317

Dengue is an arthropod-borne infectious disease caused by dengue virus (DENV) infection and transmitted by *Aedes* mosquitoes. Approximately 50–100 million people are infected with DENV each year, resulting in a high economic burden on both governments and individuals. Here, we conducted a systematic review and meta-analysis to summarize information regarding the epidemiology, clinical characteristics, and serotype distribution and risk factors for global dengue outbreaks occurring from 1990 to 2015. We searched the PubMed, Embase and Web of Science databases through December 2016 using the term "dengue outbreak." In total, 3,853 studies were identified, of which 243 studies describing 262 dengue outbreaks met our inclusion criteria. The majority of outbreak-associated dengue cases were reported in the Western Pacific Region, particularly after the year 2010; these cases were primarily identified in China, Singapore and Malaysia. The pooled mean age of dengue-infected individuals was 30.1 years; of the included patients, 54.5% were male, 23.2% had DHF, 62.0% had secondary infections, and 1.3% died. The mean age of dengue patients reported after 2010 was older than that of patients reported before 2010 (34.0 vs. 27.2 years); however, the proportions of patients who had DHF, had secondary infections and died significantly decreased after 2010. Fever, malaise, headache, and asthenia were the most frequently reported clinical symptoms and signs among dengue patients. In addition, among the identified clinical symptoms and signs, positive tourniquet test ($OR = 4.86$), ascites ($OR = 13.91$) and shock ($OR = 308.09$) were identified as the best predictors of dengue infection, DHF and mortality, respectively (both $P < 0.05$). The main risk factors for dengue infection, DHF and mortality were living with uncovered water container ($OR = 1.65$), suffering from

hypotension ($OR = 6.18$) and suffering from diabetes mellitus ($OR = 2.53$), respectively (all $P < 0.05$). The serotype distribution varied with time and across WHO regions. Overall, co-infections were reported in 47.7% of the evaluated outbreaks, and the highest pooled mortality rate (2.0%) was identified in DENV-2 dominated outbreaks. Our study emphasizes the necessity of implementing programs focused on targeted prevention, early identification, and effective treatment.

Keywords: dengue, outbreak, epidemiology, clinical characteristic, risk factor, serotype, systematic review, meat-analysis

INTRODUCTION

Only 9 countries had experienced severe dengue epidemics before 1970; however, at present, dengue fever has affected more than 100 countries in tropical and subtropical regions (Organization, 2016). It was estimated by WHO that 50–100 million dengue infections occur annually, with a 30-fold increase in global incidence observed over the past 50 years (WHO, 2012). Today, dengue virus (DENV) poses a major threat to global public health, and approximately two-fifths of the world's population is at risk of dengue infection (Lancet, 2013; Screaton et al., 2015).

Since the first dengue outbreak was reported in 1779 in Jakarta, Indonesia (Wu et al., 2011), this disease has become a public health threat that is associated with remarkable morbidity and mortality. The case fatality rate in untreated dengue patients has been reported to reach 20%, but this rate can be reduced to less than 1% under expert clinical management and with careful fluid replacement (Simmons et al., 2012). The number of dengue outbreaks caused by the four dengue virus serotypes (DENV-1 to DENV-4) has increased since 1980, mainly affecting Asia, South America and the Caribbean (Jansen and Beebe, 2010; Amarasinghe et al., 2011). The various serotypes of the DENV are transmitted predominantly by the mosquito vector, *Aedes aegypti* (Guzman and Harris, 2015); however, DENV can also be transmitted by other species of the genus *Aedes,* including *Aedes albopictus* (Barcelos, 2014). While most dengue patients recover after experiencing self-limiting illness, a small proportion progress to dengue hemorrhagic fever (DHF) (WHO/TDR, 2009). DHF may be classified into four severity grades, with grades III and IV being defined as dengue shock syndrome (DSS) (WHO/TDR, 2009). Although the characteristics of dengue infection have been well described, previous studies have mainly focused on the descriptions of single outbreaks, and few of studies have concentrated on systematically summarizing the epidemiological characteristics of dengue outbreaks worldwide. In this situation, it may difficult to keep abreast of the trends of global dengue outbreaks.

At present, little attention has been specifically paid to summarizing global dengue outbreaks. We performed a robust systematic analysis of all available data to gain a better understanding of the global epidemiology, clinical manifestations, and serotype distribution and risk factors for dengue outbreaks.

MATERIALS AND METHODS

Searching Strategy and Selection Criteria

We searched the PubMed, Embase and Web of Science databases to identify articles describing dengue outbreaks that occurred between Jan 1, 1990 to Dec 1, 2016 (**Figure 1**). The following search terms were used as a text word in each database: PubMed, "dengue outbreak" in all fields; limited to human studies; Embase, "dengue outbreak" in all fields; limited to human studies; and Web of Science, "dengue outbreak" in the topic field with the exclusion of veterinary studies. Two independent reviewers (C.C.G and Z.X.Z) screened the titles and abstracts of all related manuscripts, searched reference lists of the identified studies and obtained full texts for potentially relevant articles. Studies without any dengue outbreak data available, that described outbreaks including less than 5 dengue patients or that did not focus on a specific dengue outbreak were excluded. When different articles described the same outbreak but provided different data, all studies were included.

Data Extraction

The following data were independently extracted from each included study by two investigators (C.C.G and Z.X.Z): author, year of publication, year of outbreak, WHO region, country, city, mosquito species, patient characteristics (including demographic characteristics, risk factors, clinical symptoms and number of secondary cases), dengue serotype, number of patients (including DF, DHF, and DSS patients), and number of deaths. Any disagreements were adjudicated by a senior investigator (C.X.J).

Analysis

We described the epidemiology, clinical manifestations, risk factors and serotype distribution using the number of studies and cases, which are expressed as proportions with 95% CIs for categorical variables (sex, dengue case classification, primary or secondary infection, signs, symptoms and mortality) and means and corresponding 95% CIs for continuous variables (age). We compared the epidemiologic characteristics of dengue outbreaks occurring before 2010 and after 2010 (including 2010) using two-proportion z-tests for categorical variables and Student's *t*-tests for continuous variables. Meta-analyses were performed using Comprehensive Meta-Analysis version 2.2.064 software (Biostat Inc., NJ, USA). We assessed the level of heterogeneity across studies using P_h and I^2 (Higgins and Thompson, 2002). If a P_h-value was greater than 0.10, a fixed-effects model was used; otherwise, a random-effects model was selected (Handoll,

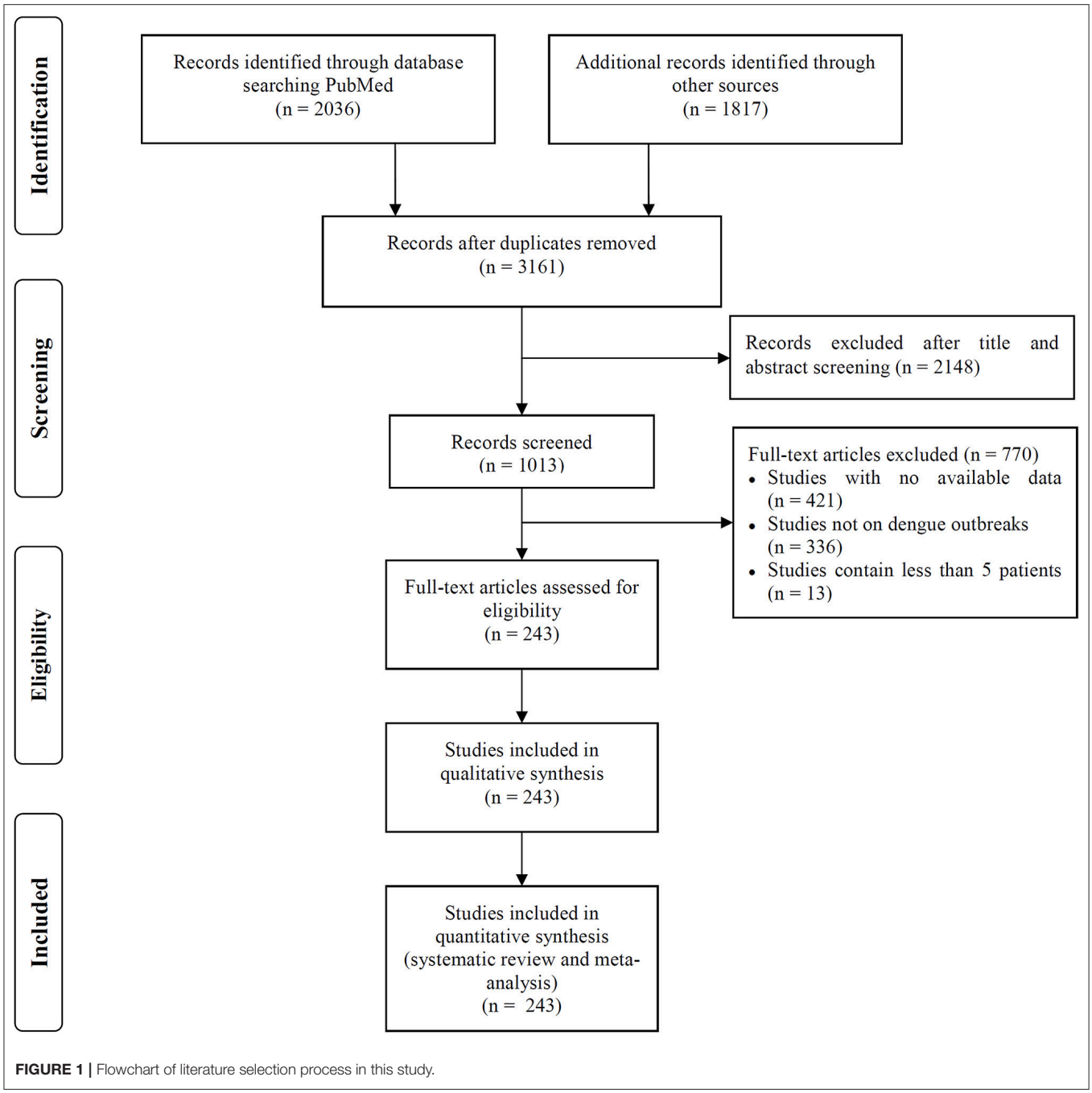

FIGURE 1 | Flowchart of literature selection process in this study.

2006). The meta-analysis corresponded with recommendations from the Preferred Reporting Items for Systematic Reviews and Meta-Analyses (PRISMA) statement (Supplementary File S2). Medians (ranges) were converted to means (SDs) using previously proposed formulas (Hozo et al., 2005). Distribution maps for global dengue outbreaks and serotypes were generated in R software, version 3.3.1 (R Core Team, Vienna, Austria), using ggplot2, maps, mapproj and sp packages. The correlations between the rates of mortality, DHF, and secondary infections were assessed by generating Spearman correlation coefficients.

RESULTS

Systematic Review

We included 243 articles describing 262 dengue outbreaks that occurred between 1990 and 2015 (**Figure 1**, Supplementary Table 1, Supplementary File S1). One hundred and twelve outbreaks described in 104 articles occurred after 2010. Among countries worldwide, the highest numbers of outbreak (58/262) are observed in India, followed by China (38/262) and Brazil (24/262) from 1990 to 2015. All the outbreaks occurred in

tropical (77/262) and subtropical (174/262) regions, except for one outbreak, which occurred in Nîmes, 2015 (Succo et al., 2016), and was considered the first considerable dengue outbreak in mainland France (**Figure 2**). Among the six WHO regions, the largest number of outbreaks occurred in the Southeast Asia region (82/262), followed by the Western Pacific region (72/262) and the American region (65/262), accounting for more than 83.6% of outbreaks overall. The European region (6/262) was least affected by dengue outbreaks, with only 4 outbreaks reported in France (three in overseas departments and regions of France and one in mainland France) and 2 outbreaks reported in Portugal. However, the Western Pacific Region had most dengue outbreaks reported after 2010 (Western Pacific: 33/112 > Southeast Asia: 27/112 > Americas: 24/112 > Eastern Mediterranean: 13/112 > Africa: 11/112 > Europe: 4/112).

Epidemiology

By the end of 2016, a total of 291,964 outbreak-associated dengue cases had been reported in the literature, mainly from China (27.9%), Singapore (27.0%) and Malaysia (15.1%). The majority (72.4%) of dengue patients were reported in the Western Pacific region, followed by the American region (19.4%), Southeast Asia Region (4.8%), Eastern Mediterranean region (1.5%), European region (1.5%) and African region (0.3%). Outbreaks occurring before 2010 (Americas > Western Pacific > South East Asia > Eastern Mediterranean > Europe > Africa) accounted for 28.6% of the total number of cases, the majority of which were reported in Cuba (28.1%), Singapore (19.3%) and Puerto Rico (13.4%), while patients in outbreaks after 2010 (Western Pacific > Americas > South East Asia > Europe > Eastern Mediterranean > Africa) were mainly from China (36.8%), Singapore (30.1%), and Malaysia (20.9%). 50.0% outbreaks occurred in urban areas (21/42), 28.6% in rural areas (12/42) and 21.4% in both urban and rural areas (9/42). It is important to note that nearly all rural outbreaks occurred after 2000 (except one in Malaysia, 1999; Cheah et al., 2006). It is consistent with the view that dengue once confined to urban areas has penetrated into the rural setup (Ishak et al., 1997). The improved road systems, better socio-economic situations and established agricultural settlements in rural areas may increase the Ae. albopictus population, and thus spread of rural dengue fever among the rural communities (Chang et al., 1997).

The pooled mean age of the patients was 30.1 years, and 54.5% were male (**Table 1**, Supplementary Table 2). The results of the meta-analyses indicated there to be significant associations between dengue infection and two variables: male gender (OR: 1.10, 95% CI: 1.01–1.20) and living with uncovered water container (OR: 1.65, 95% CI: 1.15–2.37) (**Figure 3**, Supplementary Table 3). The pooled rate of DHF was 23.2%; secondary infection (OR: 1.86, 95% CI: 1.46–2.37), diabetes mellitus (OR: 2.31, 95% CI: 1.58–3.38), hypotension (OR: 6.18, 95% CI: 1.61–23.71) and renal insufficiency (OR: 5.26, 95% CI: 1.77–15.64) were at increased odds of DHF (**Figure 3**, Supplementary Table 4). The rate of secondary infections among dengue patients was 62.0% in the meta-analysis of the 35 studies reporting these data; patients with a platelet count $< 100 \times 10^9$/L had increased odds of secondary infection (OR: 4.11, 95% CI: 1.64–10.31) (Supplementary Table 5). In addition, the pooled rate of mortality derived from the 72 studies reporting this outcome was 1.3%; patients with underlying diseases, such as diabetes

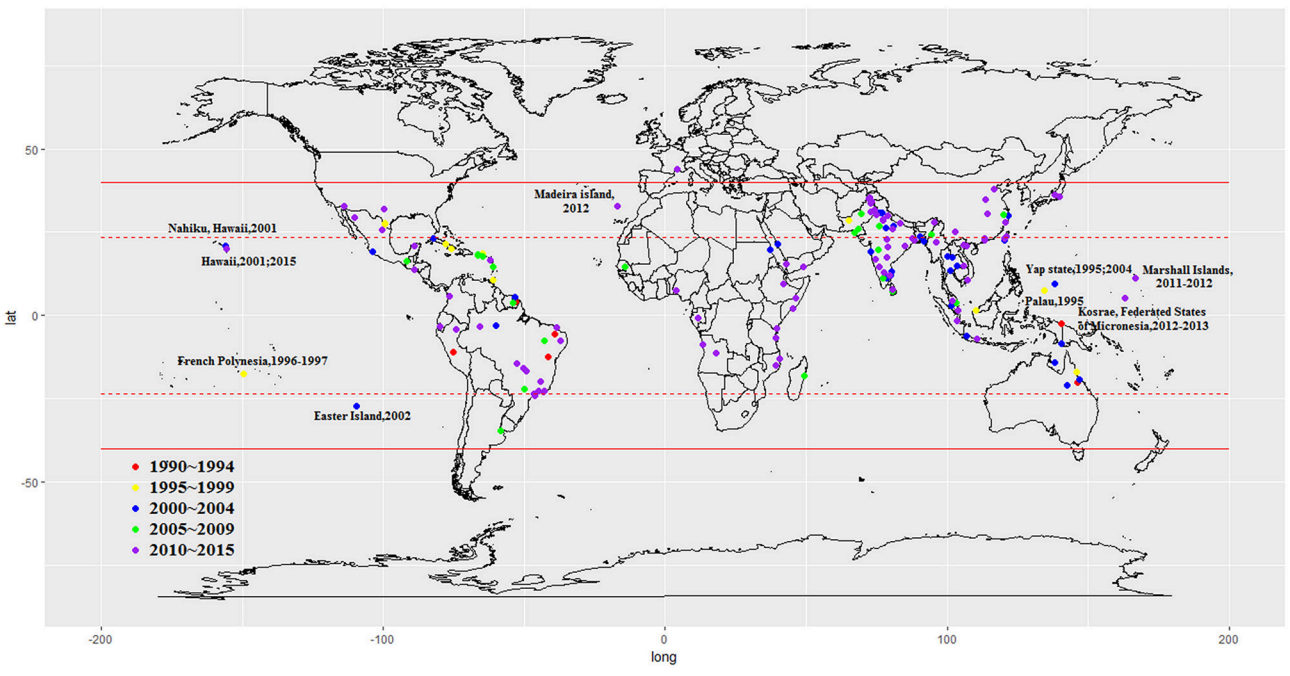

FIGURE 2 | Global dengue outbreaks distribution from 1990–2015.

mellitus (OR: 2.53, 95% CI: 1.51–4.24) and hypertension (OR: 2.36, 95% CI: 1.37–4.07) were at increased odds of mortality (**Figure 3**, Supplementary Table 6).

Patient age distributions, DHF rates, secondary infection rates and mortality rates differed significantly between outbreaks occurring before the year 2010 and occurring after 2010 (**Table 1**). Dengue patients identified in association with outbreaks occurring after 2010 were significantly older than those identified in association with outbreaks occurring before 2010 (mean, 95% CI: 34.0, 30.1–38.0 vs. 27.2, 24.5–30.0; $P = 0.006$). The rates of DHF, secondary infection and mortality significantly decreased after 2010 (all $P < 0.001$). No significant gender difference was identified between these two time periods ($P = 0.194$). The rate of DHF and rate of mortality observed in the included dengue outbreaks were significantly correlated, with an overall Spearman correlation coefficient of 0.64 ($P < 0.001$). However, no significant correlation was observed between the rate of secondary infection and the rate of mortality ($P = 0.223$).

TABLE 1 | Epidemiologic factors of dengue patients in global outbreaks.

Variables	No. studies meta-analyzed	Meta-analysis, pooled data (95% CI)*	*P* value
Mean age	96	30.1 (27.7–32.5)	0.006
Before 2010	55	27.2 (24.5–30.0)	
After 2010	41	34.0 (30.1–38.0)	
Male (%)	146	54.5 (53.2–55.7)	0.194
Before 2010	83	54.7 (52.6–56.7)	
After 2010	63	54.3 (52.5–56.0)	
DHF (%)	107	23.2 (18.3–29.0)	<0.001
Before 2010[a]	85	18.8 (14.3–24.3)	
After 2010[a]	22	15.7 (7.6–29.6)	
Secondary infection (%)	35	62.0 (53.5–69.8)	<0.001
Before 2010	20	66.7 (55.1–76.6)	
After 2010	15	55.9 (43.8–67.3)	
Fatal cases (%)	72	1.3 (0.9–2.0)	<0.001
Before 2010	46	1.9 (1.2–2.9)	
After 2010	26	0.7 (0.3–1.8)	

**Random-effects model unless otherwise specified.*

[a]Removed articles contained all DHF patients; P-value, two-proportion z-test for categorical factors and Student's t-test for continuous factors.

Clinical Symptoms and Signs

Fever was the most commonly observed clinical symptom or sign (pooled proportion: 98.1, 95% CI: 97.2–98.7%), followed by malaise (76.0, 95% CI: 64.1–84.9%), headache (75.7, 95% CI: 69.5–81.0%) and asthenia (74.3, 95% CI: 45.8–90.8%), which are listed in **Table 2** (Supplementary Table 7). Hemorrhagic manifestations were observed in 25.8% (95% CI: 21.0–31.1%) of the patients, of which petechiae (22.3, 95% CI: 16.5–29.3%) was the most common.

The rates of myalgia, chill, rash, eye/retro-orbital pain, petechiae, exanthema, lethargy, lymphadenopathy, thrombocytopenia, leukopenia, conjunctival injection, and positive tourniquet test results were significantly greater in the dengue-infected group than the laboratory negative group (all $P < 0.05$). On the other hand, since most of the laboratory negative patients were infected with influenza, those patients more frequently suffered from sore throat, nasal congestion and cough than did dengue-infected patients (all $P < 0.05$) (**Figure 4**, Supplementary Table 3).

Blood manifestations (OR: 9.57, 95% CI: 4.78–19.15), pleural effusion (OR: 12.44, 95% CI: 7.07–21.91), ascites (OR: 13.91, 95% CI: 8.03–24.11) and morality (OR: 11.46, 95% CI: 4.16–31.56) were more common in DHF patients than DF patients, and other symptom and sign comparisons are shown in **Figure 4**, Supplementary Table 4. However, body-ache (OR: 0.60, 95% CI: 0.36–0.99) was identified significantly less frequently in DHF patients than DF patients.

Patients with shock symptom were at significantly increased odds of mortality (OR: 308.09, 95% CI: 42.56–2230.53). In contrast, headaches were negatively associated with mortality (OR: 0.46, 95% CI: 0.22–0.95) (**Figure 4**, Supplementary Table 6).

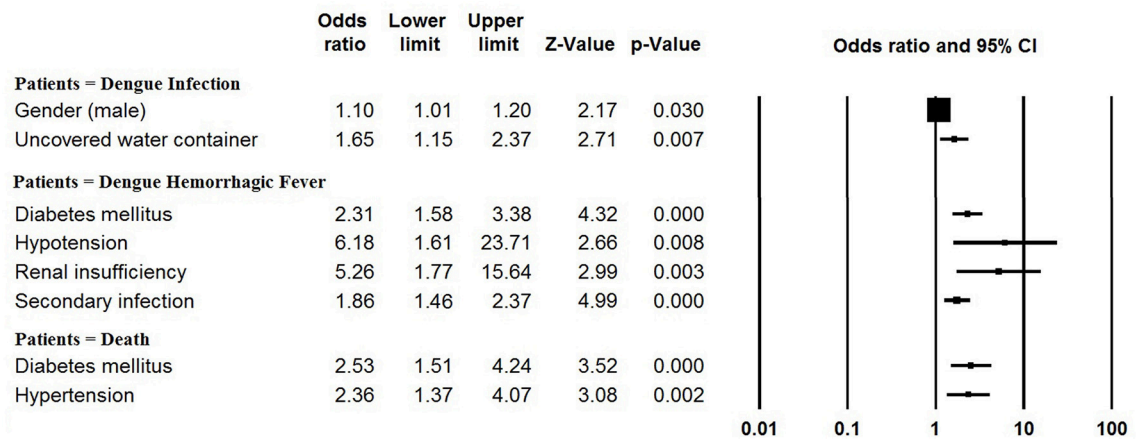

FIGURE 3 | Meta-analysis: forest plot of the associations between risk factors and dengue infection, DHF and mortality in dengue outbreaks.

TABLE 2 | Clinical symptoms and signs of patients in dengue outbreaks.

Variables	No. studies meta-analyzed	Meta-analysis, pooled data (95% CI)*
CONSTITUTIONAL		
Fever	88	98.1 (97.2–98.7)
Chills	14	65.3 (58.3–71.6)
Myalgia	65	64.2 (58.1–69.8)
Arthralgia	53	53.6 (46.0–61.0)
Lethargy	5	67.1 (32.6–89.6)
Malaise	9	76.0 (64.1–84.9)
Asthenia	6	74.3 (45.8–90.8)
Body-ache	13	67.2 (55.2–77.3)
Back pain	9	57.3 (32.2–79.1)
Sore throat	12	19.7 (13.4–28.1)
Eye pain	6	27.8 (13.7–48.1)
Retro-orbital pain	38	35.1 (27.0–44.2)
Lymphadenopathy	13	9.2 (4.4–18.2)
GASTROINTESTINAL		
Vomiting	36	39.8 (35.0–44.9)
Nausea	22	42.0 (34.0–50.4)
Diarrhea	36	20.7 (17.3–24.7)
Anorexia	17	47.8 (34.9–61.0)
Ascites	25	10.2 (5.3–18.8)
Icterus/Jaundice	13	2.8 (1.5–5.2)
Abdominal pain	61	32.4 (27.9–37.2)
Hepatomegaly	41	18.9 (12.7–27.1)
Splenomegaly	20	7.7 (5.2–11.3)
Hepatosplenomegaly	5	17.5 (8.3–33.3)
MUCOCUTANEOUS		
Rash	83	29.6 (26.1–33.3)
Pruritus	5	24.1 (19.8–29.0)
Exanthema	5	33.7 (11.2–67.1)
Itching eruption	6	24.0 (18.7–30.2)
CARDIORESPIRATORY		
Cough	29	22.9 (17.8–28.8)
Pleural effusion	23	8.3 (4.5–14.9)
Myocarditis	5	5.7 (1.2–22.5)
Hypotension	14	12.5 (7.7–19.7)
Respiratory disorders	13	8.7 (5.3–13.9)
NEUROLOGICAL		
Headache	83	75.7 (69.5–81.0)
Dizziness	9	22.8 (11.7–39.7)
Seizure	7	2.7 (1.8–3.9)**
Shock	12	9.5 (4.2–20.0)
Convulsion	5	6.1 (2.9–12.5)
Encephalopathy	8	5.0 (1.9–12.4)
HEMORRHAGIC MANIFESTATIONS		
Gingivorrhagia	16	9.7 (6.0–15.2)
Epistaxis	25	11.8 (7.6–17.9)
Hematuria	16	5.0 (3.0–8.1)
Melena	13	16.9 (8.1–31.8)
Petechiae	30	22.3 (16.5–29.3)
Hematemesis	18	13.4 (8.0–21.6)
Bleeding/Hemorrhagic manifestations	58	25.8 (21.0–31.1)

Random-effects model unless otherwise specified.
***Fixed-effects model.*

Serotype

Studies of 174 outbreaks that occurred between 1990 and 2015 reported dengue serotype data. The highest number of monoinfection outbreaks were caused by DENV-2 (36, 20.7%), followed by DENV-1 (29, 16.7%), DENV-3 (19, 10.9%) and DENV-4 (7, 4.0%). Coinfection with more than one DENV serotype was reported in 47.7% of the outbreaks; outbreaks involving all four serotypes were the most common (25, 14.4%), followed by coinfection with DENV-1 and DENV-2 (16, 9.2%) and coinfection DENV-1, DENV-2 and DENV-3 (12, 6.9%).

The longitudinal trends in serotype distribution are shown in **Figure 5**. Between 1990 and 1994, DENV-2 was most frequently identified serotype in the 6 reported outbreaks (5/6, 83.3%). During 1995–1999 and 2000–2004, DENV-2 monoinfection was the predominant serotype observed in dengue outbreaks (11/20, 55.0% and 10/45, 22.2%). Coinfection dominated subsequent (2005–2009) outbreaks (12/23, 52.2%), especially co-infection with all four serotypes (4/23, 17.4%). After 2010, DENV-1 dominated the monoinfection outbreaks (17/34, 50.0%) and co-infection with all four serotypes continued to dominate the coinfection outbreaks (17/46, 37.0%). Different serotypes were predominant in different WHO regions after 2010: DENV-1 and DENV-2 were most common in the African region and American region; DENV-1 was most common in the European region; coinfection with all four serotypes was most common in the Southeast Asia region; DENV-2 and DENV-3 were most frequently observed in the Eastern Mediterranean region, and DENV-1 was predominant in the Western Pacific region.

The highest pooled mortality rate was identified in DENV-2 dominated outbreaks at 2.0% (95% CI: 0.9–4.2%), followed by DENV-3 (1.6, 95% CI: 0.4–6.8%), DENV-4 (0.7, 95% CI: 0.0–42.3%) and DENV-1 (0.3, 95% CI: 0.1–0.9%).

DISCUSSION

Our study presents the epidemiology, clinical characteristics, and serotype distribution and risk factors for global dengue outbreaks in humans that occurred between 1990 and 2015. The majority of the 262 outbreaks occurred in developing countries, including India, China and Brazil. These high numbers might be attributed to the limited laboratory facilities and inadequate control measures in these countries (Cattand et al., 2006). The relatively low socioeconomic status of and high population density and ideal environment for the maintenance of mosquitoes in developing countries may also facilitate the transmission of DENV (Figueiredo, 2007; Saswat et al., 2015). After 2010, the majority of dengue outbreaks and dengue patients were identified in the Western Pacific region, which may be mainly attributed to cases in China, Singapore and Malaysia. In contrast, only a few dengue outbreaks were reported in the Europe region, and these outbreaks involved in only two countries (France and Portugal). The disappearance of *A. aegypti* from the European Basin between the 1950s and 2005 might be one reason for its low-prevalence of dengue outbreaks (Succo et al., 2016). It is important to note that many dengue outbreaks were influenced by the dengue epidemics

	Odds ratio	Lower limit	Upper limit	Z-Value	p-Value
Patients = Dengue Infection					
Myalgia	1.38	1.08	1.76	2.62	0.009
Chill	1.67	1.13	2.46	2.58	0.010
Rash	2.77	1.74	4.41	4.28	0.000
Eye/retro-orbital pain	1.27	1.04	1.55	2.35	0.019
Sore throat	0.47	0.23	0.96	-2.09	0.037
Nasal congestion	0.35	0.14	0.88	-2.22	0.026
Cough	0.26	0.12	0.57	-3.35	0.001
Petechiae	1.95	1.24	3.07	2.89	0.004
Exanthema	1.97	1.23	3.16	2.81	0.005
Lethargy	1.78	1.02	3.09	2.05	0.041
Lymphadenopathy	2.21	1.08	4.53	2.16	0.030
Thrombocytopenia	3.31	2.17	5.04	5.58	0.000
Leukopenia	4.42	1.75	11.18	3.14	0.002
Conjunctival injection	1.51	1.01	2.26	2.01	0.045
Positive tourniquet test	4.86	1.07	22.05	2.05	0.040
Patients = Dengue Hemorrhagic Fever					
Bodyache	0.60	0.36	0.99	-1.98	0.048
Arthralgia	1.57	1.09	2.26	2.42	0.015
Epistaxis	2.03	1.57	2.63	5.38	0.000
Petechiae	1.74	1.24	2.44	3.21	0.001
Purpura	3.15	2.04	4.87	5.17	0.000
Ecchymosis	2.75	1.20	6.31	2.39	0.017
Any blood manifestation	9.57	4.78	19.16	6.38	0.000
Melena	5.67	1.73	18.61	2.86	0.004
Hematuria	1.55	1.04	2.31	2.15	0.031
Hematemesis	3.68	1.42	9.53	2.68	0.007
Shock	2.63	1.01	6.84	1.98	0.048
Proteinuria	2.72	2.04	3.63	6.81	0.000
Hepatomegaly	6.39	4.92	8.29	13.96	0.000
Splenomegaly	6.80	4.49	10.29	9.06	0.000
Pleural effusion	12.44	7.07	21.90	8.74	0.000
Ascites	13.91	8.03	24.10	9.39	0.000
Positive tourniquet test	4.15	1.55	11.10	2.84	0.005
Raised ALT	2.31	1.82	2.93	6.89	0.000
Raised AST	2.60	1.05	6.45	2.06	0.039
Patients = Death					
Headache	0.46	0.22	0.96	-2.08	0.037
Shock	308.09	42.56	2230.39	5.67	0.000

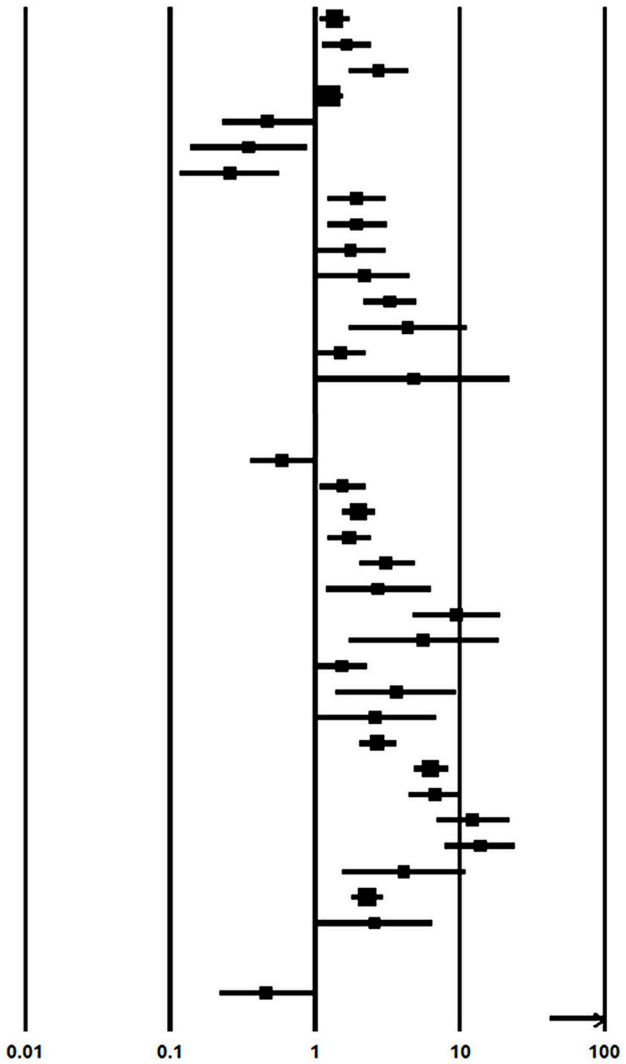

FIGURE 4 | Meta-analysis: forest plot of the associations between symptoms and signs and dengue infection, DHF and mortality in dengue outbreaks.

in nearby/neighboring countries. Wang et al. reported that the dengue virus in the Xishuangbanna and Dehong, China outbreak in 2013 was imported from Southeast Asia countries (Wang et al., 2016). Owing to the more frequent interactions between the populations of Southeast Asian countries and China, imported dengue epidemics have been documented in southern China. Additionally, the first major outbreak of dengue in Europe was reported to be most likely imported from Venezuela via travelers to Madeira (Wilder-Smith et al., 2014). Valid laboratory-based disease surveillance system and integrated vector management are required in the border regions of dengue epidemic areas so that future disease outbreaks and spread to other regions can be prevented (Guo et al., 2015).

Ongoing outbreaks likely reflect deficiencies in vector control and prevention. Originating in Africa and spreading to tropical countries in the seventeenth and eighteenth centuries, *A. aegypti* has been considered the primary dengue vector due to its enhanced viral duplication capability, thus increasing the probability of viral transmission (Gubler, 2011; Chepkorir et al., 2014; Whitehorn et al., 2015). Sixty of the articles included in our meta-analysis mentioned mosquitoes. Consistent with prior knowledge, the most prevalent mosquito was *A. aegypti* (76.7%), followed by *A. albopictus* (43.3%). In addition, the pooled mortality rate in outbreaks associated with *A. aegypti* mosquitoes (0.7, 95% CI: 0.3–1.7%) was higher than the pooled mortality rate in outbreaks associated with *A. albopictus* mosquitoes (0.4, 95% CI: 0.1–2.5%). Dengue outbreaks caused by *A. albopictus*

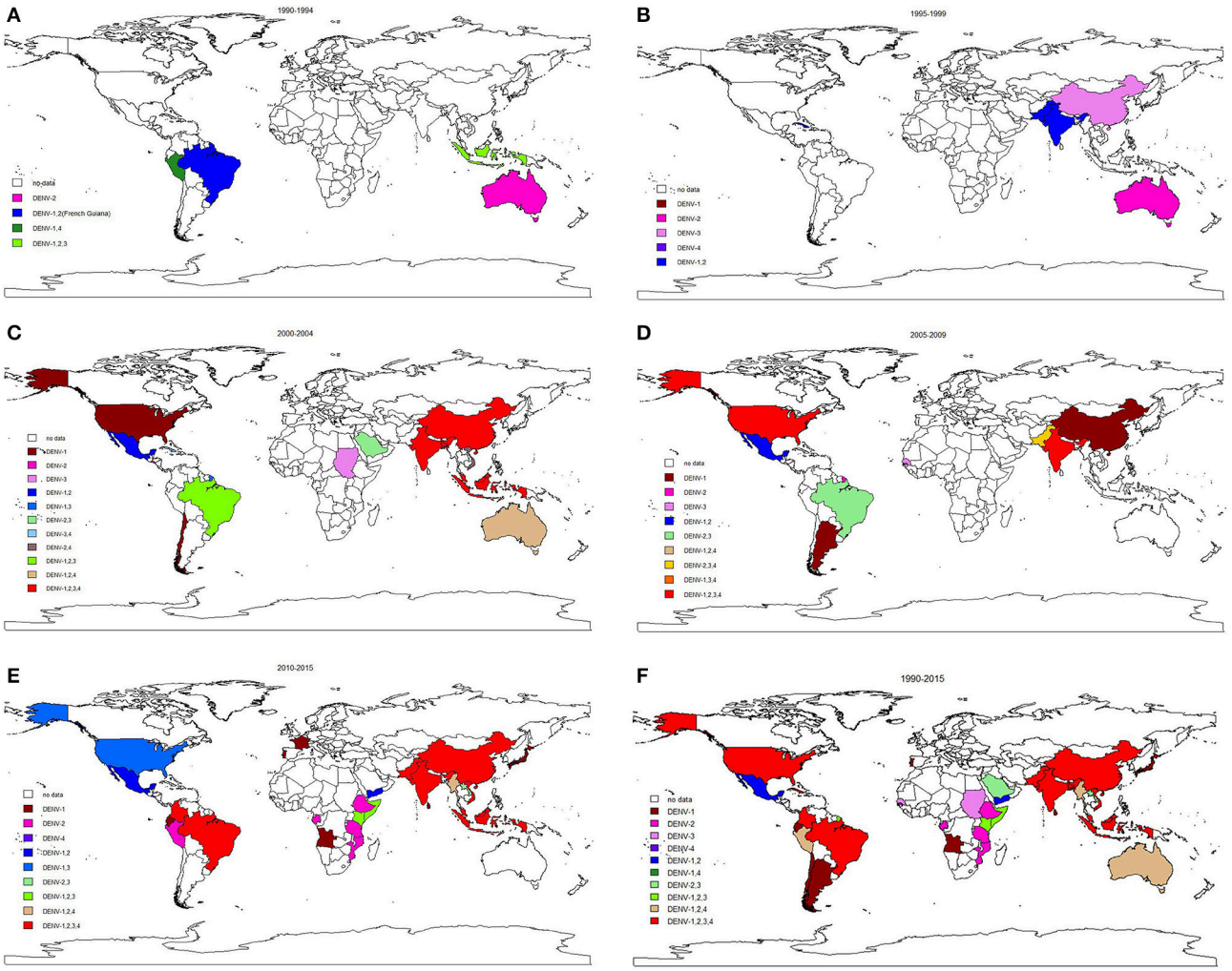

FIGURE 5 | Global serotypes distribution in dengue outbreaks from 1990–2015.

tend to be mild and short (Issack et al., 2010). Wang T. et al. (2015), Wang S. F. et al. (2015), Kim Lien et al. (2015), Kunwar and Prakash (2015), Barde et al. (2015) had reported that rainfall with the hot weather contributed to the dramatically increase of mosquitos. Rainfall provides breeding sites and stimulates egg hatching for dengue transmission vectors and temperature affects the vector's survival and their rate of development and reproduction (Johansson et al., 2009). Chepkorir et al. (2014) and Watts et al. (1987) have demonstrated a significantly higher infection rate of dengue virus at high temperatures for Ae. aegypti mosquitoes, suggesting a potentially significant role of temperature in the dynamics of dengue transmission. It may be due to that the high temperature increases virus reproduction to high titers and reduces the extrinsic incubation period for the dengue virus to be established within the vector, thus leads to the upsurge of dengue outbreaks (Lambrechts et al., 2011). Besides the traditional methods to control vectors, a potential method has been developed during the last decade; scientists released *A. aegypti* or *A. albopictus* mosquitoes infected with *Wolbachia,* which might hinder the insects' ability to transmit the dengue virus and cannot infect humans (Hoffmann et al., 2011; Callaway, 2016).

The results of our study suggested that DENV-2 was the predominant serotype in dengue outbreaks that occurred before 2000, but DENV-3 was the predominant serotype between 2000 and 2009. After 2010, DENV-1 dominated global dengue outbreaks, and DENV-4 was the least frequently identified serotype. We would like to note that at least two serotypes were identified in nearly half the outbreaks, as previous exposure to a single virus could not provide immunity against potential infections with other serotypes (Rahim and Sikder, 2005). Cross-reactive and non-neutralizing antibodies from the primary infection can also bind to the new DENV serotype and facilitate virus entry into susceptible cells. It was a phenomenon known as antibody-dependent enhancement of infection (ADE), considered as the most rational explanation for severe dengue (Simmons et al., 2007; Wang Y. et al., 2015). This can also explain the significantly association

between secondary infection and DHF in our study (OR: 1.86, 95% CI: 1.46–2.37). Additionally, we found that the pooled mortality rate was highest in DENV-2 dominated outbreaks (2.0%), with significantly higher mortality rates identified in association with this than other serotypes. Although vaccines or therapeutics for dengue are not available, Liu *et al.* previously identified multiple mosquito galactose specific C-type lectins (mosGCTLs) that facilitated dengue infection; these mosGCTLs were induced in the tissues of mosquitoes with DENV-2 and directly interacted with the DENV-2 surface envelope (E) protein and virions *in vitro* and *in vivo*. Membrane blood feeding of antisera against mosGCTLs has been found to efficiently reduce DENV-2 infections among mosquitoes, suggesting that immunization against mosGCTLs may serve as a feasible approach for preventing dengue infection (Liu et al., 2014). Additionally, to reduce the rate of mortality in dengue patients, the application of early clinical and laboratory diagnosis, intravenous rehydration, staff training and hospital reorganization should be ensured during outbreaks (Lo et al., 2007; WHO, 2012).

Dengue infections were characterized by fever (98.1%), malaise (76.0%), headache (75.7%), and asthenia (74.3%); however, in some cases, bleeding (25.8%), plasma leakage (8.3%) and organ impairment (e.g., hepatosplenomegaly, 17.5%) were observed. Although dengue was mostly mild and self-limiting in this study, when cases were misdiagnosed by untrained physicians, there may be sufficient time for virus transmission and outbreak development (Huang Xue et al., 2014). In addition to the common symptoms and signs of dengue, manifestations including bleeding (OR: 9.57), pleural effusion (OR: 12.44), and ascites (OR: 13.91) were frequently identified in DHF patients. Thus, physicians should monitor patients for hemorrhage manifestations and capillary leakage, which might indicate the onset of DHF or DSS (Trofa et al., 1997). The results of our study showed that the rates of DHF, secondary infection and mortality in dengue outbreaks were significantly lower in outbreaks occurring after 2010 than in outbreaks before 2010, which suggests that the severity of global dengue infection has somewhat decreased after 2010. Through the use of timely, appropriate clinical management, global outbreak surveillance and sustainable vector control, a great deal of effort has been devoted to achieving the goal set by the World Health Organization in 2012; however, these efforts still face a challenging situation (WHO, 2012).

We believe it is important to note that the age of dengue patients after 2010 was significantly older than that of dengue patients before 2010 (mean pooled age: 34.0 vs. 27.2). Possible reasons for this finding may be that younger people now spend more daytime in enclosed air-conditioned environments and are, therefore, less likely to be exposed to mosquitoes (Lin et al., 2012) and that older people with chronic diseases now visit the doctor more often, causing existing dengue infection to be more likely to be detected (Lee et al., 2006).

There are still some limitations to our study. First, since our study and analysis were based on published articles, some dengue outbreaks may not have been recorded; thus, the result of our study should be interpreted with caution. Second, dengue is a self-limiting disease and most infections are asymptomatic (Bordignon et al., 2008); therefore, a portion of dengue patients might go unidentified during dengue outbreaks. The actual numbers of cases associated with these outbreaks were likely considerably higher than recorded. Regardless of these limitations, we believe that our systematic review and meta-analysis provide useful information regarding the global epidemiology of dengue outbreaks. Our study indicated the countries and WHO regions most seriously affected by dengue outbreaks; the risk factors for and clinical characteristics of dengue infection, DHF and mortality; and the global dengue serotype distribution, all of which could be extremely valuable when targeting prevention and early identification efforts in dengue outbreaks worldwide.

AUTHOR CONTRIBUTIONS

GY and CJ contributed to the design of the study. CG and ZZ were involved in data acquisition. The data was then analyzed and interpreted by all authors. CG, ZZ, ZW, and YL wrote the first manuscript. GY and CJ critically revised the manuscript for important intellectual content. All authors approved the final version to be submitted.

FUNDING

This work was supported in part by Training Program of the Major Research Plan of the National Natural Science Foundation of China (Grant numbers: 91543132), National Natural Science Foundation of China (Grant numbers: 81541070, 81101267, and 30901249), Guangdong Natural Science Foundation (Grant numbers: 10151063201000036, S2011010002526, and 2016A030313089), Guangdong Province Medical Research Foundation (Grant number: A2014374 and A2015310) and Project from Jinan university (Grant number: 21612426, 21615426, JNUPHPM2016001, and JNUPHPM2016002), State Key Laboratory for Infectious Disease Prevention and Control (2015SKLID505).

ACKNOWLEDGMENTS

We would like to thank Hoi Leng Ip, Ka Yu Fu, Mei Leng Ieong, and Chong Iok Lei from Jinan University for providing precious ideas and thoughts.

SUPPLEMENTARY MATERIAL

The Supplementary Material for this article can be found online at: http://journal.frontiersin.org/article/10.3389/fcimb.2017.00317/full#supplementary-material

REFERENCES

Amarasinghe, A., Kuritsk, J. N., Letson, G. W., and Margolis, H. S. (2011). Dengue virus infection in Africa. *Emerg. Infect. Dis.* 17, 1349–1354. doi: 10.3201/eid1708.101515

Barcelos, F. L. (2014). Dengue virus 2 American-Asian Genotype identified during the 2006/2007 outbreak in Piaui, Brazil reveals a Caribbean route of introduction and dissemination of dengue virus in Brazil (vol 9, e104516, 2014). *PLoS ONE* 9:516. doi: 10.1371/journal.pone.0104516

Barde, P. V., Shukla, M. K., Kori, B. K., Chand, G., Jain, L., Varun, B. M., et al. (2015). Emergence of dengue in tribal villages of Mandla district, Madhya Pradesh, India. *Indian J. Med. Res.* 141, 584–590. doi: 10.4103/0971-5916.159517

Bordignon, J., Probst, C. M., Mosimann, A. L., Pavoni, D. P., Stella, V., Buck, G. A., et al. (2008). Expression profile of interferon stimulated genes in central nervous system of mice infected with dengue virus Type-1. *Virology* 377, 319–329. doi: 10.1016/j.virol.2008.04.033

Callaway, E. (2016). Rio fights Zika with biggest release yet of bacteria-infected mosquitoes. *Nature* 539, 17–18. doi: 10.1038/nature.2016.20878

Cattand, P., Desjeux, P., Guzman, M. G., Jannin, J., Kroeger, A., Medici, A., et al. (2006). "Tropical diseases lacking adequate control measures: dengue, leishmaniasis, and african trypanosomiasis," in *Disease Control Priorities in Developing Countries*, *2nd Edn*., eds D. T. Jamison, J. G. Breman, A. R. Measham, G. Alleyne, M. Claeson, D. B. Evans, P. Jha, A. Mills, and P. Musgrove (Washington, DC: Oxford University Press) 451–466.

Chang, M. S., Hii, J., Buttner, P., and Mansoor, F. (1997). Changes in abundance and behaviour of vector mosquitoes induced by land use during the development of an oil palm plantation in Sarawak. *Trans. R. Soc. Trop. Med. Hyg.* 91, 382–386. doi: 10.1016/S0035-9203(97)90248-0

Cheah, W. L., Chang, M. S., and Wang, Y. C. (2006). Spatial, environmental and entomological risk factors analysis on a rural dengue outbreak in Lundu District in Sarawak, Malaysia. *Trop. Biomed.* 23, 85–96. doi: 10.1038/nature.2016.20878

Chepkorir, E., Lutomiah, J., Mutisya, J., Mulwa, F., Limbaso, K., Orindi, B., et al. (2014). Vector competence of *Aedes aegypti* populations from Kilifi and Nairobi for dengue 2 virus and the influence of temperature. *Parasit. Vectors* 7:435. doi: 10.1186/1756-3305-7-435

Figueiredo, L. T. (2007). Emergent arboviruses in Brazil. *Rev. Soc. Bras. Med. Trop.* 40, 224–229. doi: 10.1590/S0037-86822007000200016

Gubler, D. J. (2011). Dengue, urbanization and globalization: the unholy trinity of the 21(st) century. *Trop. Med. Health* 39, 3–11. doi: 10.2149/tmh.2011-S05

Guo, X., Yang, H., Wu, C., Jiang, J., Fan, J., Li, H., et al. (2015). Molecular characterization and viral origin of the first dengue outbreak in Xishuangbanna, Yunnan Province, China. (2013). *Am. J. Trop. Med. Hyg.* 93, 390–393. doi: 10.4269/ajtmh.14-0044

Guzman, M. G., and Harris, E. (2015). Dengue. *Lancet* 385, 453–465. doi: 10.1016/S0140-6736(14)60572-9

Handoll, H. H. (2006). Systematic reviews on rehabilitation interventions. *Arch. Phys. Med. Rehabil.* 87:875. doi: 10.1016/j.apmr.2006.04.006

Higgins, J. P., and Thompson, S. G. (2002). Quantifying heterogeneity in a meta-analysis. *Stat. Med.* 21, 1539–1558. doi: 10.1002/sim.1186

Hoffmann, A. A., Montgomery, B. L., Popovici, J., Iturbe-Ormaetxe, I., Johnson, P. H., Muzzi, F., et al. (2011). Successful establishment of Wolbachia in Aedes populations to suppress dengue transmission. *Nature* 476, 454–457. doi: 10.1038/nature10356

Hozo, S. P., Djulbegovic, B., and Hozo, I. (2005). Estimating the mean and variance from the median, range, and the size of a sample. *BMC Med. Res. Methodol.* 5:13. doi: 10.1186/1471-2288-5-13

Huang Xue, Y., Ma Hong, X., Wang Hai, F., Du Yan, H., Su, J., Li Xing, L., et al. (2014). Outbreak of dengue fever in Central China. (2013). *Biomed. Environ. Sci.* 27, 894–897. doi: 10.3967/bes2014.125

Ishak, H., Miyagi, I., Toma, T., and Kamimura, K. (1997). Breeding habitats of *Aedes aegypti* (L) and Aedes. albopictus (Skuse) in villages of Barru, South Sulawesi, Indonesia. *Southeast. Asian J. Trop. Med. Public Health* 28, 844–850.

Issack, M. I., Pursem, V. N., Barkham, T. M. S., Ng, L. C., Inoue, M., and Manraj, S. S. (2010). Reemergence of dengue in Mauritius. *Emerg. Infect. Dis.* 16, 716–718. doi: 10.3201/eid1604.091582

Jansen, C. C., and Beebe, N. W. (2010). The dengue vector *Aedes aegypti*: what comes next. *Microbes Infect.* 12, 272–279. doi: 10.1016/j.micinf.2009.12.011

Johansson, M. A., Cummings, D. A., and Glass, G. E. (2009). Multiyear climate variability and dengue–El Nino southern oscillation, weather, and dengue incidence in Puerto Rico, Mexico, and Thailand: a longitudinal data analysis. *PLoS Med.* 6:e1000168. doi: 10.1371/journal.pmed.1000168

Kim Lien, P. T., Duoc, V. T., Gavotte, L., Cornillot, E., Nga, P. T., Briant, L., et al. (2015). Role of *Aedes aegypti* and *Aedes albopictus* during the 2011 dengue fever epidemics in Hanoi, Vietnam. *Asian Pac. J. Trop. Med.* 8, 543–548. doi: 10.1016/j.apjtm.2015.06.009

Kunwar, R., and Prakash, R. (2015). Dengue outbreak in a large military station: have we learnt any lesson? *Med. J. Armed. Forces India* 71, 11–14. doi: 10.1016/j.mjafi.2014.11.002

Lambrechts, L., Paaijmans, K. P., Fansiri, T., Carrington, L. B., Kramer, L. D., Thomas, M. B., et al. (2011). Impact of daily temperature fluctuations on dengue virus transmission by *Aedes aegypti*. *Proc. Natl. Acad. Sci. U.S.A.* 108, 7460–7465. doi: 10.1073/pnas.1101377108

Lancet, T. (2013). Dengue–an infectious disease of staggering proportions. *Lancet* 381, 2136. doi: 10.1016/s0140-6736(13)61423-3

Lee, M. S., Hwang, K. P., Chen, T. C., Lu, P. L., and Chen, T. P. (2006). Clinical characteristics of dengue and dengue hemorrhagic fever in a medical center of southern Taiwan during the 2002 epidemic. *J. Microbiol. Immunol. Infect.* 39, 121–129.

Lin, C. H., Schioler, K. L., Jepsen, M. R., Ho, C. K., Li, S. H., and Konradsen, F. (2012). Dengue outbreaks in high-income area, Kaohsiung City, Taiwan, 2003-2009. *Emerg. Infect. Dis.* 18, 1603–1611. doi: 10.3201/eid1810.111929

Liu, Y., Zhang, F., Liu, J., Xiao, X., Zhang, S., Qin, C., et al. (2014). Transmission-blocking antibodies against mosquito C-type lectins for dengue prevention. *PLoS Pathog* 10:e1003931. doi: 10.1371/journal.ppat.1003931

Lo, C. L., Yip, S. P., Cheng, P. K., To, T. S., Lim, W. W., and Leung, P. H. (2007). One-step rapid reverse transcription-PCR assay for detecting and typing dengue viruses with GC tail and induced fluorescence resonance energy transfer techniques for melting temperature and color multiplexing. *Clin. Chem.* 53, 594–599. doi: 10.1373/clinchem.2006.077446

Organization, W. H. (2016). *Dengue and Severe Dengue*. Available online at: http://www.who.int/mediacentre/factsheets/fs117/en/ (Accessed 24 Mar 2016).

Rahim, M. A., and Sikder, M. S. (2005). Clinicopathologic manifestations and outcome of dengue fever and dengue haemorrhagic fever. *Bangladesh Med. Res. Counc. Bull.* 31, 36–45.

Saswat, T., Kumar, A., Kumar, S., Mamidi, P., Muduli, S., Debata, N. K., et al. (2015). High rates of co-infection of Dengue and Chikungunya virus in Odisha and Maharashtra, India during 2013. *Infect. Genet. Evol.* 35, 134–141. doi: 10.1016/j.meegid.2015.08.006

Screaton, G., Mongkolsapaya, J., Yacoub, S., and Roberts, C. (2015). New insights into the immunopathology and control of dengue virus infection. *Nat. Rev. Immunol.* 15, 745–759. doi: 10.1038/nri3916

Simmons, C. P., Chau, T. N., Thuy, T. T., Tuan, N. M., Hoang, D. M., Thien, N. T., et al. (2007). Maternal antibody and viral factors in the pathogenesis of dengue virus in infants. *J. Infect. Dis.* 196, 416–424. doi: 10.1086/519170

Simmons, C. P., Farrar, J. J., Nguyen v, V., and Wills, B. (2012). Dengue. *N. Engl. J. Med.* 366, 1423–1432. doi: 10.1056/NEJMra1110265

Succo, T., Leparc-Goffart, I., Ferre, J., Roiz, D., Broche, B., Maquart, M., et al. (2016). Autochthonous dengue outbreak in Nimes, South of France, July to September 2015. *Eurosurveillance* 21, 5–11. doi: 10.2807/1560-7917.es.2016.21.21.30240

Trofa, A. F., DeFraites, R. F., Smoak, B. L., Kanesa-thasan, N., King, A. D., Burrous, J. M., et al. (1997). Dengue fever in US military personnel in Haiti. *JAMA* 277, 1546–1548. doi: 10.1001/jama.1997.03540430058033

Wang, B., Yang, H., Feng, Y., Zhou, H., Dai, J., Hu, Y., et al. (2016). The distinct distribution and phylogenetic characteristics of dengue virus serotypes/genotypes during the 2013 outbreak in Yunnan, China: phylogenetic characteristics of 2013 dengue outbreak in Yunnan, China. *Infect. Genet. Evol.* 37, 1–7. doi: 10.1016/j.meegid.2015.10.022

Wang, S. F., Chang, K., Lu, R. W., Wang, W. H., Chen, Y. H., Chen, M., et al. (2015). Large dengue virus type 1 outbreak in Taiwan. *Emerg. Microbes. Infect.* 4:e46. doi: 10.1038/emi.2015.46

Wang, T., Wang, M., Shu, B., Chen, X. Q., Luo, L., Wang, J. Y., et al. (2015). Evaluation of inapparent dengue infections during an outbreak in Southern China. *PLoS. Negl. Trop. Dis.* 9:e0003677. doi: 10.1371/journal.pntd.0003677

Wang, Y., Si, L., Luo, Y., Guo, X., Zhou, J., Fang, D., et al. (2015). Replacement of pr gene with Japanese encephalitis virus pr using reverse genetics reduces antibody-dependent enhancement of dengue virus 2 infection. *Appl. Microbiol. Biotechnol.* 99, 9685–9698. doi: 10.1007/s00253-015-6819-3

Watts, D. M., Burke, D. S., Harrison, B. A., Whitmire, R. E., and Nisalak, A. (1987). Effect of temperature on the vector efficiency of *Aedes aegypti* for dengue 2 virus. *Am. J. Trop. Med. Hyg.* 36, 143–152. doi: 10.4269/ajtmh.1987.36.143

Whitehorn, J., Duong Thi Hue, K., Nguyet Minh, N., Nguyen, H. L., Kyrylos, P. P., Carrington, L. B., et al. (2015). Comparative susceptibility of *Aedes albopictus* and *Aedes aegypti* to dengue virus infection after feeding on blood of viremic humans: implications for public health. *J. Infect. Dis.* 212, 1182–1190. doi: 10.1093/infdis/jiv173

WHO (2012). *Global Strategy for Dengue Prevention and Control, 2012-2020.* Geneva: World Health Organization.

WHO/TDR (2009). *Dengue Guidelines for Diagnosis, Treatment, Prevention and Control. New Edition.* Geneva: World Health Organization.

Wilder-Smith, A., Quam, M., Sessions, O., Rocklov, J., Liu-Helmersson, J., Franco, L., et al. (2014). The 2012 dengue outbreak in Madeira: exploring the origins. *Euro. Surveill.* 19:20718. doi: 10.2807/1560-7917.ES2014.19.8.20718

Wu, W., Bai, Z., Zhou, H., Tu, Z., Fang, M., Tang, B., et al. (2011). Molecular epidemiology of dengue viruses in southern China from 1978 to 2006. *Virol. J.* 8:322. doi: 10.1186/1743-422X-8-322

Conflict of Interest Statement: The authors declare that the research was conducted in the absence of any commercial or financial relationships that could be construed as a potential conflict of interest.

frontiers in Cellular and Infection Microbiology

MINI REVIEW
published: 25 July 2017
doi: 10.3389/fcimb.2017.00336

Prevention and Control Strategies to Counter Dengue Virus Infection

Irfan A. Rather[1], Hilal A. Parray[2], Jameel B. Lone[2], Woon K. Paek[3], Jeongheui Lim[3], Vivek K. Bajpai[1]* and Yong-Ha Park[1]**

[1] Department of Applied Microbiology and Biotechnology, School of Biotechnology, Yeungnam University, Gyeongsan, South Korea, [2] Department of Biotechnology, Daegu University, Gyungsan, South Korea, [3] National Science Museum, Ministry of Science, ICT and Future Planning, Daejeon, South Korea

Dengue is currently the highest and rapidly spreading vector-borne viral disease, which can lead to mortality in its severe form. The globally endemic dengue poses as a public health and economic challenge that has been attempted to suppress though application of various prevention and control techniques. Therefore, broad spectrum techniques, that are efficient, cost-effective, and environmentally sustainable, are proposed and practiced in dengue-endemic regions. The development of vaccines and immunotherapies have introduced a new dimension for effective dengue control and prevention. Thus, the present study focuses on the preventive and control strategies that are currently employed to counter dengue. While traditional control strategies bring temporary sustainability alone, implementation of novel biotechnological interventions, such as sterile insect technique, paratransgenesis, and production of genetically modified vectors, has improved the efficacy of the traditional strategies. Although a large-scale vector control strategy can be limited, innovative vaccine candidates have provided evidence for promising dengue prevention measures. The use of tetravalent dengue vaccine (CYD-TDV) has been the most effective so far in treating dengue infections. Nonetheless, challenges and limitation hinder the progress of developing integrated intervention methods and vaccines; while the improvement in the latest techniques and vaccine formulation continues, one can hope for a future without the threat of dengue virus.

Keywords: dengue virus, infection, vaccine, disease, fever

OPEN ACCESS

Edited by:
Gong Cheng,
Tsinghua University, China

Reviewed by:
Tonya Michelle Colpitts,
University of South Carolina, United States
Long Yang,
New York Medical College, United States

****Correspondence:***
Jeongheui Lim
jeongheuilim@gmail.com;
Vivek K. Bajpai
vbajpai04@yahoo.com;
Yong-Ha Park
peter@ynu.ac.kr

Received: *10 May 2017*
Accepted: *10 July 2017*
Published: *25 July 2017*

Citation:
Rather IA, Parray HA, Lone JB, Paek WK, Lim J, Bajpai VK and Park Y-H (2017) Prevention and Control Strategies to Counter Dengue Virus Infection. Front. Cell. Infect. Microbiol. 7:336. doi: 10.3389/fcimb.2017.00336

INTRODUCTION

Dengue is a mosquito-borne viral infection (Simmons et al., 2012), which has affected almost 2.5 billion people around the globe (Koh et al., 2008). It is transmitted by vector species *Aedes aegypti* and poses a global threat to humans due to its high adaptability to urban communities (Araújo et al., 2015). In 2012, WHO reported that dengue outbreaks place a large burden on communities, healthcare systems, and economies in most tropical countries worldwide. According to WHO, Asia, Americas, Africa, and the Mediterranean regions are affected by the emerging and prevailing DENV (WHO, 2012).

Recently, Bhatt et al., estimated about 390 million DENV infections occurring each year, of which 96 million were seemingly evident (Bhatt et al., 2013). The DENV infection starts with mild fever, and further leads to many other consequences (**Figure 1**). However, preventive strategies for DENV have been developed in the form of vector control, including chemical, biological, and

physical controls. Apart from general control strategies, development of vaccines have offered effective prevention and control of this disease (DeRoeck et al., 2003).

Similarly, the following study aims to discuss the prevention and control strategies to counter DENV, including the development of immunotherapies and vaccines. It also examines the challenges confronted in the effective implementation of these strategies in light of peer reviewed literature, and draws a conclusion of the research.

Prevention and Control Strategies

The prevention and control methods are divided into three categories, which have been discussed accordingly.

Physical Control

GIS Mapping of Dengue Foci

Among the advanced techniques used for location of DENV, GIS mapping has been efficient in locating dengue concentrations. By locating dengue seri-positive cases within the study area, dengue transmission can be prevented by locating dengue foci, and then treating them with diverse preventive strategies (Gandhi et al., 2017). Kittayapong et al., showed that GIS mapping not only allowed better surveillance and community-based intervention programs for suppressing dengue; it also determined the rate of successful control in the mapped areas. In their study, surveillance of the mapped dengue foci determined the major breeding sites of *A. egypti* mosquitoes to be water containers and bath basins (Kittayapong et al., 2008).

Focused and Effective Surveillance

Surveillance provides fundamental information on the assessment of risk, outbreak reaction, program evaluation and guidance, as well as delivers timely responses to prevent and control dengue (Wilder-Smith et al., 2012). Surveillance enables the understanding of spatiotemporal distribution of dengue cases, and provides entomological and epidemiological links for better planning (WHO, 2012; Scarpino et al., 2017). On the other hand, these programs are not focused on the elimination of dengue vector (Abbas et al., 2014). The eruption of dengue in Singapore, after decades of surveillance, indicated unsustainable vector control measures and ineffective surveillance (Ooi et al., 2006) in 2005 (Koh et al., 2008). An effective surveillance system aiming at vector identification (Gómez-Dantés and Willoquet, 2009) and eradication (Abbas et al., 2014), providing the underlying information regarding vector concentration and its breeding, will prove beneficial in controlling vector species.

Determination of Oviposition Sites

As determined by Morrison et al., *Aedes aegypti* females lay eggs above the water in containers or jars and so on for their survival improvement (Morrison et al., 2004). To detect and reduce the population density of dengue vectors, it is necessary to determine the behavioral pattern of vectors. Wong et al., studied the oviposition pattern of *A. aegypti* and reported that strong intra-specie affinity may be an indication of targeting vector specie. Moreover, once the oviposition sites have been determined, introduction of strategies that eliminate mosquito population at a later developmental stage will increase the efficacy of control strategies (Wong et al., 2011). Recently, introducing oviposition-based innovative techniques have shown promising results in intensifying control of vector species (Johnson et al., 2017).

Community-Based Control Programs

Community-based control programs are developed with the aim to educate the community about the measures for the extermination of mosquito breeding sites. People in a community are divided into various groups depending upon their level of education and understanding (Abbas et al., 2014). The significance of community-based programs for elimination of dengue mosquitoes in Kerala district (George et al., 2017), Mexico (Tapia-Conyer et al., 2012), and Cuba (Vanlerberghe et al., 2010) has been proven in the form of elevated awareness among the communities. Through community involvement, a variety of techniques can be integrated for maximum control of vector population (Heintze et al., 2007; Pérez-Guerra et al., 2009; Shriram et al., 2009), such as, the combination of community-based program and chemical control of *A. aegypti* have yielded significant results in Cuba (Baly et al., 2007).

Education of Prevention Strategies

It has been noted that the success of community-based strategies depends upon the knowledge, education, and behavior of the people, and strategies involved (Nam et al., 2005). Education serves as a basis for an ability of an individual to identify and deal with vector habitats, and use preventive measures. Madeira et al., emphasized that distribution of information brings awareness in order to control dengue, and provides necessary measures for the destruction of vector habitats (Madeira et al., 2002). A recent study in Thailand showed that education of prevention strategies through media also played a vital role in developing awareness (Boonchutima et al., 2017).

Biological Control

Paratransgenesis and Use of Wolbachia

Nowadays, genetic control of *A. aegypti* has risen as a set of promising techniques, among which paratransgenesis is the popular method (Araújo et al., 2015; Ogaugwu and Durvasula, 2017). This approach utilizes genetically-modified symbiotic bacteria that are reintroduced in the vector to colonize the vector population, hence limiting the transmission of disease (Araújo et al., 2015; Wilke and Marrelli, 2015). These genetically modified bacteria cause harmful effects in the host body, dysregulate its sexual cycle, decrease the host competence and interfere with the developmental processes of the vector species, thereby suppressing the vector population (Wilke and Marrelli, 2015). As reported in the study by Jeffery et al., the most effective bacterial agents used is *Wolbachia* (Jeffery et al., 2009; Saldaña et al., 2017), which is a reproductive parasite interfering with the cellular and reproductive mechanisms of the vector species (Araújo et al., 2015; Kamtchum-Tatuene et al., 2016).

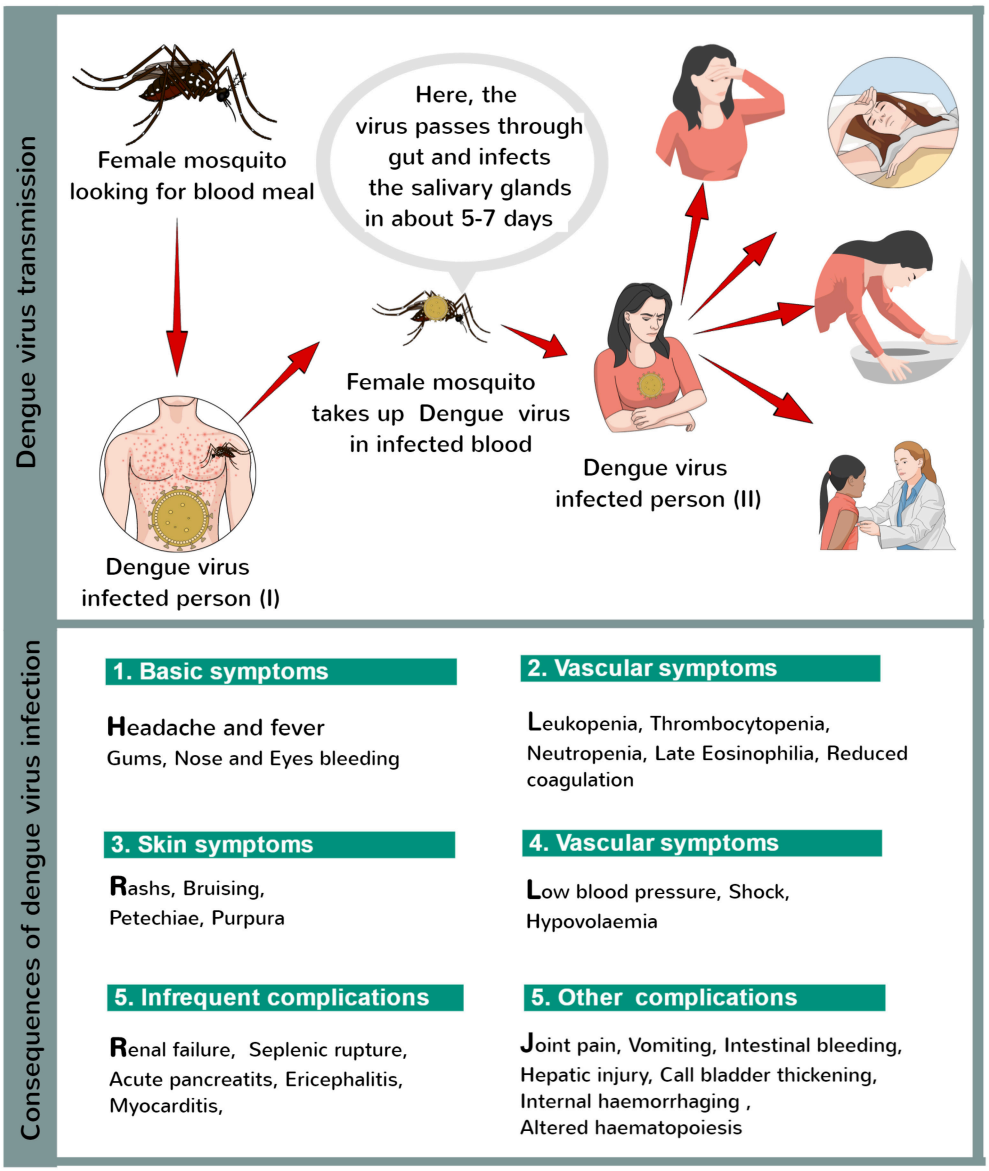

FIGURE 1 | Dengue virus infection.

Vector Specie Genetic Modification

The genetic methods for the control of *A. aegypti* aim at suppressing the population and its replacement or transformation. Therefore, the aim is designed to provide an alternate that could be accounted for providing an effector gene for reduction and inhibition of disease transmission (Reis-Castro, 2012; Carvalho et al., 2014; Jupatanakul et al., 2017). The field release of genetically modified mosquito species in Brazil showed an 85% decline in *A. aegypti* population (Pan American Health Organization, 2014), indicating that genetically modified vector species are innovative and feasible methods used for blocking the transmission of mosquito-borne diseases (Fraser, 2012; Favia, 2015).

Use of Sterile Insect Technique (SIT)

As the name indicates, SIT refers to the release of laboratory-sterilized male vectors in the target population. Once released, these male mosquitoes help in suppressing the fecundity rate in female mosquitoes and, consequently control the vector density in urban environments (Dumont and Chiroleu, 2010; Yakob et al., 2017) and transmission of vector-borne diseases (Alphey et al., 2010). According to Oliva et al., SIT is a promising strategy that helps in prevention and control of mosquito-borne diseases. After examining the irradiation effect on sterile male, they stated that sterile males were potential competitors and can help suppress the number of offsprings (Oliva et al., 2012).

Use of Larvivorous Fish and Crustacean

Since the larvae of dengue vectors reside in open water bodies, use of larvivorous fish, such as *Poecilia reticulate* (Seng et al., 2008) and *Mesocyclops formosanus* (Kalimuthu et al., 2017) comes as a cost-effective, eco-friendly, and innovate strategy in controlling the population of *A. aegypti* (Abbas et al., 2014; Han et al., 2015; Warbanski et al., 2017). A successful study in Cambodia was carried out to evaluate the efficacy of introducing larvivorous guppy fish (*Poecilia reticulata*) into heavily infested water containers. It showed that the guppy fish in test houses reduced vector larval population by 79% as compared to control houses, thus indicating successful implementation of this strategy (Seng et al., 2008).

Chemical Control

Use of Insecticides and Plant Derivatives

The chemical compounds, called insecticides, have been utilized for mosquito control for many decades. These insecticides became the most commonly used integrated strategy; nevertheless, the continuous use developed resistance in the target vector population, and can induce negative impacts on the environment (Araújo et al., 2015). To counter the effects of these compounds, researchers developed alternative control method i.e., introduction of plant-based insecticides that can sustain and induce less toxicity in environment than synthetic insecticides (Ghosh et al., 2012). These plant-based insecticides can be developed from different plant parts (leaves, stem, roots) and/or herbal extracts, such as, *Cipadessa baccifera* (Ramkumar et al., 2015), *Callistemon rigidus* (Pierre et al., 2014), *Erythrina indica, and Asparagus racemosus* (Govindarajan and Sivakumar, 2015). Furthermore, these plant derivatives are not only limited to produce insecticides; however, they have also proved their efficiency as potential repellents against *A. aegypti* (Araújo et al., 2015; Govindarajan and Sivakumar, 2015).

Use of Insect Growth Regulators (IGRs)

Among other known chemical compounds, insect growth regulators (IGRs) are used for hindering the growth and development in insects. During early stages of development, IGRs induce changes that kills the insect before becoming an adult. There are number of IGRs such as, diflubenzuron, endotoxins, and methoprene that have been used to counter viral infections spread by *A. aegypti* (Abbas et al., 2014). According to Lau et al., field population of vector species develops resistance to certain IGRs; and in their study, they found that cyromazine showed effective results in attenuating larval population indices of *A. aegypti* (Lau et al., 2015).

Use of Pheromones as "Attract-and-Kill" Approach

The practical application of pheromones as a part of integrated pest management (IPM) has been well-documented in various fields. In a recent integrated approach using pheromones, also termed attracticides, and IGRs, Nagpal et al., demonstrated the prevention of developmental stages from eggs to adults (Nagpal et al., 2015). In this study, larvae in test containers were found in a greater number than controls containers, which indicated that using attracticides hampers the progression of adulthood in *A. aegypti* and is effective in field conditions (Nagpal et al., 2015). Another study developed an uncomplicated "lethal lure control" based on attract-and-kill strategy and found that the pheromone (caproic acid)-insecticide (temephos) combination not only attracted mosquitoes, but also restricted hatching of eggs and killed the larvae, thus elaborating its significance (Ong and Jaal, 2015).

Development of Immunotherapies and Vaccines

Although no specific vaccine for dengue has been licensed at commercial scale, several candidates have been undergoing a developmental phase. Some of these are discussed below:

Live, Attenuated Dengue Vaccines

Among the vaccines having been improved, the development of live, attenuated vaccines, known as ChemariVax-Dengue (CYD)-based bivalent and tetravalent vaccines (CYD-TDV), have shown protection against DENV in a trial conducted in Mexico (Dayan et al., 2014). The study determined that the group receiving bivalent vaccine showed an immune response against CYD serotype 3, while the immune response rates of other group receiving first injection of CYD-TDV were generally higher and well-tolerated (Dayan et al., 2014). Evidences from randomized, controlled studies have emphasized the importance of tetravalent CYD vaccine in Asian (Capeding et al., 2014), Thai (Sabchareon et al., 2012), and Latin American (Villar et al., 2015) children along with adults in Singapore (Sin Leo et al., 2012), suggesting its potential in providing protection against various CYD serotypes. However, studies also suggested the lower risk of CYD in CYD-TDV vaccinated children aged 2–16 years than the unvaccinated control group (Hadinegoro et al., 2015), neutralization of antibody response to dengue serotypes, and safe profile of CYD-TDV (Qiao et al., 2011; Villar et al., 2013). The available candidates for dengue vaccine are listed in **Table 1**.

Besides live and/or attenuated vaccines, inactivated and non-replicating vaccines have also been used. The developing non-replicating vaccine approaches focus on recombinant DENV antigens, inactivated viruses, and use of non-replicating transmission agents produced specifically to extract DENV antigens *in vivo*. Using inactivated vaccines also reduce the risk of infection by conferring resistance. Also, subunit vaccines and genetic vaccination have been developed to respond to the inactivated viruses (Swaminathan and Khanna, 2010).

Recent outbreak of Zika virus (ZIKV) epidemics has raised a growing concern in many parts of the world. However, several viral diseases have been controlled using vaccination strategies. Nevertheless, for majority of arthropod transmitted viral diseases, there is no specific vaccine yet. Therefore, exploring potential transmission blocking vaccines (TBV) could halt the viral infection to humans, and could be applied to most of the arboviruses, including chikungunya, DENV, and ZIKV.

Development of Dengue Human Infection Model

In order to develop the understanding of DENV pathogenesis and effective dengue countermeasures, the evolution of the

TABLE 1 | Current Vaccine Candidates for Dengue Prevention (Source:Sandrasegaran, 2016).

Vaccine type	Developer	Process	Progress
Live, attenuated chimeric (recombinant)	Acambis/Sanofi Pasteur	Insertion of genes coding for DENV structural proteins into a yellow fever virus (17D) backbone.	Phase III tetravalent—leading candidate
	Centre for Disease Control (CDC)/Inviragen	Insertion of serotype genes into serotype II (DENV2-PDK53) DNA backbone.	Phase II monovalent
	National Institutes of Health (NIH)/University of Maryland	Insertion of serotype II and III genes into safer, more immunogenic serotype I and IV DNA backbone. Live attenuated DENV Delta-30 mutation	Phase I tetravalent
Live, traditionally attenuated	Walter-Reed Army Institute of Research (WRAIR)/GlaxoSmithKline (GSK)	Attenuation achieved by growing the virus in cultured cells and selecting strains	Phase II tetravalent; technical issues
	Mahidol Institute/Sanofi Pasteur		Phase II tetravalent
Inactivated	GSK	Viruses cultured and killed	Phase I tetravalent
Subunit	Hawaii Biotech	Viral immunogenic envelope is combined with viral non-structural protein antigens to produce recombinant 80% E subunit vaccine	Phase I tetravalent
DNA	WRAIR	Dengue prM-E DNA vaccine incorporating membrane and envelope genes into a plasmid vector	Phase I monovalent

dengue human infection model (DHIM) is also deemed necessary. Developing a DHIM requires a thorough examination of measures to reduce risks to participants and guidelines for clinical management. Moreover, DHIM serves as a promising research tool, which enables the understanding of pathways for vaccine development, examines the immunological pathogenesis, exploits protection by immune associates, supports the evolution of vaccine clinical development, and would put into effect the efforts for the development of effective vaccines (Thomas, 2013). In line with the same notion, murine infection models have also shown to be effective in examining DENV pathogenesis and evaluation of vaccine candidates and antiviral drugs (Sarathy et al., 2015).

Introducing Balance in Immunity and Reactogenicity

The two way relationship between immunity and reactigenicity has long been discussed with regards to DENV infection. It has been noticed that elevated reactogenicity may lead to a better immune response in some vaccine candidates; nonetheless, severe outcomes may be caused in others. Similarly, lower reactogenicity may result in deficient immune response (Perng et al., 2011). An ideal CYD-TVD vaccine for DENV should be able to minimize the harmful effects along with providing host responses that enhance immune protection and immune evasion. To maintain the proper balance between reactogenicity and immunity, the vital components in the CYD-TDV vaccine play an important role (Perng et al., 2011; Kirkpatrick et al., 2015), which remains a crucial yet biggest task to the vaccine development strategies.

Mitigation of the Risk of Autoimmunity

During current vaccine development strategies, the role of cross-reactive antibodies as mediators of DENV infection has not been the center of attention among the vaccine developers (Nikin-Beers and Ciupe, 2015). Thus, the cross-reactivity of these antibodies has not been considered as a part of the efficacy evaluation index in the clinical trials of CYD-TDV vaccines. However, the details of the protein sequencing in viral antigens eliciting autoimmunity have been well-documented (Perng et al., 2011). Moreover, the significant side effects can be lessened and safety profile of dengue vaccines can be enhanced by applying a strategy, which requires modification of viral genomes genetic code sequence and alteration of these determinants in these altered viral strains (Cheng et al., 2009; Perng et al., 2011).

Enhancement of the Efficacy of Antibody-Producing Plasma Cells

During vaccine development program, the significance of antibody-producing B cells is highly observed. Of the main strategies proposed to improve vaccine potential is the high survivability of plasma or memory B cells (Nothelfer et al., 2015). Furthermore, it has been determined that cysteine-rich interdomain region 1α (CIDR1α) of the *P. falciparum* can defend and save plasma cells from death. Hence, integrating CIDR1α as an additional component with live and/or attenuated dengue vaccines can improve the survivability and functional potential of the plasma cells (Perng et al., 2011).

Synthetic Nucleic Acid Antibody Immunotherapy

Since none of the current vaccines could provide a balanced protection against DENV, Flingai et al., reported that production of single intramuscular engineered DNA plasmids with human antiviral neutralizing antibodies (nAbs) protected murine models against antibody-modified DENV (Flingai et al., 2015). While the currently used vaccines produce traditional antibodies, the authors emphasized that plasmid-encoded LALA antibodies that defend against DENV and antibody-dependent enhancement (ADE)-induced disease can act as an alternative or become an incentive for traditional vaccine strategies. In fact, this synthetic nucleic acid immunotherapy can also be utilized for traveling

population to increase protection against viral infections and reduce the dengue epidemic (Flingai et al., 2015).

Challenges and Limitations to Dengue Prevention Strategies

Just as new strategies and vaccines are devised for prevention and control of DENV, there is always a gap left in the form of challenges and limitations for perfect implementation of such strategies (Achee et al., 2015). Since prevention and control strategies to counter dengue have not shown satisfactory results in reducing disease transmission, the utilization of vaccines as cost-effective and potential resistance has become the main priority to restore public health. However, the complicated immunopathology of dengue has perplexed the development of vaccines. These vaccines also confront various challenges, such as unavailability of suitable models for disease and the want for eligible markers of immunity protection (Ghosh and Dar, 2015).

CONCLUSION

As the pandemic outbreak of DENV continues to prevail in today's world, the development of safe, cost-effective, and potential preventive and control measures, including development of new and improved vaccines, evidently promise the reduction of dengue viral infection. As the strategies grow and are used in an integrated manner with other methods, advanced combinations have also predicted attenuation of vector population. Among the vaccines developed, the approbation of recombinant, live and attenuated tetravalent dengue vaccine has proved safe and tolerable, as well as protective against dengue. With more research and experimentation of novel methods and techniques, the future could enjoy better control with protective immunity to DENV.

AUTHOR CONTRIBUTIONS

IR wrote the paper and designed figure; HP, JBL, and WP. collected the literature; JL, VB, and YP. designed, analyzed approved the paper.

ACKNOWLEDGMENTS

This work was supported by National Research Foundation of Korea (2013M3A9A504705 and 2017M3A9A5048999).

REFERENCES

Abbas, A., Abbas, R. Z., Khan, J. A., Iqbal, Z., Bhatti, M. M. H., Sindhu, Z. U. D., et al. (2014). Integrated strategies for the control and prevention of dengue vectors with particular reference to *Aedes aegypti*. *Pak. Vet. J.* 34, 1–10. doi: 10.1097/QCO.0b013e3283638104

Achee, N. L., Gould, F., Perkins, T. A., Reiner, R. C., Morrison, A. C., Ritchie, S. A., et al. (2015). A critical assessment of vector control for dengue prevention. *PLoS Negl. Trop. Dis.* 9:e0003655. doi: 10.1371/journal.pntd.0003655

Alphey, L., Benedict, M., Bellini, R., Clark, G. G., Dame, D. A., Service, M. W., et al. (2010). Sterile-insect methods for control of mosquito-borne diseases: an analysis. *Vector Borne Zoonotic Dis.* 10, 295–311. doi: 10.1089/vbz.2009.0014

Araújo, H. R. C., Carvalho, D. O., Ioshino, R. S., Costa-da-Silva, A. L., and Capurro, M. L. (2015). *Aedes aegypti* control strategies in Brazil: incorporation of new technologies to overcome the persistence of dengue epidemics. *Insects* 6, 576–594. doi: 10.3390/insects6020576

Baly, A., Toledo, M. E., Boelaert, M., Reyes, A., Vanlerberghe, V., Ceballos, E., et al. (2007). Cost effectiveness of *Aedes aegypti* control programmes: participatory versus vertical. *Trans. R. Soc. Trop. Med. Hyg.* 101, 578–586. doi: 10.1016/j.trstmh.2007.01.002

Bhatt, S., Gething, P. W., Brady, O. J., Messina, J. P., Farlow, A. W., Moyes, C. L., et al. (2013). The global distribution and burden of dengue. *Nature* 496, 504–507. doi: 10.1038/nature12060

Boonchutima, S., Kachentawa, K., Limpavithayakul, M., and Prachansri, A. (2017). Longitudinal study of Thai people media exposure, knowledge, and behavior on dengue fever prevention and control. *J. Infect. Public Health* S1876–0341, 30051–30055. doi: 10.1016/j.jiph.2017.01.016

Capeding, M. R., Tran, N. H., Hadinegoro, S. R. S., Ismail, H. I. H. M., Chotpitayasunondh, T., Chua, M. N., et al. (2014). Clinical efficacy and safety of a novel tetravalent dengue vaccine in healthy children in Asia: a phase 3, randomised, observer-masked, placebo-controlled trial. *Lancet* 384, 1358–1365. doi: 10.1016/S0140-6736(14)61060-6

Carvalho, D. O., Costa-da-Silva, A. L., Lees, R. S., and Capurro, M. L. (2014). Two step male release strategy using transgenic mosquito lines to control transmission of vector-borne diseases. *Acta Trop.* 132, 1–8. doi: 10.1016/j.actatropica.2013.09.023

Cheng, H.-J., Lin, C.-F., Lei, H.-Y., Liu, H.-S., Yeh, T.-M., Luo, Y.-H., et al. (2009). Proteomic analysis of endothelial cell autoantigens recognized by anti-dengue virus nonstructural protein 1 antibodies. *Exp. Biol. Med.* 234, 63–73. doi: 10.3181/0805-RM-147

Dayan, G. H., Galán-Herrera, J. F., Forrat, R., Zambrano, B., Bouckenooghe, A., Harenberg, A., et al. (2014). Assessment of bivalent and tetravalent dengue vaccine formulations in flavivirus-naive adults in Mexico. *Hum. Vaccin. Immunother.* 10, 2853–2863. doi: 10.4161/21645515.2014.972131

DeRoeck, D., Deen, J., and Clemens, J. (2003). Policymakers' views on dengue fever/dengue haemorrhagic fever and the need for dengue vaccines in four southeast Asian countries. *Vaccine* 22, 121–129. doi: 10.1016/S0264-410X(03)00533-4

Dumont, Y., and Chiroleu, F. (2010). Vector control for the Chikungunya disease. *Math. Biosci. Eng.* 7, 313–345. doi: 10.3934/mbe.2010.7.313

Favia, G. (2015). Engineered mosquitoes to fight mosquito borne diseases: not a merely technical issue. *Bioeng. Bugs* 6, 5–7. doi: 10.4161/21655979.2014.988556

Flingai, S., Plummer, E. M., Patel, A., Shresta, S., Mendoza, J. M., Broderick, K. E., et al. (2015). Protection against dengue disease by synthetic nucleic acid antibody prophylaxis/immunotherapy. *Sci. Rep.* 5, 1–9. doi: 10.1038/srep12616

Fraser, M. J. (2012). Insect transgenesis: current applications and future prospects. *Annu. Rev. Entomol.* 57, 267–289. doi: 10.1146/annurev.ento.54.110807.090545

Gandhi, G., Chapla, J., Reddya Naik, B., and Gujju Gandhi, C. (2017). Data mapping of vector borne disease with geographical information system & global position system technology: in tribal areas Khammam District, Telangana State. *Int. J. Mosq. Res.* 39, 39–43.

George, L. S., Paul, N., and Leelamoni, K. (2017). Community based interventional study on dengue awareness and vector control in a rural population in Ernakulam, Kerala. *Int. J. Commun. Med. Public Health* 4, 962–967. doi: 10.18203/2394-6040.ijcmph20170984

Ghosh, A., and Dar, L. (2015). Dengue vaccines: challenges, development, current status and prospects. *Indian J. Med. Microbiol.* 33, 3–15. doi: 10.4103/0255-0857.148369

Ghosh, A., Chowdhury, N., and Chandra, G. (2012). Plant extracts as potential mosquito larvicides. *Indian J. Med. Res.* 135, 581–598.

Gómez-Dantés, H., and Willoquet, J. R. (2009). Dengue in the Americas: challenges for prevention and control. *Cad. Saúde Pública* 25, S19–S31. doi: 10.1590/S0102-311X2009001300003

Govindarajan, M., and Sivakumar, R. (2015). Laboratory evaluation of Indian medicinal plants as repellents against malaria, dengue, and filariasis vector mosquitoes. *Parasitol. Res.* 114, 601–612. doi: 10.1007/s00436-014-4222-0

Hadinegoro, S. R., Arredondo-García, J. L., Capeding, M. R., Deseda, C., Chotpitayasunondh, T., Dietze, R., et al. (2015). Efficacy and long-term safety of a dengue vaccine in regions of endemic disease. *N. Engl. J. Med.* 373, 1195–1206. doi: 10.1056/NEJMoa1506223

Han, W., Lazaro, A., McCall, P., and George, L. (2015). Efficacy and community effectiveness of larvivorous fish for dengue vector control. *Trop.Med. Int. Health* 20, 1239–1256. doi: 10.1111/tmi.12538

Heintze, C., Garrido, M. V., and Kroeger, A. (2007). What do community-based dengue control programmes achieve? A systematic review of published evaluations. *Trans. R. Soc. Trop. Med. Hyg.* 101, 317–325. doi: 10.1016/j.trstmh.2006.08.007

Jeffery, J. A. L., Thi Yen, N., Nam, V. S., Nghia, L. T., Hoffmann, A. A., Kay, B. H., et al. (2009). Characterizing the *Aedes aegypti* population in a vietnamese village in preparation for a wolbachia-based mosquito control strategy to eliminate dengue. *PLoS Negl. Trop. Dis.* 3:e552. doi: 10.1371/journal.pntd.0000552

Johnson, B., Ritchie, S., and Fonseca, D. (2017). The state of the art of lethal oviposition trap-based mass interventions for arboviral control. *Insects* 8:5. doi: 10.3390/insects8010005

Jupatanakul, N., Sim, S., Angleró-Rodríguez, Y. I., Souza-Neto, J., Das, S., Poti, K. E., et al. (2017). Engineered *Aedes aegypti* JAK/STAT pathway-mediated immunity to dengue virus. *PLoS Negl. Trop. Dis.* 11:e0005187. doi: 10.1371/journal.pntd.0005187

Kalimuthu, K., Panneerselvam, C., Chou, C., Tseng, L.-C., Murugan, K., Tsai, K.-H., et al. (2017). Control of dengue and Zika virus vector *Aedes aegypti* using the predatory copepod *Megacyclops formosanus*: synergy with *Hedychium coronarium*- synthesized silver nanoparticles and related histological changes in targeted mosquitoes. *Process Safety Environ. Protect.* 109, 82–96. doi: 10.1016/j.psep.2017.03.027

Kamtchum-Tatuene, J., Makepeace, B. L., Benjamin, L., Baylis, M., and Solomon, T. (2016). The potential role of Wolbachia in controlling the transmission of emerging human arboviral infections. *Curr. Opin. Infect. Dis.* 30, 108–116. doi: 10.1097/qco.0000000000000342

Kirkpatrick, B. D., Durbin, A. P., Pierce, K. K., Carmolli, M. P., Tibery, C. M., Grier, P. L., et al. (2015). Robust and balanced immune responses to all 4 dengue virus serotypes following administration of a single dose of a live attenuated tetravalent dengue vaccine to healthy, flavivirus-naive adults. *J. Infect. Dis.* 212, 702–710. doi: 10.1093/infdis/jiv082

Kittayapong, P., Yoksan, S., Chansang, U., Chansang, C., and Bhumiratana, A. (2008). Suppression of dengue transmission by application of integrated vector control strategies at sero-positive GIS-based foci. *Am. J. Trop. Med. Hyg.* 78, 70–76.

Koh, B. K. W., Lee, C. N., Kita, Y., Choon, S. T., Li, W. A., Kit, Y. W., et al. (2008). The 2005 dengue epidemic in Singapore: epidemiology, prevention and control. *Ann. Acad. Med. Singapore* 37, 538–545.

Lau, K. W., Chen, C. D., Lee, H. L., Norma-Rashid, Y., and Sofian-Azirun, M. (2015). Evaluation of insect growth regulators against field-collected *Aedes aegypti* and *Aedes albopictus* (Diptera: Culicidae) from Malaysia. *J. Med. Entomol.* 52, 199–206. doi: 10.1093/jme/tju019

Madeira, N. G., Macharelli, C. A., Pedras, J. F., and Delfino, M. C. N. (2002). Education in primary school as a strategy to control dengue. *Rev. Soc. Bras. Med. Trop.* 35, 221–226. doi: 10.1590/S0037-86822002000300004

Morrison, A. C., Gray, K., Getis, A., Astete, H., Sihuincha, M., Focks, D., et al. (2004). Temporal and geographic patterns of *Aedes aegypti* (Diptera: Culicidae) production in Iquitos, Peru. *J. Med. Entomol.* 41, 1123–1142. doi: 10.1603/0022-2585-41.6.1123

Nagpal, B. N., Ghosh, S. K., Eapen, A., Srivastava, A., Sharma, M. C., Singh, V. P., et al. (2015). Control of *Aedes aegypti* and *Ae. albopictus*, the vectors of dengue and chikungunya, by using pheromone C21 with an insect growth regulator: results of multicentric trials from 2007-12 in India. *J. Vector Borne Dis.* 52, 224–231.

Nam, V. S., Yen, N. T., Phong, T. V., Ninh, T. U., Mai, L. Q., Lo, L. V., et al. (2005). Elimination of dengue by community programs using Mesocyclops (copepoda) against *Aedes aegypti* in central Vietnam. *Am. J. Trop. Med. Hyg.* 72, 67–73.

Nikin-Beers, R., and Ciupe, S. M. (2015). The role of antibody in enhancing dengue virus infection. *Math. Biosci.* 263, 83–92. doi: 10.1016/j.mbs.2015.02.004

Nothelfer, K., Sansonetti, P. J., and Phalipon, A. (2015). Pathogen manipulation of B cells: the best defence is a good offence. *Nat. Rev. Microbiol.* 13, 173–184. doi: 10.1038/nrmicro3415

Ogaugwu, C. E., and Durvasula, R. V. (2017). "Developing the arsenal against pest and vector dipterans: inputs of transgenic and paratransgenic biotechnologies," in *Biological Control of Pest and Vector Insects*, ed V. D. C. Shields (Rijeka: InTech). doi: 10.5772/66440

Oliva, C. F., Jacquet, M., Gilles, J., Lemperiere, G., Maquart, P. O., Quilici, S., et al. (2012). The sterile insect technique for controlling populations of *Aedes albopictus* (Diptera: Culicidae) on Reunion Island: mating vigour of sterilized males. *PLoS ONE* 7:49414. doi: 10.1371/journal.pone.0049414

Ong, S.-Q., and Jaal, Z. (2015). Investigation of mosquito oviposition pheromone as lethal lure for the control of *Aedes aegypti* (L.) (Diptera: Culicidae). *Parasit. Vectors* 8, 28. doi: 10.1186/s13071-015-0639-2

Ooi, E. E., Goh, K. T., and Gubler, D. J. (2006). Dengue prevention and 35 years of vector control in Singapore. *Emerging Infect. Dis.* 12, 887–893. doi: 10.3201/eid1206.051210

Pan American Health Organization (2014). (PAHO). *Technical Note on Transgenic Mosquitoes Engineered for Aedes Aegypti Control*. Washington, DC. Available online at: http://www2.paho.org/hq/index.php?option=com_docman&task=doc_view&gid=28197&Itemid=1994

Pérez-Guerra, C. L., Zielinski-Gutierrez, E., Vargas-Torres, D., and Clark, G. G. (2009). Community beliefs and practices about dengue in Puerto Rico. *Rev. Panam. Salud Publica* 25, 218–226. doi: 10.1590/S1020-49892009000300005

Perng, G. C., Lei, H.-Y., Lin, Y.-S., and Chokephaibulkit, K. (2011). Dengue vaccines: challenge and confrontation. *World J. Vaccin.* 1, 109–130. doi: 10.4236/wjv.2011.14012

Pierre, D. Y., Okechukwu, E. C., and Nchiwan, N. E. (2014). Larvicidal and phytochemical properties of *Callistemon rigidus* R. Br. (Myrtaceae) leaf solvent extracts against three vector mosquitoes. *J. Vector Borne Dis.* 51, 216–223.

Qiao, M., Shaw, D., Forrat, R., Wartel-Tram, A., and Lang, J. (2011). Priming effect of dengue and yellow fever vaccination on the immunogenicity, infectivity, and safety of a tetravalent dengue vaccine in humans. *Am. J. Trop. Med. Hyg.* 85, 724–731. doi: 10.4269/ajtmh.2011.10-0436

Ramkumar, G., Karthi, S., Muthusamy, R., Natarajan, D., and Shivakumar, M. S. (2015). Adulticidal and smoke toxicity of *Cipadessa baccifera* (Roth) plant extracts against *Anopheles stephensi*, *Aedes aegypti*, and *Culex quinquefasciatus*. *Parasitol. Res.* 114, 167–173. doi: 10.1007/s00436-014-4173-5

Reis-Castro, L. (2012). Genetically modified insects as a public health tool: discussing the different bio-objectification within genetic strategies. *Croat. Med. J.* 53, 635–638. doi: 10.3325/cmj.2012.53.635

Sabchareon, A., Wallace, D., Sirivichayakul, C., Limkittikul, K., Chanthavanich, P., Suvannadabba, S., et al. (2012). Protective efficacy of the recombinant, live-attenuated, CYD tetravalent dengue vaccine in Thai schoolchildren: a randomised, controlled phase 2b trial. *Lancet* 380, 1559–1567. doi: 10.1016/S0140-6736(12)61428-7

Saldaña, M. A., Hegde, S., and Hughes, G. L. (2017). Microbial control of arthropod-borne disease. *Mem. Inst. Oswaldo. Cruz.* 112, 1–13. doi: 10.1590/0074-02760160373

Sandrasegaran, A. (2016). Primary prevention of dengue: a comparison between the problems and prospects of the most promising vector control and vaccination approaches. *Aust. Med. Stud. J.* 7, 51–54.

Sarathy, V. V., White, M., Li, L., Gorder, S. R., Pyles, R. B., Campbell, G. A., et al. (2015). A lethal murine infection model for dengue virus 3 in AG129 mice deficient in type I and II interferon receptors leads to systemic disease. *J. Virol.* 89, 1254–1266. doi: 10.1128/JVI.01320-14

Scarpino, S. V., Meyers, L. A., and Johansson, M. A. (2017). Design Strategies for efficient arbovirus surveillance. *Emerging Infect. Dis.* 23, 642–644. doi: 10.3201/eid2304.160944

Seng, C. M., Setha, T., Nealon, J., Socheat, D., Chantha, N., and Nathan, M. B. (2008). Community-based use of the larvivorous fish *Poecilia reticulata* to control the dengue vector *Aedes aegypti* in domestic water storage containers in rural Cambodia. *J. Vector Ecol.* 33, 139–144. doi: 10.3376/1081-1710(2008)33[139:CUOTLF]2.0.CO;2

Shriram, A. N., Sugunan, A. P., Manimunda, S. P., and Vijayachari, P. (2009). Community-centred approach for the control of *Aedes* spp. in a peri-urban zone in the Andaman and Nicobar Islands using temephos. *Natl. Med. J. India* 22, 116–20.

Simmons, C. P., Farrar, J. J., Nguyen, V. C., and Wills, B. (2012). Dengue. *N. Engl. J. Med.* 366, 1423–1432. doi: 10.1056/NEJMra1110265

Sin Leo, Y., Wilder-Smith, A., Archuleta, S., Shek, L. P., Chong, C. Y., Nam Leong, H., et al. (2012). Immunogenicity and safety of recombinant tetravalent dengue vaccine (CYD-TDV) in individuals aged 2–45 years. *Hum. Vaccin. Immunother.* 8, 1259–1271. doi: 10.4161/hv.21224

Swaminathan, S., and Khanna, N. (2010). Dengue vaccine - current progress and challenges. *Curr. Sci.* 98, 369–378.

Tapia-Conyer, R., Méndez-Galván, J., and Burciaga-Zú-iga, P. (2012). Community participation in the prevention and control of dengue: the patio limpio strategy in Mexico. *Paediatr. Int. Child Health* 32(Suppl. 1), 10–13. doi: 10.1179/2046904712Z.00000000047

Thomas, S. J. (2013). Dengue human infection model. *Hum. Vaccin. Immunother.* 9, 1587–1590. doi: 10.4161/hv.24188

Vanlerberghe, V., Toledo, M. E., Rodríguez, M., Gómez, D., Baly, A., Benítez, J. R., et al. (2010). Community involvement in dengue vector control: cluster randomised trial. *MEDICC Rev.* 12, 41–47. doi: 10.1136/bmj.b1959

Villar, L. Á., Rivera-Medina, D. M., Arredondo-García, J. L., Boaz, M., Starr-Spires, L., Thakur, M., et al. (2013). Safety and immunogenicity of a recombinant tetravalent dengue vaccine in 9–16 year olds a randomized, controlled, phase ii trial in Latin America. *Pediatr. Infect. Dis. J.* 32, 1102–1109. doi: 10.1097/INF.0b013e31829b8022

Villar, L., Dayan, G. H., Arredondo-García, J. L., Rivera-Medina, D. M., Cunha, R., Deseda, C., et al. (2015). Efficacy of a Tetravalent dengue vaccine in children in Latin America. *N. Engl. J. Med.* 372, 113–123. doi: 10.1056/NEJMoa1411037

Warbanski, M. L., Marques, P., Frauendorf, T. C., Phillip, D. A. T., and El-Sabaawi, R. W. (2017). Implications of guppy (*Poecilia reticulata*) life-history phenotype for mosquito control. *Ecol. Evol.* 7, 1–11. doi: 10.1002/ece3.2666

WHO (2012). *Global Strategy for Dengue Prevention and Control 2012–2020.* Geneva: World Health Organization.

Wilder-Smith, A., Renhorn, K. E., Tissera, H., Bakar, S. A., Alphey, L., Kittayapong, P., et al. (2012). Dengue tools: innovative tools and strategies for the surveillance and control of dengue. *Glob. Health Action* 5. doi: 10.3402/gha.v5i0.17273

Wilke, A. B. B., and Marrelli, M. T. (2015). Paratransgenesis: a promising new strategy for mosquito vector control. *Parasit. Vectors* 8, 342. doi: 10.1186/s13071-015-0959-2

Wong, J., Stoddard, S. T., Astete, H., Morrison, A. C., and Scott, T. W. (2011). Oviposition site selection by the dengue vector *Aedes aegypti* and its implications for dengue control. *PLoS Negl. Trop. Dis.* 5:e1015. doi: 10.1371/journal.pntd.0001015

Yakob, L., Funk, S., Camacho, A., Brady, O., and Edmunds, W. J. (2017). *Aedes aegypti* control through modernized, integrated vector management. *PLoS Curr.* 9:8747. doi: 10.1371/currents.outbreaks.45deb8e03a438c4d088afb4fafae8747

Conflict of Interest Statement: The authors declare that the research was conducted in the absence of any commercial or financial relationships that could be construed as a potential conflict of interest.

frontiers in Cellular and Infection Microbiology

ORIGINAL RESEARCH
published: 04 August 2017
doi: 10.3389/fcimb.2017.00356

DEAD-Box Helicase DDX25 Is a Negative Regulator of Type I Interferon Pathway and Facilitates RNA Virus Infection

*Tingting Feng, Ta Sun, Guanghao Li, Wen Pan, Kezhen Wang and Jianfeng Dai **

Jiangsu Key Laboratory of Infection and Immunity, Institute of Biology and Medical Sciences, Soochow University, Suzhou, China

Dengue is a mosquito-borne viral disease that rapidly spread in tropic and subtropic area in recent years. DEAD (Glu-Asp-Ala-Glu)-box RNA helicases have been reported to play important roles in viral infection, either as cytosolic sensors of viral nucleic acids or as essential host factors for the replication of different viruses. In this study, we reported that DDX25, a DEAD-box RNA helicase, plays a proviral role in DENV infection. The expression levels of DDX25 mRNA and protein were upregulated in DENV infected cells. During DENV infection, the intracellular viral loads were significantly lower in *DDX25* silenced cells and higher in *DDX25* overexpressed cells. Meanwhile, the expression level of type I interferon (IFN) was increased in *DDX25* siRNA treated cells during viral infection. Consistent with the *in vitro* findings, the *Ddx25*-transgenic mice have an increased susceptibility to lethal vesicular stomatitis virus (VSV) virus challenge. The viremia was significantly higher while the anti-viral cytokine levels were lower in *Ddx25*-transgenic mice. Further, DDX25 modulated RIG-I signaling pathway and blocked IFNβ production, by interrupting IFN regulatory factor 3 (IRF3) and NFκB activation. Thus, DDX25 is a novel negative regulator of IFN pathway and facilitates RNA virus infection.

Keywords: DDX25, interferon, innate immune response, dengue virus, IRF3, NFκB

OPEN ACCESS

Edited by:
Shelton S. Bradrick, University of Texas Medical Branch, United States

Reviewed by:
Kui Li, University of Tennessee Health Science Center, United States
Alan G. Goodman, Washington State University, United States

****Correspondence:***
Jianfeng Dai
daijianfeng@suda.edu.cn

Received: *19 April 2017*
Accepted: *25 July 2017*
Published: *04 August 2017*

Citation:
Feng T, Sun T, Li G, Pan W, Wang K and Dai J (2017) DEAD-Box Helicase DDX25 Is a Negative Regulator of Type I Interferon Pathway and Facilitates RNA Virus Infection. Front. Cell. Infect. Microbiol. 7:356. doi: 10.3389/fcimb.2017.00356

INTRODUCTION

Dengue virus (DENV) is a mosquito-borne viral pathogen, which is mainly transmitted by *Aedes aegypti* and *Aedes albopicuts*. Dengue imposes a significant burden on human health around the world and is endemic in more than 100 countries in tropical and subtropical areas, especially in Southeast Asia, the Americas, the Western Pacific, Africa, and Eastern Mediterranean regions (Guzman and Harris, 2015). Currently, there is no effective treatment for DENV infections. The first DENV vaccine was recently licensed for use after several decades of efforts, unfortunately, it confers only partial protection to all DENV serotypes (Gan, 2014; Thisyakorn and Thisyakorn, 2014).

Viruses have limited genetic capacity and as such rely on cellular factors to complete their life cycle. Thus, viruses interact with cellular proteins to acquire activities not encoded in the viral genome, to evade host immune defenses, and to manipulate cellular pathways to facilitate their replication (Khadka et al., 2011). However, while viruses attempt to hijack host cell machinery, the host cells attempt to halt, or slow down viral efficacy. DENV infection would normally activate the

host antiviral response, in which the type I interferon pathway is crucial for host natural immunity. RNA helicases of DEAD-box protein family modulate the RNA structure and are crucial in many fundamental biological processes (de la Cruz et al., 1999; Rocak and Linder, 2004; Jankowsky, 2010). In addition to the traditional functions in RNA metabolism, DEAD-box RNA helicases have been reported as mediators of anti-viral innate immunity, or essential host factors for viral replication (Steimer and Klostermeier, 2012; Fullam and Schroder, 2013). Thus, DEAD-box RNA helicases family members play either a proviral or antiviral role during viral infection.

DDX3 is one of the first host cell DEAD-box RNA helicases identified as flavivirus cofactor, which is important for replication of viral RNA (Ariumi et al., 2007). For example, DDX3 colocalizes with NS3 near the nucleus during West Nile virus infection (Chahar et al., 2013). Another cellular helicase, DDX1 can directly bind to poly (I:C) (Zhang et al., 2011a). DDX21 and DHX36 are located downstream of DDX1 and both DDX21 and DHX36 interact with the downstream protein TIR-domain-containing-adapter-inducing interferon-β (TRIF). This suggests that DDX1 senses dsRNA and then triggers signaling via DDX21 and DHX36 to TRIF (Zhang et al., 2011a). DDX1 has also been reported to be important for the human immunodeficiency virus type 1 (HIV-1) replication as it binds to and serves as a cofactor of the HIV-1 Rev protein (Fang et al., 2004). DDX41 binds to STING (stimulator of interferon genes), which are located on the endoplasmic reticulum membrane (Zhang et al., 2011b; Parvatiyar et al., 2012).

In our previous study, 40 genes of DEAD-box family were screened using the RNAi approach to identify the putative host factors for DENV infection. Our result showed host DDX family members, DDX3X and DDX25, played an antiviral and a proviral role respectively during DENV infection (Li G. et al., 2015). DDX25, also named as Gonadotropin-regulated testicular RNA helicase (GRTH), is well-known as an essential testis-specific protein for completion of spermatogenesis in mouse model (Kavarthapu and Dufau, 2015). The expression profile and the role of DDX25 during viral infection has not been reported yet. We here reported that DDX25 interrupts the IFN-signaling pathway by inhibiting IRF3 and NFκB activation, which negatively regulated IFNβ activity, thereby facilitates RNA virus infection.

MATERIALS AND METHODS

Ethics Statements and Mice

C57BL/6 adult wild type mice (ages 6–8 week) were purchased from Shanghai Laboratory Animal Center (Shanghai, China). C57BL/6-*Ddx25* transgenic mice (*Ddx25*-Tg) were produced by Shanghai Biomodel Organism Science & Technology Development Co., Ltd. (Shanghai, China). Microinjections and mouse transgenesis experiments were performed by inserting CAG-*Ddx25*-IRES-Luciferase-polyA plasmid into the genome of fertilized egg of C57BL/6 mice using a PiggyBAC Transposon system. Mice were genotyped by tails snips and PCR at 3 weeks of age. The genotyping primers were TCCAAGGGG CACCGAAGTCACCAA (forward), and GCGCCGGGCCTT TCTTTATGTTTT (reverse).

All mice were housed in specific pathogen free facilities in accordance with the Guide of National Animal Care and Use committee. All animal experiments were approved by the Institutional Laboratory Animal Care and Use Committee of Soochow University.

Virus, Tissues, Cell Culture, and Infection

DENV-2 virus (DENV New Guinea C stain) were propagated in mosquito C6/36 cells (ATCC® CRL-1660). Sendai virus (SeV) was propagated in 10 days old embryonated chicken eggs (Bejing Laboratory Animal Research Center, Beijing, China), and the virus titer was detected by hemagglutination assay using chicken red blood cells (BeNa Culture Collection, Bejing, China). The VSV and VSV-green fluorescent protein (GFP) virus that expresses GFP as a non-structural protein was provided by Dr. Chunsheng Dong (Soochow University). The VSV-GFP virus was grown on a Vero E6 cell in Dulbecco's modified Eagle's medium (Invitrogen, Carlsbad, CA) containing 2% fetal bovine serum, titrated in Vero E6 cells.

The HEK293T cells were cultured in Dulbecco's modified eagle medium supplemented with fetal bovine serum (10%) and penicillin/streptomycin (1%). Cells were maintained at 37°C in a 5% CO_2 laboratory incubator that was routinely cleaned and decontaminated. HEK293T cells were infected with DENV, SeV, or VSV-GFP at a multiplicity of infection (MOI) of 1, unless otherwise stated.

For *in vivo* VSV intranasal infections, 1×10^6 *pfu* of VSV in 50 μl of endotoxin-free PBS were inhaled by isoflurane-anesthetized C57BL/6 wild type and *Ddx25*-Tg mice, with PBS-only as control. Thereafter, mice were monitored daily for weight loss and symptoms of disease.

Human tumor tissue samples were obtained from the First Affiliated Hospital of Soochow University (Suzhou, China) under institutional guidelines and used in gene expression analysis.

Plasmid Constructs

Recombinant plasmid for DDX25 expression was constructed using standard protocols by inserting the *DDX25* open reading frame into the pcDNA3.1 vector. Reporter plasmids NFκB-luc and pRL-TK were purchased from Clontech (USA) and used for dual luciferase reporter assays. Luciferase reporter plasmids IFNβ-luc, IRF3-luc, and ISRE-luc were kindly provided by Dr. Rongtuan Lin, McGill University, Canada (Zhao et al., 2007).

siRNA and Transfections

Transfections of HEK293T cells with plasmid DNA and siRNA were conducted using Lipofectamine 2000 (Invitrogen, USA) according to the manual of the manufacturer. The siRNA sequences for human *DDX25* gene were target I-GCAGCTAAT TCACTCTTAA, target II-GCAATGTTAAGCAGAGTTA, and target III-GCCACCAGGTGTCTTTGTT, respectively (RiboBio Co., Guangzhou, China). RNAi efficiency was confirmed through quantitative reverse transcription polymerase chain reaction (qRT-PCR). Then, the cells were infected with DENV at an MOI

of 1 for 48 h (except for the cases noted in the text) to test the influence of DDX25 silencing on DENV replication.

$TCID_{50}$ Assay and Viral Growth Kinetics

The cell-free supernatants were collected and the titers of DENV and VSV were assayed with a $TCID_{50}$ assay according to standard protocols on Vero cells (ATCC® CCL-81) as described previously (Wang et al., 2016). The viral replication levels inside cells, in terms of the transcript levels of the DENV-2 envelop gene (E) or VSV glycoprotein gene (G), were quantified by qRT-PCR and normalized to *β-actin* gene.

RNA Isolation and Real-Time PCR

Total RNA was isolated using an RNA extraction Kit (Omega, Netherlands) and reverse-transcribed into cDNA using the first strand cDNA Synthesis Kit (Takara, Japan). qRT-PCR was performed using a SYBR Green with gene-specific primers (Applied Biosystems, USA) and normalized to *β-actin* gene. (oligo-primer sequences for qRT-PCR of this study were shown in Table S1 in the Supplemental Materials).

Luciferase Reporter Assays

For luciferase reporter assays, 70% confluent HEK293T cells were transfected with 10 ng of pRL-TK reporter plasmid (herpes simplex virus thymidine kinase promoter driving *Renilla* luciferase, internal control), 100 ng of IFNβ luciferase reporter plasmid (firefly luciferase, experimental reporter), 50 ng of IFNβ activators (RIG-IN, MAVS, TBK1, IKKε, IKKα, NFκB, or IRF3), as well as either 100 ng of recombinant expressing plasmids or siRNAs [Vector, DDX25, 50 nM negative control (N.C.), or DDX25 siRNA]. For measuring the activation of transcription factor NFκB and IRF3, NFκB and IRF3 responsive element specific reporter plasmids were used in the luciferase reporter assays. Subconfluent HEK293T cells were transfected with 10 ng of pRL-TK reporter, 100 ng of NFκB (pNFκB-Luc), or IRF3 (pPRD(III–I)-Luc) luciferase reporter plasmid, various doses of recombinant expression plasmids (Vector or DDX25), along with 50 ng of expression plasmids of RIG-IN. At 24 h post-transfection, cells were infected with DENV-2 at an MOI of 1 and incubated further for 24 h. Luciferase activity was measured using a Promega Dual Glow Kit according to the instructions of the manufacturer (Promega, USA).

Immunofluorescence Microscopy

HEK293T cells were transfected with siRNA (N.C. or DDX25 siRNA) using Lipofectamine 2000 to examine the effect of DDX25 silencing on DENV infection. At 24 h post-transfection, cells were infected with DENV-2 at an MOI of 1. Cells were fixed in 1% paraformaldehyde and permeabilized with 1% Triton X100 at 48 h post-infection. DENV envelope proteins were probed with mouse anti-DENV E antibody (Santa Cruz, USA) and stained with FITC-labeled anti-mouse IgG (Jackson ImmunoResearch). Cell nuclei were stained with DAPI. Cells were then examined using a fluorescence microscope.

Western Blot

HEK293T Cells were transfected with pcDNA-DDX25 (or pcDNA3.1 vector) and infected with DENV-2 at an MOI of 10. At 24 h post-infection, cell lysates were subjected to SDS-PAGE and transferred onto a PVDF membrane for western blotting. Non-reducing native PAGE was performed to detect the dimerization of IRF3. Briefly, cell lysates were prepared in a native sample buffer without SDS and electrophoresed on a 10% non-reducing polyacrylamide gel without SDS.

The following primary antibodies were used for western blotting: anti-human Actin polyclonal Ab (Proteintech, USA), His-tag polyclone antibody (GenScript, USA), IRF3 polyclonal antibody (Biolegend, USA), anti-IRF3 (phospho S386) Ab (Cell Signaling, USA). HRP-conjugated donkey anti-rabbit IgG and rabbit anti mouse IgG mAb (Biolegend, USA) were used as secondary antibodies. The signals were detected using an ECL detection system (Merck Millipore Ltd., USA).

Enzyme-Linked Immunosorbent Assay (ELISA)

The protein concentrations of IFNβ and TNFα in VSV infected mouse serum samples were measured by ELISA Kits according to the instructions of the manufacturer (R&D Systems).

Histopathology

Two days post VSV infection, wild type and *Ddx25*-Tg mice were sacrificed and the lung tissues were fixed in 10% formalin and paraffin embedded. Hematoxylin and eosin (H&E) staining was conducted for histopathology.

Statistical Analysis

Statistical significances were calculated with an unpaired two tailed Student's *t*-test and Log-rank (Mantel-Cox) Test (for survival data only) using Prism 5 software (GraphPad).

RESULTS

DDX25 Is Upregulated upon DENV Infection

In mice, *Ddx25* was reported to be highly expressed in testis and critical for the process of spermatogenesis (Sheng et al., 2003). Contrastingly, by searching the gene expression database, we have found that human *DDX25* mRNA was expressed in almost all the human tissues (data from database of GTEx, BioGPS, Illumina Human BodyMap, and SAGE). Human DDX25 proteins are also detected in multiple tissues, such as testis, spleen, tonsil, ovary, and retina, as well as various cell lines including A549, HEK293T, SNB-75, JUNKAT, and H1734 cells (The Human Integrated Protein Expression Database, Integrated protein expression data from ProteomicsDB, PaxDb, MaxQB, and MOPED).

We further confirmed the mRNA expression profile of human *DDX25* gene by qRT-PCR. As shown in **Figure 1A**, *DDX25* mRNA is expressed in a wide range of human tissues. With the exception of breast tissue, *DDX25* is expressed in all seven tested tissues, with the highest expression in the kidney (**Figure 1A**).

We further noted an increased *DDX25* expression in human cell line HEK293T, A549, and K562 during DENV infection. Consistently, the protein level of DDX25 was also significantly induced in cells infected with DENV (**Figure 1B**). We further investigated the cellular distribution of DDX25 in HEK293T cells before and after DENV infection. Interestingly, DDX25

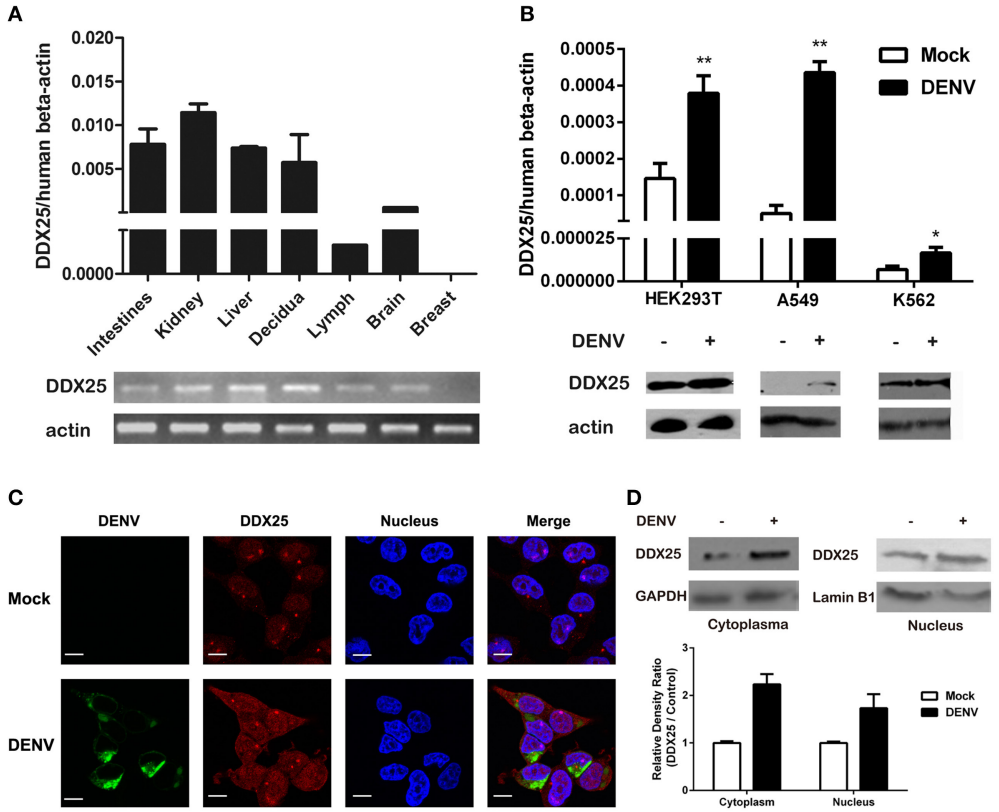

FIGURE 1 | Human DDX25 is ubiquitously expressed and upregulated after DENV infection. **(A)** qRT-PCR and electrophoresis analysis of *DDX25* expression in various human tissues. Human *β-actin* was used as an internal control. **(B)** The qRT-PCR and immunoblots analysis of DDX25 expression in HEK293T, A549, and K562 cells before and after DENV infection. **(C)** Microscopic images of immunofluorescence staining for expression and subcellular distribution of DDX25 in HEK293T with or without DENV infection. (MOI of 1 for 24 h). Scale bars, 10 μm. **(D)** Immunoblots analysis of DDX25 expression in the cytoplasm and nucleus before and after DENV infection. The relative gray density of immunoblots bands (DDX25/β-actin) was analyzed by ImageJ software. Results were expressed as the mean + the SEM. $^{*}p < 0.05$ and $^{**}p < 0.01$ (*t*-test). Representative results from at least three independent experiments.

expression was upregulated both in cytoplasm and nucleus (**Figures 1C,D**). These data demonstrate that DDX25 may have a low basal level of expression in multiple tissues and cells, and can be upregulated upon DENV infection.

DDX25 Promotes Virus Replication

Our previous studies of RNAi screening against DDX family demonstrated that DDX25 could be a proviral factor for DENV infection in HEK293T cells (Li G. et al., 2015). To confirm the role of endogenous DDX25 in DENV replication, endogenous DDX25 expression was silenced using RNAi approach. SiRNAs that targeting *DDX25* significantly reduced *DDX25* mRNA expression compared with cells transfected with scramble siRNA (N.C.) (**Figure 2A**). Cell viability was not affected after siRNA transfection, as tested through Promega Cell Viability Assay (**Figure 2B**). Silencing *DDX25* with three individual or pooled siRNAs significantly impaired DENV replication at 24 h post-infection (**Figure 2C**) [The intracellular viral loads were determined by measuring the transcript levels of the DENV envelop gene (E) and normalized to human *β-actin*]. Further experiment confirmed that the DENV viral load were decreased by ∼2 to 4-fold ($p < 0.05$) in *DDX25*-silenced cells compared with control cells after DENV infection at 12, 24, and 48 h, respectively (**Figure 2D**). Similar results were observed in *DDX25* silenced K562 cells infected with DENV (Data not shown). In line with this, immunofluorescence assay showed DENV viral burden [as determined by staining of viral envelop (E) protein] were decreased in *DDX25* silenced cells (**Figure 2E**). Conversely, we noted a ∼4-fold increase in viral load in *DDX25* overexpressing HEK293T cell at 48 h post-infection (**Figure 2F**). Consistently, the titers of DENV in cell supernatants, as determined by $TCID_{50}$ assay, were significantly higher in DDX25 overexpressed cells (**Figure 2G**). Moreover, we observed elevated viral loads in DDX25 overexpressing HEK293T cells after infection with VSV-GFP virus (**Figures 2H–J**). Overall, these data suggest that DDX25 could promote DENV and VSV replication.

DDX25 Regulates IFNβ Production

The aforementioned results clearly demonstrate the importance of DDX25 in promoting DENV infection *in vitro*. We next evaluated whether DDX25 influence the immune response to

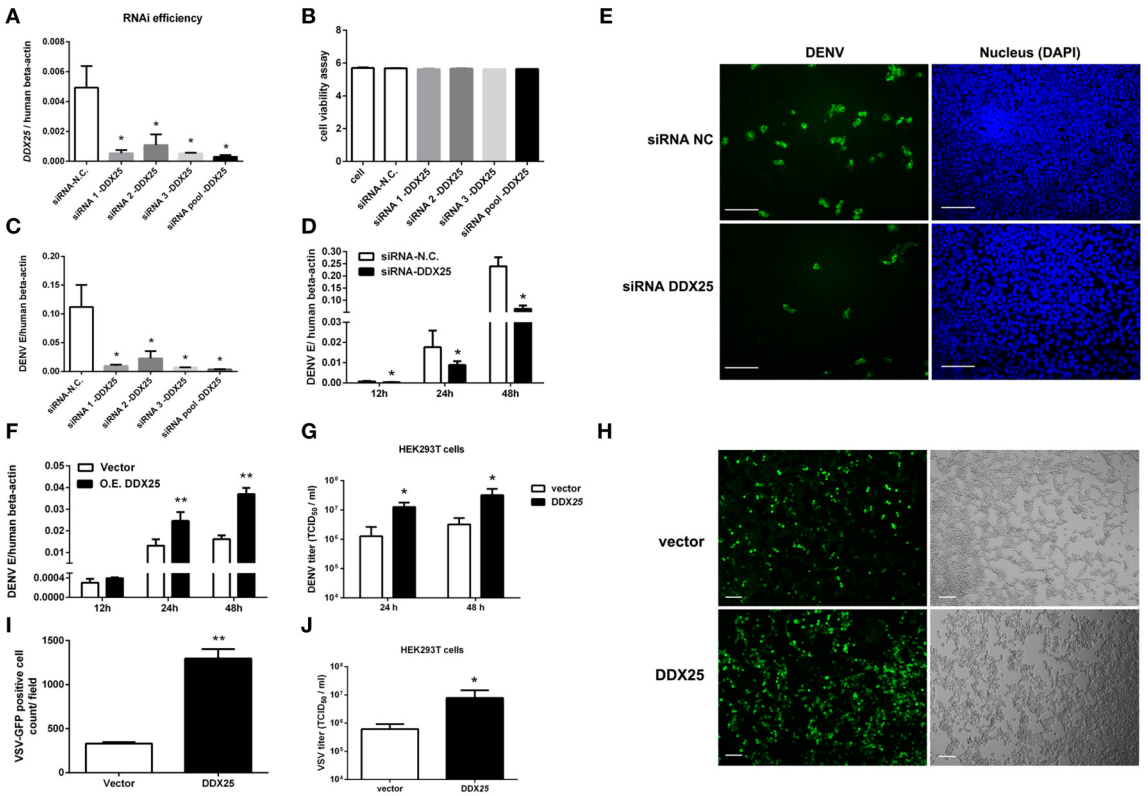

FIGURE 2 | DDX25 promotes virus replication. **(A)** The RNAi efficiency of three individual or pooled siRNAs that targeting *DDX25* were tested in transfected HEK293T cells by qRT-PCR. **(B)** RNAi of *DDX25* showed no cytotoxic effect to HEK 293T cells (Measured by Cell Viability assay, Promega). **(C)** DENV viral loads in *DDX25* siRNAs (or NC siRNA) treated HEK293T cells at 24 h post DENV infection (MOI of 1). The viral burdens were analyzed by measuring the virus E gene copy using qRT-PCR, and normalized to human *β-actin*. **(D)** DENV viral loads in *DDX25* siRNA (or NC siRNA) treated HEK293T cells at 12, 24, and 48 h post DENV infection (MOI of 1). **(E)** Microscopic images of immunofluorescence staining for DENV E antigen in *DDX25* siRNA (or NC siRNA) treated HEK293T after DENV infection for 24 h (MOI of 1). Scale bars, 100 μm. **(F)** qRT-PCR analysis of DENV viral loads in HEK293T cells with or without DDX25 overexpression at 12, 24, and 48 h post DENV infection. **(G)** Viral titers in supernatants of DENV infected HEK293T cells determined by $TCID_{50}$ assay on Vero cells. **(H,I)** Fluorescence microscopy analysis of VSV-GFP infection of HEK293T cells transfected with vector or DDX25 plasmid. Viral infection rates were indicated with GFP signal and quantified with ImageJ software. Scale bars, 100 μm. **(J)** VSV titers in supernatants of HEK293T cells infected with VSV-GFP (MOI of 1) at 24 h. Results were expressed as the mean + the SEM. $^*p < 0.05$ and $^{**}p < 0.01$ (*t*-test). Representative results from at least three independent experiments.

viral infection. The mRNA expression of *IFNβ* was increased by 1.5- and 1.4-fold at 24 and 48 h post DENV infection respectively, in *DDX25* silenced cells compared with controls (**Figure 3A**). *DDX25* silencing also enhanced the IFNβ promoter-driven luciferase (IFNβ-Luc) expression in HEK293T cells infected with other RNA viruses, such as VSV and sendai virus (SeV) (**Figure 3B**). Conversely, we noted a decreased *IFNβ* mRNA level on 24 h in DDX25-overexpressed HEK293T cells post DENV infection (**Figure 3C**). While, at 48 h post-infection, the *IFNβ* mRNA level was increased in DDX25 overexpressed cells (**Figure 3C**). We hypothesized that this was due to the expansion of DENV burdens in those cells at the late time point, which induced more IFNs that DDX25 could not fully suppressed. Consistent with the qPCR results, overexpression of DDX25 could decrease the transcription of IFNβ-Luc reporter after DENV (**Figure 3D**) and other RNA virus infection (**Figure 3E**). These results suggest that DDX25 negatively regulates innate immune-signaling processes and suppress type I IFN production during virus infection.

DDX25 Transgenic Mice Were More Susceptible to RNA Virus Infection

DDX25 null mice are sterile due to a defect in spermiogenesis (Tsai-Morris et al., 2004). So we constructed *Ddx25*-Tg mice that overexpress DDX25 to identify the role of *Ddx25* in virus infection *in vivo* (**Figure 4A**). Since immunocompetent wild-type mice do not show dengue hemorrhagic fever-like symptoms upon DENV infection, we used a VSV-infection mouse model to evaluate the importance of DDX25 in RNA viral infection *in vivo*. Consistent with the *in vitro* data, the *Ddx25* mRNA in total blood cells was upregulated after VSV virus infection in wild type mice (**Figure 4B**). Wild-type (W.T.) and *Ddx25*-Tg mice were infected intranasally with a lethal dose of VSV (1×10^6 *pfu*). All infected *Ddx25*-Tg mice show increased body weight loss compared with wide type controls (**Figure 4C**). Approximately 90% of *Ddx25*-Tg mice died within 10 days post-infection (**Figure 4D**), while only 40% of the wide type control mice died due to the VSV infection. This suggested that *Ddx25*-Tg mice are more susceptible to VSV infection. The viremia, in terms of the copy number of VSV

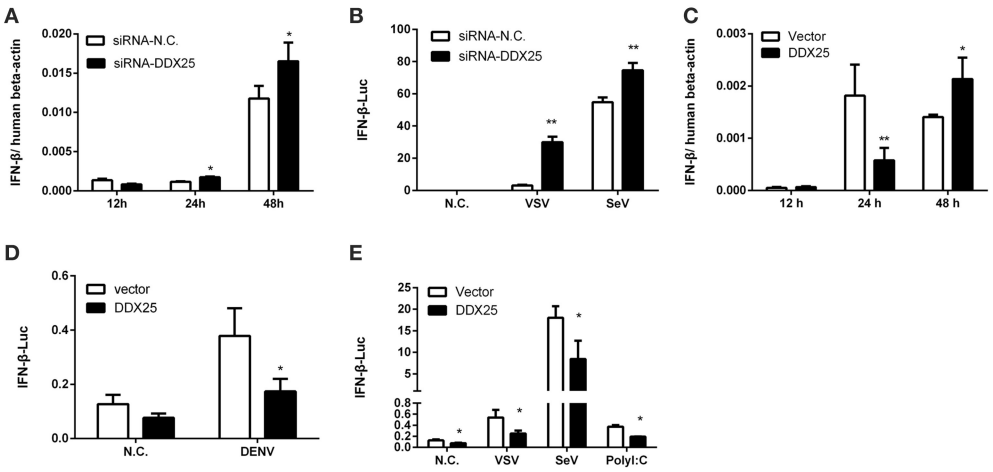

FIGURE 3 | DDX25 negatively regulates IFNβ production. **(A)** qRT-PCR analysis of the mRNA levels of IFNβ in HEK293T cells with *DDX25* RNAi during DENV infection for 12, 24, and 48 h. **(B)** VSV and SeV induced IFNβ transcriptional activities were enhanced in *DDX25* silenced HEK293T cells compared to controls. **(C)** qRT-PCR analysis of the mRNA levels of *IFNβ* in control and *DDX25* overexpressed HEK293T cells during DENV infection for 12, 24, and 48 h. **(D,E)** Luciferase reporter assay of IFNβ transcriptional activity in *DDX25* overexpressed HEK293T cells during DENV **(D)**, VSV, SeV, and Poly I:C **(E)** stimulation. Results were expressed as the mean + the SEM. $^{*}p < 0.05$ and $^{**}p < 0.01$ (*t*-test). Representative results from at least three independent experiments.

glycoprotein gene (VSV-G) in blood cells and infectious viral particles in serum, were significantly higher in *Ddx25*-Tg mice compared with W.T. mice at day 1 and day 3 after infection. We also found that VSV titers were higher in the liver, kidney, and spleen of *Ddx25*-Tg mice than in those organs of W.T. mice (**Figure 4E**). Meanwhile, the mRNA expression of *Ifnα*, *Ifnβ*, *Ifnγ, Tnfα,* and selective chemokines (*Cxcl1*, *Cxcl2*, and *Ccl5*) by leukocytes was lower in the blood of *Ddx25*-Tg mice on day 1 post-infection (**Figure 4F**). The IFNβ and TNFα proteins in the serum were also significantly lower in *Ddx25*-Tg mice compared with those in controls (**Figure 4G**). While, *Ifnα* and *Ifnβ* expression on day 3 post-infection were increased in *Ddx25*-Tg mice, this may be the secondary effect of the increased viremia (**Figure 4H**). The protein levels of IFNβ and TNFα were consistent with their mRNA levels (**Figure 4I**). Histological analysis by H&E staining indicated that the bronchial lumen and alveolar both exhibit healthy integrity in the non-infected W.T. and *Ddx25*-Tg mice. However, the W.T. mice infected virus displayed mucosal edema, inflammatory cell infiltration (submucosal and mucosal layers), as well as the increased number of eosinophils (EOS) in the airway walls. Compared to the virus infected W.T. mice group, a significantly increased inflammatory cell infiltration and serious immunopathological tissue damage were observed in VSV infected *Ddx25*-Tg mice (**Figure 4J**). These data suggested that DDX25 could promote RNA virus infection and suppress *Ifnβ* and other cytokines production *in vivo*.

DDX25 Inhibits IFN Production by Interrupting IRF3 and NFκB Activation

We next sought to understand how DDX25 suppresses of IFNβ induction. Particularly, RNA recognition by RIG-I emanates an activation signal that is passed on sequentially to mitochondrial antiviral signaling protein (MAVS), TBK1, IKKε, IRF3, and IRF7 (Sharma et al., 2003; Liu et al., 2015; Yoneyama et al., 2015). Therefore, the action point of DDX25 can be determined by assessing its suppressive effects on a series of transducer proteins. As the first step, we chose to evaluate the impact of DDX25 on the IFN-inducing activity of RIG-I-signaling pathway components, including the active caspase recruitment domain (CARD) containing form of RIG-I (RIG-IN), MDA5, MAVS, TBK1 kinase, and the active form of IRF3 (IRF3/5D) (Lin et al., 1998), or IKKα and p65. DDX25-expressing plasmids, together with one of the IFN pathway activators, RIG-IN, MDA5, MAVS, TBK1, IRF3/5D, IKKα, or p65, were co-transfected into HEK293T cells. All the expression constructs of IFN pathway activators induced an IFNβ-Luc or NFκB-Luc reporter activity. Interestingly, DDX25 was found to potently inhibit IFNβ-Luc activity induced by RIG-IN, MDA5, MAVS, TBK1, and IRF3/5D (**Figure 5A**), as well as NFκB-Luc reporter activity induced by RIG-IN, IKKα and p65 (**Figure 5B**). These results indicate that DDX25 inhibits the IFN antiviral response at or downstream of IRF3 and NFκB.

To further validate the step in which DDX25 inhibits IRF3 and NFκB activation, IRF3 and NFκB-specific luciferases activity were induced by coexpression of RIG-IN. In the presence of DDX25, the IRF3 and NFκB activities induced by RIG-IN were reduced in a DDX25 dose-dependent manner (**Figures 5C,D**), which imply that DDX25 inhibits both IRF3 and NFκB transcriptional activity directly.

IRF3 and NFκB activation requires the association of distinct signaling molecules (Baeuerle and Baichwal, 1997; Barnes and Karin, 1997). Phosphorylation of IRF3 induces a conformational change, leading to IRF3 dimerization and nuclear translocation. While activation of the NFκB is initiated by the signal-induced degradation of IκB proteins. IκB proteins mask the nuclear localization signals (NLS) of NFκB proteins and keep them

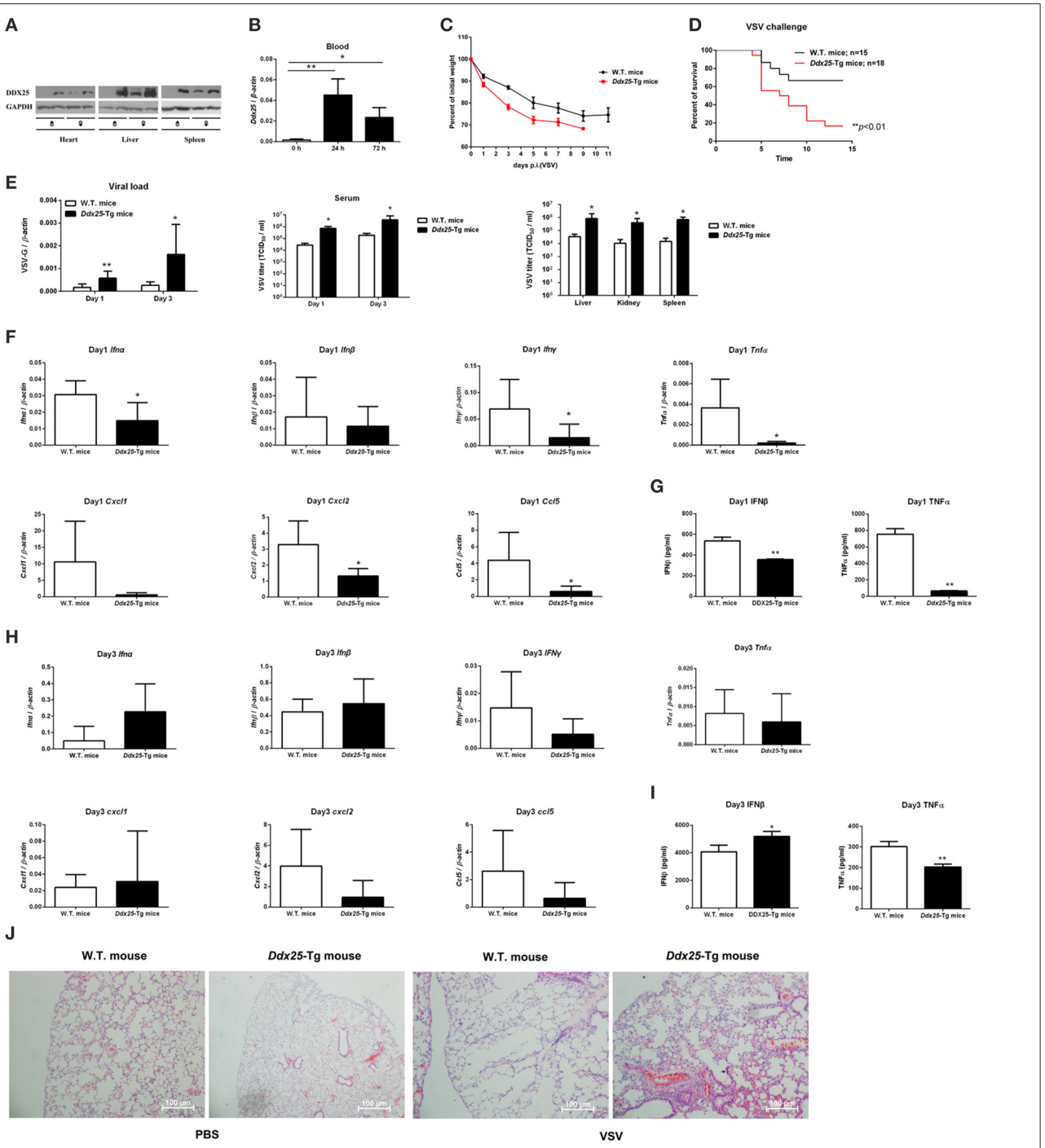

FIGURE 4 | Exacerbated VSV pathogenesis in *Ddx25* transgenic mice. Seven to eight weeks old, sex-matched, C57BL/6 (W.T.), and *Ddx25*-Tg mice were challenged with VSV (1×10^6 *pfu*/mouse). **(A)** Immunoblots of DDX25 in various tissues of W.T. and *Ddx25*-Tg mice, suggesting the evaluated expression of DDX25 in *Ddx25*-Tg mice. **(B)** qRT-PCR quantification of *Ddx25* mRNA in whole blood cells of wild type (W.T.) mice during VSV infection for 0, 24, and 72 h. **(C,D)** Changes in body weight **(C)** and survival rate **(D)** of W.T., *Ddx25*-Tg mice infected VSV, as monitored daily until days 11 and 14 post-infection, respectively. **(E)** VSV titers in the blood and tissue lysates of liver, kidney, and spleen from infected mice were measured via qRT-PCR and $TCID_{50}$ assay. **(F–I)** The expression levels of the selective cytokines/chemokines (*Ifnα*, *Ifnβ*, *Ifnγ*, *Cxcl1*, *Cxcl2*, *Ccl5*, and *Tnfα*) in total leukocytes of W.T. and *Ddx25*-Tg mice ($N = 10$ each) at day 1 **(F,G)** and day 3 **(H,I)** post-infection. Expression levels of mRNAs were determined by qRT-PCRs **(F,H)**. Protein levels of IFNβ and TNFα in serums at day 1 **(G)** and day 3 **(I)** were determined by ELISA. Results were expressed as the mean + the SEM. $^*p < 0.05$ and $^{**}p < 0.01$ (*t*-test). Representative results from at least three independent experiments. **(J)** H&E staining of lung tissues of W.T. and *Ddx25*-Tg mice at 2 days post mock infection (PBS) or VSV infection. Scale bars, 100 μm.

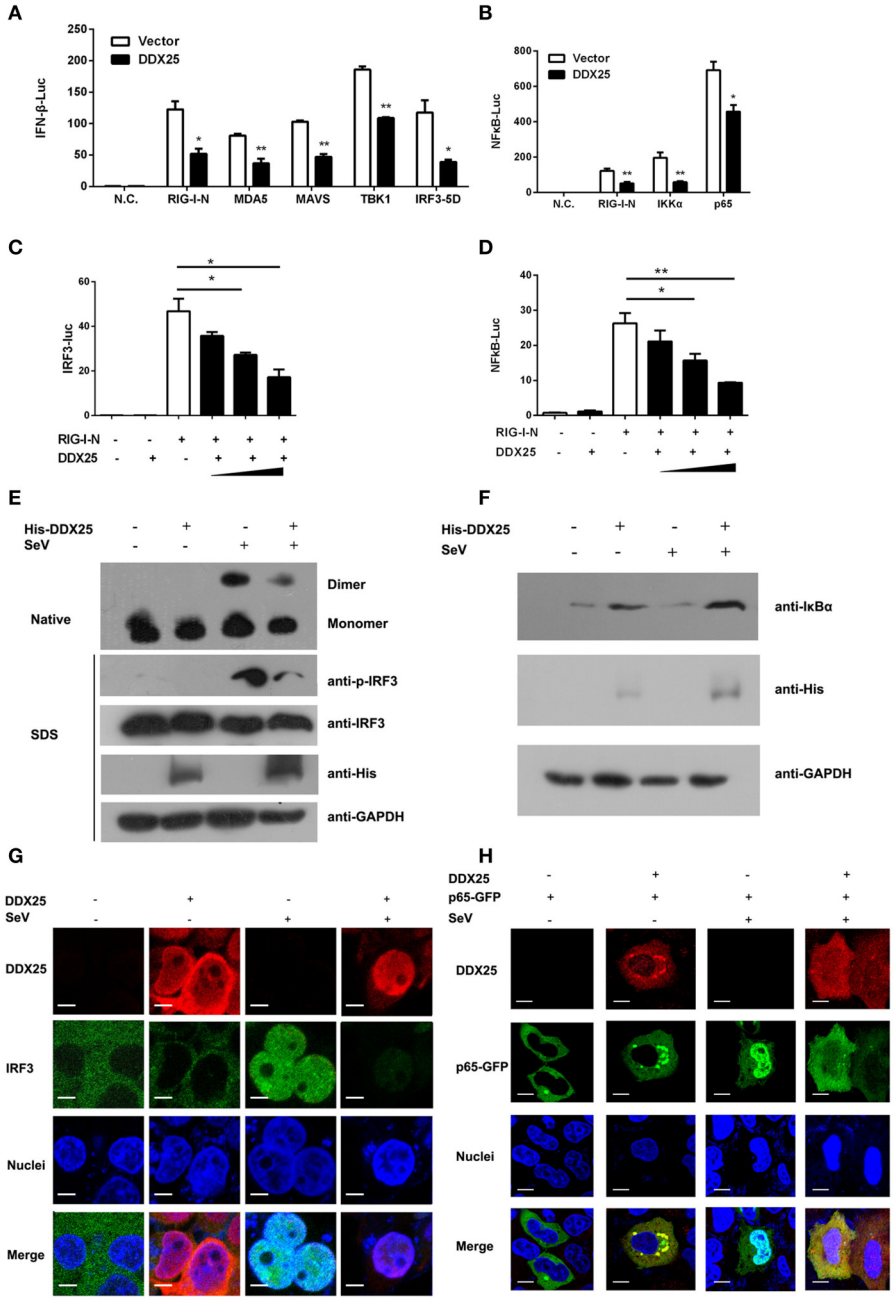

FIGURE 5 | DDX25 interrupts the IFN-signaling pathway by blocking IRF3 and NFκB activation. **(A)** Overexpression of DDX25 inhibits RIG-IN, MDA-5, MAVS, TBK1, and IRF3-5D directed IFNβ promoter activation. IFNβ-Luc assay was performed in vector or DDX25 transfected HEK293T cells. IFNβ promoter activations were driven by co-expression of distinct RIG-I signaling pathway molecules. **(B)** Overexpression of DDX25 inhibits IG-IN, IKKα, and NFκB p65 induced NFκB promoter activation. NFκB promoter was activated by transfecting RIG-IN, IKKα, or NFκB p65, and measured by a NFκB-Luc. **(C,D)** DDX25 suppresses RIG-IN directed IRF3-Luc **(C)** and NFκB-Luc **(D)** in a dose dependent manner. Results are expressed as the mean + the SEM. $^{*}p < 0.05$ and $^{**}p < 0.01$ (*t*-test). Representative results from at least three independent experiments. **(E)** Overexpression of DDX25 impaired SeV induced IRF3 phosphorylation and dimerization. **(F)** Overexpression of DDX25 suppressed SeV induced IκB degradation. **(G,H)** Nucleic translocation of IRF3 **(G)** and NFκB p65 **(H)** in SeV stimulated HEK293T cells were impaired by DDX25. Immunofluorescence assay were performed in control or DDX25 overexpressed HEK293T cells with or without SeV infection. IRF3, DDX25 were probed with specific primary antibodies followed by TRITC or FITC labeled secondary antibodies. NFκB p65 was visualized by a fused GFP protein. Scale bars, 10 μm.

sequestered in an inactive state in the cytoplasm of unstimulated cells. To investigate whether IRF3 and NFκB activation were directly or indirectly affected by DDX25, we examined the protein level of IκBα and phosphorylation of IRF3 in the DDX25 overexpressed cells. Western blot results revealed that SeV induced the phosphorylation of IRF3 and the degradation of

IκBα was inhibited by DDX25 (**Figures 5E,F**). Complementary to phosphorylation, SeV infection induced the dimerization of IRF3 and is also inhibited by DDX25 overexpression (**Figure 5E**). These results suggest that DDX25 inhibits IRF3 phosphorylation and NFκB activation.

To strengthen our existing data, immunofluorescence was carried out to investigate whether DDX25 prevented the nuclear translocation of IRF3 and NFκB p65 subunit. In mock-treated HeLa cells, IRF3, and p65 localized exclusively to the cytoplasm. SeV infection induced nuclear translocation of IRF3 and p65 in cells, while ectopic expression of DDX25 impaired the nuclear translocation of IRF3 and p65 (**Figures 5G,H**). Taken together, these results indicate that DDX25 inhibits the host antiviral response, by repressing the IFN antiviral response by suppressing IRF3 and NFκB transcriptional activity, and thereby inhibited the host antiviral response.

DISCUSSION

Previous work suggested that GRTH/DDX25 is highly expressed in testis and essential for completion of spermatogenesis in mouse mode (Mendelson, 2013). In this report, we further suggested that DDX25 is expressed in multiple human tissues and cell lines. Strikingly, we observed an increased production of DDX25 both *in vivo* and *in vitro* during viral infection. We further discovered DDX25 promotes the replication of RNA viruses, including DENV, VSV (**Figures 2G,H**), and Zika virus (ZIKV) (data not shown). *In vivo* data also demonstrates that DDX25 promotes RNA virus replication. As such, DDX25 has additional function for viral infection in human cells and mouse models.

The IFN system is triggered after viral infection via cellular recognition of viral components. Mammalian cells utilize multiple pattern recognition receptors, e.g., TLRs, RLRs, NLRs, or cGAS/STING, to detect the incoming viral particles in the cytoplasm or inside specific cellular compartments and trigger intracellular signaling pathways, which lead to the induction of IFN through the action of the transcription factor IRF3 (Chattopadhyay and Sen, 2016). Viral infection activates IRF3 by causing phosphorylation of its specific serine residues and its translocation to the nucleus, where it binds to the promoters of the target genes (Lin et al., 1998; Sato et al., 1998). On the other hand, NFκB is rapidly activated after exposure to pathogens (Rahman and McFadden, 2011). Once IκB is degraded, the NFκB complex is translocated to the nucleus where it functions as a transcription factor for numerous effector genes including type I IFN. Our data here indicated that DDX25 may negatively regulate these processes. Recently, the DEAD/H-box helicase family members have been drawing more and more attention not only for their powerful capacities in detecting invading pathogen-associated molecular patterns (PAMPs) as direct sensors (Fullam and Schroder, 2013; Mitoma et al., 2013), but also for their key roles involved in viral replication (Wang et al., 2009; Fullam and Schroder, 2013; Yasuda-Inoue et al., 2013; Zhou et al., 2013). RIG-I (DDX58) is reported to be a key sensor for viral RNA mediated innate immune signaling processes (Schmidt et al., 2012). Several other RNA helicases, such as DDX19 (Li J. et al., 2015), DDX41 (Jiang et al., 2017), DHX9 and DHX36 (Kim et al., 2010), are also implicated in the regulation of host defense processes. DDX3X and DDX24 function downstream of nucleic acid recognition to affect multi-protein signaling complexes required for efficient primary innate immune gene transcription (Ma et al., 2013; Li G. et al., 2015).

To evade the antiviral response of host cells, many viruses utilize the host factors to interfere with IRF3 or NFκB signaling by sophisticated mechanisms (Rahman and McFadden, 2011; Ye et al., 2013). Here, we demonstrate that DDX25 interfered with the activation of IRF3 and NFκB induced by DENV and other RNA viruses. Our findings suggested that DDX25 alters the phosphorylation level of IRF3 and the degradation of IκBα mediated by SeV.

DDX25 plays a negative regulatory role for IFNβ during DENV replication, confirming that inhibition of nuclear-cytoplasmic protein transport is a strategy for a virus to prevent the antiviral response of host cells. In summary, our data demonstrated that DDX25 interferes with the nuclear translocation of IRF3 and NFκB induced by RNA virus. Via this mechanism, DDX25 suppresses the induction of type I IFN in host cells during viral infection. These findings reveal a novel strategy for DENV to utilize a host factor to evade the host innate immune response and provide us new insight into the function of DDX25.

AUTHOR CONTRIBUTIONS

TF and JD designed the experiments and analyzed the data. TF, TS, GL, KW, and WP performed the experiments. TF and JD wrote the manuscript with all the authors contributing to writing, discussion, and agreeing with the conclusion presented in the manuscript.

ACKNOWLEDGMENTS

This work was supported by the National Natural Science Foundation of China (31300714, 31400737, 81471571, 81271792, and 31500700), Suzhou Science and Technology Development Project (SNG201607), China Postdoctoral Science Foundation (2013M541725), the Priority Academic Program Development of Jiangsu Higher Education Institutions, Program for Changjiang Scholars and Innovative Research Team in University (PCSIRT), and Jiangsu Natural Science Foundation (BK20140322).

SUPPLEMENTARY MATERIAL

The Supplementary Material for this article can be found online at: http://journal.frontiersin.org/article/10.3389/fcimb.2017.00356/full#supplementary-material

REFERENCES

Ariumi, Y., Kuroki, M., Abe, K., Dansako, H., Ikeda, M., Wakita, T., et al. (2007). DDX3 DEAD-box RNA helicase is required for hepatitis C virus RNA replication. *J. Virol.* 81, 13922–13926. doi: 10.1128/JVI.01517-07

Baeuerle, P. A., and Baichwal, V. R. (1997). NF-kappa B as a frequent target for immunosuppressive and anti-inflammatory molecules. *Adv. Immunol.* 65, 111–137. doi: 10.1016/S0065-2776(08)60742-7

Barnes, P. J., and Karin, M. (1997). Nuclear factor-kappaB: a pivotal transcription factor in chronic inflammatory diseases. *N. Engl. J. Med.* 336, 1066–1071. doi: 10.1056/NEJM199704103361506

Chahar, H. S., Chen, S., and Manjunath, N. (2013). P-body components LSM1, GW182, DDX3, DDX6 and XRN1 are recruited to WNV replication sites and positively regulate viral replication. *Virology* 436, 1–7. doi: 10.1016/j.virol.2012.09.041

Chattopadhyay, S., and Sen, G. C. (2016). RIG-I-like receptor-induced IRF3 mediated pathway of apoptosis (RIPA): a new antiviral pathway. *Protein Cell* 8, 165–168. doi: 10.1007/s13238-016-0334-x

de la Cruz, J., Kressler, D., and Linder, P. (1999). Unwinding RNA in *Saccharomyces cerevisiae*: DEAD-box proteins and related families. *Trends Biochem. Sci.* 24, 192–198. doi: 10.1016/S0968-0004(99)01376-6

Fang, J., Kubota, S., Yang, B., Zhou, N., Zhang, H., Godbout, R., et al. (2004). A DEAD box protein facilitates HIV-1 replication as a cellular co-factor of Rev. *Virology* 330, 471–480. doi: 10.1016/j.virol.2004.09.039

Fullam, A., and Schroder, M. (2013). DExD/H-box RNA helicases as mediators of anti-viral innate immunity and essential host factors for viral replication. *Biochim. Biophys. Acta* 1829, 854–865. doi: 10.1016/j.bbagrm.2013.03.012

Gan, V. C. (2014). Dengue: moving from current standard of care to state-of-the-art treatment. *Curr. Treat. Options Infect. Dis.* 6, 208–226. doi: 10.1007/s40506-014-0025-1

Guzman, M. G., and Harris, E. (2015). Dengue. *Lancet* 385, 453–465. doi: 10.1016/S0140-6736(14)60572-9

Jankowsky, E. (2010). RNA helicases at work: binding and rearranging. *Trends Biochem. Sci.* 36, 19–29. doi: 10.1016/j.tibs.2010.07.008

Jiang, Y., Zhu, Y., Liu, Z. J., and Ouyang, S. (2017). The emerging roles of the DDX41 protein in immunity and diseases. *Protein Cell* 8, 83–89. doi: 10.1007/s13238-016-0303-4

Kavarthapu, R., and Dufau, M. L. (2015). Germ cell nuclear factor (GCNF/RTR) regulates transcription of gonadotropin-regulated testicular RNA helicase (GRTH/DDX25) in testicular germ cells–the androgen connection. *Mol. Endocrinol.* 29, 1792–1804. doi: 10.1210/me.2015-1198

Khadka, S., Vangeloff, A. D., Zhang, C., Siddavatam, P., Heaton, N. S., Wang, L., et al. (2011). A physical interaction network of dengue virus and human proteins. *Mol. Cell. Proteomics* 10:M111.012187. doi: 10.1074/mcp.M111.012187

Kim, T., Pazhoor, S., Bao, M., Zhang, Z., Hanabuchi, S., Facchinetti, V., et al. (2010). Aspartate-glutamate-alanine-histidine box motif (DEAH)/RNA helicase A helicases sense microbial DNA in human plasmacytoid dendritic cells. *Proc. Natl. Acad. Sci. U.S.A.* 107, 15181–15186. doi: 10.1073/pnas.1006539107

Li, G., Feng, T., Pan, W., Shi, X., and Dai, J. (2015). DEAD-box RNA helicase DDX3X inhibits DENV replication via regulating type one interferon pathway. *Biochem. Biophys. Res. Commun.* 456, 327–332. doi: 10.1016/j.bbrc.2014.11.080

Li, J., Hu, L., Liu, Y., Huang, L., Mu, Y., Cai, X., et al. (2015). DDX19A senses viral RNA and mediates NLRP3-dependent inflammasome activation. *J. Immunol.* 195, 5732–5749. doi: 10.4049/jimmunol.1501606

Lin, R., Heylbroeck, C., Pitha, P. M., and Hiscott, J. (1998). Virus-dependent phosphorylation of the IRF-3 transcription factor regulates nuclear translocation, transactivation potential, and proteasome-mediated degradation. *Mol. Cell. Biol.* 18, 2986–2996. doi: 10.1128/MCB.18.5.2986

Liu, S., Cai, X., Wu, J., Cong, Q., Chen, X., Li, T., et al. (2015). Phosphorylation of innate immune adaptor proteins MAVS, STING, and TRIF induces IRF3 activation. *Science* 347:aaa2630. doi: 10.1126/science.aaa2630

Ma, Z., Moore, R., Xu, X., and Barber, G. N. (2013). DDX24 negatively regulates cytosolic RNA-mediated innate immune signaling. *PLoS Pathog.* 9:e1003721. doi: 10.1371/journal.ppat.1003721

Mendelson, C. R. (2013). GRTH: a key to understanding androgen-mediated germ cell signaling. *Endocrinology* 154, 1967–1969. doi: 10.1210/en.2013-1395

Mitoma, H., Hanabuchi, S., Kim, T., Bao, M., Zhang, Z., Sugimoto, N., et al. (2013). The DHX33 RNA helicase senses cytosolic RNA and activates the NLRP3 inflammasome. *Immunity* 39, 123–135. doi: 10.1016/j.immuni.2013.07.001

Parvatiyar, K., Zhang, Z., Teles, R. M., Ouyang, S., Jiang, Y., Iyer, S. S., et al. (2012). The helicase DDX41 recognizes the bacterial secondary messengers cyclic di-GMP and cyclic di-AMP to activate a type I interferon immune response. *Nat. Immunol.* 13, 1155–1161. doi: 10.1038/ni.2460

Rahman, M. M., and McFadden, G. (2011). Modulation of NF-kappaB signalling by microbial pathogens. *Nat. Rev. Microbiol.* 9, 291–306. doi: 10.1038/nrmicro2539

Rocak, S., and Linder, P. (2004). DEAD-box proteins: the driving forces behind RNA metabolism. *Nat. Rev. Mol. Cell Biol.* 5, 232–241. doi: 10.1038/nrm1335

Sato, M., Tanaka, N., Hata, N., Oda, E., and Taniguchi, T. (1998). Involvement of the IRF family transcription factor IRF-3 in virus-induced activation of the IFN-beta gene. *FEBS Lett.* 425, 112–116. doi: 10.1016/S0014-5793(98)00210-5

Schmidt, A., Rothenfusser, S., and Hopfner, K. P. (2012). Sensing of viral nucleic acids by RIG-I: from translocation to translation. *Eur. J. Cell Biol.* 91, 78–85. doi: 10.1016/j.ejcb.2011.01.015

Sharma, S., tenOever, B. R., Grandvaux, N., Zhou, G. P., Lin, R., and Hiscott, J. (2003). Triggering the interferon antiviral response through an IKK-related pathway. *Science* 300, 1148–1151. doi: 10.1126/science.1081315

Sheng, Y., Tsai-Morris, C. H., and Dufau, M. L. (2003). Cell-specific and hormone-regulated expression of gonadotropin-regulated testicular RNA helicase gene (GRTH/Ddx25) resulting from alternative utilization of translation initiation codons in the rat testis. *J. Biol. Chem.* 278, 27796–27803. doi: 10.1074/jbc.M302411200

Steimer, L., and Klostermeier, D. (2012). RNA helicases in infection and disease. *RNA Biol.* 9, 751–771. doi: 10.4161/rna.20090

Thisyakorn, U., and Thisyakorn, C. (2014). Latest developments and future directions in dengue vaccines. *Ther. Adv. Vaccines* 2, 3–9. doi: 10.1177/2051013613507862

Tsai-Morris, C. H., Sheng, Y., Lee, E., Lei, K. J., and Dufau, M. L. (2004). Gonadotropin-regulated testicular RNA helicase (GRTH/Ddx25) is essential for spermatid development and completion of spermatogenesis. *Proc. Natl. Acad. Sci. U.S.A.* 101, 6373–6378. doi: 10.1073/pnas.0401855101

Wang, H., Kim, S., and Ryu, W. S. (2009). DDX3 DEAD-Box RNA helicase inhibits hepatitis B virus reverse transcription by incorporation into nucleocapsids. *J. Virol.* 83, 5815–5824. doi: 10.1128/JVI.00011-09

Wang, K., Wang, J., Sun, T., Bian, G., Pan, W., Feng, T., et al. (2016). Glycosphingolipid GM3 is indispensable for dengue virus genome replication. *Int. J. Biol. Sci.* 12 872–883. doi: 10.7150/ijbs.15641

Yasuda-Inoue, M., Kuroki, M., and Ariumi, Y. (2013). Distinct DDX DEAD-box RNA helicases cooperate to modulate the HIV-1 Rev function. *Biochem. Biophys. Res. Commun.* 434, 803–808. doi: 10.1016/j.bbrc.2013.04.016

Ye, J., Zhu, B., Fu, Z. F., Chen, H., and Cao, S. (2013). Immune evasion strategies of flaviviruses. *Vaccine* 31 461–471. doi: 10.1016/j.vaccine.2012.11.015

Yoneyama, M., Onomoto, K., Jogi, M., Akaboshi, T., and Fujita, T. (2015). Viral RNA detection by RIG-I-like receptors. *Curr. Opin. Immunol.* 32, 48–53. doi: 10.1016/j.coi.2014.12.012

Zhang, Z., Kim, T., Bao, M., Facchinetti, V., Jung, S. Y., Ghaffari, A. A., et al. (2011a). DDX1, DDX21, and DHX36 helicases form a complex with the adaptor molecule TRIF to sense dsRNA in dendritic cells. *Immunity* 34, 866–878. doi: 10.1016/j.immuni.2011.03.027

Zhang, Z., Yuan, B., Bao, M., Lu, N., Kim, T., and Liu, Y. J. (2011b). The helicase DDX41 senses intracellular DNA mediated by the adaptor STING in dendritic cells. *Nat. Immunol.* 12, 959–965. doi: 10.1038/ni.2091

Zhao, T., Yang, L., Sun, Q., Arguello, M., Ballard, D. W., Hiscott, J., et al. (2007). The NEMO adaptor bridges the nuclear factor-kappaB and interferon regulatory factor signaling pathways. *Nat. Immunol.* 8, 592–600. doi: 10.1038/ni1465

Zhou, X., Luo, J., Mills, L., Wu, S., Pan, T., Geng, G., et al. (2013). DDX5 facilitates HIV-1 replication as a cellular co-factor of Rev. *PLoS ONE* 8:e65040. doi: 10.1371/journal.pone.0065040

Conflict of Interest Statement: The authors declare that the research was conducted in the absence of any commercial or financial relationships that could be construed as a potential conflict of interest.

frontiers in Cellular and Infection Microbiology

ORIGINAL RESEARCH
published: 26 October 2017
doi: 10.3389/fcimb.2017.00456

E. fischeriana Root Compound Dpo Activates Antiviral Innate Immunity

Jingxuan Chen[1†], Hongqiang Du[1†], Shuang Cui[2], Tong Liu[3], Guang Yang[4], Huaping Sun[5], Weiwei Tao[6], Baoping Jiang[7], Li Yu[7] and Fuping You[1, 4*]*

[1] Department of Immunology, Institute of Systems Biomedicine, School of Basic Medical Sciences, Peking University Health Science Center, Beijing, China, [2] Key Laboratory for Neuroscience, Neuroscience Research Institute, Peking University Beijing, National Health and Family Planning Commission of the People's Republic of China (NHFPC), Ministry of Education, Beijing, China, [3] College of Animal Science and Veterinary Medicine, Heilongjiang Bayi Agricultural University, Daqing, China, [4] Department of Parasitology, Department of Public Health and Preventive Medicine, School of Basic Medical Sciences, Jinan University, Guangzhou, China, [5] Jiangsu Hospital of Traditional Chinese Medicine, Affiliated Hospital of Nanjing University of Chinese Medicine, Nanjing, China, [6] Center for Translational Systems Biology and Neuroscience, School of Basic Biomedical Science, Nanjing University of Chinese Medicine, Nanjing, China, [7] Jiangsu Key Laboratory for High Technology Research of TCM Formulae, Jiangsu Collaborative Innovation Center of Chinese Medicinal Resources Industrialization, Pharmacy College, Nanjing University of Chinese Medicine, Nanjing, China

E. fischeriana has long been used as a traditional Chinese medicine. Recent studies reported that some compounds of E. fischeriana exhibited antimicrobial and immune enhance activity. Innate immune system is essential for the immune surveillance of inner and outer threats, initial host defense responses and immune modulation. The role of natural drug compounds, including E. fischeriana, in innate immune regulation is largely unknown. Here we demonstrated that E. fischeriana compound Dpo is involved in antiviral signaling. The genome wide RNA-seq analysis revealed that the induction of ISGs by viral infection could be synergized by Dpo. Consistently, Dpo enhanced the antiviral immune responses and protected the mice from death during viral infection. Dpo however was not able to rescue STING deficient mice lethality caused by HSV-1 infection. The enhancement of ISG15 by Dpo was also impaired in STING, IRF3, IRF7, or ELF4 deficient cells, demonstrating that Dpo activates innate immune responses in a STING/IRFs/ELF4 dependent way. The STING/IRFs/ELF4 axis is therefore important for Dpo induced ISGs expression, and can be used by host to counteract infection.

Keywords: innate immunity, viruses, RLR signalling, STING, compound

OPEN ACCESS

Edited by:
Penghua Wang,
New York Medical College,
United States

Reviewed by:
Feng Qian,
Fudan University, China
Xin Zhao,
Institute of Microbiology (CAS), China

***Correspondence:**
Li Yu
lyu@njutcm.edu.cn;
Fuping You
fupingyou@hsc.pku.edu.cn

† These authors have contributed equally to this work.

Received: *29 August 2017*
Accepted: *11 October 2017*
Published: *26 October 2017*

Citation:
Chen J, Du H, Cui S, Liu T, Yang G, Sun H, Tao W, Jiang B, Yu L and You F (2017) E. fischeriana Root Compound Dpo Activates Antiviral Innate Immunity. Front. Cell. Infect. Microbiol. 7:456. doi: 10.3389/fcimb.2017.00456

INTRODUCTION

Virus infection poses serious threats to public health. Innate immunity is the sentinel for the host health and is promptly activated after infection. The pattern recognition receptors (PRRs) are the first line of innate immunity to sense the invading pathogens and other danger signals. Antiviral immune responses are triggered after viral recognition by host PRRs, including several Toll-like receptors (TLR3, TLR7/8, TLR9; Schulz et al., 2005; Hoshino et al., 2006), RIG-I like receptors (RIG-I and Mda5; Yoneyama et al., 2004, 2005), and cytosolic double strand DNA (dsDNA) receptors (DAI, IFI16, DDX41, and cGAS; Takaoka et al., 2007; Unterholzner et al., 2010; Zhang et al., 2011; Sun et al., 2013). RIG-I like receptors recognize cytoplasmic viral RNA, and recruit the adaptor MAVS (Mitochondrial Antiviral Signaling Protein; Seth et al., 2005; Xu et al., 2005; Kumar et al., 2006; Liu et al., 2015). MAVS localizes on mitochondria and peroxisomes, and after receiving danger signals from RLRs, recruits downstream molecules to form a signal complex. This

signal complex then triggers the activation of signaling events, leading to the transcription of NFκB and IRF3/7-dependent genes. STING (Stimulator of Interferon Genes Protein, also named ERIS or MITA) was initially identified as an adaptor protein downstream of cytosolic DNA sensing pathway (Ishikawa and Barber, 2008; Zhong et al., 2008; Sun et al., 2009). The recent studies showed that STING was able to recognize the secondary message cGAMP (Cyclic GMP-AMP) synthetized by cGAS (Sun et al., 2013). After binding with cGAMP, STING recruited TBK1 to form a signal complex, and initiated the transcription of type I IFNs and related antiviral genes in an IRF3/7-dependent way.

The Euphorbia is the largest genus (Li et al., 2009) of Euphorbiaceae, which is one of the largest families of higher plants. The species are distributed worldwide (Vasas and Hohmann, 2014) throughout tropical and temperate regions, mainly growing in southern USA, the Mediterranean basin, the Middle East, South Africa and north China. Many of them have been used as folk medicine with a long history (Wang et al., 2006; Ghanadian et al., 2013). For their extensive biological activities, Euphorbia species have been used for treatment of yellow fever (Korin et al., 2002), viral hepatitis (Hezareh, 2005), edema, ascites, warts (Wang et al., 2006), cancer (Wang et al., 2009), multi-drug resistance (Wesolowska et al., 2007), skin diseases, gonorrhea, and migraine (Shi et al., 2008). Some studies focused on their antiviral activities. Abdelgaleil et al. (2001) described the compounds from *Euphorbia paralias* L. (growing in Egypt and entire Mediterranean region), which inhibited HIV (human immunodeficiency virus) induced cytopathicity in MT-4 cells. Akihisa et al. (2002) and Tanaka et al. (2000) used Raji cells, the Epstein-Barrvirus (EBV) genome-carrying human lymphoblastoid cells to assay the compounds from *Euphorbia antiquorum* L. and *Euphorbia chamaesyce* L. Seven and one of them showed inhibitory effects respectively on EBV early antigen (EBV-EA), induced by the tumor promoter 12-O-tetradecanoylphorbol-13-acetate (TPA).

Euphorbia fischeriana Steud is a perennial herbaceous plant, which produces a milky juice. The roots of E. fischeriana had long been used as a traditional Chinese medicine for the treatment of cancer, edema, and ascites. Accumulating studies are uncovering its role in antiviral immune responses. A phorbol ester from Euphorbia species (Sun and Liu, 2011), prostratin, is well-known for the notable induction activity on viral reservoirs. There are more potent analogs of prostratin, in which phorbol-13-stearate showed at least 10-fold more potent than prostratin on the activation of HIV-1 gene (Márquez et al., 2008). Besides prostratin, the role of other compounds of E. fischeriana in antiviral immunity awaited to be brought to light. The association between natural drug and innate immunity also is an interesting topic to be explored.

In present study, we demonstrated that a compound, named Dpo, which was isolated from Euphorbia fischeriana Steud, was able to activate the antiviral immunity in type I IFNs independent manner. Dpo up-regulated a group of ISGs (interferon stimulated gene) and inflammatory genes but type I IFNs. Dpo protected wild type mice from lethality due to virus infection but not STING deficient mice. We further found Dpo exerted its antiviral function through STING and IRFs. Therefore, we here revealed a new antiviral pathway triggered by Dpo.

RESULT

Dpo Is an Antiviral Compound from Euphorbia Fischeriana Steud

To investigate the function of E. fischeriana in host defense, we isolated a list of chemical compounds from it and examined their antiviral activity. Dpo is the only compound that was able to suppress the infection of VSV, a negative-sense single strand RNA virus (**Figure 1A** and Supplementary Figure 1). However, the replication of VSV was not affected by the treatment of prostratin, which is known as a HIV-1 inhibitor. This indicated that Dpo employed a different mechanism to restrict virus infection. To gain additional insight of the function of Dpo, we infected wild type bone marrow derived macrophages with VSV-G-HIV-1 and HSV-1 (Herpes simplex virus 1), a double strands DNA virus after Dpo treatment (**Figures 1B,C**). Viral replication was also inhibited by Dpo but not by other compounds. We further observed that Dpo restricted virus in a dose dependent manner (**Figures 1D,E**). Thus, Dpo suppressed the infection of different types of viruses significantly, suggesting that Dpo is a general anti-viral compound without virus specificity. To further evaluate the physiological function of Dpo, we challenged the wild type mice with HSV-1. The control group mice were much more susceptible to HSV-1 than Dpo treated group (**Figure 1F**). Therefore, Dpo is an active anti-viral compound from E. fischeriana.

Dpo Induces Expression of Interferon-Stimulated Genes

Type I IFN is one of the most potent defensive element against virus infection. IFNβ is the earliest induced IFN during viral infection. Dpo however did not affect the production of IFNβ (**Figure 2A**). Interestingly CCL5 and IL1-β were up-regulated slightly after Dpo treatment (**Figures 2B,C**), indicating that Dpo might exert its anti-viral function in a chemokines and inflammatory cytokines dependent way. To gain further insight of the mechanism of how Dpo direct antiviral immune responses, we performed a genome wide RNA-seq to identify Dpo regulated signaling and genes. Interestingly Dpo treatment led to significant alteration of antiviral pathways in bone marrow derived macrophages, including TLR, RLR, NLR, and cytosolic DNA sensing pathway. Dpo also induced or suppressed a group of genes associated with Hepatitis A Virus, Hepatitis B Virus, Hepatitis C Virus, influenza virus, HSV and Epstein-barr virus (Supplementary Figure 2). This further suggested that Dpo suppressed virus via regulating innate immune signaling. In addition to IFNβ, IFNαs are the main effector to eliminate infected virus. Similar to IFNβ, Dpo did not induce IFNαs production in macrophages (**Figure 2D**). We next measured the expression of the known innate immune signaling molecules after Dpo treatment. Dpo significantly enhanced the induction of IRF7 during viral infection (**Figure 2E**). As IRF7 is an interferon stimulated genes (ISG). We then reason that Dpo might be

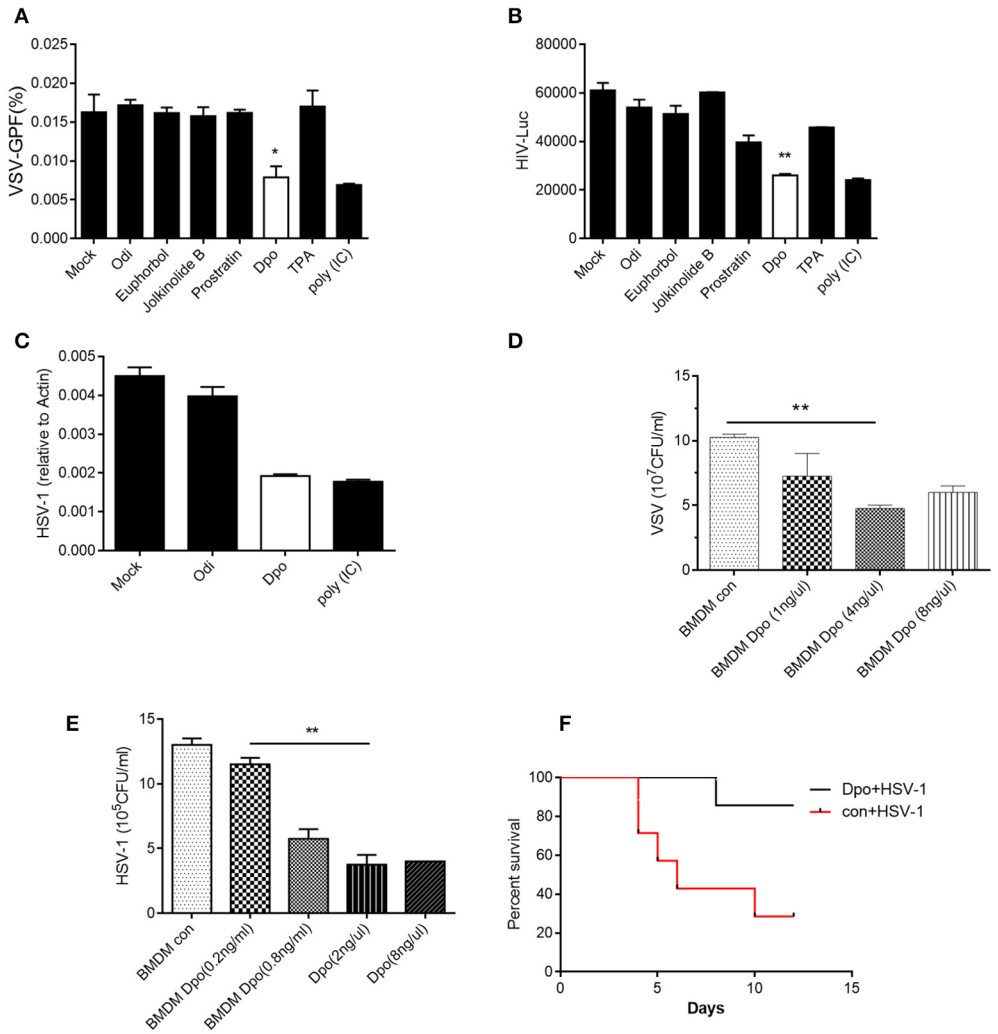

FIGURE 1 | Dpo is an antiviral compound from Euphorbia fischeriana Steud. **(A–C)** Bone marrow derived macrophages were treated with indicated compounds (1 ng/ul). Four hours later, these cells were infected with VSV **(A)**, HIV-1 **(B)**, and HSV-1 **(C)**. Twenty-four hours later, the viral load were measured by plaque assay. **(D,E)** Bone marrow derived macrophages were treated with increasing amount of Dpo. Four hours later, these cells were infected with VSV **(D)** and HSV-1 **(E)**. Twenty-four hours later, the viral load were measured by plaque assay. **(F)** Wild type C57BL/6 mice were treated with Dpo, 24 h later infected with HSV-1, and monitored daily for 15 days. $^*P < 0.05$. **(A–E)** The data represent mean values ± SEM ($n = 3$); $^*P < 0.05$, $^{**}P < 0.01$, significant compared to control, Student's *t*-test. The data represent mean values ± SEM ($n = 6$ mice per group); **(F)** $^*P < 0.05$, significance compared to the control group, non-parametric Mann–Whitney analysis.

involved in ISG regulation. A list of ISGs were induced by viral infection, and further enhanced by Dpo (**Figure 2F**). NFκB is a key transcription factor that plays a pivotal role in innate immune signaling, including the defense against virus. The RNA-seq analysis showed that Dpo regulated NFκB pathway. The q-PCR results further verified that Dpo up-regulated the adaptor proteins, including: IRAK2, TRADD, TRAF1, and MyD88 (**Figure 2G**), and transcription factors, including: NFκB2, NFκBIB, NFκBil1, and NFil3 (**Figure 2H**). Accordingly, Dpo enhanced the expression of many inflammatory cytokines (**Figure 2I**) and chemokine during virus infection (**Figure 2J**). Therefore, Dpo enhanced virus induced immune genes expression, particularly the ISGs induction, which is critical for its anti-viral function.

Sting Is Required for Dpo Mediated Anti-Viral Immune Responses

Innate immunity is considered to act as the first line of host defense and is critical for virus surveillance. Toll like receptor (TLR) is the first identified PRRs family in mammals that is able to recognize the pattern recognition proteins (PRPs) from different types of pathogens including parasite, fungi, bacteria and virus. All of the TLRs transduce danger signals through adaptor protein MyD88 (Häcker et al., 2000; Takeuchi et al., 2000a,b) except TLR3 that utilize TRIF (Yamamoto et al., 2002) as the adaptor. We first examined the possibility that Dpo was sensed by TLRs. However, the ISG15 induction by Dpo was intact in MyD88 or TRIF deficient macrophages (**Figure 3A**), so was the inhibition of viral replication (**Figure 3B**). Consistently Dpo

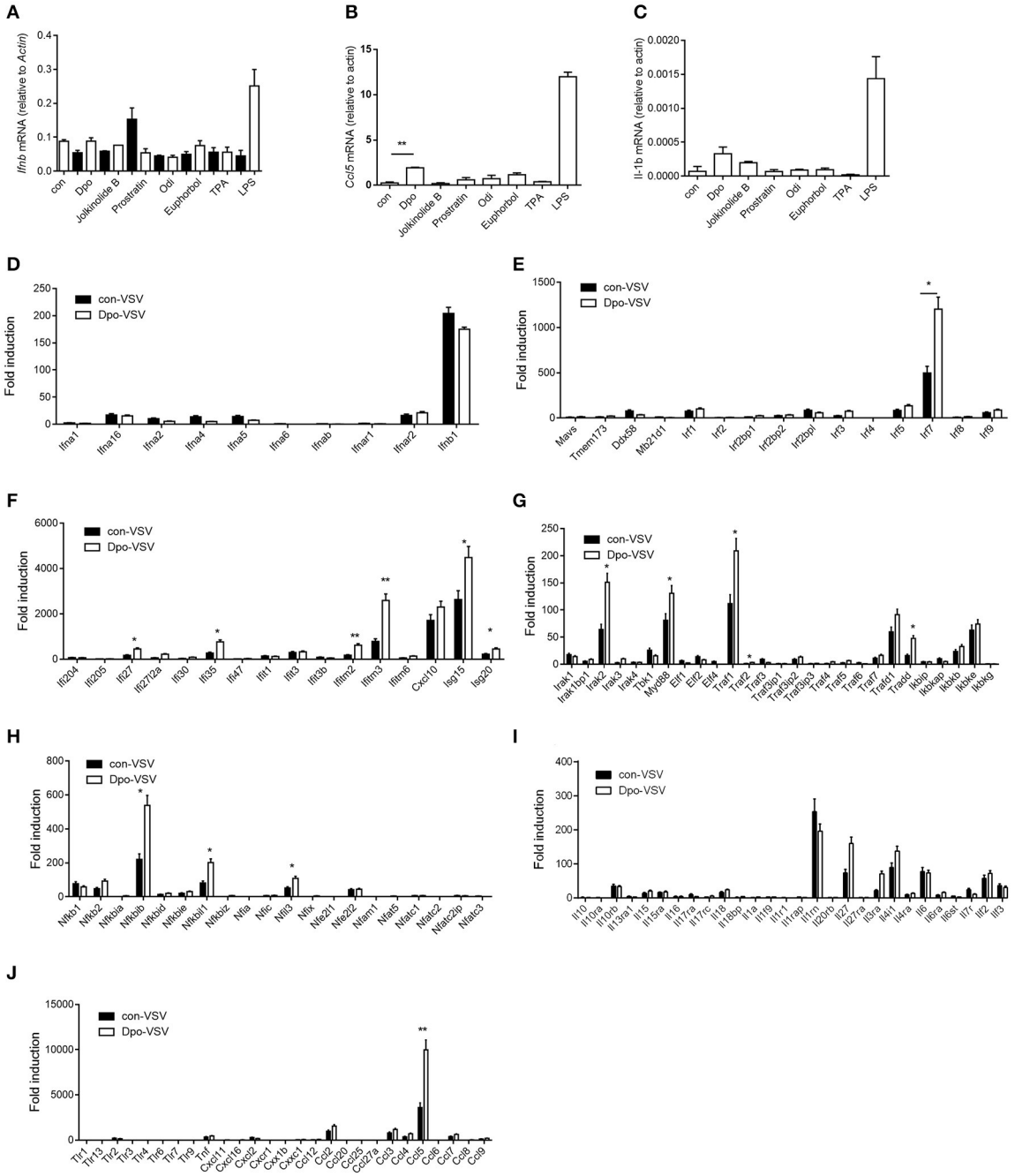

FIGURE 2 | Dpo induces expression of interferon-stimulated genes. **(A–C)** Bone marrow derived macrophages were treated with indicated compounds (1 ng/ul). Four hours later, the mRNA level of IFNβ, CCl5, and IL-β were measured by qPCR. **(D–J)** Bone marrow derived macrophages were treated with Dpo. Four hours later, these cells were infected with VSV. Twenty-four hours later, the indicated cytokines and genes were measured by qPCR. **(A–J)** The data represent mean values ± SEM ($n = 3$); $^*P < 0.05$, $^{**}P < 0.01$, significant compared to control, Student's *t*-test.

also could protect TLR4 deficient mice from lethality after HSV-1 infection (**Figure 3C**). Thus, Dpo did not activate innate immune signaling through TLRs. RLR, including RIG-I and Mda5, is responsible for sensing the cytosolic RNA virus. MAVS is the adaptor protein downstream of RIG-I and Mda5 and critical for RLR signaling. MAVS transduces the signal from RLR to kinase TBK1, which in turn phosphorylate and activate IRF3. Activated IRF3 then translocate from cytoplasm to nucleus to initiate transcription of type I IFNs. We observed that Dpo was able to inhibit virus replication in RIG-I or MAVS deficient macrophages (**Figures 3D,E**), demonstrating that Dpo was not involved in RLR signaling. We then investigated the role of Dpo

in cytosolic double strands DNA sensing pathway. STING is the key signal molecule of this pathway. We noted that Dpo enhanced immune responses were greatly attenuated in STING deficient cells during viral infection (**Figure 3F**). In line with this, Dpo treatment could not rescue STING deficient mice from death caused by viral infection (**Figure 3G**). Collectively these results demonstrated that Dpo modulated cytosolic double strands DNA sensing signaling in STING dependent manner.

Dpo Induces ISGs Via IRFs/ELF4

We have found that Dpo was able to enhance the induction of ISGs by viral infection. We then checked the possibility whether Dpo could induce ISGs expression by itself in the non-infected cells. q-PCR analysis showed that Dpo was able to up-regulated the expression of CCl5 and ISG15 without virus challenging (**Figures 4A–E**). It is established that the robust induction of ISGs is directly mediated by innate transcription factors. We next assessed the role of known transcription factors in ISGs regulation after Dpo treatment. Dpo could not suppress virus replication in IRF3 or IRF7 deficient macrophages (**Figures 4F,G**). Consistently the induction of ISG15 by Dpo was attenuated in IRF3 or IRF7 deficient macrophages (**Figure 4H**), demonstrating that Dpo related anti-viral function is mediated by IRFs. ELF4 is an ETS domain containing transcription factor. Our previous study showed that it was critical for antiviral immunity. ELF4 cooperated with IRF3/IRF7 to initiate the transcription of antiviral genes. We thus evaluated the function of ELF4 in Dpo mediated immune responses. The plaque assay showed that Dpo inhibited the virus replication in wild type but not ELF4 deficient macrophages (**Figure 4I**). The induction of ISG15 was also impaired in ELF4 deficient cells (**Figure 4J**). CGAS is the cytosolic DNA sensor that synthetizes cGAMP to activate STING and TBK1. We found that TBK1 was indispensable for Dpo mediated ISG induction but cGAS was dispensable (**Figures 4K,L**). Therefore, Dpo regulates ISGs induction in a TBK1/IRF3/IRF7/ELF4 dependent way.

DISCUSSION

E. fischeriana root has been used to cure immune diseases in Chinese medicine for thousands years. The active compounds within it and the mechanism of how they modulate host immune system is largely unknown. There are approximate 60 compounds of E. fischeriana root isolated since the 1970s. EtOH and H_2O extracts of E. fischeriana were found to inhibit the growth of Lewis lung carcinoma and ascetichepatoma in mice (Yang, 1993). Several studies on jolkinolide B (Uemura and Hirata, 1972) have been conducted in order to better understand the underlying mechanism of the antitumor activity of E. fischeriana. In addition, five extracts exhibited antibacterial activities against tuberculous bacillus and Prostratin was useful in the treatment of HIV. However, their function in innate immune pathway is unclear.

We here demonstrated that the E. fischeriana root compound Dpo enhanced antiviral innate immunity. The mechanism is different from prostratin mediated anti-HIV responses. The main mechanisms of HIV-1 inhibition effects by prostratin involved: (1) down-regulation of CD4 receptor expression as well as HIV-1 coreceptors, C-X-C chemokine receptor type 4 (CXCR4) and C-C chemokine receptor type 5 (CCR5; Kulkosky et al., 2001) and leading to protecting CD4+ T cells from HIV-1 infection. (2) up-regulation of activation receptor. (3) Leading to virus replication in latently infected cells. As a protein kinase C (PKC) agonist, prostratin activates PKC and cause phosphorylation of IκB kinase, which leads to NF-κB entering into the cell nucleus and promoting antiviral gene expression. This induction activity facilitate the eradication of viruses through elimination of their reservoirs. However, Dpo exerted its anti-viral function by activating innate immune signaling. STING is known as a type I IFNs stimulator localized on endoplasmic reticulum. Recent studies revealed its role as a sensor that recognized the secondary messager cGAMP (Cyclic GMP-AMP). Our *in vivo* and *in vitro* results showed that STING was essential for Dpo induced immune response. The detailed mechanism how Dpo activates STING signaling is still interesting to further explore. Similar to cGAMP, Dpo is a small molecule compound. It is possible that Dpo act as an agonist sensed by STING, and then activate downstream signaling.

ISGs are interferon stimulated genes that direct antiviral responses and immune homeostasis. The canonical induction of ISGs signaling are triggered by interferon through interferon receptors. Previous study had showed that viral infection was able to up-regulate the expression of ISGs directly through MAVS signaling without activation of IFN receptor signaling (Dixit et al., 2010). We here reported that Dpo initiated ISGs production in STING dependent but type I IFNs independent way. IRF3/7 and ELF4 are key transcription factors for type I IFN expression. Our previous study has shown that EICE (ETS–ISRE composition element) mediated the cooperation between IRFs and ELF4 in type I IFN transcription. IRF3/IRF7 and ELF4 are required for the induction of ISGs by Dpo, which should be bridged by EICE. Thus, our study uncover the role of an E. fischeriana root compound Dpo in innate immunity, and a STING/IRFs/ELF4 dependent pathway in ISGs regulation.

MATERIALS AND METHODS

Mice, Cells, Viruses, and Reagents

Sting$^{gt/gt}$ mice, which lack a functional STING protein, were a gift from R. Vance (University of California, Berkeley). The *Mavs*$^{-/-}$ mice were from Jackson laboratory (Stock No: 008634) and the *Tlr4*$^{-/-}$ mice were purchased from National Resource Center of Model Mice (NRCMM, Nanjing; N000192). All procedures followed the Peking University Guidelines for "Using Animals in Intramural Research" and were approved by the Animal Care and Use Committee of Peking University. iBMDM cells were a gift from Feng Shao (National Institute of Biological Sciences, Beijing). Elf4$^{-/-}$, Irf3$^{-/-}$, Irf7$^{-/-}$, Myd88$^{-/-}$, and Trif$^{-/-}$ iBMDM were generated by Crispr-Cas9 system. HEK 293T (Human Embryonic Kidney 293 cells transformed by expression of the large T antigen from SV40), HeLa (Henrietta Lacks strain of cancer cells), Vero cell (normal African green monkey kidney epithelial cells), were cultured in Dulbecco's modified Eagle medium (DMEM). Bone marrow-derived macrophages

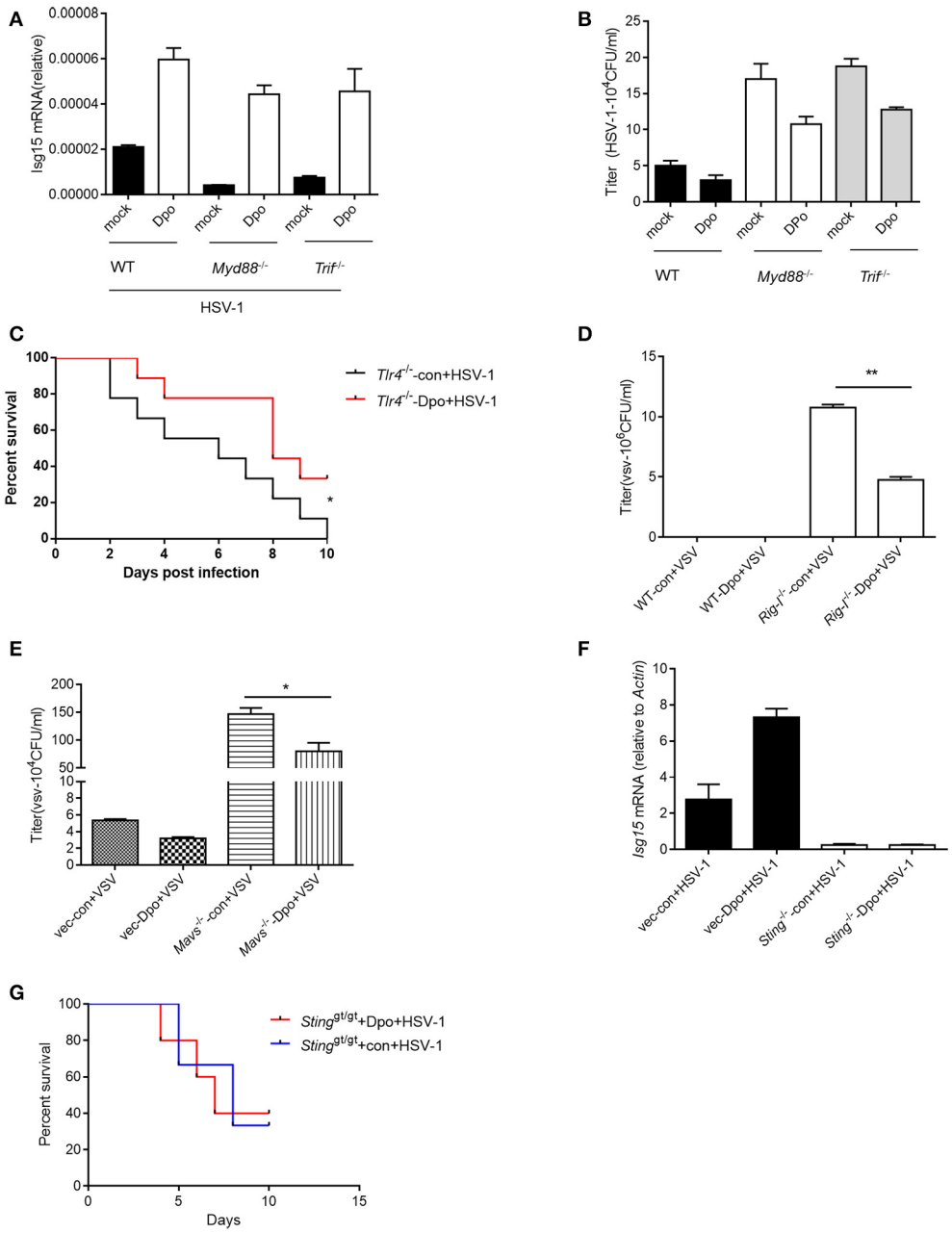

FIGURE 3 | STING is required for Dpo mediated anti-viral immune responses. **(A,B)** WT, *Trif*$^{-/-}$, *Myd88*$^{-/-}$ peritoneal macrophages were treated with Dpo. Four hours later, these cells were infected with HSV-1. Twenty-four hours later, the mRNA level of ISG15 were measured by qPCR **(A)**, and the viral load were measured by plaque assay **(B)**. **(C)** *Tlr4*$^{-/-}$ C57BL/6 mice were treated with Dpo, 24 h later infected with HSV-1, and monitored daily for 15 days. **(D,E)** WT, *Ddx58*$^{-/-}$ **(D)**, *Mavs*$^{-/-}$ **(E)** peritoneal macrophages were treated with Dpo. Four hours later, these cells were infected with VSV. Twenty-four hours later, and the viral load were measured by plaque assay **(F)**. Wild type or *Sting*$^{gt/gt}$ peritoneal macrophages were treated with Dpo, 4 h later infected with HSV-1, and the mRNA level of ISG15 were measured by qPCR. **(G)** *Sting*$^{gt/gt}$ C57BL/6 mice were treated with Dpo, 24 h later infected with HSV-1, and monitored daily for 15 days. **(A,B,D–F)** The data represent mean values ± SEM ($n = 3$); $^{*}P < 0.05$, $^{**}P < 0.01$ significant compared to control, Student's *t*-test. The data represent mean values ± SEM ($n = 6$ mice per group); **(C–G)** $^{*}P < 0.05$, significance compared to the control group, non-parametric Mann–Whitney analysis.

(BMDMs), and macrophages was performed as previously described (Chen et al., 2011). Cells were cultured in 10 cm petri-dish at 37°C for 5 days. The medium for BMDCs is RPMI-1640 medium containing GM-CSF at 100 U/mL and TNF at 50 U/mL. VSV-GFP (Indiana strain) was gift from Dr. John Rose (Yale University) and HSV-1 was from Dr. Akiko Iwasaki (Yale University). LPS (lipopolysaccharides, L4391) was from Sigma. Lipofectamine 2000 (Invitrogen) was used for lipid transfection.

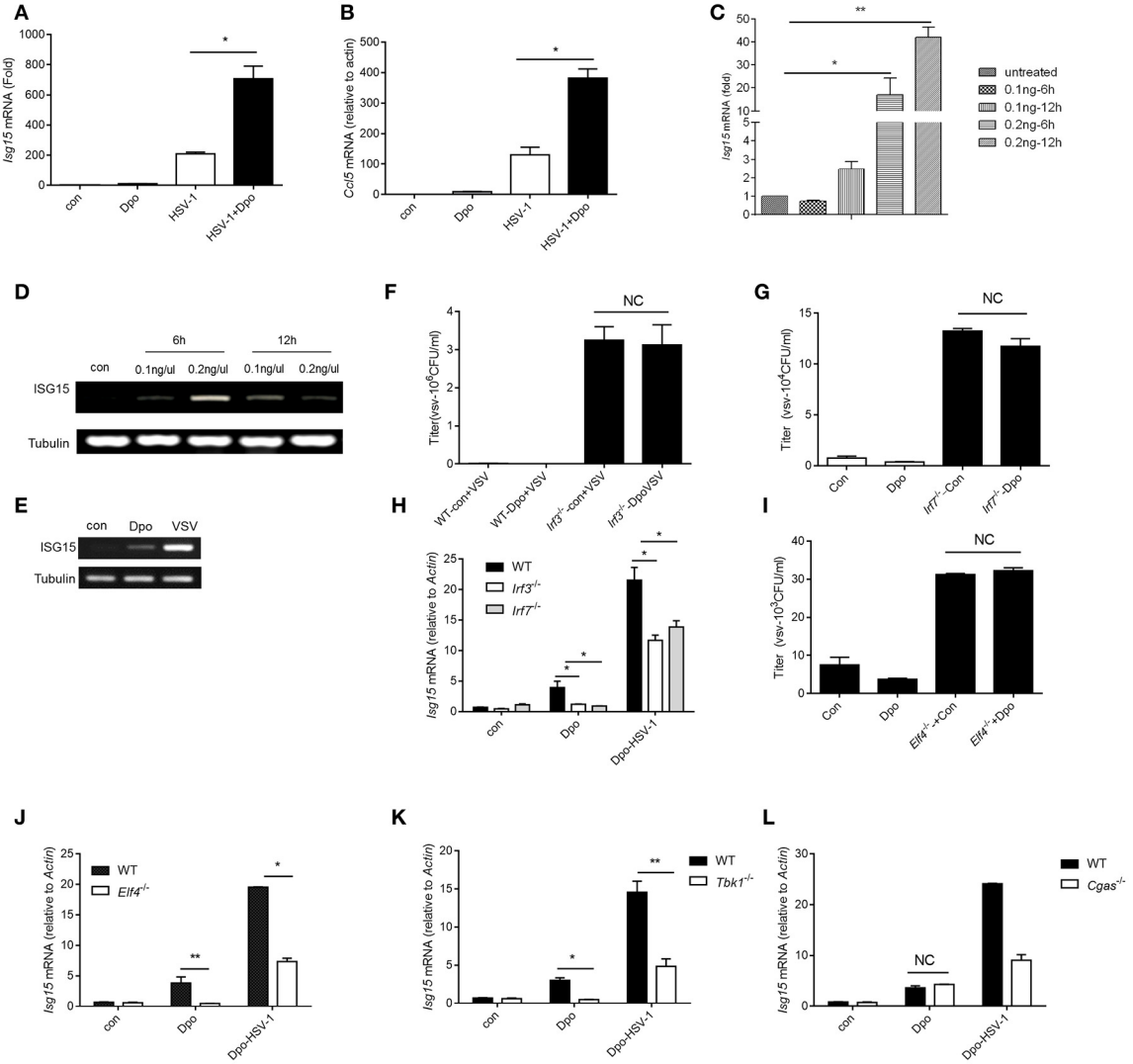

FIGURE 4 | Dpo induces ISGs via IRFs/ELF4. **(A,B)** Bone marrow derived macrophages were treated with Dpo. Four hours later, these cells were infected with HSV-1. Twenty-four hours later, the mRNA level of ISG15 **(A)** and CCl5 **(B)** were measured by qPCR. **(C)** Bone marrow derived macrophages were treated with increasing amount of Dpo. Twenty-four hours later, the mRNA level of ISG15 was measured by qPCR. **(D,E)** DC2.4 cells and peritoneal macrophages were treated with Dpo or infected with VSV. Twenty-four hours later, the mRNA level of ISG15 were measured by RT-PCR. **(F–H)** WT, *Irf3*$^{-/-}$ or *Irf7*$^{-/-}$ iBMDM were treated with Dpo. Four hours later, these cells were infected with VSV. Twenty-four hours later, and the viral load were measured by plaque assay **(F,G)**, the mRNA level of ISG15 was measured by qPCR **(H)**. **(I,J)** WT or *Elf4*$^{-/-}$ iBMDM were treated with Dpo. Four hours later, these cells were infected with HSV-1. Twenty-four hours later, and the viral load were measured by plaque assay **(I)**, the mRNA level of ISG15 was measured by qPCR **(J)**. **(A–C,F–J)** The data represent mean values ± SEM ($n = 3$); *$P < 0.05$, **$P < 0.01$ significant compared to control, Student's *t*-test. WT, *Tbk1*$^{-/-}$ **(K)** or *Cgas*$^{-/-}$ **(L)** iBMDM were treated with Dpo. Four hours later, these cells were infected with HSV-1. Twenty-four hours later, the mRNA level of ISG15 was measured by qPCR.

In Vivo Dpo Treatment and Virus Infection

The C57BL/6 STING$^{-/-}$, TLR4$^{-/-}$ mice were breeding by ourselves. Age-and sex-matched C57BL/6 littermate were produced and used in all the experiments.

Seven-week-old mice were distribution into two groups: control group and experimental group. Before infection the mice with viruses, control group mice were treatment with PBS (200 μl/mouse), and experimental group mice with Dpo (10 μg/mouse) by intravenous injection. Twenty-four hours later, both group mice were infection with HSV-1 with 2 × 108 plaque-forming units (PFU) of viruses per mouse by intravenous. The survival state of the mice was monitored accordingly.

Pseudo Typed HIV-1 Production and Infection

Vesicular Stomatitis Virus Glycoprotein (VSV-G)-pseudotyped HIV or YU2-HIV were produced from 293T cells using the standard phosphate calcium transfection protocol. HEK293T cells were seeded at a density of 8 × 105 cells per well in 6-well plates. Twelve hours after plating, cells were transfected with

VSV-G (0.07 μg) or YU2 (1.33 μg), pOPRIgagpol (1.5 μg), Ps-ReV (0.33 μg) and HIVec2GFP (0.66 μg), media was replaced 16 h after transfection and viruses were harvested 48 h later, filtered at 0.2 mm, and stored at −20°C in aliquots (After 10 min centrifugation at 14 krpm, virus-containing supernatant was transferred to a fresh tube, and stored at −20°C in aliquots). HEK293T (2×10^5) and TZM-bl cells (1×10^5) were plated on 24 well-plates 12 h before infection. Infection was performed by addition of 300 μL virus-containing supernatant. After a 12-h incubation, supernatants were removed and replaced with fresh media. Luciferase assay was measured 48 h after infection.

Quantitative Real-Time PCR

Total RNA was isolated from cells using the RNeasy RNA extraction kit (Qiagen) and cDNA synthesis was performed using 1 μg of total RNA (iScriptcDNA Synthesis kit). Quantitative PCR was done with gene-specific primers and 6FAM-TAMRA (6-carboxyfluorescein–N,N,N′,N′-tetramethyl-6-carboxyrhodamine) probes or inventoried gene expression kits from Applied Biosystems [6FAM-MGB (6-carboxyfluorescein minor groove binder) probes]. The sequence of the primers were listed in the Supplementary Table 1.

Plaque Assay

For the HSV-1 plaque assays, cells ($\sim 1 \times 10^5$) were first infected with virus. Twenty-four hours later, supernatants were collected and used to infect confluent Vero cells. One hour later, supernatants were removed and cells were washed with PBS and culture medium containing 2% (wt/vol) methylcellulose was overlaid for 60 h, cells were fixed for 30 min with 0.5% (vol/vol) glutaraldehyde and were stained with 1% (wt/vol) crystal violet dissolved in 70% ethanol. Plaques were counted and average counts were multiplied by the dilution factor to determine the viral titer as plaque-forming units per ml. The VSV plaque assay was performed as previously described (You et al., 2009).

RNA Seq

Macrophages were treated with Dpo or medium. We harvested these cell and control cells, and purified whole RNA by using RNeasy Mini Kit (Qiagen NO. 74104). The transcriptome library for sequencing was generated using VAHTSTM mRNA-seq v2 Library Prep Kit for Illumina® (Vazyme Biotech Co., Ltd, Nanjing, China) following the manufacturer's recommendations. After clustering, the libraries were sequenced on IlluminaHiseq X Ten platform using (2 × 150 bp) paired-end module. The raw images were transformed into raw reads by base calling using CASAVA (http://www. illumina.com/ support/ documentation.ilmn). Then, raw reads in a fastq format were first processed using in-house perl scripts. Clean reads were obtained by removing reads with adapters, reads in which unknown bases were more than 5% and low quality reads (the percentage of low quality bases was over 50% in a read, we defined the low quality base to be the base whose sequencing quality was no more than 10. At the same time, Q20, Q30, GC content of the clean data were calculated (Vazyme Biotech Co., Ltd, Nanjing, China). The original data of the RNA-seq was uploaded to the GEO DataSets (GEO Accession No. GSE104236).

Statistical Analysis

Statistical comparisons were performed with the mean ± standard error of the mean (SEM) for continuous variables. All data were statistically analyzed by unpaired 2 sample *t*-test with $p < 0.05$ indicative of statistical significance. All analyses were performed using GraphPad Prism 6.

AUTHOR CONTRIBUTIONS

FY: Designed the study and analyzed the data and wrote or revised the paper. JC, TL, HD: Performed experiments. LY: Analyzed the data and provided expertise and contributed to animal work. SC: Provided expertise and contributed to RNAseq screening. WT, HS, BJ, GY: Provide technical help. LY: Provided expertise and contributed to experiment with viral infection.

ACKNOWLEDGMENTS

We thank Zhengfan Jiang (Peking University) for the reporter plasmids. This work was supported by the National Natural Science Foundation of China (31570891) and the Open Project Program of Jiangsu Key Laboratory for High Technology Research of TCM Formulae and Jiangsu Collaborative Innovation Center of Chinese Medicinal Resources Industrialization (No. FJGJS-2015-07).

SUPPLEMENTARY MATERIAL

The Supplementary Material for this article can be found online at: https://www.frontiersin.org/articles/10.3389/fcimb.2017.00456/full#supplementary-material

REFERENCES

Abdelgaleil, S. A., Kassem, S. M., Doe, M., Baba, M., and Nakatani, M. (2001). Diterpenoids from *Euphorbia paralias*. *Phytochemistry* 58, 1135–1139. doi: 10.1016/S0031-9422(01)00393-4

Akihisa, T., KithsiriWijeratne, E. M., Tokuda, H., Enjo, F., Toriumi, M., Kimura, Y., et al. (2002). Eupha-7,9(11),24-trien-3beta-ol ("antiquol C") and other triterpenes from *Euphorbia antiquorum* latex and their inhibitory effects on Epstein-Barr virus activation. *J. Nat. Prod.* 65, 158–162. doi: 10.1021/np010377y

Chen, H., Sun, H., You, F., Sun, W., Zhou, X., Chen, L., et al. (2011). Activation of STAT6 by STING is critical for antiviral innate immunity. *Cell* 147, 436–446. doi: 10.1016/j.cell.2011.09.022

Dixit, E., Boulant, S., Zhang, Y., Lee, A. S., Odendall, C., Shum, B., et al. (2010). Peroxisomes are signaling platforms for antiviral innate immunity. *Cell* 141, 668–681. doi: 10.1016/j.cell.2010.04.018

Ghanadian, M., Choudhary, M. I., Ayatollahi, A. M., Mesaik, M. A., Abdalla, O. M., and Afsharypour, S. (2013). New cyclomyrsinolditerpenes from Euphorbia aellenii with their immunomodulatory effects. *J. Asian Nat. Prod. Res.* 15, 22–29. doi: 10.1080/10286020.2012.742073

Häcker, H., Vabulas, R. M., Takeuchi, O., Hoshino, K., Akira, S., and Wagner, H. (2000). Immune cell activation by bacterial CpG-DNA through myeloid differentiation marker 88 and tumor necrosis factor receptor-associated factor (TRAF) 6. *J. Exp. Med*. 192, 595–600. doi: 10.1084/jem.192.4.595

Hezareh, M. (2005). Prostratin as a new therapeutic agent targeting HIV viral reservoirs. *Drug News Perspect*. 18, 496–500. doi: 10.1358/dnp.2005.18.8.944543

Hoshino, K., Sugiyama, T., Matsumoto, M., Tanaka, T., Saito, M., Hemmi, H., et al. (2006). IkappaB kinase-alpha is critical for interferon-alpha production induced by Toll-like receptors 7 and 9. *Nature* 440, 949–953. doi:10.1038/nature04641

Ishikawa, H., and Barber, G. N. (2008). STING is an endoplasmic reticulum adaptor that facilitates innate immune signalling. *Nature* 455, 674–678. doi: 10.1038/nature07317

Korin, Y. D., Brooks, D. G., Brown, S., Korotzer, A., and Zack, J. A. (2002). Effects of prostratin on T-cell activation and human immunodeficiency virus latency. *J. Virol*. 76, 8118–8123. doi: 10.1128/JVI.76.16.8118-8123.2002

Kulkosky, J., Culnan, D. M., Roman, J., Dornadula, G., Schnell, M., Boyd, M. R., et al. (2001). Prostratin: activation of latent HIV-1 expression suggests a potential inductive adjuvant therapy for HAART. *Blood* 98, 3006–3015. doi: 10.1182/blood.V98.10.3006

Kumar, H., Kawai, T., Kato, H., Sato, S., Takahashi, K., Coban, C., et al. (2006). Essential role of IPS-1 in innate immune responses against RNA viruses. *J. Exp. Med*. 203, 1795–1803. doi: 10.1084/jem.20060792

Li, X. L., Li, Y., Wang, S. F., Zhao, Y. L., Liu, K. C., Wang, X. M., et al. (2009). Ingol and ingenolditerpenes from the aerial parts of Euphorbia royleana and their antiangiogenic activities. *J. Nat. Prod*. 72, 1001–1005. doi: 10.1021/np800816n

Liu, S., Cai, X., Wu, J., Cong, Q., Chen, X., Li, T., et al. (2015). Phosphorylation of innate immune adaptor proteins MAVS, STING, and TRIF induces IRF3 activation. *Science* 347:aaa2630. doi: 10.1126/science.aaa2630

Márquez, N., Calzado, M. A., Sánchez-Duffhues, G., Pérez, M., Minassi, A., Pagani, A., et al. (2008). Differential effects of phorbol−13 - monoesters on human immunodeficiency virus reactivation. *Biochem. Pharmacol*. 75, 1370–1380. doi: 10.1016/j.bcp.2007.12.004

Schulz, O., Diebold, S. S., Chen, M., Näslund, T. I., Nolte, M. A., Alexopoulou, L., et al. (2005). Toll-like receptor 3 promotes cross-priming to virus-infected cells. *Nature* 433, 887–892. doi: 10.1038/nature03326

Seth, R. B., Sun, L., Ea, C. K., and Chen, Z. J. (2005). Identification and characterization of MAVS, a mitochondrial antiviral signaling protein that activates NF-κB and IRF 3. *Cell* 122, 669–682. doi: 10.1016/j.cell.2005.08.012

Shi, Q. W., Su, X. H., and Kiyota, H. (2008). Chemical and pharmacological research of the plants in genus Euphorbia. *Chem. Rev*. 108, 4295–4327. doi: 10.1021/cr078350s

Sun, L., Wu, J., Du, F., Chen, X., and Chen, Z. J. (2013). Cyclic GMP-AMP synthase is a cytosolic DNA sensor that activates the type I interferon pathway. *Science* 339, 786–791. doi: 10.1126/science.1232458

Sun, W., Li, Y., Chen, L., Chen, H., You, F., Zhou, X., et al. (2009). ERIS, an endoplasmic reticulum IFN stimulator, activates innate immune signaling through dimerization. *Proc. Natl. Acad. Sci. U.S.A*. 106, 8653–8658. doi: 10.1073/pnas.0900850106

Sun, Y. X., and Liu, J. C. (2011). Chemical constituents and biological activities of Euphorbia fischerianaSteud. *Chem. Biodivers*. 8, 1205–1214. doi: 10.1002/cbdv.201000115

Takaoka, A., Wang, Z., Choi, M. K., Yanai, H., Negishi, H., Ban, T., et al. (2007). DAI (DLM-1/ZBP1) is a cytosolic DNA sensor and an activator of innate immune response. *Nature* 448, 501–505. doi: 10.1038/nature06013

Takeuchi, O., Hoshino, K., and Akira, S. (2000a). Cutting edge: TLR2-deficient and MyD88-deficient mice are highly susceptible to *Staphylococcus aureus* infection. *J. Immunol*. 165, 5392–5396. doi: 10.4049/jimmunol.165.10.5392

Takeuchi, O., Takeda, K., Hoshino, K., Adachi, O., and Ogawa, T. (2000b). Cellular responses to bacterial cell wall components are mediated through MyD88-dependent signaling cascades. *Int. Immunol*. 12, 113–117. doi: 10.1093/intimm/12.1.113

Tanaka, R., Kasubuchi, K., Kita, S., Tokuda, H., Nishino, H., and Matsunaga, S. (2000). Bioactive steroids from the whole herb of *Euphorbia chamaesyce*. *J. Nat. Prod*. 63, 99–103. doi: 10.1021/np990394b

Uemura, D., and Hirata, Y. (1972). Two new diterpenoids, jolkinolides A and B, obtained from euphorbia *Jolkini boiss* (Euphorbiaceae). *Tetrahedron Lett*. 13, 1387–1390. doi: 10.1016/S0040-4039(01)84635-9

Unterholzner, L., Keating, S. E., Baran, M., Horan, K. A., Jensen, S. B., Sharma, S., et al. (2010). IFI16 is an innate immune sensor for intracellular DNA. *Nat. Immunol*. 11, 997–1004. doi: 10.1038/ni.1932

Vasas, A., and Hohmann, J. (2014). Euphorbia diterpenes: isolation, structure, biological activity, and synthesis (2008-2012). *Chem. Rev*. 114, 8579–8612. doi: 10.1021/cr400541j

Wang, Y. B., Huang, R., Wang, H. B., Jin, H. Z., Lou, L. G., and Qin, G. W. (2006). Diterpenoids from the roots of Euphorbia fischeriana. *J. Nat. Prod*. 69, 967–970. doi: 10.1021/np0600088

Wang, Y., Ma, X., Yan, S., Shen, S., Zhu, H., Gu, Y., et al. (2009). 17-hydroxy-jolkinolide B inhibits signal transducers and activators of transcription 3 signaling by covalently cross-linking Janus kinases and induces apoptosis of human cancer cells. *Cancer Res*. 69, 7302–7310. doi: 10.1158/0008-5472.CAN-09-0462

Wesolowska, O., Wisniewski, J., Duarte, N., Ferreira, M. J., and Michalak, K. (2007). Inhibition of MRP1 transport activity by phenolic and terpenic compounds isolated from Euphorbia species. *Anticancer Res*. 27, 4127–4133.

Xu, L. G., Wang, Y. Y., Han, K. J., Li, L. Y., Zhai, Z., and Shu, H. B. (2005). VISA is an adapter protein required for virus-triggered IFN-beta signaling. *Mol. Cell* 19, 727–740. doi: 10.1016/j.molcel.2005.08.014

Yamamoto, M., Sato, S., Mori, K., Hoshino, K., Takeuchi, O., Takeda, K., et al. (2002). Cutting edge: a novel Toll/IL-1 receptor domain-containing adapter that preferentially activates the IFN-beta promoter in the toll-like receptor signaling. *J. Immunol*. 169, 6668–6672. doi: 10.4049/jimmunol.169.12.6668

Yang, C. L. (1993). *MateriaMedica of Toxic Herbs*. Beijing: Chinese Medicine and Materials Publisher.

Yoneyama, M., Kikuchi, M., Matsumoto, K., Imaizumi, T., Miyagishi, M., Taira, K., et al. (2005). Shared and unique functions of the DExD/H-box helicases RIG-I, MDA5, and LGP2 in antiviral innate immunity. *J. Immunol*. 175, 2851–2858. doi: 10.4049/jimmunol.175.5.2851

Yoneyama, M., Kikuchi, M., Natsukawa, T., Shinobu, N., Imaizumi, T., Miyagishi, M., et al. (2004). The RNA helicase RIG-I has an essential function in double-stranded RNA-induced innate antiviral responses. *Nat. Immunol*. 5, 730–737. doi: 10.1038/ni1087

You, F., Sun, H., Zhou, X., Sun, W., Liang, S., Zhai, Z., et al. (2009). PCBP2 mediates degradation of the adaptor MAVS via the HECT ubiquitin ligase AIP4. *Nat. Immunol*. 10, 1300–1308. doi: 10.1038/ni.1815

Zhang, Z., Yuan, B., Bao, M., Lu, N., Kim, T., and Liu, Y. J. (2011). The helicase DDX41 senses intracellular DNA mediated by the adaptor STING in dendritic cells. *Nat. Immunol*. 12, 959–965. doi: 10.1038/ni.2091

Zhong, B., Yang, Y., Li, S., Wang, Y. Y., Li, Y., Diao, F., et al. (2008). The adaptor protein MITA links virus-sensing receptors to IRF3 transcription factor activation. *Immunity* 29, 538–535. doi: 10.1016/j.immuni.2008.09.003

Conflict of Interest Statement: The authors declare that the research was conducted in the absence of any commercial or financial relationships that could be construed as a potential conflict of interest.

frontiers in Cellular and Infection Microbiology

ORIGINAL RESEARCH
published: 17 January 2018
doi: 10.3389/fcimb.2017.00542

Dengue Virus Capsid Interacts with DDX3X–A Potential Mechanism for Suppression of Antiviral Functions in Dengue Infection

Rinki Kumar[1,2], *Nirpendra Singh*[3], *Malik Z. Abdin*[2], *Arvind H. Patel*[4] and *Guruprasad R. Medigeshi*[1]*

[1] Clinical and Cellular Virology Lab, Vaccine and Infectious Disease Research Center, Translational Health Science and Technology Institute, NCR-Biotech Science Cluster, Faridabad, India, [2] Department of Biotechnology, Jamia Hamdard, New Delhi, India, [3] Regional Center for Biotechnology, NCR-Biotech Science Cluster, Faridabad, India, [4] MRC-University of Glasgow Centre for Virus Research, Glasgow, United Kingdom

Dengue virus is a pathogen of global concern and has a huge impact on public health system in low- and middle-income countries. The capsid protein of dengue virus is least conserved among related flavivirus and there is very limited information on the role of cytosolic proteins that interact with dengue virus capsid. We identified DEAD (Asp-Glu-Ala-Asp) Box Helicase 3, an X-Linked (DDX3X), cytosolic ATP-dependent RNA helicase as a dengue virus capsid-interacting protein. We show that the N-terminal region of capsid is important for interaction with DDX3X, while the N-terminal domain of DDX3X seems to be involved in interaction with dengue capsid. DDX3X was down-regulated in dengue virus infected cells at later stages of infection. Our results show that DDX3X is an antiviral protein as suppression of DDX3X expression by siRNA led to an increase in viral titers and overexpression of DDX3X led to inhibition of viral replication. Knock-down of DDX3X did not affect induction of type I interferon response upon infection suggesting that the effect of DDX3X knock-down is independent of the interferon-dependent pathways that DDX3X modulates under normal conditions. Thus, our study identifies DDX3X as a dengue virus capsid interacting protein and indicates a potential link between the antiviral functions of DDX3X and dengue capsid at later stages of dengue infection.

Keywords: Dengue virus, capsid, DDX3X, siRNA, antiviral

Edited by:
James Drew Brien,
Saint Louis University, United States

Reviewed by:
Penghua Wang,
New York Medical College, United States
Sunnie R. Thompson,
University of Alabama at Birmingham, United States
Tonya Michelle Colpitts,
National Emerging Infectious Diseases Laboratories (NEIDL), Boston University, United States

***Correspondence:**
Guruprasad R. Medigeshi
gmedigeshi@thsti.res.in

Received: *18 August 2017*
Accepted: *26 December 2017*
Published: *17 January 2018*

Citation:
Kumar R, Singh N, Abdin MZ, Patel AH and Medigeshi GR (2018) Dengue Virus Capsid Interacts with DDX3X–A Potential Mechanism for Suppression of Antiviral Functions in Dengue Infection. Front. Cell. Infect. Microbiol. 7:542. doi: 10.3389/fcimb.2017.00542

INTRODUCTION

Dengue is the most common mosquito-borne viral disease in tropical and subtropical areas, with an estimated 50–100 million infections occurring each year. Dengue virus (DENV) is a member of *Flaviviridae* family, which consists of a group of enveloped, positive sense, single-stranded, RNA viruses. DENV genome encodes three structural proteins, namely core (C), membrane (prM/M), and envelope (E), and seven non-structural proteins, (NS1, NS2A, NS2B, NS3, NS4A, NS4B, and NS5), which are produced via proteolytic processing of the single polyprotein by viral serine protease (NS2B-NS3) and cellular proteases (Medigeshi, 2011). Sequential cleavages of the anchored capsid protein by viral protease and host signalase result in removal of the C-terminal trans-membrane region to yield the 100-residue mature form,

which is a highly basic 12 kDa protein (Amberg et al., 1994; Yamshchikov and Compans, 1995; Sangiambut et al., 2008, 2013). While the mechanism by which encapsidation occurs is not completely understood, it is proposed that the capsid protein interacts with the viral genome to form the nucleocapsid, possibly via interactions with basic surfaces on the solvent-exposed side of the protein (Jones et al., 2003; Ma et al., 2004). A number of host proteins have been identified as capsid-interacting proteins for various flaviviruses and these studies implicate capsid in a variety of functions such as lipid metabolism, apoptosis and stress granule formation (Byk and Gamarnik, 2016). West Nile virus capsid protein has been proposed to activate pro-survival pathways by blocking apoptosis through a phosphatidylinositol (PI) 3-kinase-dependent pathway (Urbanowski and Hobman, 2013). However, another study showed an opposite role for capsid where, WNV capsid was shown to induce apoptosis in a p53-dependent manner (Yang et al., 2008). Recent studies have also proposed a role for JEV capsid protein in blocking stress granule formation and relieving translation repression by interaction with Caprin-1 (Katoh et al., 2013). DENV capsid was shown to colocalize with MX1/MxA, an interferon-induced GTPase involved in antiviral signaling in primary endothelial cells infected with DENV-2 suggesting a role for capsid protien in blocking antiviral pathways (Kanlaya et al., 2010).

Many groups have identified capsid-interacting proteins some of which include nucleolin, histone proteins H2A, H2B, H3, H4, and importin-α (Bhuvanakantham et al., 2009; Netsawang et al., 2010; Colpitts et al., 2011; Balinsky et al., 2013; Bhuvanakantham and Ng, 2013; Mairiang et al., 2013). Overexpression of capsid protein leads to nuclear localization, therefore, it is not surprising, that most of the capsid-interacting proteins identified above are nuclear proteins. Although the C protein of dengue virus localizes to the nucleus of mammalian cells and remains at high levels throughout the course of infection (Wang et al., 2002; Sangiambut et al., 2008), its role in the nucleus is not yet understood. Given the role of C in promoting encapsidation of the viral RNA and subsequent assembly of infectious virus particles, it is imperative to identify non-nuclear capsid-interacting proteins to further elucidate the role of capsid in dengue virus life-cycle. In this study, we adopted an in-solution interaction approach and identified 16 proteins interacting with DENV capsid by proteomics and mass spectrometry. One of the capsid-interacting proteins identified was DDX3X, a DEAD (Asp-Glu-Ala-Asp)-box helicase. DEAD-box RNA helicases belong to helicase superfamily 2 and consist of two large domains, the N- terminal and C-terminal domains which consist of 9 conserved sequence motifs (Garbelli et al., 2011b). DDX3X shuttles between cytoplasm and the nucleus and plays a multifunctional role such as RNA splicing, transcriptional and translational regulation, mRNA export and translation initiation, and it also contributes to the nuclear export of RNA (Owsianka and Patel, 1999; Yedavalli et al., 2004; Lai et al., 2008; Schroder, 2011). DDX3X has also been shown to regulate innate immune responses through its interaction with components of antiviral signaling such as mitochondrial antiviral signaling protein, TANK-binding kinase-1 and I-kappa-B kinase epsilon which results in IRF3 and IRF7 activation and interferon-β production (Schröder et al., 2008; Soulat et al., 2008; Mulhern and Bowie, 2010; Oshiumi et al., 2010b). Recent reports suggests that many viruses usurp the function of DDX3X to promote viral RNA replication or prevent DDX3X functions (Valiente-Echeverría et al., 2015). Therefore, we further characterized the role of DDX3X in dengue infection as a capsid-interacting partner. We show that DDX3X is an antiviral protein and interaction of DENV capsid with DDX3X may counter the antagonistic effect of DDX3X in DENV life-cycle.

MATERIALS AND METHODS

Cells and Viruses

All the cell lines, virus strain used in this study and virus titering protocols have been described previously (Agrawal et al., 2013; Medigeshi et al., 2016). Huh-7, HEK293T, A549 cells were grown in Dulbecco's modified Eagle medium (DMEM) supplemented with 10% fetal bovine serum (FBS), 1 mM L-glutamine, 100 units/ml penicillin-streptomycin-glutamine and non-essential amino acids at 37°C and 5% CO2. BHK-21 and C6/36 cells were grown in the minimal essential medium (MEM) containing 10% FBS, Earl's salts and PSG in the concentration mentioned above. Dengue virus serotype 2 obtained from National Institute of virology, India (Dengue virus 2 isolate P23085 INDI-60-GenBank: KJ918750.1) was used throughout the study. The virus was cultured in C6/36 cell lines and titered by plaque assay in BHK21 cells as described previously (Agrawal et al., 2013).

Antibodies

Mouse monoclonal antibodies for anti-6X his-tag (Abcam - ab18184) (1:1,000), HA (Biolegend 901501) (1:1,000), α-tubulin (Clone 12G10 from Developmental Studies Hybridoma Bank, University of Iowa) (1:5,000) and viral envelope (Merck-Millipore MAB10216) (1:1,000) were used. Rabbit polyclonal antibodies for GAPDH (1:5,000) were from Cell Signaling Technology (CST 2118). Rabbit polyclonal dengue-capsid antibody was used for immunoblotting (1:1,000) (Agrawal et al., 2013). Rabbit polyclonal DDX3X (R648) antibody (1:2,000 for western blotting and 1:1,000 for immunofluorescence) has been described before (Angus et al., 2010). Anti-rabbit (Merck-Millipore) or anti-mouse (Sigma) IgG secondary antibodies raised in goat and conjugated with horseradish peroxidase (HRP) (1:2,000) were used. HRP-conjugated secondary antibodies specific to IgG-light chain (Jackson's Immunoresearch Lab) were used (1:10,000) for probing blots of immunoprecipitation.

Cloning, Expression, and Purification of DENV2 Capsid

DENV2 full-length capsid construct was generated by PCR and cloning into pET-23b vector using the forward primer 5′-TAC ATATGAATAACCAACGGAAAAAGG-3′ and reverse primer 5′-GACTCGAGTCTGCGTCTCCTGTTCAAG-3′ using NdeI & XhoI sites. Capsid clone in a mammalian expression vector pEF1/*myc*hisC was generated using the forward primer 5′-TAGG TACCATGAATAACCAACGGAAAAAG-3′ and reverse primer 5′-TAGCGGCCGCTCAGTGGTGGTGGTGGTG-3′ with KpnI and NotI restriction sites.

Capsid deletion constructs were generated in pEF1/*myc*hisA with KpnI & NotI sites using the following primers: α2-4-capsid (26-100 a.a) 5′-TAGGTACCATGAAACTGTTCATGGCCC-3′ (forward) and 5′-TAGCGGCCGCTCAGTGGTGGTGGTGGTGGT G-3′ (reverse). α3-4-capsid (63–100 a.a) 5′-TAGGTACCATGG CAGGGATATTGAAGA-3′(forward) and 5′ TAGCGGCCGCT CAGTGGTGGTGGTGGTG-3′ (reverse). α4-capsid (74–100 a.a) 5′-TAGGTACCATGAAATCAAAAGC-3′ (forward) and 5′-TAG CGGCCGCTCAGTGGTGGTGGTGGTG-3′ (reverse). Plasmids were constructed by standard PCR methods using Expand Hi fidelity^{plus} PCR system (Roche). Clones were verified by sequencing.

Protein Purification

The His-tagged full length DENV2 capsid clone was generated in pET23b vector as described above, and expressed in BL21DE3pLysS cells for protein purification as per standard procedures. Briefly, an overnight culture of pET23b-capsid was inoculated into fresh Luria-Bertani (LB) media containing ampicillin and chloramphenicol. At an O.D$_{600}$ of 0.4–0.5, protein expression was induced using isopropyl-beta-D-thiogalactoside (IPTG) to a final concentration of 1 mM for 4 h at 37°C. Cells were harvested by centrifugation at 4,000 × *g* for 20 min. Cell pellet was resuspended in cold lysis buffer (50 mM NaH_2PO_4, 150 mM NaCl, and phenylmethanesulfonylfluoride (PMSF), pH 8.0) followed by sonication. All steps were carried out at 4°C. The crude extract was centrifuged at 17,000 × *g*. Triton-X-100 and imidazole was added to a final concentration of 1% and 20 mM respectively. Lysate was incubated with pre-washed Ni-NTA beads (Qiagen) for 2 h. The beads were washed three times with wash buffer (50 mM NaH_2PO_4, 150 mM NaCl, 1% Triton-X-100, 50 mM imidazole, pH 8.0). Capsid protein was eluted using 100, 250, and 500 mM imidazole buffer pH 8.0. The purified capsid protein was dialyzed overnight using a dialysis cassette with a cut-off value of 2 kDa (ThermoFisher Scientific) in dialysis buffer (50 mM NaH_2PO_4, 150 mM NaCl, 20 mM imidazole and 0.1% triton).

Interaction Studies

Huh-7 (human hepatocyte) cells from a confluent T150 flask were used for each interaction experiment. The cells were lysed in cold lysis buffer (50 mM NaH_2PO_4, 150 mM NaCl, 0.1% Triton-X-100, protease inhibitor cocktail (PIC), sodium orthovanadate and PMSF). The lysate was centrifuged at 17,000 × *g* at 4°C and supernatant was collected. 5 mg of the Huh-7 lysate protein was incubated with pre-washed Ni-NTA beads for 1 h as a pre-clearing step. 2 mg of dialyzed His-capsid protein was added to the pre-cleared Huh-7 lysate and incubated at 4°C for 2 h with continuous mixing. Prewashed Ni-NTA slurry was added to the lysate mixture and further incubated for 1 h at 4°C. The beads were washed with buffer containing (50 mM NaH_2PO_4, 150 mM NaCl, 0.1% Triton-X-100, 50 mM imidazole) and protein was eluted using 100 and 250 mM imidazole elution buffers. The eluates were precipitated overnight at 4°C using 10% trichloroacetic acid (TCA). Protein pellet was washed with 2% sodium acetate in ethanol, air-dried, and resuspended in 8 M urea buffer (UB).

Filter-Aided Sample Processing (FASP) for Mass Spectrometry

The TCA precipitated protein sample was resuspended in 200 µl of 8 M UB, loaded in a 3 kDa filter unit (Amicon-Millipore) and centrifuged at 14,000 × *g* for 15 min. Sample was washed by adding 200 µl of UB and centrifuged at 14,000 × *g* for 15 min. 100 µl of 0.05 M iodoacetamide (IAA) prepared in UB was added and mixed at 600 rpm for 1 min and incubated without mixing for 20 min. This was followed by centrifugation at 14,000 × *g* for 10 min. Washing was done twice by adding 100 µl of UB and centrifugation at 14,000 × *g* for 15 min. This was followed by two washes with 100 µl of 0.05 M ammonium bicarbonate (ABC) and centrifuged at 14,000 × *g* for 10 min. 40 µl ABC with trypsin (Promega V511A) (enzyme to protein ratio 1:100) was added and mixed at 600 rpm for 1 min, and then incubated in a water bath at 37°C for 16–18 h. The digested peptides were eluted at 14,000 × *g* for 10 min. Any remaining peptides were eluted with another 20–30 µl of ABC. The eluted sample was acidified with 0.1% formic acid and concentrated to 10 µl by speed vac. LC MS/MS was done using AB SCIEX Triple TOF 5600. The peptides were identified by searching the MS data against the MASCOT and PARAGON search engines. Proteins were selected for further study based on a 5% false-discovery rate cut-off and a minimum of 2-peptide-per-protein.

Cloning of DDX3X Plasmid Constructs

HA-DDX3X was a gift from Robin Reed (Addgene plasmid # 44975). All plasmid constructs of DDX3X were generated in pSELECT-CHA-zeo and pSELECT-cGFP-Blas with Age-I & Bam-HI sites using the following primers: DDX3X-full length (FL) was generated using 5′-TAACCGGTATG AGTCATGTGGCAGTG-3′ (forward) and 5′-ATGGATCCGT TACCCCACCAGTCAA-3′ (reverse). DDX3X-Δ351-661 was generated using primers 5′-TAACCGGTATGAGTCATGTGG CAGTG-3′ (forward) and 5′-GGATCCATCAGCTTCATCTA A-3′ (reverse). DDX3X-Δ385-661 was generated using 5′-TAACCGGT ATGAGTCATGTGGCAGTG-3′ (forward) and 5′GGATCCAGTAGCACTAAACATCAT3′ reverse). DDX3X-Δ1-222Δ351-661 was generated using 5′-TAACCGGTATGTGT GCCCAAACAGGG-3′ (forward) 5′-GGATCCATATCCAACA TCCGATC-3′ (reverse). DDX3X-Δ1-381 was generated using 5′-TAACCGGTATGGCTACTTTTCCTAAG-3′ (forward) 5′ATG GATCCGTTACCCCACCAGTCAA3′ (reverse). Plasmids were constructed by standard PCR methods using Expand Hi fidelity^{plus} PCR system (Roche). Clones were verified by sequencing.

Immunoprecipitation (IP)

For transient transfection experiments, His-tagged capsid and HA-DDX3X plasmid constructs were co-transfected in HEK293T cells using Lipofectamine-2000 (Invitrogen). 24 h post-transfection, cell lysates were prepared in cold lysis buffer (0.5% Triton-X-100 in PBS containing PIC and PMSF). The lysates were pre-cleared using protein A sepharose beads (GE healthcare) and rabbit IgG for 1 h at 4°C on a tube rotator. The supernatant was collected and incubated with capsid antibody overnight on a rotator at 4°C. Next day, pre-washed protein A

sepharose beads were added and incubated for 2 h. The beads were washed with cold lysis buffer three times, and once with cold PBS. The beads were boiled in Laemmli buffer at 95°C for 5 min, loaded on SDS PAGE and transferred to PVDF membrane. Blots were probed with capsid and HA antibody. IgG light chain-specific secondary-HRP antibody was used to probe the blots. For DENV infection experiments, Huh-7 cells were plated in 3 cm dishes and infected with DENV at 5 MOI. At 24 h pi cells were collected in cold lysis buffer (0.5% Triton-X-100 in 1X TBS containing PIC, PMSF and sodium orthovanadate). The lysates were processed as described above and immunoprecipitation was performed using Capsid or DDX3X antibody. For RNAse treatment of lysates, infected Huh-7 cell lysates were treated with 200 μg/ml of bovine pancreatic RNAse A for 2 h at 4°C as per previous reports (Höck et al., 2007). The untreated and treated lysates were then used for pre-clearing with protein A sepharose beads followed by immunoprecipitation with DDX3X antibody as described above.

Pull-Down of HA-DDX3X using His-Capsid

HA-DDX3X deletion constructs were transfected into HEK293T cells. 24 h p.t, cell lysates were prepared in cold lysis buffer (0.5% Triton-X-100, 20 mM Tris-Cl and 150 mM NaCl, PIC, PMSF, and sodium orthovanadate). Purified capsid protein (20 μg) was added to the 80 μg of lysate (equivalent amount of all HA-tagged protein normalized to expression levels) and incubated for 2 h at 4°C. Then 20 mM imidazole and pre-washed Ni-NTA slurry were added and incubated for 1 h at 4°C with constant mixing. The beads were washed with buffer containing 20 mM Tris-Cl,150 mM NaCl and 20 mM imidazole and boiled in 1X Laemmli buffer and processed for western blot analysis with anti-HA and capsid antibodies.

Western Blotting, siRNA Transfection, Real Time PCR, and Immunofluorescence

Cell lysates were prepared and processed for western blot analysis as described previously (Agrawal et al., 2013). siRNA targeting the human DDX3X were purchased from Dharmacon (Cat. No. L-006874-02, J-006874-07, and J-006874-18) and transfections were performed as described previously (Kumar et al., 2016).

Total RNA isolation and real-time PCR conditions for DENV viral RNA levels has been described before (Agrawal et al., 2013; Kumar et al., 2016). Briefly, total RNA was isolated using Trizol reagent (Life Technologies). cDNA was synthesized using gDNA eraser Takara cDNA synthesis kit. qRT-PCR was performed by one-step or two-step methods using either Taqman or SYBR green chemistry. Two hundred nanogram of total RNA was used to determine viral genome copy numbers using Taqman one-step qRT-PCR using primers and probe for DEN-UTR and normalized to GAPDH. DDX3X knock-down levels were verified by SYBR green chemistry using the following primers: Forward 5′ GGAGGAAGTACAGCCAGCAAAG 3′ and reverse 5′ CTGCCAATGCCATCGTAATCACTC 3′. Immunofluorescence was performed by fixing cells with methanol as described previously (Haridas et al., 2013) and stained with DDX3X, dengue envelope protein and HA antibody. Interferon beta mRNA was using the following forward and reverse primers: 5′-AAACTCATGAGCAGTCTGCA-3′ and 5′-AGGAGATCTTCAGTTTCGGAGG-3′ (Jaworska et al., 2007).

Cell Proliferation Assay

Cell proliferation was assessed using Promega's CellTiter 96® AQueous One Solution cell proliferation assay kit as per the manufacturer's protocol. Briefly, knockdown of DDX3X was performed in Huh-7 cells using smart-pool siRNAs (si-DDX3X) and single siRNA (si-DDX3X-1) in 96 well plate. At 48 h p.t cells, 20 μl of the AQueous One Solution was added to each well containing 100 μl of media and incubated for 3 h. The reaction was stopped by adding 25 μl of 10% SDS. The supernatant was diluted 1:5 in PBS and absorbance was measured at 490 nm. OD_{490} from media alone with the AQueous One Solution was used to subtract background.

Flow Cytometry

Cells were collected by trypsinization and washed with FACS buffer (PBS+0.25% FBS). The fixable viability stain (BD EF-780) was added at 1:1,000 dilution and cells were incubated at RT for 10 min followed by washing with FACS buffer. Cells were centrifuged at 700 × *g* for 5 min and fixed in 3% PFA for 10 min on ice. Subsequently all steps were carried out at 4°C. Cells were washed once with FACS buffer and permeabilized with IMF buffer (20 mM HEPES pH 7.5, 0.1% triton-X 100, 150 mM NaCl, 5 mM EDTA, 0.02% sodium azide) for 20 min. The cells were washed with FACS buffer and pelleted by centrifugation. Primary anti-dengue envelope antibody conjugated to APC was prepared in IMF buffer at a dilution of 1:400, added to the cells and incubated for 1 h. The cells were washed twice with FACS buffer and resuspended in 1X PBS and acquired in BD FACS Canto-II. 50,000 cells were acquired in forward vs. side scatter in a linear scale. Data was analyzed using FlowJo (Treestar).

Statistical Analysis

GraphPad Prism software was used for all graphical representations and statistical analysis. All experiments were performed with two or three technical triplicates and all experiments have been performed two or more times. Non parametric, two tailed *t*-tests were performed to calculate *p*-values. $^{*}p < 0.05$, $^{**}p < 0.005$, and $^{***}p < 0.0005$.

RESULTS

Identification of DDX3X as a DENV Capsid-Interacting Protein

Previous studies have identified a number of cellular proteins that interact with dengue capsid using yeast-two-hybrid system and co-immunoprecipitation studies (Limjindaporn et al., 2007; Netsawang et al., 2010; Balinsky et al., 2013; Mairiang et al., 2013). Interestingly, these studies focused on the nuclear proteins that bound to capsid and elucidated the mechanism of capsid transport to the nucleus and possible link of host gene regulation due to the interaction of host proteins with capsid (Bhuvanakantham et al., 2009; Balinsky et al., 2013). To identify cytosolic proteins that interact with DENV capsid, we expressed

and purified DENV capsid protein without the membrane anchor domain in a bacterial expression system (**Figure S1**). The purified His-tagged capsid protein was allowed to interact in-solution with cell lysates prepared from Huh-7 cells. Ni-NTA beads were added to the reaction mix to pull down the capsid and any other interacting proteins. As capsid protein expressed in bacteria lacks post-translational modifications compared to the capsid protein in mammalian cells, it is likely that many interacting partners whose interaction depends on post-translational modifications would be missed by our approach. Nevertheless, the proteins bound to the beads were eluted and were digested with trypsin and processed for LC MS/MS to identify interacting proteins. The identification of peptides was performed by searching the Mascot and Paragon search engines and proteins were selected with a 5% false-discovery rate cut-off and a minimum of 2-peptide-per-protein. Using these criteria, 16 proteins were identified as potential DENV capsid interacting proteins (**Table 1**). Of these, DDX3X, which was identified consistently in four experiments, with the highest number of peptides was selected for further characterization.

Domain Mapping of DENV Capsid and DDX3X Interaction

We validated the mass spectrometry data by confirming the pull-down of DDX3X in the eluates from capsid and Huh-7 lysate interaction experiment by western blot analysis and identified DDX3X in interactions that had both the capsid protein and cell lysates but not with beads that were incubated with Huh-7 cell lysate without capsid (**Figure 1A**). We next used HEK293T cells for co-transfection of His-capsid and HA-DDX3X plasmids. Capsid-DDX3X interaction was verified by performing immunoprecipitation (IP) of capsid and western blot analysis for DDX3X. DDX3X was found to co-immunoprecipitate with capsid (**Figure 1B**). We next performed IP with either DDX3X antibody or capsid antibody in cell lysates prepared from Huh-7 cells infected with 5 MOI of DENV2. We observed co-IP of capsid and DDX3X respectively demonstrating the interaction of dengue capsid and DDX3X in the context of dengue infection (**Figures 1C,D**). The interaction of DDX3X with capsid was unaffected by pre-treatment of lysates with RNAse suggesting that the interaction was not bridged by RNA (**Figure S2**). Earlier studies with Hepatitis C virus core protein have shown that the N-terminal region of the core protein is sufficient for interaction with DDX3X (Owsianka and Patel, 1999). We generated truncated versions of DENV2 capsid based on the alpha-helical regions (Ma et al., 2004). However, we were able to detect expression of only the capsid construct lacking the first α-helix (α2-4-capsid) (**Figure S3**). Next, we transfected either full-length or α2-4-capsid constructs into HEK293T cells and verified co-IP of endogenous DDX3X with capsid antibody. As expected, DDX3X pull-down was observed with full-length capsid and the same was drastically reduced with α2-4-capsid suggesting that the N-terminal 45 amino acids of DENV capsid is required for interaction with DDX3X (**Figure 2A**). To further identify the capsid-interacting region in DDX3X, we generated HA-tagged DDX3X constructs with C-terminal deletions (DDX3X-Δ351-661, DDX3X-Δ385-661), N-terminal deletion (DDX3X-Δ1-381) and a double deletion mutant (DDX3X-Δ1-222, Δ351-661) and the full-length DDX3X (DDX3X-FL) (**Figure 2B**). We verified the expression of these deletion constructs in HEK293T cells and observed that the expression of DDX3X-Δ1-381 was highest, followed by DDX3X-Δ351-661. DDX3X-FL and DDX3X-Δ385-661 constructs had comparable expression levels. The double deletion mutant (DDX3X-Δ1-222, Δ351-661) had the lowest expression compared to all other constructs (**Figure 2C**, i). As we faced technical difficulties with co-immunoprecipitation of capsid using HA antibodies from infected cells, these HA-tagged constructs were expressed in HEK293T cells and equal quantity of lysates (normalized to HA-DDX3X expression levels) containing the recombinant HA-tagged proteins were incubated with purified His-capsid by in-solution interaction method as described in methods section. His-capsid was pulled down using Ni-NTA and co-elution of capsid protein was observed with all the HA-DDX3X constructs except the N-terminal deletion mutant (DDX3X-Δ1-381) (**Figure 2C**, ii). It is important to note that pull-down of HA-tagged DDX3X was observed in the presence of endogenous DDX3X present in the lysate which would act as a competitor for binding to capsid protein. Therefore, the low amounts of HA-DDX3X observed cannot be interpreted as weak interaction. The same lysates incubated with Ni-NTA beads alone failed to pull down any of the HA-tagged proteins ruling out non-specific interaction with the beads alone (**Figure 2C**, iii). The double deletion mutant (DDX3X-Δ1-222, Δ351-661) was capable of co-eluting with capsid, albeit at a lower levels relative to other constructs, and the DDX3X-Δ351-661 was most efficient in interaction with capsid under these conditions. Therefore, our data indicate that the N-terminal

TABLE 1 | List of identified potential capsid interacting proteins from mass spectrometry analysis.

Identified protein	No. of peptides (95% confidence)
DDX3X: DEAD (Asp-Glu-Ala-Asp) box, X-Linked, ATP dependent RNA helicase 3	25
Heterogeneous nuclear ribonucleoprotein Q	13
cDNA FLJ54373, highly similar to 60 kDa heat shock protein, mitochondrial	9
60S ribosomal protein L35	7
Heterogeneous nuclear ribonucleoprotein A0	6
Heterogeneous nuclear ribonucleoprotein A1	6
Histone H1.4	6
Heterogeneous nuclear ribonucleoprotein U	4
40S ribosomal protein S13	3
40S ribosomal protein S11	3
40S ribosomal protein S15a	2
40S ribosomal protein S8	2
60S ribosomal protein L23a	2
Pyrroline-5-carboxylate reductase 2	2
cDNA, FLJ94136, highly similar to Homo sapiens synaptotagmin binding, cytoplasmic RNA interacting protein (SYNCRIP)	2
cDNA FLJ53662, highly similar to Actin, alpha skeletal muscle	2

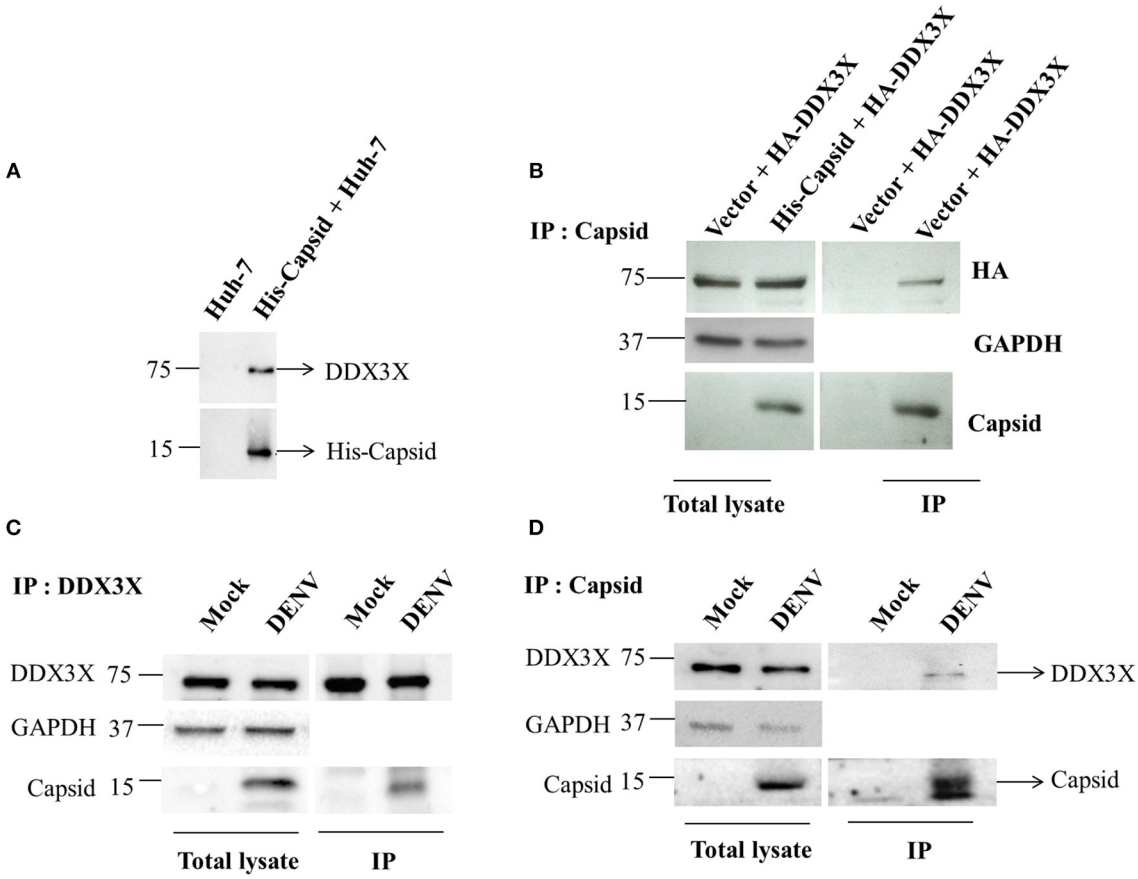

FIGURE 1 | Capsid coimmunoprecipitates with DDX3X from cell lysates. **(A)** In-solution interaction of purified His-tagged DENV capsid and Huh-7 lysate was followed by pull-down of interacting proteins using Ni-NTA beads. Pull down with Huh-7 lysate alone is used as a control. **(B)** His-tagged DENV capsid and HA-DDX3X were co-transfected in HEK293T cells. 24 h p.t. lysate was prepared and capsid was immunoprecipitated using DENV capsid antibody. Total lysate and immunoprecipitated proteins were analyzed by western blots probed for capsid, HA and GAPDH. **(C,D)** Huh-7 cells were infected with DENV at an MOI of 5. At 24 h pi mock and DENV-infected Huh-7 cell lysates were prepared, endogenous DDX3X **(C)** or DENV capsid **(D)** was immunoprecipitated from total lysates using DDX3X or DENV capsid antibody respectively. Total lysate and immunoprecipitated proteins were analyzed by western blots probed for capsid and DDX3X.

domain consisting of amino acids 223-350 is the minimal domain required for efficient interaction of DDX3X with DENV capsid.

DENV Down-Regulates DDX3X at Later Stages of Infection

The role of DDX3X in viral infections is poorly characterized. DDX3X has been shown to act as either a necessary factor or an inhibitor in viral replication (Yedavalli et al., 2004; Chang et al., 2006; Kalverda et al., 2009; Angus et al., 2010; Oshiumi et al., 2010a; Garbelli et al., 2011a; Chahar et al., 2013; Lai et al., 2013; Li et al., 2014, 2015; Pène et al., 2015). We analyzed the effect of DENV infection on DDX3X protein levels in different cell lines. A549 and Huh-7 cells were infected with DENV and DDX3X levels were monitored by western blot analysis at 24 and 48 h pi. We observed a significant decrease in DDX3X protein levels at 48 h pi in both the cell lines (**Figures 3A–C**). We further verified if the reduction in the DDX3X protein levels is reflected at the mRNA levels by measuring the transcripts of DDX3X in dengue infection in Huh-7 cells. We observed a significant reduction in the mRNA levels of DDX3X at 48 h pi suggesting that DENV infection suppresses the expression of DDX3X at mRNA level at later stages of infection (**Figure 3D**). The reduction in DDX3X levels were further confirmed by immunofluorescence analysis where DDX3X levels were lower in infected cells at 48 h pi however there was no significant change in distribution of DDX3X in infected cells and we observed no co-localization with viral envelope (**Figure S4**). Colocalization studies with viral capsid could not be performed as both DDX3X and capsid antibodies were raised in rabbit.

DDX3X Inhibits DENV Replication

To further assess the role of DDX3X in DENV infection, we performed the knock-down of DDX3X expression using siRNAs in Huh-7 cells. Cells were treated with either DDX3X smart-pool siRNAs or a non-targeting control (NTC) siRNA followed by infection with DENV2. Supernatants were collected at 24 h pi for plaque assay and total RNA was isolated from cells for RT-PCR. Knockdown of DDX3X was confirmed by western blot

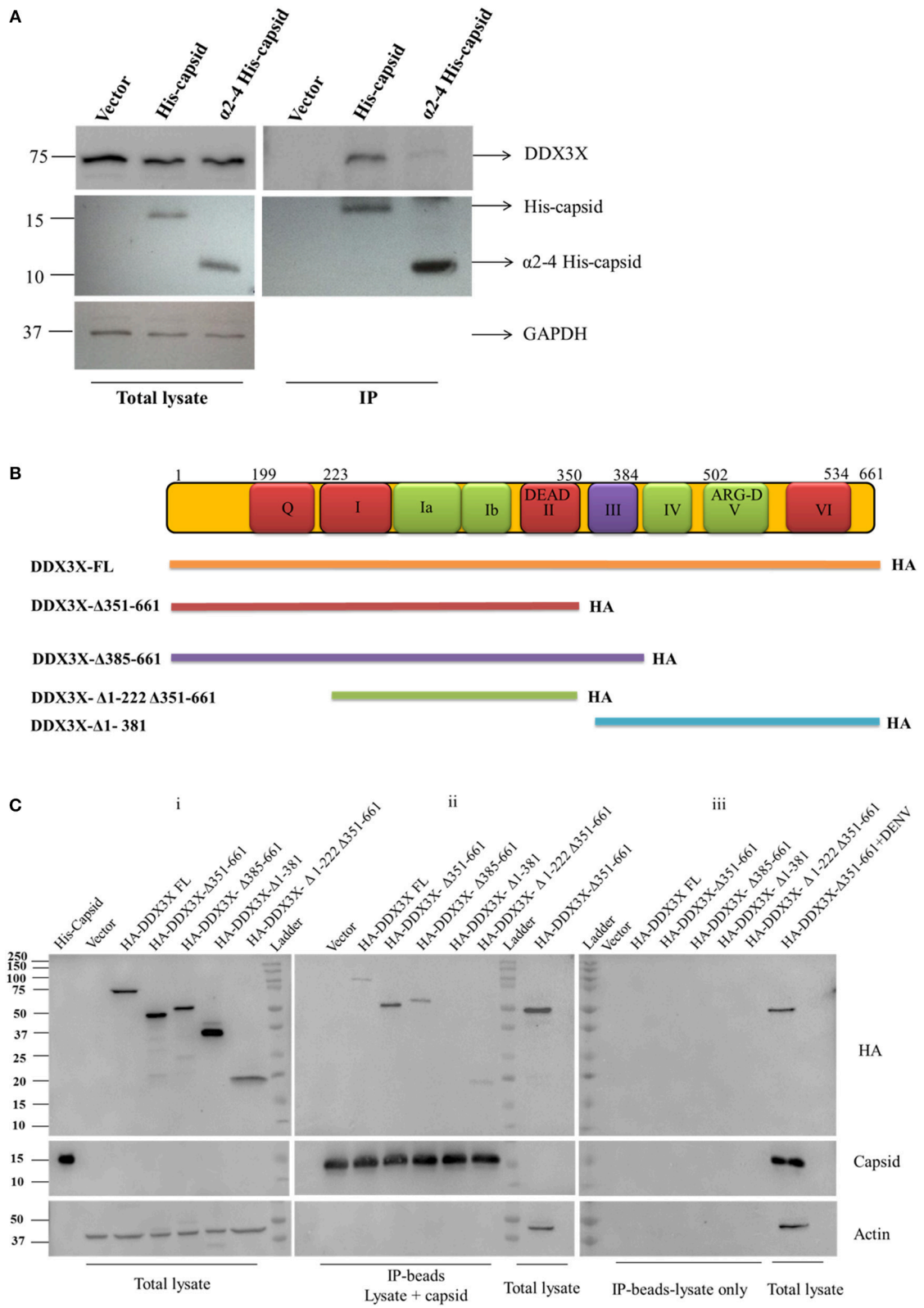

FIGURE 2 | Co-immunoprecipitation and pull-down of recombinant capsid and DDX3X. **(A)** Full length His-capsid and α2-4 His-capsid were transfected in HEK293T cells and lysates were prepared 24 h p.t. Lysates were used for IP with capsid antibody and blots were probed for capsid, DDX3X and GAPDH. **(B)** Map of the

(Continued)

FIGURE 2 | HA-DDX3X deletion constructs. **(C)** Total lysates were prepared from HEK293T cells transfected with HA-DDX3X-FL and HA-DDX3X deletion constructs at 24 h p.t. Purified His-capsid was added to the lysate for in-solution interaction and protein complexes were pulled down by Ni-NTA beads. Lysates incubated with Ni-NTA beads only were used as negative control. The beads were washed, boiled in Laemmli buffer and loaded on SDS PAGE and probed for HA-tag, capsid and Actin. In the first lane of blot (i) purified His-capsid was loaded as a positive control for capsid antibody. Total lysate of HEK293T cells transfected with HA-DDX3X-Δ351-661 and total lysate of HEK293T cells transfected with HA-DDX3X-Δ351-661 and infected with DENV was loaded as positive controls respectively in blots (ii) and (iii) for HA, capsid and actin antibodies.

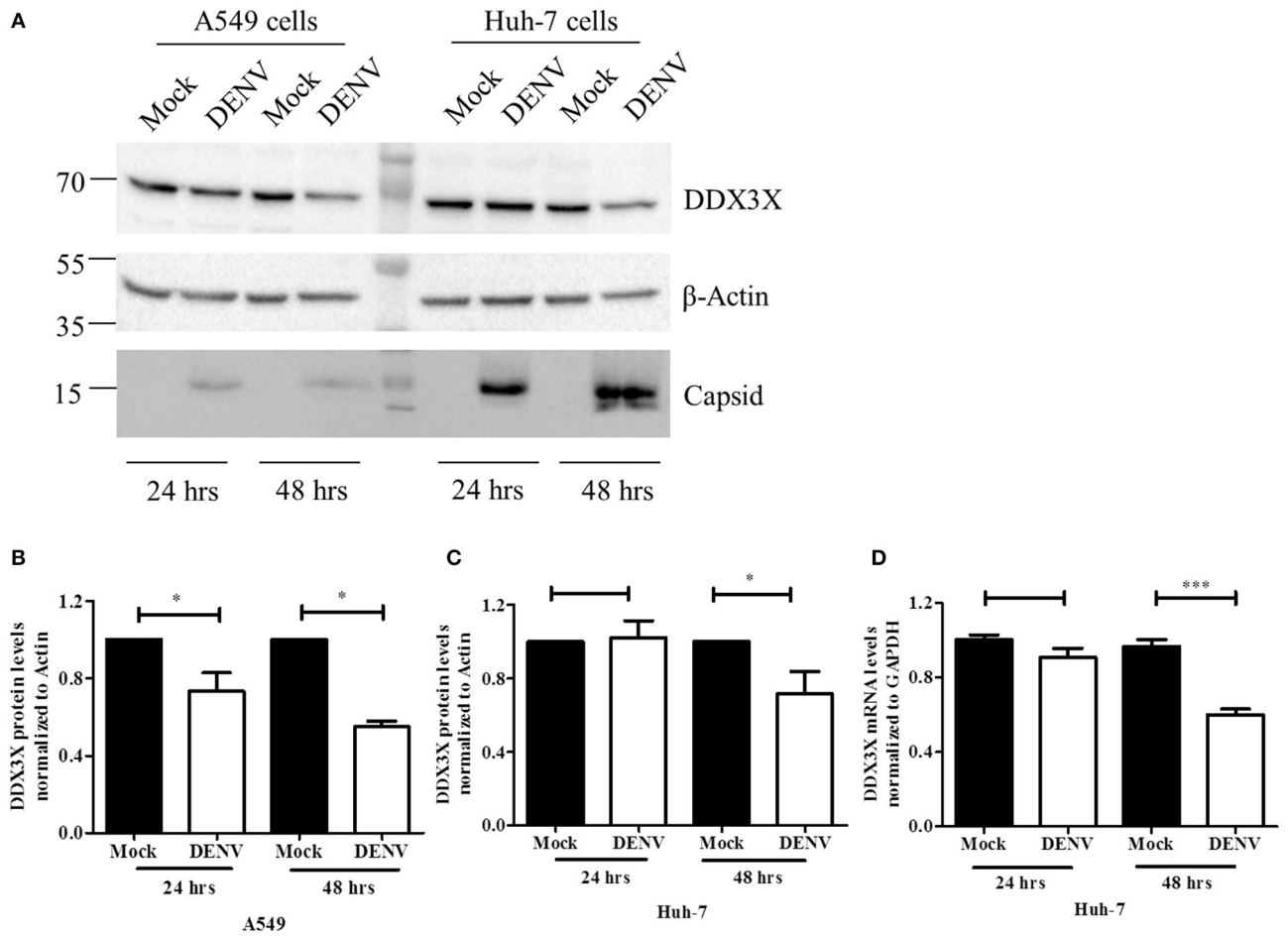

FIGURE 3 | DENV down-regulates DDX3X at later stages of infection. A549 and Huh-7 cells were infected with DENV at 3 MOI. Cells were collected at 24 and 48 h pi for either lysate preparation or for total RNA isolation. **(A)** Cell lysates were used for western blot analysis for DDX3X, GAPDH and capsid in both cell lines. **(B)**. Densitometry quantitation of the blots for A549 cells ($n = 4$). **(C)** Quantitation of blots for Huh-7 cells ($n = 4$). **(D)** Total RNA was used to estimate mRNA levels of DDX3X by real-time PCR from 3 independent experiments performed in triplicates ($n = 9$). Data is represented as mean ±SEM. $^{*}P < 0.05$ and $^{***}P < 0.0005$, ns = not significant.

analysis with cell lysates (**Figure 4A**). There was about three-fold increase in viral titers in the supernatants of cells where DDX3X expression was knocked down as compared to the NTC (**Figure 4B**). We further confirmed this observation by using single siRNAs (siDDX3X-1 and siDDX3X-2) to knock-down DDX3X in order to rule out off-target effects of smart-pool siRNAs (siDDX3X). A similar increase in viral titers was observed when individual siRNAs were used to knock-down DDX3X expression (**Figure 4C**) further confirming that the increase in viral titers is not due to the off-target effect of smart pool siRNAs. The increase in viral titers due to DDX3X knock-down suggested enhanced viral entry, replication or egress due to reduced DDX3X expression. To further identify the stage of DENV life cycle that DDX3X may be involved in, we performed time-course experiments and evaluated the DENV genome levels at 1, 12, 24, and 48 h pi in Huh-7 cells transfected with NTC or DDX3X siRNAs. We observed around 1.4 fold increase in DENV RNA levels at 24 h pi which further increased to 2.5-fold at 48 h pi in DDX3X knock-down cells as compared to NTC (**Figure 4D**). The viral RNA levels at 1 h pi did not show any difference between si-DDX3X and NTC samples indicating that the effect observed is not due to enhanced viral entry. The knock-down of

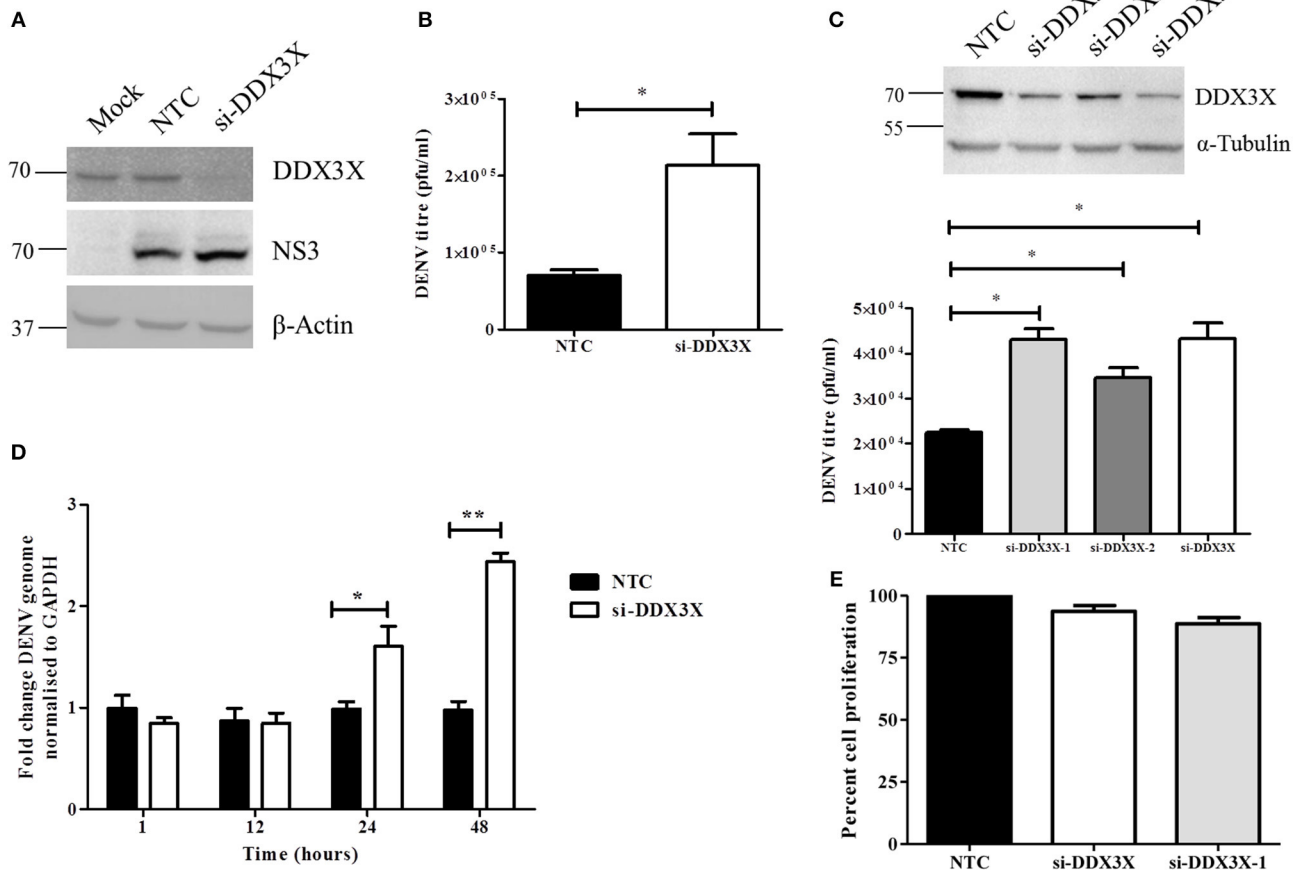

FIGURE 4 | Knockdown of DDX3X enhances DENV infection. Knockdown of DDX3X was performed in Huh-7 cells using smartpool siRNAs (si-DDX3X) and at 48 h p.t cells were infected with DENV at 1 MOI. Viral titres and RNA levels were verified at 24 h p.i. **(A)** Western blot analysis to verify knockdown of DDX3X. β-actin level is shown as a loading control and DENV-NS3 antibody was used to detect infection levels. **(B)** Viral titers were estimated by plaque assay. **(C)** DDX3X expression was knocked down by a single siRNA (si-DDX3X-1 or si-DDX3X-2) or using smartpool siRNAs (si-DDX3X) in Huh-7 cells and 48 h p.t. cells were infected with DENV at 1 MOI. Upper panel shows the western blot for knockdown efficiency. Lower panel shows viral titres estimated at 24 h pi. Figure is representative of three independent experiments performed with triplicate samples **(D)** Kinetics of infection in Huh-7 cells after DDX3X knockdown. Cells were collected at 1, 12, 24, and 48 h pi and DENV genome levels were estimated by real-time PCR. Data from two independent experiments performed with triplicate samples ($n = 6$) is represented as mean ± SEM. **(E)** Knockdown of DDX3X was performed in Huh-7 cells using smartpool siRNAs (si-DDX3X) and single siRNA (si-DDX3X-1) and cell proliferation was assessed as described in the methods section at 48 h post-transfection. *$P < 0.05$ and **$P < 0.005$.

DDX3X by siRNAs did not affect cell proliferation (**Figure 4E**). Similar results were obtained with A549 cells where knock-down of DDX3X led to enhanced DENV RNA levels and viral titers as compared to NTC (**Figures S5A–D**). These results clearly suggest that DDX3X may exert its antiviral effect at a post-entry stage which may have a direct or indirect effect on DENV RNA replication.

As silencing DDX3X expression led to increased DENV titers, we speculated that overexpression of DDX3X would lead to an enhanced antiviral state and inhibit DENV infection. We tested this by transfecting HA-DDX3X plasmid and its vector in HEK293T cells. At 24 h p.t, cells were fixed and stained with HA and DENV envelope antibody. Viral titers in the supernatants were measured by plaque assay. DENV infection was absent in cells expressing HA-DDX3X while un-transfected cells showed DENV positivity (**Figure 5A**). HA-DDX3X overexpression led to a 50% reduction in DENV infection (**Figure 5B**), which further correlated with a five-fold reduction in viral titers (**Figure 5C**). Similar results were obtained in Huh-7 cells transfected with HA-DDX3X where we observed 50% reduction in both viral titers and DENV RNA levels under DDX3X overexpression conditions (**Figures S6A,B**). Our results with DDX3X knock-down and overexpression suggest an antiviral role for DDX3X in DENV infection.

The N-Terminal 1-350 aa Domain of DDX3X Is Required for the Antiviral Activity

DDX3X performs multiple functions due to its multiple functional domains, which include the RNA helicase, ATPase and RNA binding activities (Garbelli et al., 2011b; Soto-Rifo and Ohlmann, 2013; Valiente-Echeverría et al., 2015). To further verify the domain required for the antiviral activity of DDX3X

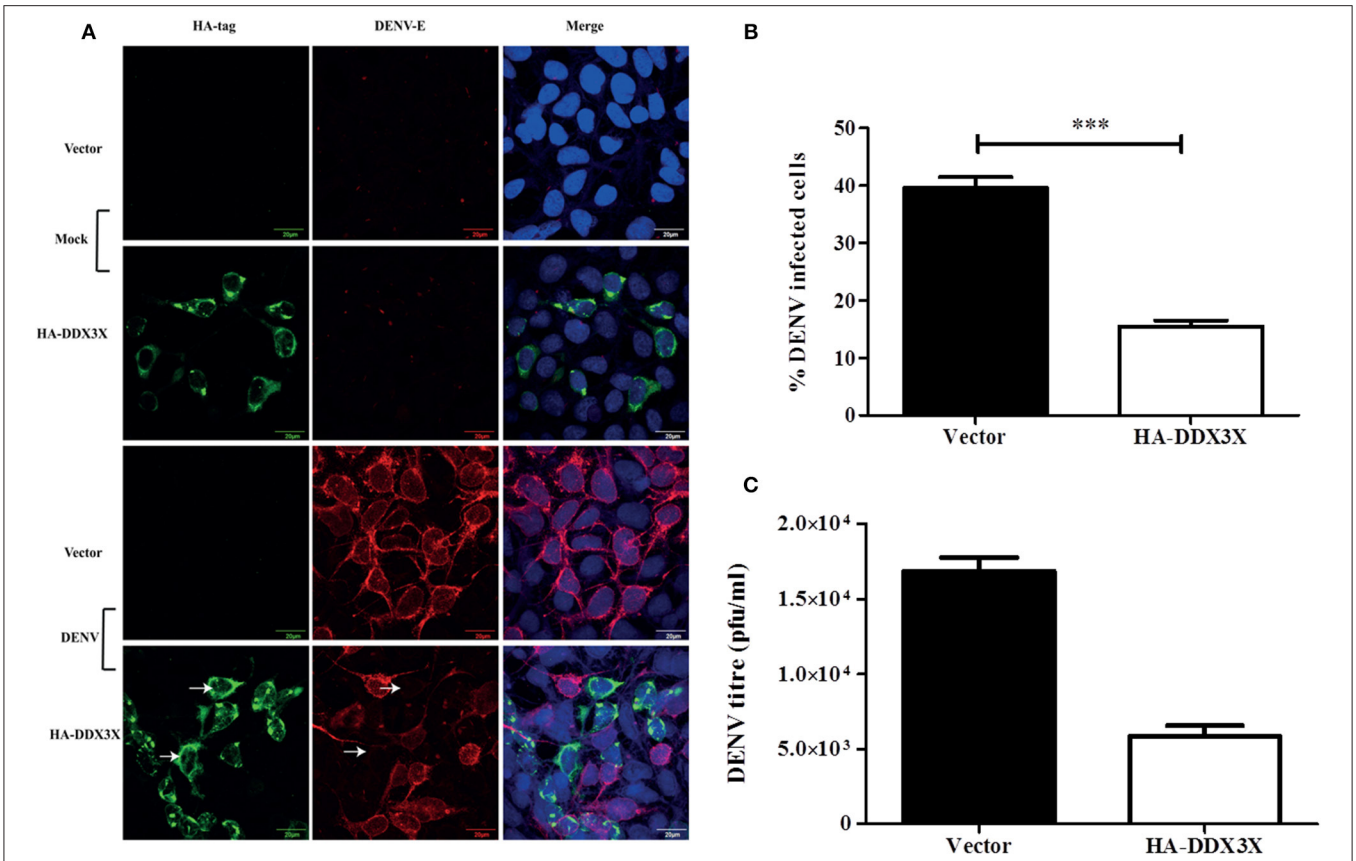

FIGURE 5 | DDX3X overexpression suppresses dengue infection. **(A)** HA-DDX3X plasmid or the vector was transfected in HEK293T cells. 24 h p.t. cells were infected with DENV at 5 MOI. Cells were fixed and stained for dengue envelope and HA at 24 h pi. **(B)** Percentage of infected cells was counted in ten fields each in three independent experiments (~3000 cells were counted) **(C)** Viral titres were estimated by plaque assay at 24 h pi. Data is represented as mean ± SEM. ***$P < 0.0005$.

by flow cytometry we created truncations in the DDX3X protein by generating the following GFP-tagged constructs: full length DDX3X (DDX3X-FL) and constructs lacking the c-terminal domains (DDX3X-Δ351-661, DDX3X-Δ385-661). The plasmids were transfected in HEK293T and at 24 h post-transfection, the cells were infected with DENV at 5 MOI and at 24 h pi cells were fixed and DENV infection in GFP^{high} cells was assessed by staining with DENV-E antibody conjugated with allophycocyanin (APC) using flow cytometry (**Figure S7**). Cells expressing GFP-tagged-DDX3X-FL showed a 50% decrease in infection as compared to the GFP-vector alone (**Figures 6A,B**). The antiviral activity of GFP-DDX3X was less as compared to HA-DDX3X (**Figure 4**) most probably due to differences in the expression levels of these constructs and also due to altered sub-cellular localization of GFP-DDX3X most likely due to the larger GFP-tag (**Figure S8**). Cells expressing DDX3X-Δ351-661 (34.6%) and DDX3X-Δ385-661 (31.2%) also showed a significant inhibition of DENV infection (**Figures 6C,D**), although the effect was slightly less than full-length DDX3X (**Figure 6E**). Overexpression of any of these constructs had no effect on cell viability (**Figures S9A–D**). We also generated the N-terminal deletion construct GFP-DDX3X-Δ1-381 which was found to localize to the nucleus suggesting that the c-terminal region of the protein is necessary for proper localization of the protein. Therefore, although this construct was useful in *in vitro* assays to demonstrate binding to capsid, the same was not appropriate for performing cellular interactions and antiviral functions due to altered localization. As the loss of aa 351-661 retained the antiviral activity, these results indicate that the N-terminal region of DDX3X, 1-350 aa, which contains the motifs Q, I, Ia, Ib, and DEAD box is sufficient for the antiviral functions of DDX3X. Such an effect may be expected as this region contains conserved motifs that are involved in ATP and RNA binding (Bol et al., 2015).

In a previous report, the antiviral function of DDX3X was attributed to its role in the induction of interferon-β as knock-down of DDX3X led to suppression of IFN-β production and increase in DENV titers (Li et al., 2015). To confirm this under our infection conditions, we measured the mRNA levels of IFN-β in cells with si-DDX3X transfection. We did not observe any significant difference in the basal levels of IFN-β transcript when DDX3X expression was suppressed in Huh-7 cells. Moreover, induction of IFN-β was not impaired upon dengue infection in both NTC and si-DDX3X cells indicating that DDX3X was not essential for induction of IFN-β in DENV infection or the residual levels of DDX3X present in knock-down cells may

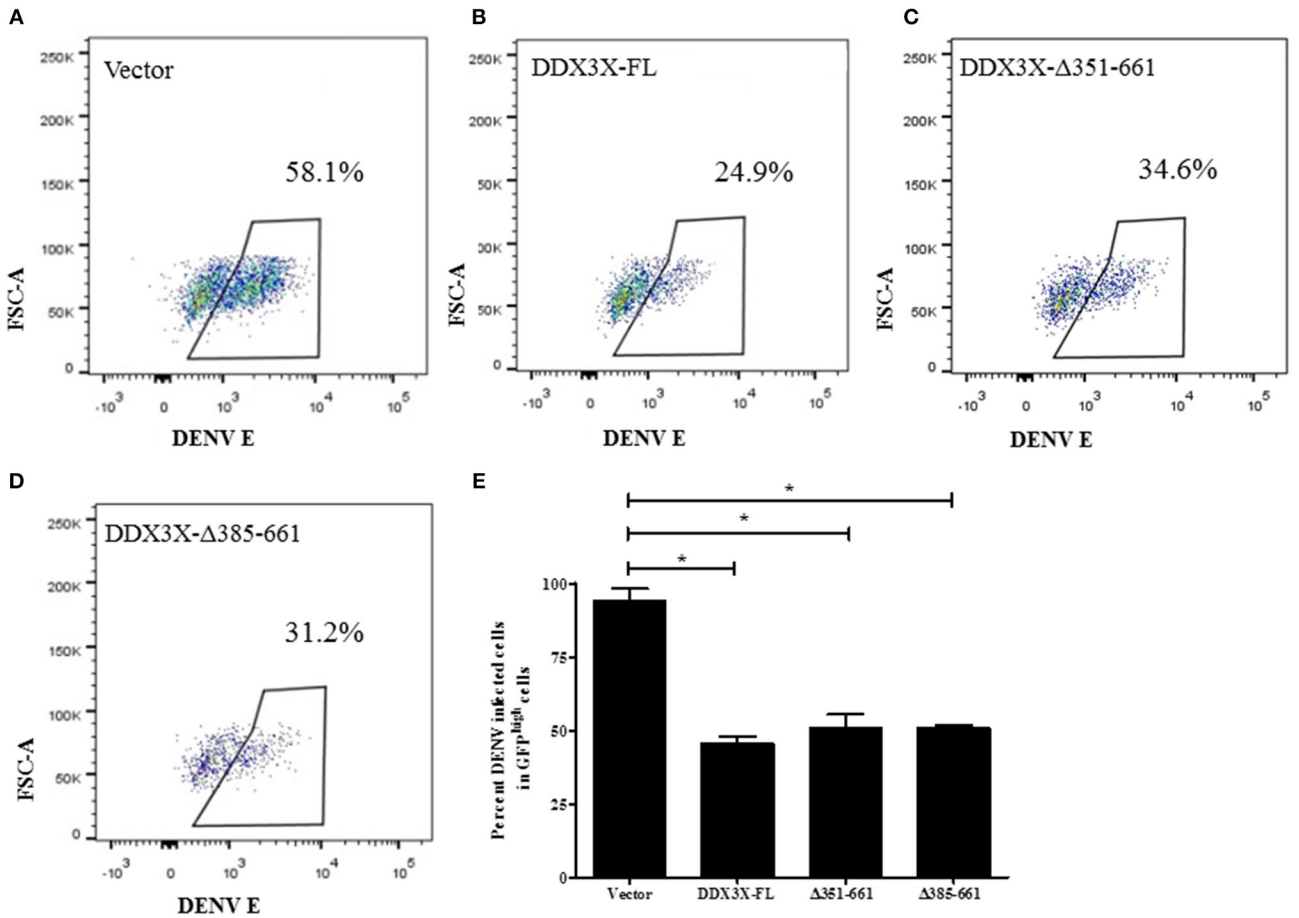

FIGURE 6 | Domain mapping of DDX3X antiviral activity. GFP tagged-DDX3X plasmids were transfected in HEK-293T cells and at 24 h p.t, cells were infected with DENV at 5 MOI. Cells were fixed and stained at 24 h pi with dengue envelope antibody. Cells were acquired in FACS and GFP signal was used to identify transfected cells. **(A–D)** Representative plots for percent DENV positive in GFP^{high} cells for each GFP-DDX3X construct. **(E)** Quantitation of DENV positivity in GFP^{high} for all GFP-DDX3X constructs. The experiment was performed twice with two replicates in each. Data is represented as mean ±SEM. $^{*}P < 0.05$.

be sufficient for IFN-β production (**Figure S10**). These results indicate that the antiviral effect of DDX3X in dengue infection is independent of interferon induction pathways.

DISCUSSION

Previous studies have shown the role of DDX3X in viral infections and in innate immune signaling (Yedavalli et al., 2004; Chang et al., 2006; Kalverda et al., 2009; Angus et al., 2010; Oshiumi et al., 2010a; Garbelli et al., 2011a; Chahar et al., 2013; Lai et al., 2013; Li et al., 2014, 2015; Pène et al., 2015). We have identified DDX3X as a DENV capsid-interacting protein and further confirm its anti-viral role in DENV infection. We show that the N-terminal 45 amino acids including the α-helix-1 of DENV-C was essential for interaction with DDX3X. Interestingly, HCV core protein was also shown to interact with DDX3X via its N-terminal domain and abrogation of DDX3X and HCV core interaction by mutagenesis had no effect on viral replication and infectious virus production indicating that HCV core and DDX3X interaction may have an indirect effect on host functions (Angus et al., 2010). In addition, DDX3X was also identified as a host factor in HCV infection by a genome-wide genetic screening and was shown to be involved at late stages of viral replication (Li et al., 2009). DDX3X was shown to sequester HCV RNA to lipid droplets and this was proposed to be an immune evasion strategy (Ariumi et al., 2011). Although HCV is a member of the family *Flaviviridae,* it belongs to a different genus (Hepacivirus) and has a different mode of RNA replication. The HCV core was shown to bind c-terminal domain of DDX3X and knock-down of DDX3X led to reduction in viral replication which is contrary to our observations with dengue virus. Therefore, these viruses may utilize DDX3X in different ways. The role of DDX3X in HIV replication is one of the well-characterized examples. DDX3X along with its binding partner Chromosome Maintenance-1 (CRM-1) was involved in the nuclear export of HIV RNA by Rev-Rev Response Element (RRE) complex (Yedavalli et al., 2004).

In addition, DDX3X was also shown to promote translation initiation of HIV mRNA (Soto-Rifo et al., 2013). DDX3X been shown to be required for viral replication in the case of murine norovirus (Yedavalli et al., 2004; Angus et al., 2010; Vashist et al., 2012). DDX3X has also been shown to act as an antiviral protein owing to its involvement in the upstream events leading to IFN-β induction (Schröder et al., 2008; Soulat et al., 2008; Oshiumi et al., 2010b). Therefore, in contrast to its proviral role in the case of HCV and HIV, DDX3X has been shown to play an antiviral role in vaccinia virus, hepatitis B virus and vesicular stomatitis virus infections (Oshiumi et al., 2010b; Wang and Ryu, 2010; Schroder, 2011). In the case of flaviviruses, DDX3X and other components of P bodies and stress granules were shown to be redistributed to viral replication compartments in West Nile virus infected cells although the relevance of this finding is yet to be determined (Chahar et al., 2013). In the case of Japanese encephalitis virus, DDX3X knock-down led to inhibition of viral titers, however, overexpression of DDX3X or any of the mutants under knock-down conditions suggested that the helicase activity of DDX3X is involved in JEV replication in BHK-21 cells. DDX3X was shown to play a role in translation of JEV proteins by interacting with viral non-structural proteins and 5′ and 3′ untranslated regions of viral RNA (Li et al., 2014). As JEV is a neurotropic virus, these observations need further validation in cells of central nervous system or at least in immortalized human cell lines. In a siRNA screening to identify DEAD-box family genes involved in DENV infection, Li et. al., identified DDX3X and DDX50 as the two DEAD-box family members which, when suppressed by siRNAs, led to significant upregulation of viral replication and DDX25 and DDX26 knock-down led to downregulation of DENV replication (Li et al., 2015). We have made a similar observation in our study where knock-down of DDX3X led to increase in viral titers and intracellular viral RNA levels without affecting viral entry and overexpression of DDX3X led to inhibition of virus replication. We were not successful in our attempts to purify DDX3X protein in prokaryotic expression system, therefore, a direct binding between DDX3X and dengue capsid could not be demonstrated. Nevertheless, we show by indirect methods that the motifs within the N-terminal region are important for the anti-viral role of DDX3X, since C-terminal deletions up to 350 a.a retained anti-viral functions of DDX3X. The N-terminal region of the protein consists of motifs Q, I, Ia, Ib, and DEAD box, which are involved in ATP and RNA binding (Cordin et al., 2006; Henn et al., 2012; Bol et al., 2015), and thus may be important in anti-viral response in the cell. This clearly demonstrates the antiviral function of DDX3X in cells infected with dengue virus and we show downregulation of DDX3X at later stages of DENV infection which could be an immune evasion strategy.

Huh-7 cells are deficient in TLR3-mediated pathway and rely on RIG-I pathway for induction of type I interferons (Li et al., 2005). We observed that DDX3X knock-down did not hamper the induction of IFN-β suggesting that reduction in type I interferons is not a reason for higher viral titers observed in these cells. We speculate that DDX3X may mediate anti-viral effects independent of IFN-β response by other stress response pathways. We have shown recently that drugs that induced autophagy acted as potent inhibitors of DENV replication (Medigeshi et al., 2016). Therefore, it would be interesting to investigate the role of DDX3X in autophagy. DDX3X is a phosphorylation target of TANK-binding kinase-1 (TBK-1), which has been shown to be a crucial bridge between innate immune responses and autophagy (Weidberg and Elazar, 2011; Pilli et al., 2012). It is possible that DDX3X may regulate autophagy through some of its interacting partners such as TBK-1, which warrants further investigation.

Recent reports have suggested a prominent role for DDX3X in stress granule formation and many viruses have been shown to hijack DDX3X to modulate/utilize this function (Chahar et al., 2013). We have not investigated the role of stress granules in our study. However, it should be noted that the list of proteins identified by mass spectrometry included ribonucleoproteins (RNPs) hnRNPQ, hnRNPA0, hnRNPA1 and hnRNPU of which all except hnRNPA0 have been shown to be components of stress granules and P bodies (Guil et al., 2006; Gallois-Montbrun et al., 2007; Quaresma et al., 2009). Recent reports have demonstrated the role of ribonucleoproteins in dengue virus replication as NS-1 and capsid-interacting partners (Chang et al., 2001; Brunetti et al., 2015; Dechtawewat et al., 2015; Diwaker et al., 2016). Further studies are required to understand if the hnRNPs identified in our study also play a similar role in DENV infection. It is plausible that DDX3X is part of a multifunctional protein complex involving RNPs, which interact with DENV capsid and future studies may focus on probing this further. The other capsid-interacting proteins identified in our study are various 60S and 40S ribosomal proteins which have been shown to be involved in ribosomal biogenesis. A putative protein which is highly similar to 60 kDa heat shock protein was also identified in this study. Interestingly, HSP60 has been shown to be involved in viral infections such as rotavirus, hepatitis B virus and dengue virus by either modulating apoptotic pathways or immune responses (Tanaka et al., 2004; Padwad et al., 2009; Chattopadhyay et al., 2017). In addition, as in this study, previous reports have also identified histone proteins as binding partners of DENV capsid further indicating that the list of proteins that we have identified are relevant for DENV biology (Colpitts et al., 2011). The relevance of other identified proteins such as the mitochondrial protein Pyrroline-5-carboxylate reductase 2 which catalyzes the conversion of pyrroline-5-carboxylate to proline, and other putative proteins similar to synaptotagmin binding, cytoplasmic RNA interacting protein (SYNCRIP) and skeletal muscle α-actin remains to be explored.

AUTHOR CONTRIBUTIONS

RK performed experiments, analyzed data and wrote the manuscript. NS performed experiments and analyzed data. MA analyzed data and provided critical inputs. AP contributed reagents, designed experiments, analyzed data and provided critical inputs. GM conceived the study, designed and performed

experiments, analyzed data and wrote the manuscript. All authors have reviewed the final version of the manuscript.

FUNDING

This work was supported by intramural funding to GM from the institute. GM is also supported by Intermediate fellowship from Wellcome trust-DBT India alliance (IA/S/14/1/501291). Work in AHP's laboratory is supported by the Medical Research Council, UK (grant number MC_UU_12014/2). RK received fellowship from Council for Scientific and Industrial Research, India (CSIR file No. 09/1049(0003)/2012-EMR-I). The funders had no role in study design, data collection and interpretation or the decision to submit the work for publication.

ACKNOWLEDGMENTS

We would like to thank Mr. Madhav Rao and Mr. Nagavara Prasad (Regional Center for Biotechnology) for their assistance with the mass spectrometry. We thank Ms. Meenakshi Kar, Mr. Naseem Ahmed Khan, and Mr. Amresh Kumar Singh for technical support and all members of CCV lab for their critical inputs and support.

SUPPLEMENTARY MATERIAL

The Supplementary Material for this article can be found online at: https://www.frontiersin.org/articles/10.3389/fcimb.2017.00542/full#supplementary-material

Figure S1 | Purification of His-capsid protein. **(A)** Purification of the His-capsid protein as described in methodology using Ni-NTA beads. **(B)** Western blot showing purified His-capsid probed using anti-His antibody.

Figure S2 | Interaction between capsid and DDX3X is not mediated via RNA. Huh-7 cells were infected with DENV at an MOI of 5. At 24 h pi mock and DENV-infected Huh-7 cell lysates were prepared and treated with RNAse prior to immunoprecipitation. DDX3X was immunoprecipitated from total lysates (untreated) and RNAse-treated lysates using DDX3X antibody at 4°C. Total lysate and immunoprecipitated proteins were detected by western blots.

Figure S3 | Deletion constructs of capsid. **(A)** Graphical representation of His-capsid deletion constructs. **(B)** HEK293T cells were transfected with plasmids encoding various capsid constructs. Total lysates were prepared at 24 h p.t. and expression of recombinant His-tagged proteins were analyzed by western blotting with capsid antibody. GAPDH levels are shown as loading controls.

Figure S4 | DENV infection downregulates DDX3X in Huh-7 cells at later stages of infection. **(A)** Huh-7 cells were infected at 1 MOI and fixed at 24 and 48 h pi. Cells were stained for DDX3X (red), dengue envelope (green) and nuclei with DAPI (blue). **(B)** The fluorescence intensity of DDX3X staining was quantitated using Fluoview software. Quantitation of DDX3X fluorescence intensity (AU) at 24 and 48 h pi. ($n = 15$) $^{***}P < 0.0005$.

Figure S5 | DDX3X downregulation enhances DENV infection in A549 cells. **(A)** Cells were transfected with si-NTC or si-DDX3X and at 48 h p.t. knock-down efficiency was measured by real-time PCR from total RNA. **(B)** Cells transfected with si-NTC or si-DDX3X were infected with DENV at 3 MOI at 48 h p.t. Viral titres were estimated at 24 h pi by plaque assay and viral genome levels were analyzed by real-time and normalized to GAPDH **(C)** Data represents three independent experiments performed with triplicates samples ($n = 9$). (**D)** Viral entry was assessed in DDX3X knockdown cells. Cells were collected after 1 h of virus adsorption and viral genome levels was analyzed by real-time PCR. Data presented are from two independent experiments performed with three replicates each ($n = 6$). Data is represented as mean ±SEM. $^{**}P < 0.005$ and $^{***}P < 0.0005$, ns = not significant.

Figure S6 | Overexpression of HA-DDX3X in Huh-7 cells inhibits virus replication. HA-DDX3X was transfected in Huh-7 cells, and at 24 h p.t, cells were infected with DENV at 3 MOI and viral titers were measured by plaque assay at 24 h pi **(A)** DENV viral genome levels were estimated by real-time PCR. Data is from three independent experiments performed in triplicates ($n = 9$). **(B)** Data is represented as mean ± SEM. $^{**}P < 0.005$.

Figure S7 | Gating strategy for dengue infection in GFP-DDX3X transfected cells. HEK293T cells transfected with GFP-DDX3X constructs were infected with DENV2 at 5 MOI at 24 h pt. At 24 h pi, cells were fixed and stained with APC-conjugated anti-DENV envelope antibody. Single cell population was gated in FSC-H vs. FSC-A plot and SSC-A vs. FSC-A plot. Live cells were gated for analysis. Dengue-E positive cells were gated in total GFP, GFP^{low} and GFP^{high} respectively.

Figure S8 | Overexpression of HA-DDX3X and GFP-DDX3X. HA- or GFP-tagged DDX3X constructs were transfected in HEK-293T cells and at 48 h p.t, cells were fixed and HA-DDX3X transfection samples were stained with HA antibody followed by secondary antibody conjugated with Alexa-488. Nuclei was stained with DAPI.

Figure S9 | Overexpression of DDX3X plasmids does not affect cell viability. GFP-tagged DDX3X constructs were transfected in HEK-293T cells and at 24 h p.t, cells were infected with DENV at 5 MOI. **(A–D)** The fixable live-dead viability stain (BD EF-780) was added at 1:1000 dilution and incubated at RT for 10 min and then washed with FACS buffer. Cells were processed by flow cytometry.

Figure S10 | IFN-β levels in Huh-7 in DDX3X knockdown and DENV infection. siRNA knockdown of DDX3X was done in Huh-7. Forty-eight hour p.t, cells were either mock or DENV infected at 10 MOI. Twenty-four hour p.i the IFN-β mRNA levels were assessed by real-time PCR. Data is represented as mean ± SEM.

REFERENCES

Agrawal, T., Schu, P., and Medigeshi, G. R. (2013). Adaptor protein complexes-1 and 3 are involved at distinct stages of flavivirus life-cycle. *Sci. Rep.* 3:1813. doi: 10.1038/srep01813

Amberg, S. M., Nestorowicz, A., Mccourt, D. W., and Rice, C. M. (1994). NS2B-3 proteinase-mediated processing in the yellow fever virus structural region: *in vitro* and *in vivo* studies. *J. Virol.* 68, 3794–3802.

Angus, A. G., Dalrymple, D., Boulant, S., Mcgivern, D. R., Clayton, R. F., Scott, M. J., et al. (2010). Requirement of cellular DDX3 for hepatitis C virus replication is unrelated to its interaction with the viral core protein. *J. Gen. Virol.* 91, 122–132. doi: 10.1099/vir.0.015909-0

Ariumi, Y., Kuroki, M., Kushima, Y., Osugi, K., Hijikata, M., Maki, M., et al. (2011). Hepatitis C virus hijacks P-body and stress granule components around lipid droplets. *J. Virol.* 85, 6882–6892. doi: 10.1128/JVI.02418-10

Balinsky, C. A., Schmeisser, H., Ganesan, S., Singh, K., Pierson, T. C., and Zoon, K. C. (2013). Nucleolin interacts with the dengue virus capsid protein and plays a role in formation of infectious virus particles. *J. Virol.* 87, 13094–13106. doi: 10.1128/JVI.00704-13

Bhuvanakantham, R., Chong, M. K., and Ng, M. L. (2009). Specific interaction of capsid protein and importin-alpha/beta influences West Nile virus production. *Biochem. Biophys. Res. Commun.* 389, 63–69. doi: 10.1016/j.bbrc.2009.08.108

Bhuvanakantham, R., and Ng, M. L. (2013). West Nile virus and dengue virus capsid protein negates the antiviral activity of human Sec3 protein through the proteasome pathway. *Cell. Microbiol.* 15, 1688–1706. doi: 10.1111/cmi.12143

Bol, G. M., Vesuna, F., Xie, M., Zeng, J., Aziz, K., Gandhi, N., et al. (2015). Targeting DDX3 with a small molecule inhibitor for lung cancer therapy. *EMBO Mol. Med.* 7, 648–669. doi: 10.15252/emmm.201404368

Brunetti, J. E., Scolaro, L. A., and Castilla, V. (2015). The heterogeneous nuclear ribonucleoprotein K (hnRNP K) is a host factor required for

dengue virus and Junin virus multiplication. *Virus Res.* 203, 84–91. doi: 10.1016/j.virusres.2015.04.001

Byk, L. A., and Gamarnik, A. V. (2016). Properties and functions of the dengue virus capsid protein. *Annu. Rev. Virol.* 3, 263–281. doi: 10.1146/annurev-virology-110615-042334

Chahar, H. S., Chen, S., and Manjunath, N. (2013). P-body components LSM1, GW182, DDX3, DDX6 and XRN1 are recruited to WNV replication sites and positively regulate viral replication. *Virology* 436, 1–7. doi: 10.1016/j.virol.2012.09.041

Chang, C. J., Luh, H. W., Wang, S. H., Lin, H. J., Lee, S. C., and Hu, S. T. (2001). The heterogeneous nuclear ribonucleoprotein K (hnRNP K) interacts with dengue virus core protein. *DNA Cell Biol.* 20, 569–577. doi: 10.1089/104454901317094981

Chang, P. C., Chi, C. W., Chau, G. Y., Li, F. Y., Tsai, Y. H., Wu, J. C., et al. (2006). DDX3, a DEAD box RNA helicase, is deregulated in hepatitis virus-associated hepatocellular carcinoma and is involved in cell growth control. *Oncogene* 25, 1991–2003. doi: 10.1038/sj.onc.1209239

Chattopadhyay, S., Mukherjee, A., Patra, U., Bhowmick, R., Basak, T., Sengupta, S., et al. (2017). Tyrosine phosphorylation modulates mitochondrial chaperonin Hsp60 and delays rotavirus NSP4-mediated apoptotic signaling in host cells. *Cell. Microbiol.* 19:e12670. doi: 10.1111/cmi.12670

Colpitts, T. M., Barthel, S., Wang, P., and Fikrig, E. (2011). Dengue virus capsid protein binds core histones and inhibits nucleosome formation in human liver cells. *PLoS ONE* 6:e24365. doi: 10.1371/journal.pone.0024365

Cordin, O., Banroques, J., Tanner, N. K., and Linder, P. (2006). The DEAD-box protein family of RNA helicases. *Gene* 367, 17–37. doi: 10.1016/j.gene.2005.10.019

Dechtawewat, T., Songprakhon, P., Limjindaporn, T., Puttikhunt, C., Kasinrerk, W., Saitornuang, S., et al. (2015). Role of human heterogeneous nuclear ribonucleoprotein C1/C2 in dengue virus replication. *Virol. J.* 12:14. doi: 10.1186/s12985-014-0219-7

Diwaker, D., Mishra, K. P., Ganju, L., and Singh, S. B. (2016). Dengue virus non-structural 1 protein interacts with heterogeneous nuclear ribonucleoprotein H in human monocytic cells. *Asian Pac. J. Trop. Med.* 9, 112–118. doi: 10.1016/j.apjtm.2016.01.015

Gallois-Montbrun, S., Kramer, B., Swanson, C. M., Byers, H., Lynham, S., Ward, M., et al. (2007). Antiviral protein APOBEC3G localizes to ribonucleoprotein complexes found in P bodies and stress granules. *J. Virol.* 81, 2165–2178. doi: 10.1128/JVI.02287-06

Garbelli, A., Beermann, S., Di Cicco, G., Dietrich, U., and Maga, G. (2011a). A motif unique to the human DEAD-box protein DDX3 is important for nucleic acid binding, ATP hydrolysis, RNA/DNA unwinding and HIV-1 replication. *PLoS ONE* 6:e19810. doi: 10.1371/journal.pone.0019810

Garbelli, A., Radi, M., Falchi, F., Beermann, S., Zanoli, S., Manetti, F., et al. (2011b). Targeting the human DEAD-box polypeptide 3 (DDX3) RNA helicase as a novel strategy to inhibit viral replication. *Curr. Med. Chem.* 18, 3015–3027. doi: 10.2174/092986711796391688

Guil, S., Long, J. C., and Cáceres, J. F. (2006). hnRNP A1 relocalization to the stress granules reflects a role in the stress response. *Mol. Cell. Biol.* 26, 5744–5758. doi: 10.1128/MCB.00224-06

Haridas, V., Rajgokul, K. S., Sadanandan, S., Agrawal, T., Sharvani, V., Gopalakrishna, M. V., et al. (2013). Bispidine-amino acid conjugates act as a novel scaffold for the design of antivirals that block Japanese encephalitis virus replication. *PLoS Negl. Trop. Dis.* 7:e2005. doi: 10.1371/journal.pntd.0002005

Henn, A., Bradley, M. J., and De La Cruz, E. M. (2012). ATP utilization and RNA conformational rearrangement by DEAD-box proteins. *Annu. Rev. Biophys.* 41, 247–267. doi: 10.1146/annurev-biophys-050511-102243

Höck, J., Weinmann, L., Ender, C., Rüdel, S., Kremmer, E., Raabe, M., et al. (2007). Proteomic and functional analysis of Argonaute-containing mRNA-protein complexes in human cells. *EMBO Rep.* 8, 1052–1060. doi: 10.1038/sj.embor.7401088

Jaworska, J., Gravel, A., Fink, K., Grandvaux, N., and Flamand, L. (2007). Inhibition of transcription of the beta interferon gene by the human herpesvirus 6 immediate-early 1 protein. *J. Virol.* 81, 5737–5748. doi: 10.1128/JVI.02443-06

Jones, C. T., Ma, L., Burgner, J. W., Groesch, T. D., Post, C. B., and Kuhn, R. J. (2003). Flavivirus capsid is a dimeric alpha-helical protein. *J. Virol.* 77, 7143–7149. doi: 10.1128/JVI.77.12.7143-7149.2003

Kalverda, A. P., Thompson, G. S., Vogel, A., Schröder, M., Bowie, A. G., Khan, A. R., et al. (2009). Poxvirus K7 protein adopts a Bcl-2 fold: biochemical mapping of its interactions with human DEAD box RNA helicase DDX3. *J. Mol. Biol.* 385, 843–853. doi: 10.1016/j.jmb.2008.09.048

Kanlaya, R., Pattanakitsakul, S. N., Sinchaikul, S., Chen, S. T., and Thongboonkerd, V. (2010). The ubiquitin-proteasome pathway is important for dengue virus infection in primary human endothelial cells. *J. Proteome Res.* 9, 4960–4971. doi: 10.1021/pr100219y

Katoh, H., Okamoto, T., Fukuhara, T., Kambara, H., Morita, E., Mori, Y., et al. (2013). Japanese encephalitis virus core protein inhibits stress granule formation through an interaction with Caprin-1 and facilitates viral propagation. *J. Virol.* 87, 489–502. doi: 10.1128/JVI.02186-12

Kumar, R., Agrawal, T., Khan, N. A., Nakayama, Y., and Medigeshi, G. R. (2016). Identification and characterization of the role of c-terminal Src kinase in dengue virus replication. *Sci. Rep.* 6:30490. doi: 10.1038/srep30490

Lai, M. C., Lee, Y. H., and Tarn, W. Y. (2008). The DEAD-box RNA helicase DDX3 associates with export messenger ribonucleoproteins as well as tip-associated protein and participates in translational control. *Mol. Biol. Cell* 19, 3847–3858. doi: 10.1091/mbc.E07-12-1264

Lai, M. C., Wang, S. W., Cheng, L., Tarn, W. Y., Tsai, S. J., and Sun, H. S. (2013). Human DDX3 interacts with the HIV-1 Tat protein to facilitate viral mRNA translation. *PLoS ONE* 8:e68665. doi: 10.1371/journal.pone.0068665

Li, C., Ge, L. L., Li, P. P., Wang, Y., Dai, J. J., Sun, M. X., et al. (2014). Cellular DDX3 regulates Japanese encephalitis virus replication by interacting with viral un-translated regions. *Virology* 449, 70–81. doi: 10.1016/j.virol.2013.11.008

Li, G., Feng, T., Pan, W., Shi, X., and Dai, J. (2015). DEAD-box RNA helicase DDX3X inhibits DENV replication via regulating type one interferon pathway. *Biochem. Biophys. Res. Commun.* 456, 327–332. doi: 10.1016/j.bbrc.2014.11.080

Li, K., Foy, E., Ferreon, J. C., Nakamura, M., Ferreon, A. C., Ikeda, M., et al. (2005). Immune evasion by hepatitis C virus NS3/4A protease-mediated cleavage of the Toll-like receptor 3 adaptor protein TRIF. *Proc. Natl. Acad. Sci. U.S.A.* 102, 2992–2997. doi: 10.1073/pnas.0408824102

Li, Q., Brass, A. L., Ng, A., Hu, Z., Xavier, R. J., Liang, T. J., et al. (2009). A genome-wide genetic screen for host factors required for hepatitis C virus propagation. *Proc. Natl. Acad. Sci. U.S.A.* 106, 16410–16415. doi: 10.1073/pnas.0907439106

Limjindaporn, T., Netsawang, J., Noisakran, S., Thiemmeca, S., Wongwiwat, W., Sudsaward, S., et al. (2007). Sensitization to Fas-mediated apoptosis by dengue virus capsid protein. *Biochem. Biophys. Res. Commun.* 362, 334–339. doi: 10.1016/j.bbrc.2007.07.194

Ma, L., Jones, C. T., Groesch, T. D., Kuhn, R. J., and Post, C. B. (2004). Solution structure of dengue virus capsid protein reveals another fold. *Proc. Natl. Acad. Sci. U.S.A.* 101, 3414–3419. doi: 10.1073/pnas.0305892101

Mairiang, D., Zhang, H., Sodja, A., Murali, T., Suriyaphol, P., Malasit, P., et al. (2013). Identification of new protein interactions between dengue fever virus and its hosts, human and mosquito. *PLoS ONE* 8:e53535. doi: 10.1371/journal.pone.0053535

Medigeshi, G. R. (2011). Mosquito-borne flaviviruses: overview of viral life-cycle and host–virus interactions. *Future Virol.* 6, 1075–1089. doi: 10.2217/fvl.11.85

Medigeshi, G. R., Kumar, R., Dhamija, E., Agrawal, T., and Kar, M. (2016). N-Desmethylclozapine, Fluoxetine, and Salmeterol inhibit postentry stages of the dengue virus life cycle. *Antimicrob. Agents Chemother.* 60, 6709–6718. doi: 10.1128/AAC.01367-16

Mulhern, O., and Bowie, A. G. (2010). Unexpected roles for DEAD-box protein 3 in viral RNA sensing pathways. *Eur. J. Immunol.* 40, 933–935. doi: 10.1002/eji.201040447

Netsawang, J., Noisakran, S., Puttikhunt, C., Kasinrerk, W., Wongwiwat, W., Malasit, P., et al. (2010). Nuclear localization of dengue virus capsid protein is required for DAXX interaction and apoptosis. *Virus Res.* 147, 275–283. doi: 10.1016/j.virusres.2009.11.012

Oshiumi, H., Ikeda, M., Matsumoto, M., Watanabe, A., Takeuchi, O., Akira, S., et al. (2010a). Hepatitis C virus core protein abrogates the DDX3 function that enhances IPS-1-mediated IFN-beta induction. *PLoS ONE* 5:e14258. doi: 10.1371/journal.pone.0014258

Oshiumi, H., Sakai, K., Matsumoto, M., and Seya, T. (2010b). DEAD/H BOX 3 (DDX3) helicase binds the RIG-I adaptor IPS-1 to up-regulate IFN-beta-inducing potential. *Eur. J. Immunol.* 40, 940–948. doi: 10.1002/eji.200940203

Owsianka, A. M., and Patel, A. H. (1999). Hepatitis C virus core protein interacts with a human DEAD box protein DDX3. *Virology* 257, 330–340. doi: 10.1006/viro.1999.9659

Padwad, Y. S., Mishra, K. P., Jain, M., Chanda, S., Karan, D., and Ganju, L. (2009). RNA interference mediated silencing of Hsp60 gene in human monocytic myeloma cell line U937 revealed decreased dengue virus multiplication. *Immunobiology* 214, 422–429. doi: 10.1016/j.imbio.2008.11.010

Pène, V., Li, Q., Sodroski, C., Hsu, C. S., and Liang, T. J. (2015). Dynamic interaction of stress granules, DDX3X, and IKK-alpha mediates multiple functions in hepatitis C virus infection. *J. Virol.* 89, 5462–5477. doi: 10.1128/JVI.03197-14

Pilli, M., Arko-Mensah, J., Ponpuak, M., Roberts, E., Master, S., Mandell, M. A., et al. (2012). TBK-1 promotes autophagy-mediated antimicrobial defense by controlling autophagosome maturation. *Immunity* 37, 223–234. doi: 10.1016/j.immuni.2012.04.015

Quaresma, A. J., Bressan, G. C., Gava, L. M., Lanza, D. C., Ramos, C. H., and Kobarg, J. (2009). Human hnRNP Q re-localizes to cytoplasmic granules upon PMA, thapsigargin, arsenite and heat-shock treatments. *Exp. Cell Res.* 315, 968–980. doi: 10.1016/j.yexcr.2009.01.012

Sangiambut, S., Keelapang, P., Aaskov, J., Puttikhunt, C., Kasinrerk, W., Malasit, P., et al. (2008). Multiple regions in dengue virus capsid protein contribute to nuclear localization during virus infection. *J. Gen. Virol.* 89, 1254–1264. doi: 10.1099/vir.0.83264-0

Sangiambut, S., Suphatrakul, A., Sriburi, R., Keelapang, P., Puttikhunt, C., Kasinrerk, W., et al. (2013). Sustained replication of dengue pseudoinfectious virus lacking the capsid gene by trans-complementation in capsid-producing mosquito cells. *Virus Res.* 174, 37–46. doi: 10.1016/j.virusres.2013.02.009

Schroder, M. (2011). Viruses and the human DEAD-box helicase DDX3: inhibition or exploitation? *Biochem. Soc. Trans.* 39, 679–683. doi: 10.1042/BST0390679

Schröder, M., Baran, M., and Bowie, A. G. (2008). Viral targeting of DEAD box protein 3 reveals its role in TBK1/IKKepsilon-mediated IRF activation. *EMBO J.* 27, 2147–2157. doi: 10.1038/emboj.2008.143

Soto-Rifo, R., and Ohlmann, T. (2013). The role of the DEAD-box RNA helicase DDX3 in mRNA metabolism. *Wiley Interdiscip. Rev. RNA* 4, 369–385. doi: 10.1002/wrna.1165

Soto-Rifo, R., Rubilar, P. S., and Ohlmann, T. (2013). The DEAD-box helicase DDX3 substitutes for the cap-binding protein eIF4E to promote compartmentalized translation initiation of the HIV-1 genomic RNA. *Nucleic Acids Res.* 41, 6286–6299. doi: 10.1093/nar/gkt306

Soulat, D., Bürckstümmer, T., Westermayer, S., Goncalves, A., Bauch, A., Stefanovic, A., et al. (2008). The DEAD-box helicase DDX3X is a critical component of the TANK-binding kinase 1-dependent innate immune response. *EMBO J.* 27, 2135–2146. doi: 10.1038/emboj.2008.126

Tanaka, Y., Kanai, F., Kawakami, T., Tateishi, K., Ijichi, H., Kawabe, T., et al. (2004). Interaction of the hepatitis B virus X protein (HBx) with heat shock protein 60 enhances HBx-mediated apoptosis. *Biochem. Biophys. Res. Commun.* 318, 461–469. doi: 10.1016/j.bbrc.2004.04.046

Urbanowski, M. D., and Hobman, T. C. (2013). The West Nile virus capsid protein blocks apoptosis through a phosphatidylinositol 3-kinase-dependent mechanism. *J. Virol.* 87, 872–881. doi: 10.1128/JVI.02030-12

Valiente-Echeverría, F., Hermoso, M. A., and Soto-Rifo, R. (2015). RNA helicase DDX3: at the crossroad of viral replication and antiviral immunity. *Rev. Med. Virol.* 25, 286–299. doi: 10.1002/rmv.1845

Vashist, S., Urena, L., Chaudhry, Y., and Goodfellow, I. (2012). Identification of RNA-protein interaction networks involved in the norovirus life cycle. *J. Virol.* 86, 11977–11990. doi: 10.1128/JVI.00432-12

Wang, H., and Ryu, W. S. (2010). Hepatitis B virus polymerase blocks pattern recognition receptor signaling via interaction with DDX3: implications for immune evasion. *PLoS Pathog.* 6:e1000986. doi: 10.1371/journal.ppat.1000986

Wang, S. H., Syu, W. J., Huang, K. J., Lei, H. Y., Yao, C. W., King, C. C., et al. (2002). Intracellular localization and determination of a nuclear localization signal of the core protein of dengue virus. *J. Gen. Virol.* 83, 3093–3102. doi: 10.1099/0022-1317-83-12-3093

Weidberg, H., and Elazar, Z. (2011). TBK1 mediates crosstalk between the innate immune response and autophagy. *Sci. Signal.* 4:pe39. doi: 10.1126/scisignal.2002355

Yamshchikov, V. F., and Compans, R. W. (1995). Formation of the flavivirus envelope: role of the viral NS2B-NS3 protease. *J. Virol.* 69, 1995–2003.

Yang, M. R., Lee, S. R., Oh, W., Lee, E. W., Yeh, J. Y., Nah, J. J., et al. (2008). West Nile virus capsid protein induces p53-mediated apoptosis via the sequestration of HDM2 to the nucleolus. *Cell. Microbiol.* 10, 165–176. doi: 10.1111/j.1462-5822.2007.01027.x

Yedavalli, V. S., Neuveut, C., Chi, Y. H., Kleiman, L., and Jeang, K. T. (2004). Requirement of DDX3 DEAD box RNA helicase for HIV-1 Rev-RRE export function. *Cell* 119, 381–392. doi: 10.1016/j.cell.2004.09.029

Conflict of Interest Statement: The authors declare that the research was conducted in the absence of any commercial or financial relationships that could be construed as a potential conflict of interest.

frontiers in Cellular and Infection Microbiology

ORIGINAL RESEARCH
published: 09 April 2018
doi: 10.3389/fcimb.2018.00113

SIRT6 Acts as a Negative Regulator in Dengue Virus-Induced Inflammatory Response by Targeting the DNA Binding Domain of NF-κB p65

*Pengcheng Li[1], Yufei Jin[1], Fei Qi[1], Fangyi Wu[1], Susu Luo[2], Yuanjiu Cheng[1], Ruth R. Montgomery[3] and Feng Qian[1]**

[1] Ministry of Education Key Laboratory of Contemporary Anthropology, School of Life Sciences, Fudan University, Shanghai, China, [2] Institute of Biothermal Science and Technology, School of Medical Instrument and Food Engineering, University of Shanghai for Science and Technology, Shanghai, China, [3] Program on Human Translational Immunology, Department of Internal Medicine, Yale University School of Medicine, New Haven, CT, United States

Dengue virus (DENV) is a mosquito-borne single-stranded RNA virus causing human disease with variable severity. The production of massive inflammatory cytokines in dengue patients has been associated with dengue disease severity. However, the regulation of these inflammatory responses remains unclear. In this study, we report that SIRT6 is a negative regulator of innate immune responses during DENV infection. Silencing of *Sirt6* enhances DENV-induced proinflammatory cytokine and chemokine production. Overexpression of SIRT6 inhibits RIG-I-like receptor (RLR) and Toll-like receptor 3 (TLR3) mediated NF-κB activation. The sirtuin core domain of SIRT6 is required for the inhibition of NF-κB p65 function. SIRT6 interacts with the DNA binding domain of p65 and competes with p65 to occupy the *Il6* promoter during DENV infection. Collectively, our study demonstrates that SIRT6 negatively regulates DENV-induced inflammatory response via RLR and TLR3 signaling pathways.

Keywords: SIRT6, dengue virus, proinflammatory cytokines, NF-κB p65, RLR, TLR3

OPEN ACCESS

Edited by:
Qiangming Sun, Institute of Medical Biology (CAMS), China

Reviewed by:
Penghua Wang, New York Medical College, United States
Tonya Michelle Colpitts, Boston University, United States
Irving Coy Allen, Virginia Tech, United States
Jianfeng Dai, Soochow University, China

***Correspondence:**
Feng Qian
fengqian@fudan.edu.cn

Received: *03 January 2018*
Accepted: *22 March 2018*
Published: *09 April 2018*

Citation:
Li P, Jin Y, Qi F, Wu F, Luo S, Cheng Y, Montgomery RR and Qian F (2018) SIRT6 Acts as a Negative Regulator in Dengue Virus-Induced Inflammatory Response by Targeting the DNA Binding Domain of NF-κB p65. Front. Cell. Infect. Microbiol. 8:113. doi: 10.3389/fcimb.2018.00113

INTRODUCTION

Dengue virus (DENV) is a mosquito-transmitted single-stranded RNA virus, causing an acute systemic viral disease and is a significant public health concern (Guzman et al., 2010). An estimated 390 million individuals worldwide are infected with DENV per year, with 96 million manifesting symptoms (Bhatt et al., 2013). Although primary infection in humans typically results in mild dengue fever, secondary infection with different DENV serotypes is associated with severe symptoms which can lead to dengue hemorrhagic fever (DHF), dengue shock syndrome (DSS) and even death (Wilder-Smith and Schwartz, 2005). It is believed that the massive production of inflammatory cytokines contributes to the pathogenesis of severe dengue disease (Pang et al., 2007). Unfortunately, there are no DENV specific therapies or widely available vaccines (Martin and Hermida, 2016).

Pattern recognition receptors (PRRs) are key components of the innate immune system that recognize pathogen associated molecular patterns (PAMPs) (Chan and Gack, 2016). DENV

infection is recognized by the innate immune system through retinoic acid-inducible gene-I (RIG-I)-like receptors (RLRs) and Toll like receptors (TLRs) (Tsai et al., 2009; Nasirudeen et al., 2011). These two recognition pathways lead to the activation of a series of signaling events and the induction of proinflammatory cytokines and chemokines. The cytosolic sensor RIG-I detects DENV after fusion and replication in infected cells. TLR3 recognizes dsRNA in endosomes (Green et al., 2014). Upon recognition of viral RNA, the caspase-recruitment domain of RIG-I binds to the mitochondrial antiviral signaling (MAVS) adaptor, while TLR3 interacts with the TIR domain containing adaptor TRIF. These adaptors then recruit E3 ligase TRAF6, and further activate the canonical IKKs, leading to the production of nuclear factor-κB (NF-κB) dependent proinflammatory cytokines (Kawai and Akira, 2009; Kumar et al., 2011).

NF-κB is a critical transcriptional factor that participates in the regulation of inflammatory mediators. After viral infection, NF-κB can be activated by several pathways including RLRs and TLRs mediated signaling (Rahman and McFadden, 2011). The most abundant form of NF-κB is a p50/p65 heterodimer, which associates with the NF-κB inhibitor α (IκBα). Following stimulation, IκBα is phosphorylated and then degraded. NF-κB translocates to the nucleus where it induces the expression of NF-κB-target genes (Li and Verma, 2002). NF-κB activation during DENV infection has been reported to lead to the induction of cell apoptosis and excessive inflammation (Jan et al., 2000). In a murine model, NF-κB activation induced by DENV protease overexpression resulted in development of dengue hemorrhage (Lin et al., 2014). In humans, increased levels of NF-κB regulated proinflammatory cytokine TNFα have been associated with the severity of dengue disease manifestations (Soundravally et al., 2014). Thus, excessive NF-κB activation should be tightly controlled. The negative regulatory mechanisms of NF-κB activation remain incompletely defined.

The sirtuins (SIRTs) are a family of nicotinamide adenine dinucleotide (NAD)-dependent deacetylases. Mammals contain seven sirtuins, which have different subcellular localizations, with a subset of sirtuins residing in mitochondrial (SIRT3, SIRT4 and SIRT5), cytosolic (SIRT2), or nuclear (SIRT1, SIRT6, and SIRT7) compartments (Haigis and Sinclair, 2010). SIRT6, predominantly a nuclear protein, has been increasing identified as a critical regulator in diverse physiological and pathological events including life span, DNA damage repair, glucose metabolism and cancer (Gertler and Cohen, 2013). SIRT6 is known to deacetylate lysine-9 of histone H3 at the promoter of many genes involved in glycolysis and lipid metabolism (Kim et al., 2010). SIRT6 is also known to mediate mono-ADP ribosylation of KAP1 and repress LINE1 retrotransposons (Van Meter et al., 2014). The *in vivo* studies have shown that SIRT6 prevent age-related disorders and premature aging. Transgenic overexpression of SIRT6 could extend lifespan in male mice (Kanfi et al., 2012). The phenotype of *Sirt6*$^{-/-}$ mice is the consequence of multiorgan degeneration associated with premature aging and chronic inflammation (Mostoslavsky et al., 2006; Xiao et al., 2012). Sirtuins may play an important role in the control of inflammation through the regulation of immune gene transcription. SIRT1, one of the most widely studied nuclear sirtuin, has been shown to suppress inflammatory responses. Resveratrol, an activator of SIRT1, inhibits inflammation by targeting NF-κB signaling (Zhu et al., 2011). SIRT2 suppresses inflammatory responses in collagen-induced arthritis (Lin et al., 2013). The role of SIRT6 in antiviral innate immune responses and whether SIRT6 is involved in the regulation of DENV-induced inflammatory response is currently unknown.

Here we demonstrate that SIRT6 negatively regulates the DENV-induced inflammatory response. SIRT6 is induced upon DENV infection, and proinflammatory cytokine production to DENV is enhanced when *Sirt6* is silenced. Further studies show that SIRT6 binds to the DNA binding domain of p65 and inhibits NF-κB function.

MATERIALS AND METHODS

Cell Lines, Viruses, and Reagents

The Raw264.7 cell line was a kind gift form Dr. Zhaojun Wang (Jiaotong University, China). HEK293T cells were obtained from Type Culture Collection of the Chinese Academy of Science. The cells were cultured at 37°C under 5% CO_2 in DMEM or RPMI 1640 medium supplemented with 10% fetal bovine serum and antibiotics (100 units/mL penicillin and 100 μg/mL streptomycin, Invitrogen). DENV New Guinea C strain serotype 2 (DENV-2) was propagated in C6/36 cells. Low molecular weight (LMW) and high molecular weight (HMW) Poly I:C were from Invivogen. The antibodies specific to SIRT6, p65, Histone H3, Caspase 3 were from Cell Signaling Technology. Anti-HA, anti-Flag, anti-p50 and anti-GAPDH antibodies were from Proteintech. HRP-conjugated secondary antibodies were from Sungene Biotechnology.

shRNAs and Lentiviral Infection

The small hairpin RNA (shRNA) target sequences were as follows: mouse *Sirt6* sh*Sirt6*-1 (5′-TCC CAA GTG TAA GAC GCA GTA-3′), sh*Sirt6*-2 (5′-GCA TGT TTC GTA TAA GTC CAA-3′), human *SIRT6* shRNA (5′-CTC CCT GGT CTC CAG CTT AAA-3′), mouse p65 shRNA (5′-GCA TGC GAT TCC GCT ATA AAT-3′) and scrambled shRNA (5′-CAA CAA GAT GAA GAG CAC CAA-3′). Lentiviruses expressing scrambled or *Sirt6* specific shRNA were used to generate control and *Sirt6*-knockdown cell lines. Lentivirus was produced by cotransfection of HEK293T cells with pLKO.1 shRNA plasmid (Addgene plasmid No. 8453), pCMV-dR8.2 dvpr packaging plasmid (Addgene plasmid No. 8455), and pCMV-VSVG envelope plasmid (Addgene plasmid No. 8454). Supernatants containing lentivirus were harvested at 36–48 h after transfection and used to infect the target cells for 24 h. Stably transduced cells were selected in media containing puromycin (5 μg/mL; Invivogen). Knockdown efficiency was analyzed by immunoblot.

Dual-Luciferase Reporter Assay

HEK293T cells were transfected in 24-well plates with indicated expression plasmids along with luciferase reporter plasmids pNF-κB-Luc (Stratagene), TNFa-Luc (kindly provided by Dr. Guang Yang, Jinan University, China) or pRL-TK (Promega) using Hieff

Trans^{TM} transfection reagent (Yeasen). The cells were incubated at 37°C under 5% CO2 for 24 h. For experiments with ligand stimulation, cells were treated with HWM or LMW Poly I:C (10 μg /mL) for 16 h. Cells were lysed, and luciferase activities were determined with Dual-Luciferase Reporter Assay System (Wang et al., 2017).

Quantitative PCR (qPCR) Analysis

Total RNA was extracted using TRI Reagent (Sigma), and cDNA was synthesized using the Reverse Transcription Reagent Kit (Takara). Amplification was performed using SYBR Green qPCR Master Mix (Biotools) with gene-specific primers in CFX96 System (Bio-Rad). Gene expression levels were normalized to the *Actin* gene. Primer sequences used for qPCR were as follows: *mSirt6* (forward: 5′-CAG TAC GTC AGA GAC ACG GTT G-3′, reverse: 5′-GTC CAG AAT GGT GTC TCT CAG C-3′), *mIl6* (forward: 5′-TAC CAC TTC ACA AGT CGG AGG C-3′, reverse: 5′-CTC AAG TCA TCA TCG TTG TTC-3′), *mTnfα* (forward: 5′-GGT GCC TAT GTC TCA GCC TCT T-3′, reverse: 5′-GCC TAG AAC TGA TGA GAG GGA G-3′), *mCcl2* (forward: 5′-GCT ACA AGA GGA TCA CCA GCA G-3′, reverse: 5′-GTC TGG ACC CAT TCC TTC TTG G-3′), *mCcl5* (forward: 5′-CCT GCT GCT TTG CCT ACC TCT C-3′, reverse: 5′-ACA CAC TTG GCG GTT CCT TCG A-3′), *mActin* (forward: 5′-CAT TGC TGA CAG GAT GCA GAA GG-3′, reverse: 5′-TGC TGA AGG TGA CAT GAG G-3′). *hIL6* (forward: 5′-AGA CAG CCA CTC ACC TCT TCA G-3′, reverse: 5′-TTC TGC CAG TGC CTC TTT GCT G-3′), *hTNFA* (forward: 5′-CTC TTC TGC CTG CTG CAC TTT G-3′, reverse: 5′-ATG GGC TAC AGG CTT GTC ACT C-3′), *hCCL2* (forward: 5′-GCT ACA AGA GGA TCA CCA GCA G-3′, reverse: 5′-GTC TGG ACC CAT TCC TTC TTG G-3′), *hCCL5* (forward: 5′-CCT GCT GCT TTG CCT ACA TTG C-3′, reverse: 5′-ACA CAC TTG GCG GTT CTT TCG G-3′), *hACTIN* (forward: 5′-AGA TCA TGT TTG AGA CCT TCA ACA C-3′, reverse: 5′-GGA GCA ATG ATC TTG ATC TTC ATT G-3′). *DENV E* (forward: 5′-CAT TCC AAG TGA GAA TCT CTT TGT CA-3′, reverse: 5′-CAG ATC TCT GAT GAA TAA CCA ACG-3′).

Cytokine ELISA Measurements

Cell supernatants were harvested from DENV infected cells. Supernatants were centrifuged for 5 min at 3,000 g to remove cellular debris and were stored at −80°C before analysis. Cytokines were quantified using ELISA MAX^{TM} Deluxe kit (Biolegend) according to the manufacturer's instructions.

Coimmunoprecipitation (CoIP) and Immunoblot Analysis

HEK293T cells transfected with expression plasmids or Raw264.7 cells were harvested using RIPA III lysis buffer containing protease inhibitor cocktail (Biotechwell). Whole cell extracts were incubated overnight at 4°C with indicated antibodies followed by incubation with protein A/G agarose beads (Santa Cruz) for 2 h at 4°C. The beads were washed five times with lysis buffer and proteins eluted by boiling for 5 min in SDS sample buffer.

For immunoblot analysis, cell lysates were subjected to SDS-PAGE and transferred onto PVDF membranes (Thermo Fisher). Immunoblots were probed with indicated antibodies and developed using NcmECL Ultra Reagent (NCM Biotech).

Immunofluorescence Microscopy

Poly I:C treated and untreated cells were fixed, permeabilized in 4% PFA/0.2 Triton-X for 20 min and blocked in PBS/10% FBS for 1 h. Cells were labeled with mouse anti-Flag and rabbit anti-HA antibodies, and detected by Alexa 488 anti-mouse and Alexa 546 anti-rabbit antibodies (Invitrogen). Images were collected using an inverted fluorescence microscope (Leica).

Chromatin Immunoprecipitation

Cells were fixed with 1% formaldehyde and quenched with glycine. Purified chromatin was sonicated to ∼500 bp using the Ultrasonic Processing (SONICS) and incubated with the indicated antibodies. DNA-protein complexes were immunoprecipitated by protein A/G agarose, followed by reverse crosslinking processes. The DNA was then purified and quantified by qPCR. PCR primer sequences for promoter regions were as follows: *Il6*-CHIP (forward: 5′-GCA GTG GGA TCA GCA CTA AC-3′, reverse: 5′-GGT GGG TAA AGT GGG TGA AG-3′), *Tnfa*-CHIP (forward: 5′-GGA GAT TCC TTG ATG CCT GG-3′, reverse: 5′-GCT CTC ATT CAA CCC TCG GA-3′).

Statistical Analysis

Statistical significance was determined by an unpaired Student's *t*-test with GraphPad Prism. Data were presented as mean ± SEM of three independent experiments. Values of $p < 0.05$ were considered statistically significant.

RESULTS

SIRT6 Negatively Regulates DENV-Induced Proinflammatory Cytokine and Chemokine Production

Macrophages and mononuclear phagocytes are the primary targets of dengue virus infection (Chen and Wang, 2002). We examined the expression pattern of SIRT6 in murine Raw264.7 macrophages upon DENV infection. The mRNA level of *Sirt6* was significantly increased after DENV infection within 12 h (**Figure 1A**). Immunoblot further confirmed the upregulation of SIRT6 protein expression in DENV infected cells (**Figure 1B**).

Macrophages are the major source of proinflammatory cytokines after DENV infection. To investigate the potential role of *Sirt6* in DENV-induced inflammatory response, we designed small hairpin RNA (shRNA) that targeted two sites of *Sirt6* and generated *Sirt6*-silenced Raw264.7 cells. Endogenous SIRT6 was silenced efficiently as quantified by immunoblot analysis (**Figure 1C**). We used qPCR to quantify mRNA expression levels of proinflammatory cytokine and chemokine in *Sirt6*-silenced cells. Notably, silencing of *Sirt6* significantly increased the transcription level of proinflammatory cytokines *Il6 and Tnfα* as well as chemokines *Ccl2* and *Ccl5* after DENV infection (**Figure 1D**). We further measured protein production of IL-6 and TNFα in *Sirt6*-silenced cells after DENV infection. In agreement with these findings, these cells produced greater

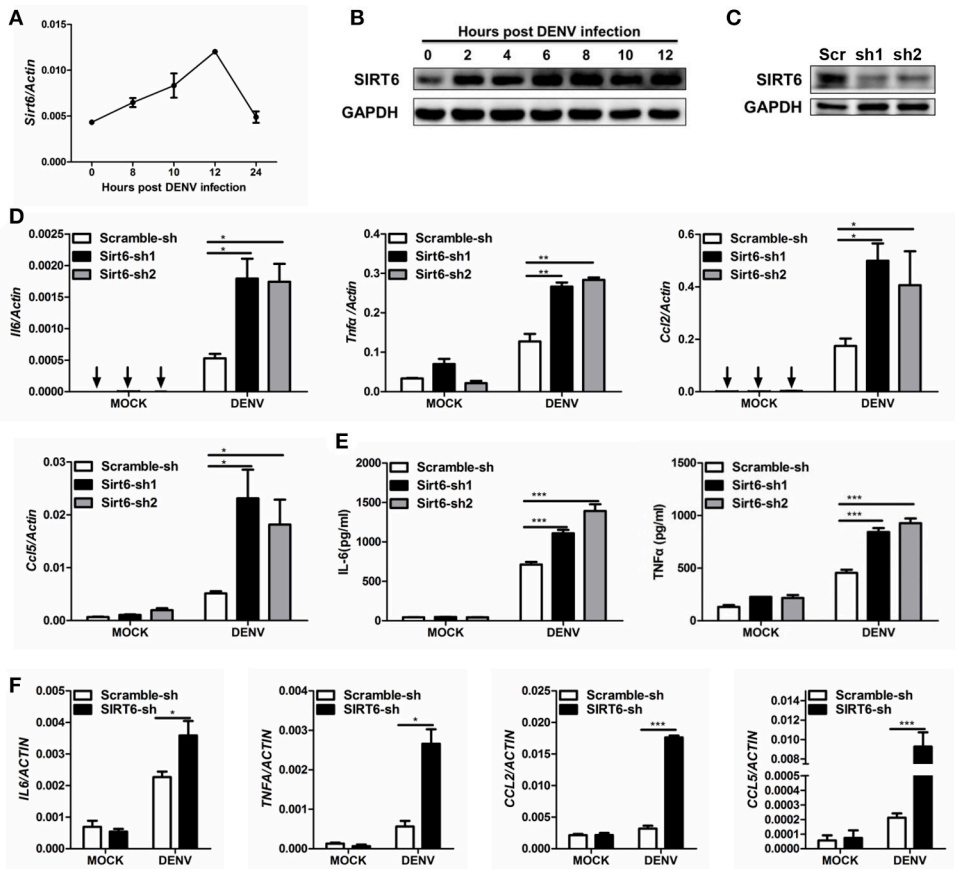

FIGURE 1 | SIRT6 negatively regulates DENV-induced proinflammatory cytokine and chemokine production. Quantification of **(A)** *Sirt6* mRNA levels by qPCR, and **(B)** SIRT6 protein expression by immunoblot in Raw264.7 cells after DENV infection (MOI = 1). **(C)** Immunoblot analysis of SIRT6 expression in Raw264.7 cells stably expressing shRNA against *Sirt6*. Quantification of **(D)** indicated cytokine and chemokine mRNA levels by qPCR and **(E)** secreted IL-6 and TNFα levels by ELISA from Raw264.7 cells stably expressing either scrambled shRNA or *Sirt6*-targeting shRNA after DENV infection for 12 h. **(F)** Quantification of indicated cytokine and chemokine mRNA levels by qPCR from HEK293T cells stably expressing either scrambled shRNA or *SIRT6*-targeting shRNA after DENV infection for 24 h. Data shown are the mean ± SEM; $^{*}p < 0.05$, $^{**}p < 0.01$, $^{***}p < 0.001$. Representative results are from at least three independent experiments.

amounts of IL-6 and TNFα protein than scrambled shRNA-treated cells (**Figure 1E**). To determine whether the function of SIRT6 is conserved across species, we generated *SIRT6*-silenced HEK293T human embryonic kidney cells. Similar to the data obtained with Raw264.7 cells, we observed that knockdown of *SIRT6* in HEK293T increased DENV-induced expression levels of *IL6, TNFA, CCL2*, and *CCL5* (**Figure 1F**). Moreover, DENV replication was reduced when *SIRT6* was silenced (**Figure S1**). These results suggest that SIRT6 is involved in the regulation of DENV-induced proinflammatory cytokine and chemokine production.

SIRT6 Inhibits RLR-Mediated Inflammatory Response

The RLR pathway is a well-characterized pathway initiating antiviral innate immune responses (Loo and Gale, 2011). The key transcription factor NF-κB contributes to the production of proinflammatory cytokines in RLR-mediated signal transduction. We examined whether SIRT6 regulated virus-induced inflammatory reactions through the RIG-I/MDA5 pathway. By transfection of a synthetic analog of double-stranded RNA (agonist of RLR pathway), we initially tested the effect of SIRT6 on RLR-dependent NF-κB activation. We found that SIRT6 significantly inhibited activation of NF-κB promoter in HEK293T cells transfected with either low-molecular-weight (LMW) Poly I:C (RIG-I activator) or high-molecular-weight (HMW) Poly I:C (MDA5 activator) (**Figures 2A,B**).

To confirm the inhibitory role of SIRT6 in RLR signaling, we tested the effect of SIRT6 on upstream components of the RLR signaling pathway in their activation of NF-κB and TNFa promoters through reporter assay. We transfected HEK293T cells with expression plasmids encoding the RLR signaling molecules ΔRIG-I (active form of RIG-I), MDA5 or MAVS (adaptor molecule), together with increasing amounts of SIRT6 and luciferase reporter constructs driven by the transcription factor NF-κB or TNFα promoter. SIRT6 overexpression significantly decreased ΔRIG-I, MDA5, and MAVS-induced NF-κB activation (**Figures 2C–E**, **Figure S2**). Furthermore, SIRT6 also inhibited

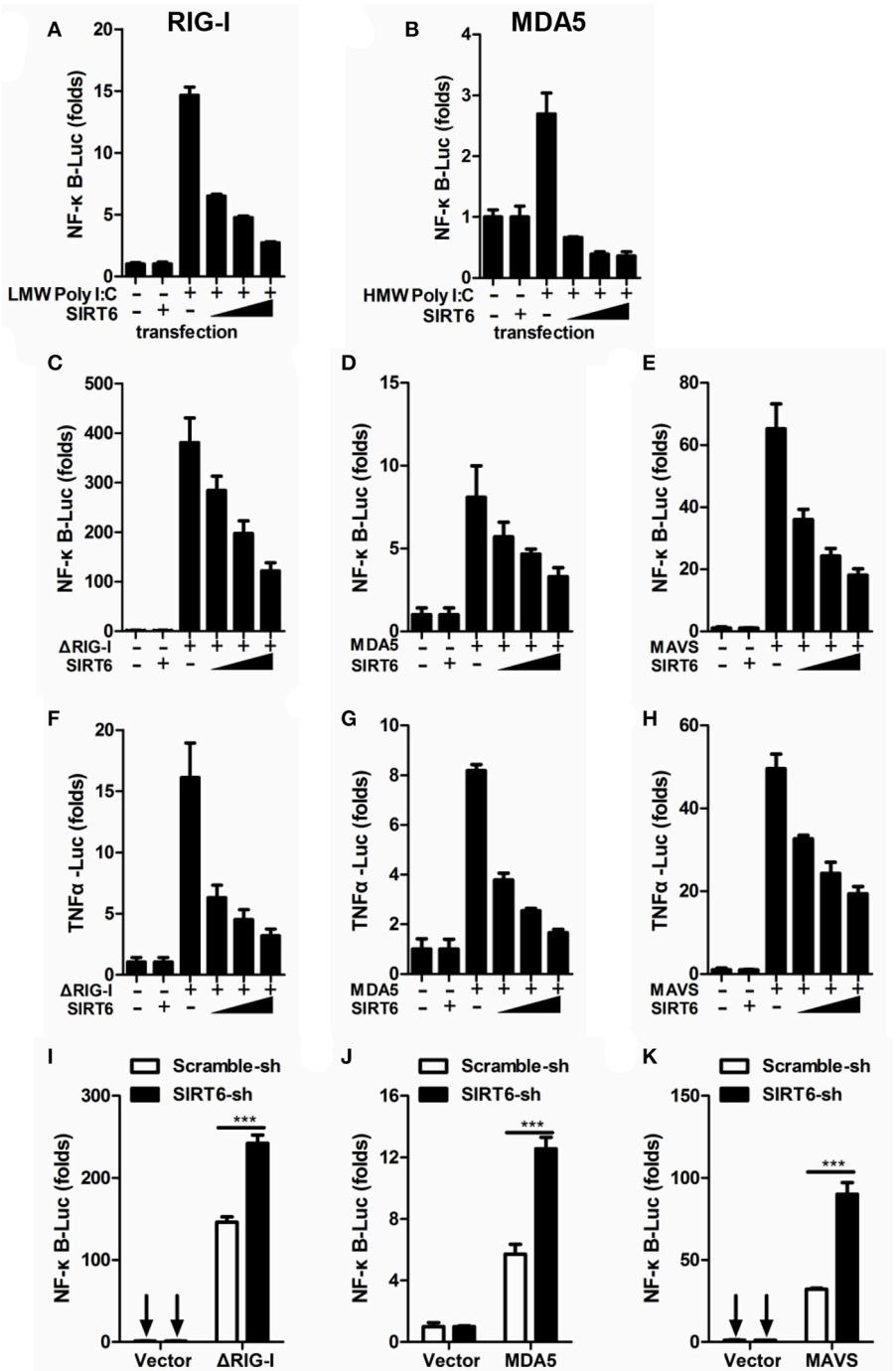

FIGURE 2 | SIRT6 inhibits RLR-mediated inflammatory response. **(A,B)** Quantification of NF-κB promoter activity of HEK293T cells transfected with either an empty vector or increasing amounts of SIRT6 plasmid and treated with LMW Poly I:C or HMW Poly I:C. Quantification of **(C–E)** NF-κB promoter activity and **(F–H)** TNFα promoter activity of HEK293T cells expressing ΔRIG-I, MDA5, or MAVS, together with increasing amounts of SIRT6. **(I–K)** Quantification of NF-κB promoter activity in scrambled shRNA or *SIRT6* shRNA treated HEK293T cells transfected with either an empty vector or ΔRIG-I, MDA5, MAVS plasmids. Data shown are the mean ± SEM; ***$p < 0.001$. Representative results are from at least three independent experiments.

ΔRIG-I, MDA5, and MAVS-induced TNFα promoter activation in a dose-dependent manner (**Figures 2F–H**). In contrast, silencing of *SIRT6* enhanced the activation of NF-κB by these RLR signaling molecules (**Figures 2I–K**). The expression level of NF-κB responsive gene *Il6* was increased in *Sirt6*-knockdown cells after SeV (agonist of the RLR signaling)

infection (**Figure S3A**). Together, these data suggest that SIRT6 is a negative regulator for the RLR signaling pathway and inhibits RLR-mediated NF-κB activation.

SIRT6 Inhibits TLR3-Mediated Inflammatory Response

In addition to RIG-I/MDA5, the Toll-like receptor 3 (TLR3) also play an important role in DENV recognition and induction of cytokine (Tsai et al., 2009). When we assessed whether SIRT6 regulated inflammatory responses via TLR3 pathway, we found that SIRT6 overexpression inhibited the activation of NF-κB promoter in HEK293T-TLR3 cells treated with extracellular Poly I:C (HMW) (**Figure 3A**). Further, when we co-expressed the TLR3 signaling adaptor, TRIF, with increasing amounts of SIRT6, SIRT6 significantly decreased the TRIF-induced NF-κB and TNFα promoter activation in a dose-dependent manner (**Figures 3B–C**). Furthermore, silencing of *SIRT6* promoted TRIF-induced NF-κB activation (**Figure 3D**) and Poly I:C (HMW) induced *Il6* production (**Figure S3B**). Taken together, these findings suggest that SIRT6 blocks TLR3-mediated inflammatory responses.

NF-κB p65 Is the Target of SIRT6

To identify the target of SIRT6 in RLR and TLR3 signaling, we expressed TRAF6, TAK1/TAB1, IKKα, IKKβ, NF-κB p65 along with increasing amounts of SIRT6. The reporter assay showed that SIRT6 inhibited NF-κB activation induced by all these signaling molecules (**Figure 4A**). These data suggested that SIRT6 might target the downstream component, NF-κB p65. Then, we determined whether SIRT6 targets p65 using coimmunoprecipitation (CoIP) assays. SIRT6 plasmid with Flag tag and p65 plasmid with HA tag were transfected into HEK293T cells. The coimmunoprecipitation results showed that SIRT6 associated with p65 (**Figure 4B**). To confirm whether SIRT6 physically interacts with the NF-κB subunit p65, we immunoprecipitated endogenous SIRT6 and immunoblot analysis revealed a specific interaction with p65. In addition, SIRT6 was detected in IPs of endogenous p65. Importantly, DENV infection promoted endogenous SIRT6 binding to p65 in Raw264.7 cells (**Figure 4C**). We also immunoprecipitated endogenous NF-κB subunit p50 to investigate whether SIRT6 associates with the p50. We did not detect the interaction between p50 and SIRT6 (**Figure S4**).

To further verify that SIRT6 associated with p65, we performed subcellular fractionation and immunofluorescence microscopy. Endogenous p65 was mainly in the cytosol of untreated cells, but it translocated to nucleus and localized together with SIRT6 after DENV infection. Increased expression of SIRT6 was detected in the nuclear fraction upon DENV infection of Raw264.7 cells (**Figure 4D**). Consistent with these results, immunofluorescence microscopy demonstrated the colocalization of SIRT6 and p65 after Poly I:C treatment (**Figure 4E**). Taken together, these findings suggest that SIRT6 interacts with p65 in the nucleus in a viral infection-inducible manner.

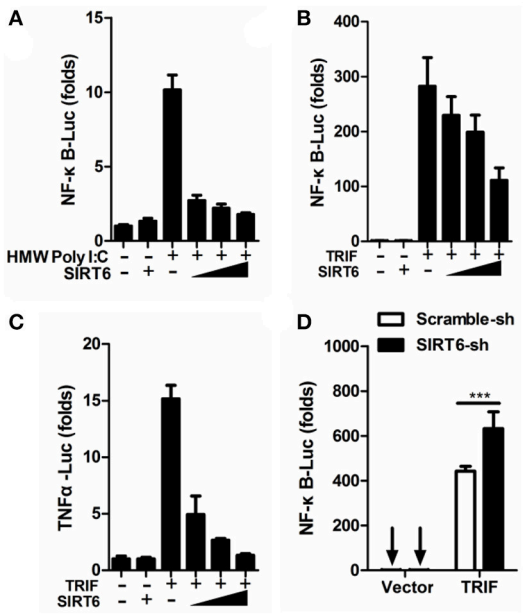

FIGURE 3 | SIRT6 inhibits TLR3-mediated inflammatory response. **(A)** Quantification of NF-κB promoter activity of HEK293T-TLR3 cells transfected with either an empty vector or increasing amounts of SIRT6 plasmid and treated with HMW Poly I:C. Quantification of **(B)** NF-κB promoter activity and **(C)** TNFα promoter activity of HEK293T cells expressing TRIF together with increasing amounts of SIRT6. **(D)** Quantification of NF-κB promoter activity in scrambled shRNA or *SIRT6* shRNA treated HEK293T cells transfected with either an empty vector or TRIF plasmid. Data shown are the mean ± SEM; $^{***}p < 0.001$. Representative results are from at least three independent experiments.

The Core Domain of SIRT6 Is Required for p65 Inhibition

We next asked which domain of SIRT6 binds to and inhibits p65 function. To determine which domain of SIRT6 was necessary for interaction with p65, we generated several SIRT6 deletion constructs (**Figure 5A**) and assessed them in coimmunoprecipitation experiments. NF-κB p65 bound strongly to full-length SIRT6, sirtuin core domain (amino acids 34–274), ΔN (amino acids 1–33 was deleted) and ΔC (amino acids 275–355 was deleted) constructs of SIRT6, while C terminus of SIRT6 lost the ability to interact with p65 (**Figure 5B**). These results suggest the core domain of SIRT6 is necessary for p65 binding. In addition, deletion of the N-terminal and C-terminal domain did not affect the inhibitory activity of SIRT6 on p65-induced NF-κB promoter activation. The core domain of SIRT6 retained a similar inhibitory effect on p65-induced NF-κB promoter activation as full-length SIRT6 (**Figure 5C**). These data suggest that the core domain of SIRT6 is required for p65 binding and inhibition.

SIRT6 Targets to the DNA Binding Domain of p65

NF-κB p65 is composed of a DNA binding domain (amino acids 1–186), a dimerizing domain (amino acids 187–286) and an activation domain (amino acids 287–551) (**Figure 6A**). To identify the SIRT6-binding domain within p65, we performed

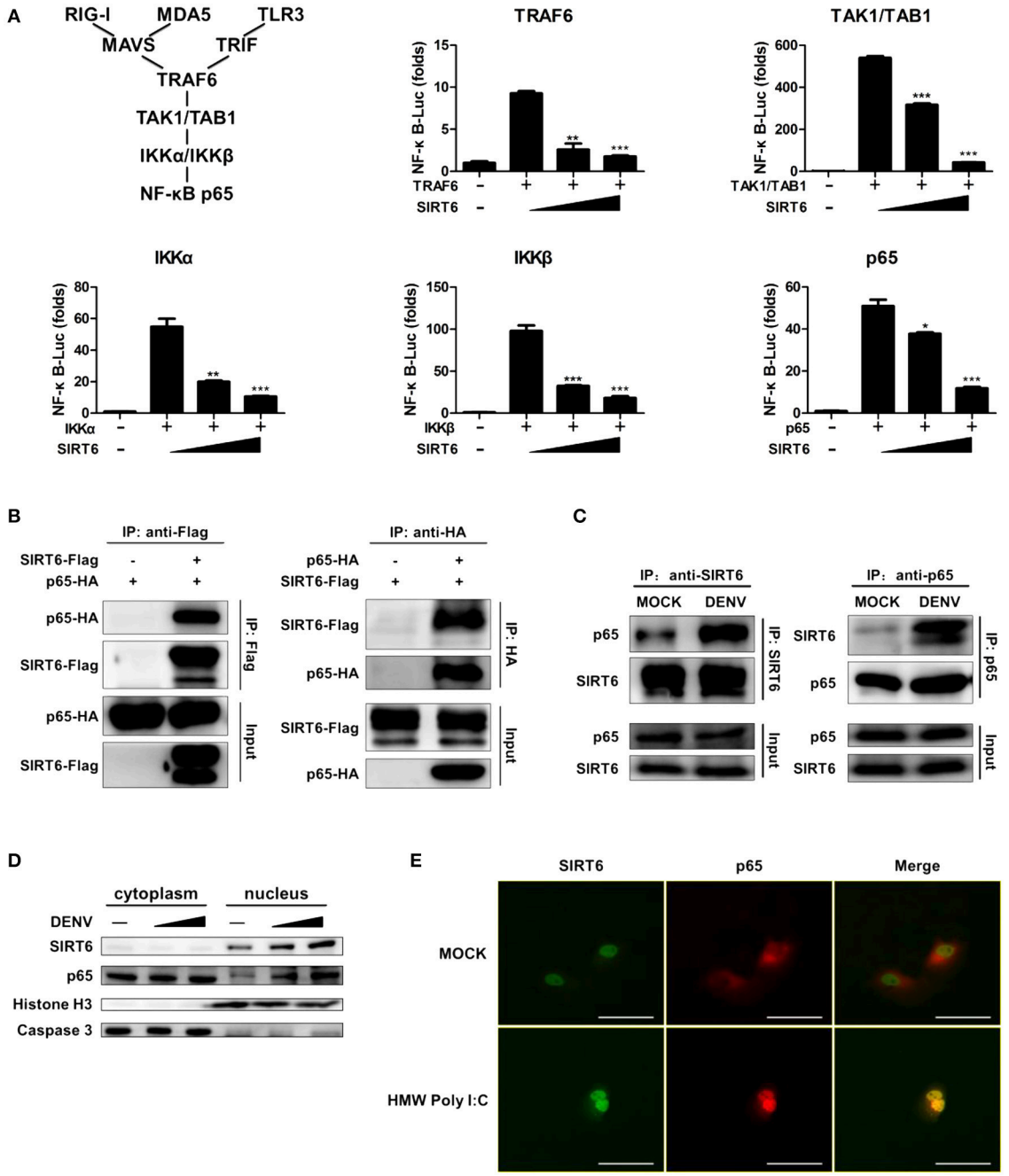

FIGURE 4 | NF-κB p65 is the target of SIRT6. **(A)** SIRT6 inhibits RLR and TLR3-activated NF-κB signaling pathway. Quantification of NF-κB promoter activity of HEK293T cells expressing increasing amounts of SIRT6 together with TRAF6, TAK1/TAB1, IKKα, IKKβ, or p65, respectively. **(B)** SIRT6 interacts with NF-κB p65. Coimmunoprecipitation (CoIP) of SIRT6 and p65 from HEK293T cells expressing Flag-SIRT6 and HA-p65 using α-Flag or α-HA antibody pull-down, followed by immunoblotting. **(C)** CoIP of endogenous SIRT6 and p65 from Raw264.7 cells infected with DENV (MOI = 1) for 12 h using α-SIRT6 or α-p65 antibody pull-down, followed by immunoblotting. **(D)** Immunoblot analysis of SIRT6, p65, Caspase 3 and Histone H3 in cytoplasm and nucleus of Raw264.7 cells after DENV infection (MOI = 1–5) for 12 h. **(E)** Immunofluorescence microscopy of HEK293T-TLR3 cells transfected with plasmids of Flag-SIRT6 (green) with HA-p65 (red) stimulated by HMW Poly I:C. White Bar: 50 um. Data shown are the mean ± SEM; $^{*}p < 0.05$, $^{**}p < 0.01$, $^{***}p < 0.001$. Representative results are from at least three independent experiments.

coimmunoprecipitation and assessed the binding of SIRT6 to several truncated forms of p65. We found that SIRT6 bound strongly to full-length, ΔAD and DNA binding domain of p65, but failed to bind to the activation domain of p65 (**Figure 6B**). Together these data suggest that SIRT6 may inhibit NF-κB activation through targeting the DNA binding domain of p65.

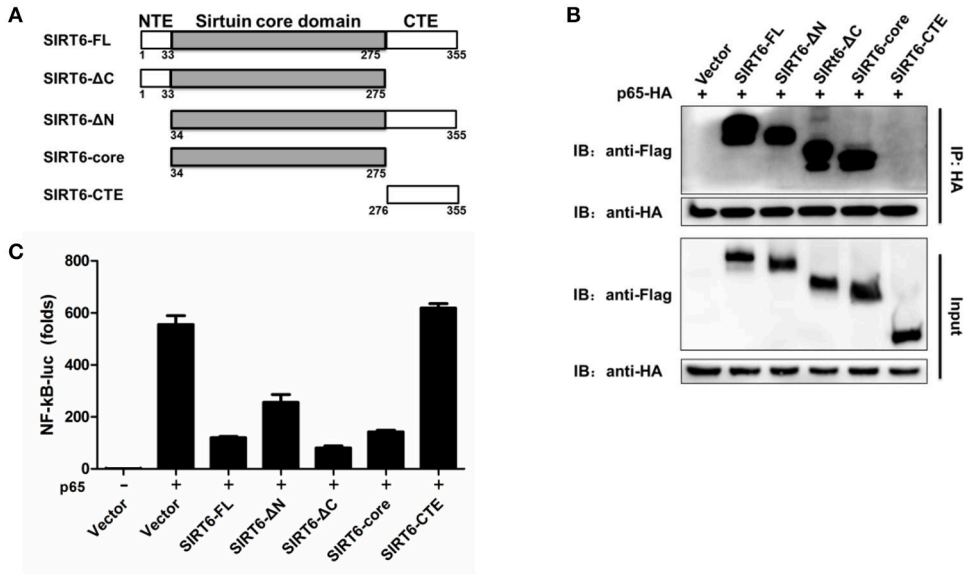

FIGURE 5 | The core domain of SIRT6 is required for p65 inhibition. **(A)** Schematic of SIRT6 deletion mutants. **(B)** Coimmunoprecipitation of NF-κB p65 and SIRT6 from HEK293T cells expressing HA-p65 together with Flag-SIRT6 variants using a HA monoclonal antibody, followed by immunoblotting. **(C)** Quantification of NF-κB promotor activity of HEK293T cells transfected with either an empty vector or SIRT6 deletion mutants together with p65 plasmid.

SIRT6 Decreases p65 Occupancy in the *Il6* Promoter

In response to viral infections, activated NF-κB translocates to the nucleus, binds to the promoter region of target genes, and induces the expression of inflammatory cytokines (Rahman and McFadden, 2011). To test whether SIRT6 occupies the p65 target gene promoter region, we performed chromatin immunoprecipitation (ChIP) assays with an anti-SIRT6 antibody. SIRT6 was detected at the promoter of p65 target gene *Il6 and Tnfa*, compared to the IgG negative control background signal. Notably, DENV infection further elevated the binding of SIRT6 to the *Il6 and Tnfa* promoter (**Figure 6C**). These data suggest that SIRT6 is enriched at the promoter region of p65 regulated genes following viral infection. To determine whether SIRT6 is recruited to p65 target gene promoter region via its interaction with p65, we designed shRNA that targeted *p65* and generated *p65*-silenced Raw264.7 cells. Silencing of p65 significantly decreased the occupancy of SIRT6 at *Il6* gene promoter (**Figure 6D**). Finally, we examined the effects of SIRT6 deficiency on p65 occupancy at target gene promoters by ChIP assay using anti-p65 antibody. In *Sirt6*-silenced cells, p65 occupancy at *Il6* gene promoter was significantly enhanced after DENV infection (**Figure 6E**). These data suggest that SIRT6 is recruited to the inflammatory gene promoter through its interaction with the DNA binding domain of p65, and impairs the binding of p65 to its target gene promoter.

DISCUSSION

Excessive inflammation is believed to play a pathologic role during host response to DENV infection (Costa et al., 2013). Increased levels of proinflammatory cytokines and chemokines occur in patients experiencing severe dengue disease (Chaturvedi et al., 2000; Soundravally et al., 2014). Therefore, elucidating the regulatory mechanisms in the DENV-induced host immune responses is a key task. Sirtuins may play an important role in the control of inflammation. In this study, we found that mRNA and protein levels of SIRT6 increased upon DENV infection. It has been reported that transcription factor AP-1 activation is induced in DENV-infected macrophages (Ceballos-Olvera et al., 2010). SIRT6 is a direct transcriptional target of AP-1 (Min et al., 2012). The DENV-induced activation of AP-1 may promote SIRT6 expression. We further investigated the role of SIRT6 in DENV-triggered immune responses. Silencing of *Sirt6* by RNA interference enhanced DENV-induced proinflammatory cytokine and chemokine production. Activation of the host innate immune system by DENV is thought to induce a strong inflammatory response. We next confirmed SIRT6 as a negative regulator in the RLR and TLR3-mediated innate immune response. Overexpression of SIRT6 significantly inhibited RIG-I/MDA5 and TLR3-induced NF-κB activation, whereas silencing of *SIRT6* had opposite effects on NF-κB activation. These findings suggest that SIRT6 has a global role in RLR and TLR signaling pathways, indicating its importance in virus induced innate immune responses.

NF-κB is a key component in the pathway from pathogen recognition to inflammatory cytokine production. NF-κB activation must be tightly regulated to prevent excessive immune responses. A20, CUEDC2, and ANGPTL8 have been identified as regulators that limit NF-κB signaling through different molecular mechanisms. A20 is a deubiquitinating enzyme that removes ubiquitin moieties from the signaling molecule TRAF6, thereby

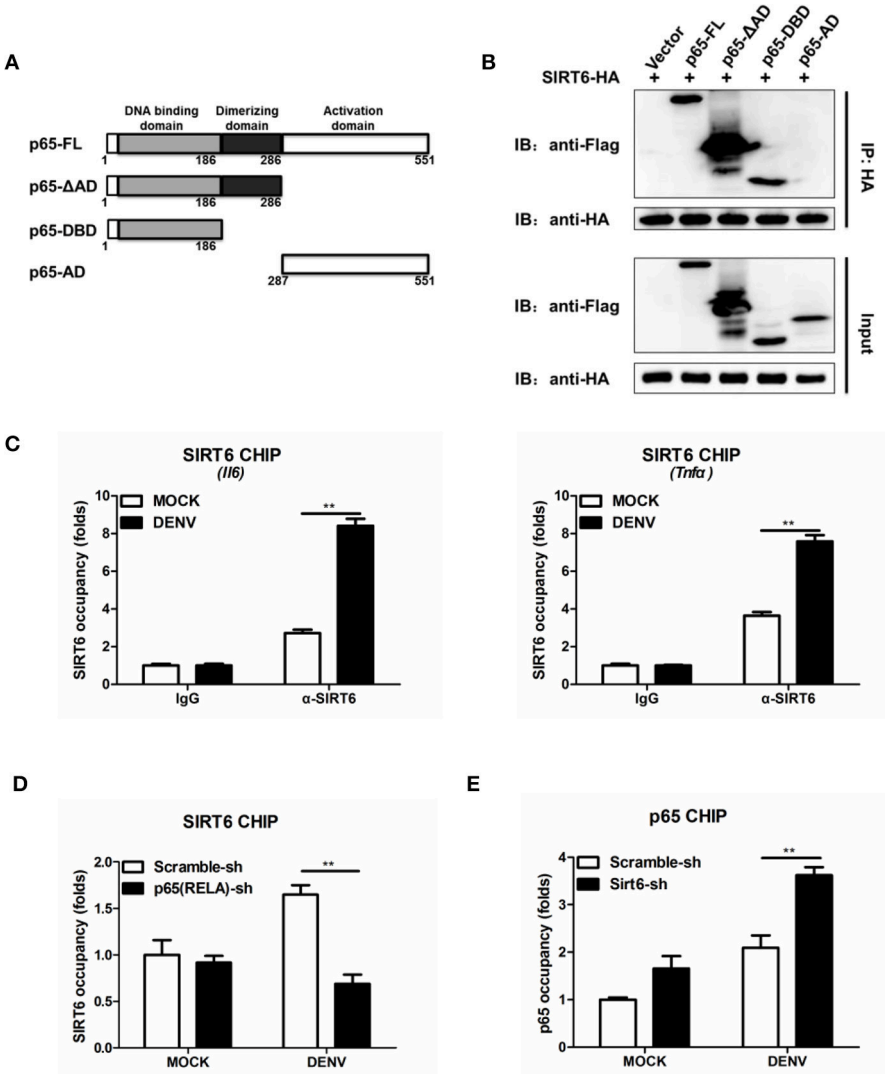

FIGURE 6 | SIRT6 interacts with the DNA binding domain of p65 and decreases p65 occupancy in the *Il6* promoter. **(A)** Schematic of p65 deletion mutants. **(B)** Coimmunoprecipitation of SIRT6 and NF-κB p65 from HEK293T cells expressing HA-SIRT6 and Flag-p65 variants using α-HA monoclonal antibody, followed by immunoblotting. **(C)** Chromatin immunoprecipitation (ChIP) assays followed by qPCR for SIRT6 in the *Il6* and *Tnfa* promoter in Raw264.7 cells infected with DENV (MOI = 1) for 12 h. **(D)** ChIP assays followed by qPCR for SIRT6 in the *Il6* promoter in Raw264.7 cells stably expressing either scrambled shRNA or *p65*-trageting shRNA after DENV infection (MOI = 1) for 12 h. **(E)** ChIP assays followed by qPCR for NF-κB p65 in the *Il6* promoter in Raw264.7 cells stably expressing either scrambled shRNA or *Sirt6*-trageting shRNA after DENV infection (MOI = 1) for 12 h. Data shown are the mean ± SEM; $^{**}p < 0.01$. Representative results are from at least three independent experiments.

terminating TLR-induced NF-κB activation (Boone et al., 2004). CUEDC2 has been reported to interact with IKKα and IKKβ and inhibit NF-κB activation by decreasing phosphorylation of IKK (Li et al., 2008). ANGPTL8 has been reported to negatively regulate NF-κB activation by facilitating p62-mediated autophagic degradation of IKKγ (Zhang et al., 2017). In this study, several lines of evidence indicate SIRT6 directly targets NF-κB p65 to inhibit NF-κB activation. First, overexpression of SIRT6 inhibits either p65-induced or upstream factors of RLR/TLR3-signaling-induced NF-κB promoter activation. Second, p65 colocalizes with SIRT6 in the nucleus after infection with DENV. Third, DENV infection promotes endogenous SIRT6 binding to p65. Domain mapping assays show that the sirtuin core domain of SIRT6 is required for the binding of p65. Our results demonstrate that SIRT6 core domain alone is sufficient for the inhibitory effect of SIRT6 on NF-κB signaling.

Our findings and those of others suggest that sirtuins could target NF-κB p65 and regulate its function through distinct mechanisms. SIRT1 was initially reported to interact with p65 and deacetylate p65 at lysine 310 (Yeung et al., 2004). Overexpression of SIRT1 and the addition of the SIRT1 agonist resveratrol protects against microglia-dependent amyloid-β toxicity through inhibiting NF-κB signaling (Chen et al., 2005). Similar studies have revealed that SIRT2 interacts

with p65 in the cytoplasm and deacetylates p65 *in vitro* and *in vivo* at lysine 310 (Rothgiesser et al., 2010). *Sirt2* deficient mice are more sensitive to DSS-induced colitis compared to wild type littermates (Lo et al., 2014). Surprisingly, SIRT5 and SIRT1/2 have opposite functions. SIRT5 could compete with SIRT2 to interact with p65 and block the deacetylation of p65 by SIRT2, leading to increased acetylation of p65 and the activation of NF-κB signaling (Qin et al., 2017). SIRT6 has been shown previously to affect NF-κB-dependent gene expression, through deacetylation of histone H3 (Kawahara et al., 2009). Our study has demonstrated SIRT6 interacts with the DNA binding domain of p65. SIRT6 is recruited to cytokines promoter regions through its interaction with p65 after DENV infection. This interaction decreased the occupancy of p65 at the NF-κB target gene promoter. Consequently, SIRT6 occupies the promoter of NF-κB target genes and mediates repression of inflammatory response.

In summary, our work identifies a critical role for SIRT6 in the control of DENV-induced innate immune responses. Mechanistically, SIRT6 targets the DNA binding domain of NF-κB p65 and blocks the NF-κB medicated transcription of inflammatory cytokines. SIRT6 may be an effective target for new therapeutic interventions against various infectious and inflammatory diseases that have been associated excessive inflammation.

AUTHOR CONTRIBUTIONS

FQia and PL designed the study. PL, YJ, and FQi performed the experiments. FW, SL, and YC provided experimental assistance. PL, FQia, and RM interpreted the data. PL and FQia drafted the manuscript. All the authors reviewed the manuscript.

ACKNOWLEDGMENTS

This work was supported by the National Natural Science Foundation of China (No. 81671393, 81370464), Doctoral Fund of Ministry of Education of China (No. 20130071120031).

SUPPLEMENTARY MATERIAL

The Supplementary Material for this article can be found online at: https://www.frontiersin.org/articles/10.3389/fcimb.2018.00113/full#supplementary-material

Figure S1 | Effect of SIRT6 on DENV replication. Quantification of intracellular DENV loads by qPCR from HEK293T cells stably expressing either scrambled shRNA or *SIRT6*-targeting shRNA after DENV infection for 36 h. Data shown are the mean ± SEM; $^{***}p < 0.001$.

Figure S2 | Effect of SIRT6 on ΔRIG-I, MDA5 and MAVS expression. Quantification of ΔRIG-I **(A)**, MDA5 **(B)**, and MAVS **(C)** protein expression levels by immunoblotting from HEK293T cells transfected with either an empty vector or indicated plasmids, together with increasing amounts of SIRT6.

Figure S3 | SIRT6 inhibits RLR- and TLR3-mediated inflammatory response. Quantification of *Il6* mRNA levels by qPCR from Raw264.7 cells stably expressing either scrambled shRNA or *Sirt6*-targeting shRNA after SeV infection **(A)** and PolyI:C (HMW) stimulation **(B)** for 12 h. Data shown are the mean ± SEM; $^{*}p < 0.05$, $^{**}p < 0.01$.

Figure S4 | SIRT6 does not associate with NF-κB subunit p50. **(A)** Coimmunoprecipitation of SIRT6 and p65 from HEK293T cells infected with DENV (MOI = 1) for 24 h using α-p65 antibody pull-down, followed by immunoblotting using α-SIRT6 antibody. **(B)** Coimmunoprecipitation of SIRT6 and p50 from HEK293T cells infected with DENV (MOI = 1) for 24 h using α-p50 antibody pull-down, followed by immunoblotting using α-SIRT6 antibody.

REFERENCES

Bhatt, S., Gething, P. W., Brady, O. J., Messina, J. P., Farlow, A. W., Moyes, C. L., et al. (2013). The global distribution and burden of dengue. *Nature* 496, 504–507. doi: 10.1038/nature12060

Boone, D. L., Turer, E. E., Lee, E. G., Ahmad, R. C., Wheeler, M. T., Tsui, C., et al. (2004). The ubiquitin-modifying enzyme A20 is required for termination of Toll-like receptor responses. *Nat. Immunol.* 5, 1052–1060. doi: 10.1038/ni1110

Ceballos-Olvera, I., Chavez-Salinas, S., Medina, F., Ludert, J. E., and Del, A. R. (2010). JNK phosphorylation, induced during dengue virus infection, is important for viral infection and requires the presence of cholesterol. *Virology* 396, 30–36. doi: 10.1016/j.virol.2009.10.019

Chan, Y. K., and Gack, M. U. (2016). Viral evasion of intracellular DNA and RNA sensing. *Nat. Rev. Microbiol.* 14, 360–373. doi: 10.1038/nrmicro.2016.45

Chaturvedi, U. C., Agarwal, R., Elbishbishi, E. A., and Mustafa, A. S. (2000). Cytokine cascade in dengue hemorrhagic fever: implications for pathogenesis. *FEMS Immunol. Med. Microbiol.* 28, 183–188. doi: 10.1111/j.1574-695X.2000.tb01474.x

Chen, J., Zhou, Y., Mueller-Steiner, S., Chen, L. F., Kwon, H., Yi, S., et al. (2005). SIRT1 protects against microglia-dependent amyloid-beta toxicity through inhibiting NF-kappaB signaling. *J. Biol. Chem.* 280, 40364–40374. doi: 10.1074/jbc.M509329200

Chen, Y. C., and Wang, S. Y. (2002). Activation of terminally differentiated human monocytes/macrophages by dengue virus: productive infection, hierarchical production of innate cytokines and chemokines, and the synergistic effect of lipopolysaccharide. *J. Virol.* 76, 9877–9887. doi: 10.1128/JVI.76.19.9877-9887.2002

Costa, V. V., Fagundes, C. T., Souza, D. G., and Teixeira, M. M. (2013). Inflammatory and innate immune responses in dengue infection: protection versus disease induction. *Am. J. Pathol.* 182, 1950–1961. doi: 10.1016/j.ajpath.2013.02.027

Gertler, A. A., and Cohen, H. Y. (2013). SIRT6, a protein with many faces. *Biogerontology* 14, 629–639. doi: 10.1007/s10522-013-9478-8

Green, A. M., Beatty, P. R., Hadjilaou, A., and Harris, E. (2014). Innate immunity to dengue virus infection and subversion of antiviral responses. *J. Mol. Biol.* 426, 1148–1160. doi: 10.1016/j.jmb.2013.11.023

Guzman, M. G., Halstead, S. B., Artsob, H., Buchy, P., Farrar, J., Gubler, D. J., et al. (2010). Dengue: a continuing global threat. *Nat. Rev. Microbiol.* 8, S7–S16. doi: 10.1038/nrmicro2460

Haigis, M. C., and Sinclair, D. A. (2010). Mammalian sirtuins: biological insights and disease relevance. *Annu. Rev. Pathol.* 5, 253–295. doi: 10.1146/annurev.pathol.4.110807.092250

Jan, J. T., Chen, B. H., Ma, S. H., Liu, C. I., Tsai, H. P., Wu, H. C., et al. (2000). Potential dengue virus-triggered apoptotic pathway in human neuroblastoma cells: arachidonic acid, superoxide anion, and NF-kappaB are sequentially involved. *J. Virol.* 74, 8680–8691. doi: 10.1128/JVI.74.18.8680-8691.2000

Kanfi, Y., Naiman, S., Amir, G., Peshti, V., Zinman, G., Nahum, L., et al. (2012). The sirtuin SIRT6 regulates lifespan in male mice. *Nature* 483, 218–221. doi: 10.1038/nature10815

Kawahara, T. L., Michishita, E., Adler, A. S., Damian, M., Berber, E., Lin, M., et al. (2009). SIRT6 links histone H3 lysine 9 deacetylation to NF-κB-dependent gene expression and organismal life span. *Cell* 136, 62–74. doi: 10.1016/j.cell.2008.10.052

Kawai, T., and Akira, S. (2009). The roles of TLRs, RLRs and NLRs in pathogen recognition. *Int. Immunol.* 21, 317–337. doi: 10.1093/intimm/dxp017

Kim, H. S., Xiao, C., Wang, R. H., Lahusen, T., Xu, X., Vassilopoulos, A., et al. (2010). Hepatic-specific disruption of SIRT6 in mice results in fatty liver formation due to enhanced glycolysis and triglyceride synthesis. *Cell Metab.* 12, 224–236. doi: 10.1016/j.cmet.2010.06.009

Kumar, H., Kawai, T., and Akira, S. (2011). Pathogen recognition by the innate immune system. *Int. Rev. Immunol.* 30, 16–34. doi: 10.3109/08830185.2010.529976

Li, H. Y., Liu, H., Wang, C. H., Zhang, J. Y., Man, J. H., Gao, Y. F., et al. (2008). Deactivation of the kinase IKK by CUEDC2 through recruitment of the phosphatase PP1. *Nat. Immunol.* 9, 533–541. doi: 10.1038/ni.1600

Li, Q., and Verma, I. M. (2002). NF-κB regulation in the immune system. *Nat. Rev. Immunol.* 2, 725–734. doi: 10.1038/nri910

Lin, J. C., Lin, S. C., Chen, W. Y., Yen, Y. T., Lai, C. W., Tao, M. H., et al. (2014). Dengue viral protease interaction with NF-κB inhibitor α/β results in endothelial cell apoptosis and hemorrhage development. *J. Immunol.* 193, 1258–1267. doi: 10.4049/jimmunol.1302675

Lin, J., Sun, B., Jiang, C., Hong, H., and Zheng, Y. (2013). Sirt2 suppresses inflammatory responses in collagen-induced arthritis. *Biochem. Biophys. Res. Commun.* 441, 897–903. doi: 10.1016/j.bbrc.2013.10.153

Lo, S. G., Menzies, K. J., Mottis, A., Piersigilli, A., Perino, A., Yamamoto, H., et al. (2014). SIRT2 deficiency modulates macrophage polarization and susceptibility to experimental colitis. *PLoS ONE* 9:e103573. doi: 10.1371/journal.pone.0103573

Loo, Y. M., and Gale, M. J. (2011). Immune signaling by RIG-I-like receptors. *Immunity* 34, 680–692. doi: 10.1016/j.immuni.2011.05.003

Martin, J., and Hermida, L. (2016). Dengue vaccine: an update on recombinant subunit strategies. *Acta Virol.* 60, 3–14. doi: 10.4149/av_2016_01_3

Min, L., Ji, Y., Bakiri, L., Qiu, Z., Cen, J., Chen, X., et al. (2012). Liver cancer initiation is controlled by AP-1 through SIRT6-dependent inhibition of survivin. *Nat. Cell Biol.* 14, 1203–1211. doi: 10.1038/ncb2590

Mostoslavsky, R., Chua, K. F., Lombard, D. B., Pang, W. W., Fischer, M. R., Gellon, L., et al. (2006). Genomic instability and aging-like phenotype in the absence of mammalian SIRT6. *Cell* 124, 315–329. doi: 10.1016/j.cell.2005.11.044

Nasirudeen, A. M., Wong, H. H., Thien, P., Xu, S., Lam, K. P., and Liu, D. X. (2011). RIG-I, MDA5 and TLR3 synergistically play an important role in restriction of dengue virus infection. *PLoS Negl. Trop. Dis.* 5:e926. doi: 10.1371/journal.pntd.0000926

Pang, T., Cardosa, M. J., and Guzman, M. G. (2007). Of cascades and perfect storms: the immunopathogenesis of dengue haemorrhagic fever-dengue shock syndrome (DHF/DSS). *Immunol. Cell Biol.* 85, 43–45. doi: 10.1038/sj.icb.7100008

Qin, K., Han, C., Zhang, H., Li, T., Li, N., and Cao, X. (2017). NAD+ dependent deacetylase Sirtuin 5 rescues the innate inflammatory response of endotoxin tolerant macrophages by promoting acetylation of p65. *J. Autoimmun.* 81, 120–129. doi: 10.1016/j.jaut.2017.04.006

Rahman, M. M., and McFadden, G. (2011). Modulation of NF-kappaB signalling by microbial pathogens. *Nat. Rev. Microbiol.* 9, 291–306. doi: 10.1038/nrmicro2539

Rothgiesser, K. M., Erener, S., Waibel, S., Luscher, B., and Hottiger, M. O. (2010). SIRT2 regulates NF-κB dependent gene expression through deacetylation of p65 Lys310. *J. Cell Sci.* 123, 4251–4258. doi: 10.1242/jcs.073783

Soundravally, R., Hoti, S. L., Patil, S. A., Cleetus, C. C., Zachariah, B., Kadhiravan, T., et al. (2014). Association between proinflammatory cytokines and lipid peroxidation in patients with severe dengue disease around defervescence. *Int. J. Infect. Dis.* 18, 68–72. doi: 10.1016/j.ijid.2013.09.022

Tsai, Y. T., Chang, S. Y., Lee, C. N., and Kao, C. L. (2009). Human TLR3 recognizes dengue virus and modulates viral replication *in vitro*. *Cell. Microbiol.* 11, 604–615. doi: 10.1111/j.1462-5822.2008.01277.x

Van Meter, M., Kashyap, M., Rezazadeh, S., Geneva, A. J., Morello, T. D., Seluanov, A., et al. (2014). SIRT6 represses LINE1 retrotransposons by ribosylating KAP1 but this repression fails with stress and age. *Nat. Commun.* 5, 5011. doi: 10.1038/ncomms6011

Wang, W., Jin, Y., Zeng, N., Ruan, Q., and Qian, F. (2017). SOD2 facilitates the antiviral innate immune response by scavenging reactive oxygen species. *Viral Immunol.* 30, 582–589. doi: 10.1089/vim.2017.0043

Wilder-Smith, A., and Schwartz, E. (2005). Dengue in travelers. *N. Engl. J. Med.* 353, 924–932. doi: 10.1056/NEJMra041927

Xiao, C., Wang, R. H., Lahusen, T. J., Park, O., Bertola, A., Maruyama, T., et al. (2012). Progression of chronic liver inflammation and fibrosis driven by activation of c-JUN signaling in Sirt6 mutant mice. *J. Biol. Chem.* 287, 41903–41913. doi: 10.1074/jbc.M112.415182

Yeung, F., Hoberg, J. E., Ramsey, C. S., Keller, M. D., Jones, D. R., Frye, R. A., et al. (2004). Modulation of NF-κB-dependent transcription and cell survival by the SIRT1 deacetylase. *EMBO J.* 23, 2369–2380. doi: 10.1038/sj.emboj.7600244

Zhang, Y., Guo, X., Yan, W., Chen, Y., Ke, M., Cheng, C., et al. (2017). ANGPTL8 negatively regulates NF-κB activation by facilitating selective autophagic degradation of IKKgamma. *Nat. Commun.* 8, 2164. doi: 10.1038/s41467-017-02355-w

Zhu, X., Liu, Q., Wang, M., Liang, M., Yang, X., Xu, X., et al. (2011). Activation of Sirt1 by resveratrol inhibits TNF-α induced inflammation in fibroblasts. *PLoS ONE* 6:e27081. doi: 10.1371/journal.pone.0027081

Conflict of Interest Statement: The authors declare that the research was conducted in the absence of any commercial or financial relationships that could be construed as a potential conflict of interest.

frontiers in Cellular and Infection Microbiology

ORIGINAL RESEARCH
published: 08 May 2018
doi: 10.3389/fcimb.2018.00148

Complete Genome Characterization of the 2017 Dengue Outbreak in Xishuangbanna, a Border City of China, Burma and Laos

Songjiao Wen[1,2,3†], Dehong Ma[4†], Yao Lin[1,2,3], Lihua Li[4], Shan Hong[1,2,5], Xiaoman Li[6], Xiaodan Wang[1,2,3], Juemin Xi[1,2,3], Lijuan Qiu[6], Yue Pan[1,2,3], Junying Chen[1,2,3], Xiyun Shan[4] and Qiangming Sun[1,2,3*]*

[1] Institute of Medical Biology, Peking Union Medical College, Chinese Academy of Medical Sciences, Kunming, China, [2] Yunnan Key Laboratory of Vaccine Research and Development on Severe Infectious Diseases, Kunming, China, [3] Yunnan Key Laboratory of Vector-borne Infectious Disease, Kunming, China, [4] Xishuangbanna Dai Autonomous Prefecture People's Hospital, Xishuangbanna, China, [5] School of Basic Medicine, Kunming Medical University, Kunming, China, [6] Institute of Pediatric Disease Research, The Affiliated Children's Hospital of Kunming Medical University, Kunming, China

OPEN ACCESS

Edited by:
Jianming Qiu,
University of Kansas Medical Center, United States

Reviewed by:
Xiao-Guang Chen,
Southern Medical University, China
Haijian Zhou,
Chinese Center for Disease Control and Prevention, China

***Correspondence:**
Xiyun Shan
sgtrhh@126.com
Qiangming Sun
qsun@imbcams.com.cn

† These authors have contributed equally to this work.

Received: 23 December 2017
Accepted: 20 April 2018
Published: 08 May 2018

Citation:
Wen S, Ma D, Lin Y, Li L, Hong S, Li X, Wang X, Xi J, Qiu L, Pan Y, Chen J, Shan X and Sun Q (2018) Complete Genome Characterization of the 2017 Dengue Outbreak in Xishuangbanna, a Border City of China, Burma and Laos.
Front. Cell. Infect. Microbiol. 8:148.
doi: 10.3389/fcimb.2018.00148

A dengue outbreak abruptly occurred at the border of China, Myanmar, and Laos in June 2017. By November 3rd 2017, 1184 infected individuals were confirmed as NS1-positivein Xishuangbanna, a city located at the border. To verify the causative agent, complete genome information was obtained through PCR and sequencing based on the viral RNAs extracted from patient samples. Phylogenetic trees were constructed by the maximum likelihood method (MEGA 6.0). Nucleotide and amino acid substitutions were analyzed by BioEdit, followed by RNA secondary structure prediction of untranslated regions (UTRs) and protein secondary structure prediction in coding sequences (CDSs). Strains YN2, YN17741, and YN176272 were isolated from local residents. Stains MY21 and MY22 were isolated from Burmese travelers. The complete genome sequences of the five isolates were 10,735 nucleotides in length. Phylogenetic analysis classified all five isolates as genotype I of DENV-1, while isolates of local residents and Burmese travelers belonged to different branches. The three locally isolates were most similar to the Dongguan strain in 2011, and the other two isolates from Burmese travelers were most similar to the Laos strain in 2008. Twenty-four amino acid substitutions were important in eight evolutionary tree branches. Comparison with DENV-1SS revealed 658 base substitutions in the local isolates, except for two mutations exclusive to YN17741, resulting in 87 synonymous mutations. Compared with the local isolates, 52 amino acid mutations occurred in the CDS of two isolates from Burmese travelers. Comparing MY21 with MY22, 17 amino acid mutations were observed, all these mutations occurred in the CDS of non-structured proteins (two in NS1, 10 in NS2, two in NS3, three in NS5). Secondary structure prediction revealed 46 changes in the potential nucleotide and protein binding sites of the CDSs in local isolates. RNA secondary structure prediction

also showed base changes in the 3′UTR of local isolates, leading to two significant changes in the RNA secondary structure. To our knowledge, this study is the first complete genome analysis of isolates from the 2017 dengue outbreak that occurred at the border areas of China, Burma, and Laos.

Keywords: dengue outbreak, complete genome, phylogenetic trees, RNA secondary structure, protein secondary structure

INTRODUCTION

Dengue virus (DENV) is a member of the family *Flaviviridae* and genus *Flavivirus*, which has four closely related serotypes (DENV-1 to DENV-4) (Anez et al., 2017). Among these serotypes, DENV-1 has five distinct genotypes (I–V) (Sasmono et al., 2015). DENV is a single-stranded positive-sense RNA virus approximately 11 kb in length, comprising an open reading frame (ORF) and 5′ and 3′untranslated regions (UTRs). Translation of the ORF encodes three structural proteins (capsid [C], membrane [PrM/M], and envelope [E]) and seven non-structural proteins (NS1, NS2A, NS2B, NS3, NS4A, NS4B, and NS5) (Nukui et al., 2006; Parameswaran et al., 2017).

Dengue is a highly prevalent disease spread by the mosquito species *Aedes albopictus* and *Ae. aegypti* (Lustig et al., 2017). This virus is endemic to more than 100 countries worldwide, especially in cities and semi-urban areas of tropical and subtropical countries (Imrie et al., 2010; Anez et al., 2017). A recent study estimated that 390 million cases of dengue infection occur worldwide each year, representing a 30-fold increase in the past 50 years (Anez et al., 2017). Dengue virus has become a worldwide public problem (Santos-Sanz et al., 2014). The World Health Organization (WHO) classified dengue disease as dengue fever (DF), dengue hemorrhagic fever (DHF), and dengue shock syndrome (DSS) in 1997 (Narvaez et al., 2011). However, in 2008, the WHO proposed a new classification system, classifying dengue into dengue without warning signs (DWWS), dengue with warning signs (DWS), and severe dengue (SD) (Lima et al., 2013).

The first dengue outbreak in China was reported in Foshan, Guangdong Province, in 1978. Since then, dengue epidemics have been reported in Guangdong, Jiangsu, Hainan, Fujian, Guangxi, Zhejiang, and Henan (Huang et al., 2014; Liu et al., 2014; Xiong and Chen, 2014; Chen and Liu, 2015; Ren et al., 2015). In 2008, an unexpected dengue outbreak occurred in Ruili, a city on the border of China and Burma (Zhang et al., 2013). In 2013 and 2015, large-scale dengue outbreaks occurred in Xishuangbanna, Yunnan Province, a Chinese city on the border of China, Burma, and Laos. In 2014 and 2016, sporadic cases of dengue fever were also reported. In June 2017, a dengue outbreak developed abruptly at the borders of China, Burma, and Laos. By 03 November 2017, 1,184 infected individuals in Xishuangbanna had been confirmed as dengue NS1-positive.

MATERIALS AND METHODS

Ethics Statement

Each participant was informed of the purpose of the study. Written informed consent was obtained from all participants. The study protocol was approved by the Institutional Ethics Committee (Institute of Medical Biology, Chinese Academy of Medical Sciences, and Peking Union Medical College). The study was conducted in accordance with the Declaration of Helsinki for Human Research of 1974 (last modified in 2000).

Dengue Virus RNA Extraction and Identification

Serum samples were collected from DENV NS1-positive patients at Xishuangbanna Dai Autonomous Prefecture People's Hospital. The serum samples were separated from the collected blood, followed by viral RNA extraction. Viral RNA was extracted from 140 μl of dengue virus-infected serum using the QIAamp viral RNA mini kit (Qiagen, Hilden, Germany; No. 52906). The RNA was eluted in 60 μl of nuclease-free water and stored at −80°C. Viral RNA was reverse transcribed into cDNA using the PrimeScript™ II 1st Strand cDNA Synthesis Kit (Takara Bio, Shiga, Japan; No. 6210A). The cDNA was amplified by using dengue universal, 1, 2, 3, 4-type primers (Supplementary Table 1) for specific identification. The reaction conditions in each 25-μl volume were denaturation at 94°C for 5 min, followed by 35 cycles of denaturation at 94°C for 30 s, annealing at 55°C for 30 s, and elongation at 72°C for 30 s; with a final elongation step at 72°C for 7 min. The PCR products were then subjected to gel electrophoresis.

Primer Design

A total of 21 synthetic oligonucleotide primer pairs (Supplementary Table 2) were designed to amplify overlapping fragments with sizes between 200 and 900 nucleotides (nt) spanning the entire viral genome of DENV-1. All primers were selected online from Primer-BLAST at the NCBI website, based on the strain WestPac (GenBank accession no. U88535.1). All primers were synthesized and purified by Shuo GE Biotechnology Co., Ltd. (Kunming, China).

Genome Synthesis for Amplification and Sequencing

PCR was performed with the following protocol (50 μl volume): denaturation at 98°C for 2 min, followed by 40 cycles of denaturation at 98°C for 10 s, annealing at 56°C for 10 s, and elongation at 72°C for 30 s; with a final elongation step at 72°C for 1 min. The PCR products were confirmed by agarose gel electrophoresis and sequenced at Shuo GE Biotechnology Co. Ltd. Forward and reverse sequencing were done.

Analysis of Molecular Characteristics

A total of 21 nucleotide sequences were assembled using BioEdit7.1.3 (http://www.mbio.ncsu.edu/bioedit/bioedit.html).

Complete genome sequences of five DENV-1 isolates were submitted to the NCBI GenBank database with accession numbers of MF681692 (for YN2), MF683116 (YN1774), MF681693 (YN176272), MG679800 (MY21), and MG679801 (MY22). Nucleotide sequences and translated amino acid sequences were analyzed by BioEdit7.1.3. The secondary structure of isolates and reference strains CDS and UTR was predicted with the Predict Protein server (https://www.predictprotein.org/) and RNA fold web server (http://rna.tbi.univie.ac.at/cgi-bin/RNAWebSuite/RNAfold.cgi), respectively.

Phylogenetic Analysis

The sequences were assembled using BioEdit 7.1.3. Phylogenetic analysis based on the whole genome genes was conducted using the Molecular Evolutionary Genetics Analysis (MEGA) software version 6.0 (Maximum Likelihood method (ML), Bootstrap1000, Jones-Taylor-Thornton (JTT) model). The reference viral sequences used to construct the distinct phylogenetic branches were collected from the GenBank sequence database under the following country accession numbers: China (JQ048541, KP7752, KU365900, DQ193572, FJ176780, AB608788, KU094071, and KT827374), Singapore (GU370049, KJ806945, M87512, JN544411, and GQ357692), Malaysia (KX452068 and KX452065), South Korea (KP406802), Indonesia (KC762646), Japan (AB178040), Thailand (HM469966 and AF180817), Myanmar (AY726554 and AY726553), Laos (KC172829, KC172835, and KC172834), Cambodia (HQ624984), Viet Nam (JQ045660), Hawaii (EU848545, DQ672564, and DQ672562), Western Pacific (U88535), South Pacific (JQ915076), Brazil (AF226685), Haiti (KT279761), USA (FJ390379), India (KF289072), and standard strains (M29095, M93130, and AF326573).

RESULTS

Geographic Analysis of the Outbreak

Xishuangbanna has become the central area of dengue fever epidemics occurring at the borders of China, Myanmar, and Laos. The latest was an abrupt onset outbreak that began in June 2017. As of November 3rd 2017, 1,184 infected individuals had been confirmed as dengue NS1-positive as of November 3rd in Xishuangbanna, Yunnan, China. These cases included 71 cases involving non-residents of Xishuangbanna and 1,113 local cases.

Base Sequence Analysis of the Complete Genome Sequences of Five DENV Isolates

The complete genome sequences of five isolates were obtained by amplifying 21 overlapping fragments. Two of the five complete genome sequences were obtained from travelers from Burma. The remaining three genome sequences were obtained from local residents. Sequencing and clustering, All isolates were 10,735 nt in length. The 5′ and3′UTRs of the five isolates were 94 and 465 nt in length, respectively. The ORF of all five isolates was located between nt 95 and 10270, and encoded 3,392 amino acids.

Phylogenetic Analysis

The whole genome of the five isolates was aligned and compared with 40 sequences from standard strains of four serotypes and some typical DENV-1 strains of various geographical origins obtained from the NCBI GenBank database. The phylogenetic analysis was constructed with the ML method. The five isolates belonged to DENV-1 and were further classified as genotype. Three local isolates were located in one cluster of the ML tree, with the closest relationship to the Dongguan strain of China (2011, JQ048541). Additionally, three isolates were also closely related to the following strains: China (Hubei 2014 KP772252, Taiwan 2014 KU365900, and Fujian 2005 DQ193572), Singapore (2008, GU370049), and Malaysia (2014 KX452068 and KX452065). However, two isolates obtained from Burmese travelers were located in another cluster of the ML tree and were most similar to the Laos strain in 2008 (KC172834). DENV-3 (M93130), DENV-4 (AF326573), and DENV-2 (M29095) were outgroups (**Figure 1A**).

We further analyzed the relationship between the evolutionary tree branching and amino acid substitution of genotype ? of DENV-1. A total of 24 amino acid substitutions were detected that had important roles in eight evolutionary treebranches. Particularly, A1843S, I2392V, D2921E, S3372L, and E3386D resulted in branch 1; N75S, K1345R, R2871K, K3044R, V3280I, and E3326G resulted in branch 2; I781V, K945R, M1172I, C1184S, V2264D, A2738V, and Y3142H resulted in branch 3; and S3059A, I1937V/A2863T, N90S, H2620Y, and I2628M resulted in branches 4–8, respectively (**Figures 1B**, **2**).

Base Substitution and Amino Acid Mutation Analysis of Coding DNA Sequences (CDSS) From the Isolated Strains

Base substitution and amino acid mutation analyses were performed by comparison with the DENV-1 standard strain (DENV-1SS) (Hawaii, 1944, NO. EU848545). The results revealed 187 base substitutions in the structural protein (C/PrM/E) in three local isolates, of which 155 substitutions were non-synonymous. These were 471 base substitutionsin non-structural protein regions in the three local isolates, leading to 416 non-synonymous mutations (Supplementary Figure 1). The genome sequence of the three local isolates was almost the same, except for nt 3786(C→T) and 10630(A→G) in isolate YN17741. All the isolates harbored a base deletion (T) at nt 79 of the 5′UTR, and a few base substitutions occurred in the 3′UTRs in all the isolates.

The two isolates obtained from Burmese travelers were different from the three local isolates. Compared with local isolates, a total of 52 amino acid mutations occurred in the CDS of the two isolates (MY21 and 22) obtained from Burmese travelers. There were also differences between MY21 and 22. Comparison of MY21with MY22 revealed 17 amino acid mutations, which all occurred in CDS of non-structural proteins. Of these, two amino acid mutations (R874Q, D995V) occurred in the non-structural protein NS1, three amino acid

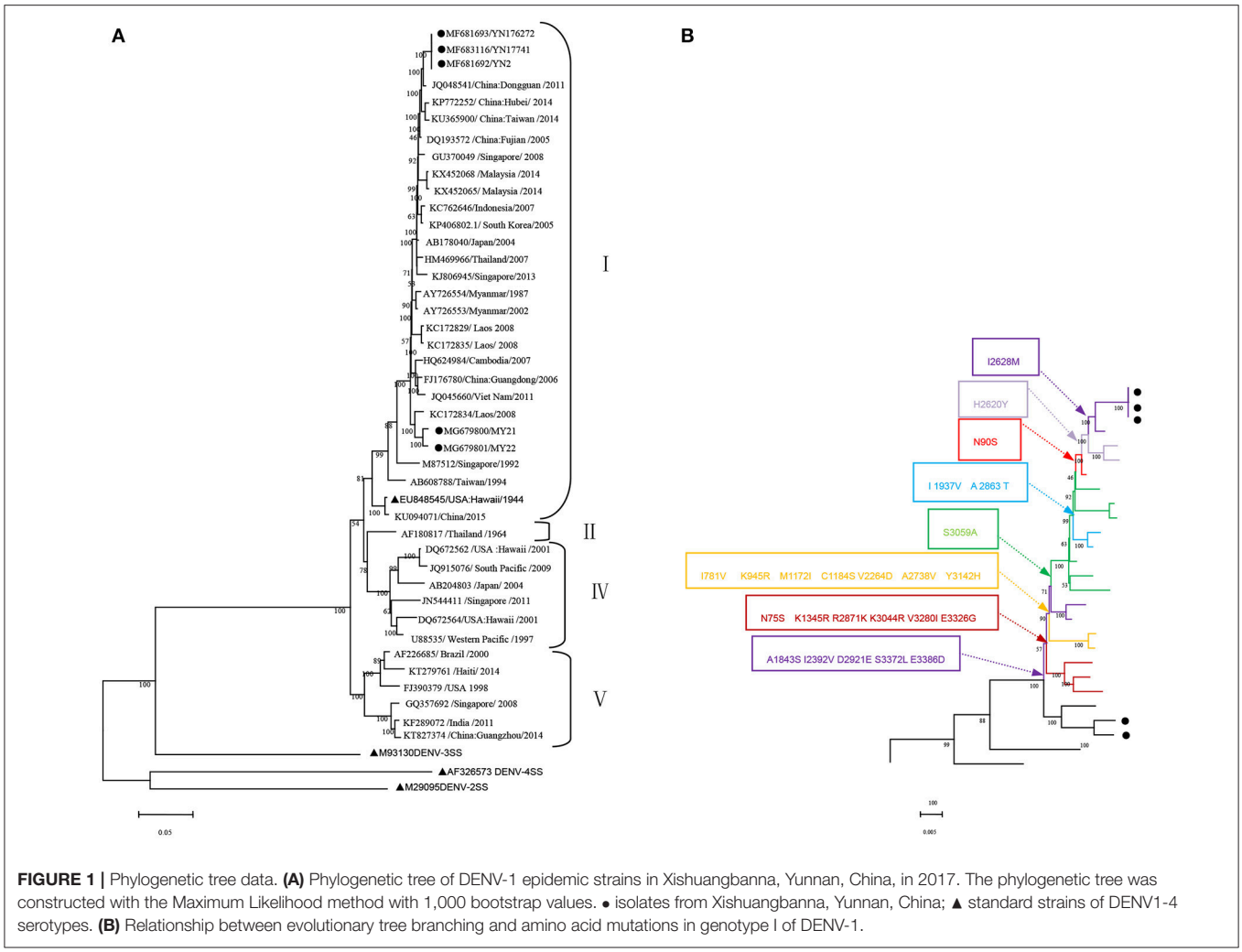

FIGURE 1 | Phylogenetic tree data. **(A)** Phylogenetic tree of DENV-1 epidemic strains in Xishuangbanna, Yunnan, China, in 2017. The phylogenetic tree was constructed with the Maximum Likelihood method with 1,000 bootstrap values. ● isolates from Xishuangbanna, Yunnan, China; ▲ standard strains of DENV1-4 serotypes. **(B)** Relationship between evolutionary tree branching and amino acid mutations in genotype I of DENV-1.

mutations (A1317T, V1331L, G1340K) occurred in the non-structural protein NS2A, seven amino acid mutations (D1350N, G1355A, G1364S, A1365S, E1368K, G1369N, G1374A) occurred in the non-structural protein NS2B, two amino acid mutations (D1960S, I2096V) occurred in the non-structural protein NS3, and three amino acid mutations (H2778Y, S3122L, S3239G) occurred in the non-structural protein NS5 (**Figure 3**).

Compared to the closest Dongguan strain (China 2011, JQ048541), a total of 14 amino acid mutations occurred in the CDS of the local isolates (**Figure 4**). Three mutations leading to changes in amino acid polarity occurred in non-structural protein regions. At amino acid 1031in L1031Y, the amino acid changed from a non-polar to a polar residue, while the change was from polar to non-polar residues in positions S1183L and V1615L).

Prediction of the RNA Secondary Structure Based on the Untranslated Regions of the Standard and Local Isolated Strains

All sequences wereconserved in the UTRs. Compared to the standard strain, only one base deletion occurred, and thus the predicted RNA structure of the 5′UTR was only marginally changed (Supplementary Figures 2A,B). Comparison with the 3′UTR of the standard strains revealed that all local isolates had eight substitutions (nt 10273 [A→G], nt 10276 [T→C], nt 10286 [C→T], nt 10293 [C→T], nt 10408 [G→A], nt 10467 [C→T], nt 10536 [A→G], nt 10621 [C→T]) and 3 inserts (nt 10455 [G], nt 10479 [A], and nt 10730 [C]). In addition to these mutations, an additional mutation at nt 10630 [A→G] was observed in YN17741. RNA secondary structure prediction results showed that some base changes in the 3′UTR of the local isolates lead to two significant changes in the RNA secondary structure. In contrast to the long interior loop in the standard strain, a 47 bp stem downstream of nt 10277 was formed in the isolates. Long stem and loop structures were formed before nt 10734 in the standard strain, while the stem and loops were shorter in the isolates before nt 10719 (Supplementary Figures 2C,D).

Potential Secondary Structure of the CDS Regions

The potential secondary structures of the CDS regions of the local isolates were predicted and compared with that of the standard strain. In structural proteins C/prM/E, there were 13 changes inputative nucleotide/protein binding sites among the 775 amino

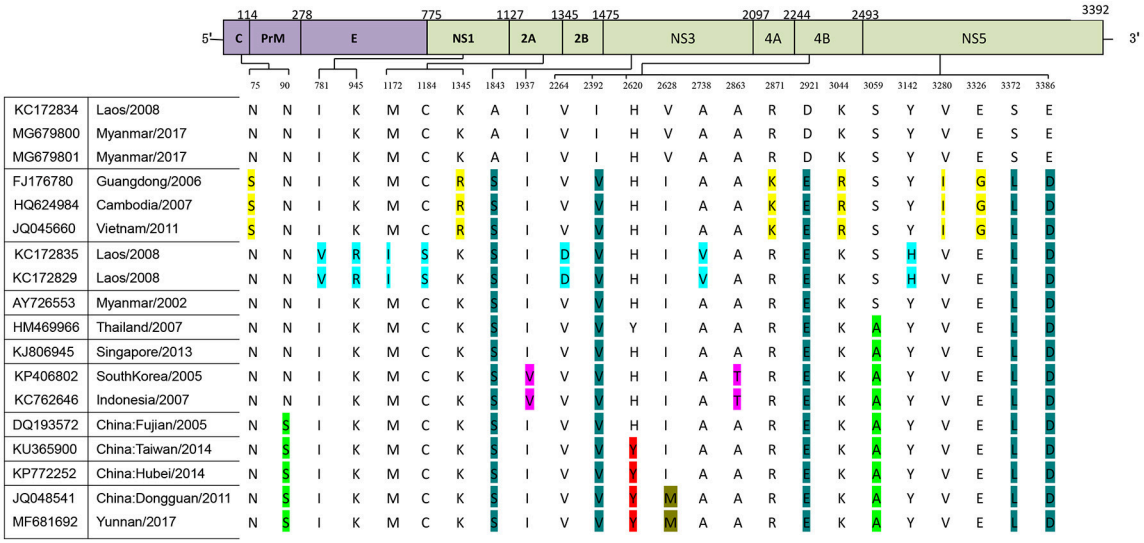

FIGURE 2 | Identification of variations among genotype I of DENV-1. Variations are presented in accordance with their location in the viral genome. The various colors indicate the different variations described in **Figure 1B**.

acids. Among these, six putative protein-binding sites (sites 8, 68, 87, 161, 335, and 436) were detected only in the isolates. However, five potential protein-binding sites (sites 1, 7, 21, 86, and 429) and two nt-binding sites (sites 6 and 7) were lost compared to the standard strain. Approximately eight distinct changes appeared in the helix and strand regions. Two distinct changes were found in the exposed and buried regions and the disordered regions. The helical transmembrane regions in the local isolates were highly consistent with those in the standard strain (Supplementary Figure 3). In the non-structural protein NS1, comparison with the standard strain revealed only one potential nucleotidesite (site 118) and protein binding site (site 99) in the isolates. Approximately four distinct changes were found in the helix and strand regions (Supplementary Figure 3B). In the non-structural protein NS2A, three changes were observed in putative protein binding sites among the 218 amino acids. Among these changes, four potential protein-binding sites were increased, and two other sites (118 and 180) were lost in the isolated strains (Supplementary Figure 3C). In the non-structural protein NS2B, comparison with reference strain revealed only one change (site 49) in the putative protein binding sites of the isolates (Supplementary Figure 3D). In the non-structural protein NS3, 15 changes were observed in the putative nucleotide and protein binding sites among the 619 amino acids. Among these changes, five potential protein-binding sites (sites 132, 134, 143, 338, and 471) were increased in the isolates, while 10 putative protein-binding sites (sites 107, 161, 172, 304, 461, 481, 483, 531, 539, and 593) were lost compared with the standard strain (Supplementary Figure 3E). In the non-structural protein NS4A, only two distinct changes were found in the exposed and buried regions and disordered regions (Supplementary Figure 3F). In the non-structural protein NS4B, the isolates lost potential nucleotide (site 249) and protein binding sites (site 243) compared to the standard strain (Supplementary Figure 3G). In the non-structural protein NS5, 11 changes were detected in putative nucleotide and protein binding sites among the 899 amino acids. Four putative protein-binding sites (sites 51, 289, 558, and 691) and two nucleotide-binding sites (sites 598, 853) were increased in the isolated strains, while five putative protein-binding sites (sites 350, 465, 499, 502, and 895) were lost. In addition, three distinct changes were found in the disordered regions (Supplementary Figure 3H).

DISCUSSION

Yunnan Province is located on the southwest border of China. The northwest corner is closely attached to the Tibet autonomous region. The west borders Myanmar and the south is connected with Laos and Vietnam. Yunnan is located in the vast expanse of the Asian continent, south of the Indian Ocean and the Pacific Ocean. The region is influenced by monsoons that originate to the southeast and southwest, and also by the Tibetan plateau area. These climatic influences have produced a complex and diverse natural geographical environment. The region is a popular touristic destination. These and other factors have made this area important for the prevention and control of dengue fever in Asia.

A 2006 study revealed the existence of DENV infection in the Dushan and Xingyi areas of the Yunnan-Guizhou Plateau, China (Liu et al., 2006). In 2008, 48 imported cases and one native case were reported in Yunnan Ruili. This was the first report of a dengue outbreak in Yunnan. Of the 49 confirmed cases, 18 involved people from Mujie City, Myanmar, 30 cases involved Chinese residents who had returned to Myanmar from elsewhere, and one native case. This outbreak was caused by DENV-1 and DENV-3 (Zhang et al., 2013). A DENV-2 isolate was obtained from a patient with fever who returned from Laos in 2009 (Guo et al., 2013). The first aboriginal outbreak occurred in

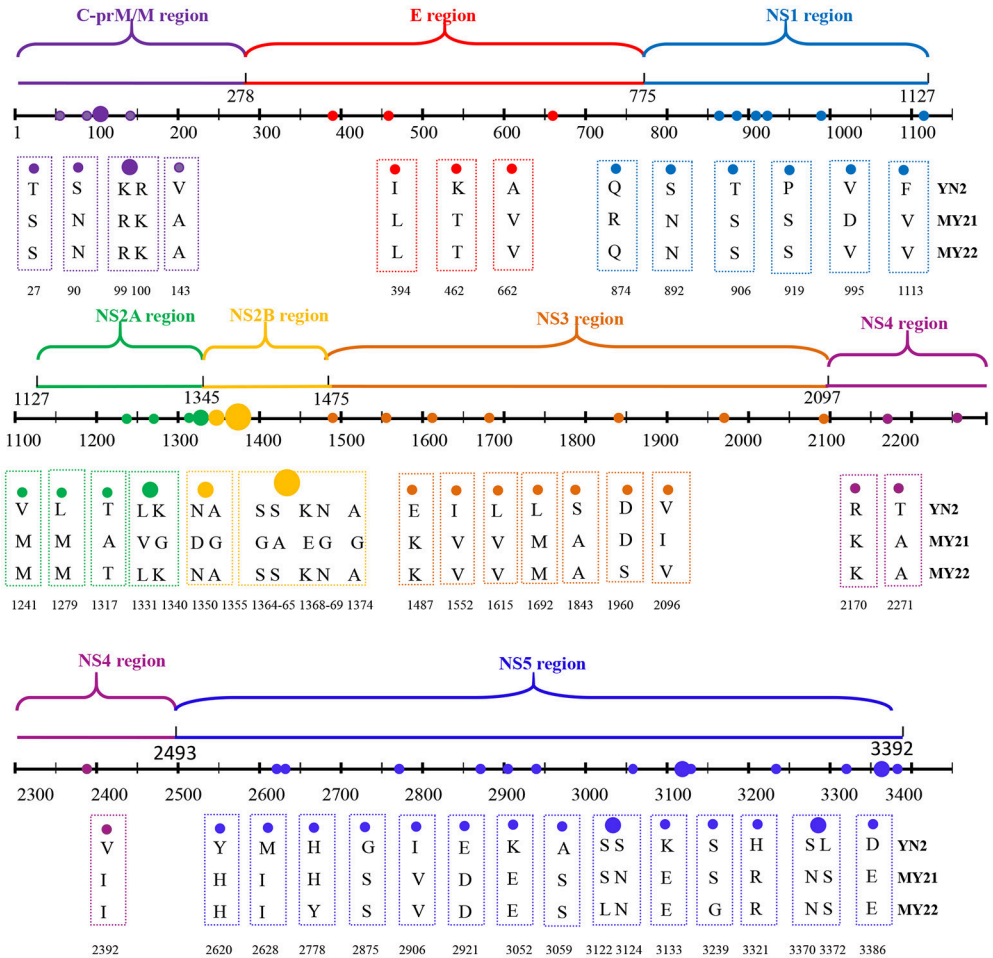

FIGURE 3 | Amino acid mutations between CDS of locally isolated strains and two strains isolated from Myanmar (2017).

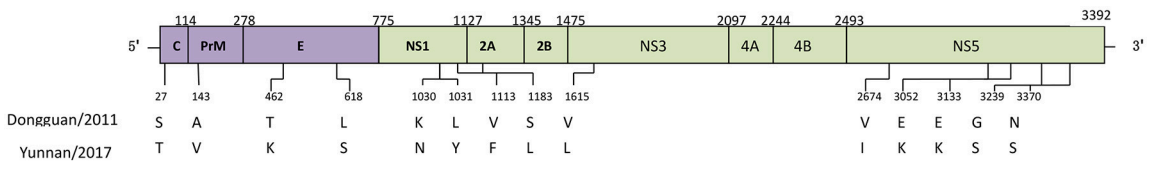

FIGURE 4 | Amino acid mutations between CDS of Dongguan strain (2011) and Yunnan strains (2017).

Xishuangbanna Dai Autonomous Prefecture, Yunnan Province, China, in 2013. This outbreak was caused by DENV-3 and 1,331 cases were confirmed. A mixed outbreak of DENV-1 and DENV-2 appeared in Ruili in Dehong prefecture, with 246 dengue fever cases recorded (Zhang et al., 2014; Guo et al., 2015; Wang et al., 2017). From June to December of 2014, a total of 292 cases of dengue fever were diagnosed in Ruili City. These included 139 local cases and 153 imported cases caused by DENV-1, DENV-2, and DENV-4. In 2015, 240 DENV-1 cases were reported in Lincang, and 1,067 DENV-2 cases were reported in Xishuangbanna (Guo et al., 2016; Zhao et al., 2016). In 2016, 25 isolates were obtained from the sera of dengue fever patients. These included 15 local cases and 10 imported cases from Burma. These cases were caused by DENV-1, DENV-2, DENV-3, and DENV-4. A dengue fever outbreak caused by DENV-1occurred in Xishuangbanna, Yunnan Province, in 2017. This was the first known outbreak due to DENV-1in this area. According to government statistics, as of 03 November 2017, a total of 1,184 infected cases have been verified, including 71 imported cases and 1,113 local cases. Interestingly, large-scale dengue outbreak shave occurred in Xishuangbanna every 2 years since 2013, involving different serum types of DENV.

In the present study, viral RNA was extracted from the sera of patients from China and Myanmar, followed by amplification of overlapping fragments to obtain five complete genomes (YN2, YN17741, YN176272, MY21, and MY22). Two isolates (MY21 and MY22) were obtained from Burmese travelers. The five isolates were 10,735 bp in length. YN2 and YN176272 displayed the same genome sequence. Compared with YN2, YN17741 possessed has two base changes at nt 3786 (C→T) and nt 10630 (A→G). These base changes were non-synonymous. However, the two isolates from Burmese travelers were different from three isolated strains from local residents. Compared with locally isolated strains, a total of 52 amino acid mutations occurred in the CDS of the two isolates from Burmese travelers. These two isolates differed from each other. Comparison of MY21 and MY22 revealed 17 amino acid mutations. All occurred in CDS of non-structured proteins. These results indicate that the 2017 dengue outbreak in Xishuangbanna was not caused by the imported DENV-1, but rather was a local outbreak. The 2017 dengue outbreak in the border areas around Xishuangbanna was not caused by only one DENV-1 source strain, but belong to a single genotype.

The 5′ and 3′ UTRs of dengue virus play an important role in the genome replication of RNA (Wei et al., 2008; Vashist et al., 2009). According to different conservative levels, the 3′ UTR is divided into three regions: (1) a variable area directly following the ORF; (2) a highly conserved cyclization sequence motif (CS1) and stable stem-loop structure; and (3) the region between the variable and 3-terminal regions, which have modest conservative levels and contain several hairpin motifs (Bryant et al., 2005). The 3′UTR is dispensable for the replication of dengue type 1 virus *in vitro* (Tajima et al., 2006). The variable area in the 3' UTR of Japanese encephalitis virus (JEV) reportedly did not affect its growth *in vitro* or its pathogenicity in mice (Kato et al., 2012). However, a previous report showed that the variable area of DENV-2 can enhance viral replication in baby hamster kidney cells, although this area is dispensable in mosquito cells (Alvarez et al., 2005). Another study showed that VR mutations of DENV-1 might not affect the translation process (Tajima et al., 2007). In the present study, mutations were observed in the 3′UTRs of the isolates compared to those of the reference strains. Nucleotide changes in 3′UTRs of the isolates lead to two significant changes in the RNA secondary structure. In contrast to the long interior loop in the standard strain, a 47-bp stem downstream of nt 10277 was formed in the isolated strains. Long stem and loop structures were formed before nt 10734 in the standard strain, while the stem and loops were shorter in the isolated strains before nt 10719, especially in the variable area. The effect of these changes on dengue type 1 replication needs further clarification.

In recent years, several studies reported that the mutation of amino acids in some special sites has a significant impact on the virulence, replication, and infectivity of flaviviruses. An alanine-to-valine amino acid substitution at residue 188 of the NS1 protein promotes the infectivity of Zika virus (ZIKV) Asian genotype in mosquitoes (Delatorre et al., 2017; Liu et al., 2017). A single mutation (S139N) in the PrM protein of Zika virus promotes fetal microcephaly (Yuan et al., 2017). The single mutation G66A in the NS2A gene of Japanese encephalitis-live vaccine virus reduces neurovirulence and neuroinvasiveness in mice(Ye et al., 2012). The mutation of putative N-glycosylation sites (Asn-58 and Asn-62) affects the biological function of DENV NS4B in the viral replication complex (Naik and Wu, 2015). A DENV-2 vaccine strain (PDK53) has three mutations that are critical for the attenuated state of PDK53 (Butrapet et al., 2000). The present results indicate that the region of the viral structural protein is relatively conserved, with less amino acid substitutions, with mutations being more prevalent in the non-structural protein regions in genotype I of DENV-1. Based on phylogenetic analysis, we identified a total of 24 amino acid substitutions that play an important role in evolutionary tree branching. These substitutions included two important amino acid substitutions (N90S and S3059A) in Chinese strains (DQ193572, KU365900, KP772252, JQ048541, and MF681692), and an amino acid substitution (I2628M) in the local isolated strains and the Dongguan strain of China (JQ048541). The effects of these amino acid substitutions on virulence, replication, infection, and other functions of the virus are unclear.

In 2017, there have been extensive outbreaks of dengue fever in many areas including Yunnan, Guangdong, Zhejiang, Shandong, Taiwan, Xianggang, Macao, and other areas (Chen et al., 2017). Xishuangbanna is geographically near Myanmar, Laos, and Vietnam. The present study is the first report on the complete genome characterization of the 2017 Xishuangbanna DENV outbreak. The present study should serve as a reference to follow-up studies of DENV outbreaks in Southeast Asia in 2017. The findings are a reference for future research on the virulence, replication, infection, pathogenicity, and vaccine development of DENV.

AUTHOR CONTRIBUTIONS

XS and QS contributed to the design of the study. SW and DM were involved in data acquisition and analysis. YL, LL, SH, and XL provided software technology support. XW, JX, YP, LQ, and JC provided experiment technology support. All the authors agree to the final version of the submission.

FUNDING

This research was supported by the Foundation of the CAMS Initiative for Innovative Medicine (CAMS-I2M) (grant no. 2016-I2M-1-19), the Natural Science Foundation of Yunnan Province (2016FA029), Yunnan Medical Discipline Leader Project (D-201605), Kunming Science and Technology Innovation Team Project (grant no. 2015-1-R-00956), the National Twelfth Five Year major new drug discovery technology major project (grant no. 2012ZX09104-302), the Jointly Supported Foundation of the National Project in Yunnan Province (2013GA018), and the National Natural Science Foundation of China (81171946).

ACKNOWLEDGMENTS

We would like to thank Dr. Penghua Wang of Department of Microbiology and Immunology, School of Medicine, New York Medical College for proofreading and reviewing our manuscript.

SUPPLEMENTARY MATERIAL

The Supplementary Material for this article can be found online at: https://www.frontiersin.org/articles/10.3389/fcimb.2018.00148/full#supplementary-material

REFERENCES

Alvarez, D. E., De Lella Ezcurra, A. L., Fucito, S., and Gamarnik, A. V. (2005). Role of RNA structures present at the 3'UTR of dengue virus on translation, RNA synthesis, and viral replication. *Virology* 339, 200–212. doi: 10.1016/j.virol.2005.06.009

Añez, G., Volkova, E., Jiang, Z., Heisey, D. A. R., Chancey, C., and Fares, R. C. G. (2017). Collaborative study to establish World Health Organization international reference reagents for dengue virus Types 1 to 4 RNA for use in nucleic acid testing. *Transfusion* 57, 1977–1987. doi: 10.1111/trf.14130

Bryant, J. E., Vasconcelos, P. F., Rijnbrand, R. C., Mutebi, J. P., Higgs, S., and Barrett, A. D. (2005). Size heterogeneity in the 3' noncoding region of South American isolates of yellow fever virus. *J. Virol.* 79, 3807–3821. doi: 10.1128/JVI.79.6.3807-3821.2005

Butrapet, S., Huang, C. Y., Pierro, D. J., Bhamarapravati, N., Gubler, D. J., and Kinney, R. M. (2000). Attenuation markers of a candidate dengue type 2 vaccine virus, strain 16681 (PDK-53), are defined by mutations in the 5' noncoding region and nonstructural proteins 1 and 3. *J. Virol.* 74, 3011–3019. doi: 10.1128/JVI.74.7.3011-3019.2000

Chen, B., and Liu, Q. (2015). Dengue fever in China. *Lancet* 385, 1621–1622. doi: 10.1016/S0140-6736(15)60793-0

Chen, Q., Song, W., Mou, D., Li, Y., Yin, W., Li, Z., et al. (2017). Analysis on epidemiological characteristics of dengue fever in China, as of 31th August,2017. *Dis. surveill.* 10, 801–804. doi: 10.3784/j.issn.1003-9961.2017.10/11.005

Delatorre, E., Mir, D., and Bello, G. (2017). Tracing the origin of the NS1 A188V substitution responsible for recent enhancement of Zika virus Asian genotype infectivity. *Mem. Inst. Oswaldo Cruz* 112, 793–795. doi: 10.1590/0074-02760170299

Guo, X., Yang, H., Wu, C., Jiang, J., Fan, J., Li, H., et al. (2015). Molecular characterization and viral origin of the first dengue outbreak in Xishuangbanna, Yunnan Province, China, 2013. *Am. J. Trop. Med. Hyg.* 93, 390–393. doi: 10.4269/ajtmh.14-0044

Guo, X., Yang, M., Jiang, J., Li, H., Zhu, C., Gui, Q., et al. (2016). [Molecular characteristics of dengue virus outbreak in China-Myanmar border region, Yunnan province, 2015]. *Zhonghua Liu Xing Bing Xue Za Zhi* 37, 398–401. doi: 10.3760/cma.j.issn.0254-6450.2016.03.022

Guo, X., Zhao, Q., Wu, C., Zuo, S., Zhang, X., Jia, N., et al. (2013). First isolation of dengue virus from Lao PDR in a Chinese traveler. *Virol. J.* 10:70. doi: 10.1186/1743-422X-10-70

Huang, X. Y., Ma, H. X., Wang, H. F., Du, Y. H., Su, J., Li, X. L., et al. (2014). Outbreak of dengue Fever in central China, 2013. *Biomed. Environ. Sci.* 27, 894–897. doi: 10.1186/s12916-015-0336-1

Imrie, A., Roche, C., Zhao, Z., Bennett, S., Laille, M., Effler, P., et al. (2010). Homology of complete genome sequences for dengue virus type-1, from dengue-fever- and dengue-haemorrhagic-fever-associated epidemics in Hawaii and French Polynesia. *Ann. Trop. Med. Parasitol.* 104, 225–235. doi: 10.1179/136485910X12647085215570

Kato, F., Kotaki, A., Yamaguchi, Y., Shiba, H., Hosono, K., Harada, S., et al. (2012). Identification and characterization of the short variable region of the Japanese encephalitis virus 3' NTR. *Virus Genes* 44, 191–197. doi: 10.1007/s11262-011-0685-6

Lima, F. R., Croda, M. G., Muniz, D. A., Gomes, I. T., Soares, K. R., Cardoso, M. R., et al. (2013). Evaluation of the traditional and revised World Health Organization classifications of dengue cases in Brazil. *Clinics* 68, 1299–1304. doi: 10.6061/clinics/2013(10)02

Liu, C., Liu, Q., Lin, H., Xin, B., and Nie, J. (2014). Spatial analysis of dengue fever in Guangdong Province, China, 2001-2006. *Asia Pac. J. Public Health* 26, 58–66. doi: 10.1177/1010539512472356

Liu, W., Zuo, L., and Zhou, Y. (2006). The distribution of DEN infected people in Dushan and Xingyi area of Yunnan-Guizhou Plateau, China. *Cell. Mol. Immunol.* 3, 473–476.

Liu, Y., Liu, J., Du, S., Shan, C., Nie, K., Zhang, R., et al. (2017). Evolutionary enhancement of Zika virus infectivity in Aedes aegypti mosquitoes. *Nature* 545, 482–486. doi: 10.1038/nature22365

Lustig, Y., Wolf, D., Halutz, O., and Schwartz, E. (2017). An outbreak of dengue virus (DENV) type 2 Cosmopolitan genotype in Israeli travellers returning from the Seychelles, April 2017. *Euro Surveill.* 22:30563. doi: 10.2807/1560-7917.ES.2017.22.26.30563

Naik, N. G., and Wu, H. N. (2015). Mutation of putative N-glycosylation sites on dengue virus NS4B decreases RNA replication. *J. Virol.* 89, 6746–6760. doi: 10.1128/JVI.00423-15

Narvaez, F., Gutierrez, G., Pérez, M. A., Elizondo, D., Nuñez, A., Balmaseda, A., et al. (2011). Evaluation of the traditional and revised WHO classifications of Dengue disease severity. *PLoS Negl. Trop. Dis.* 5:e1397. doi: 10.1371/journal.pntd.0001397

Nukui, Y., Tajima, S., Kotaki, A., Ito, M., Takasaki, T., Koike, K., et al. (2006). Novel dengue virus type 1 from travelers to Yap State, Micronesia. *Emerging Infect. Dis.* 12, 343–346. doi: 10.3201/eid1202.050733

Parameswaran, P., Wang, C., Trivedi, S. B., Eswarappa, M., Montoya, M., Balmaseda, A., et al. (2017). Intrahost selection pressures drive rapid dengue virus microevolution in acute human infections. *Cell Host Microbe* 22, 400–410.e405. doi: 10.1016/j.chom.2017.08.003

Ren, H., Ning, W., Lu, L., Zhuang, D., and Liu, Q. (2015). Characterization of dengue epidemics in mainland China over the past decade. *J. Infect. Dev. Ctries.* 9, 970–976. doi: 10.3855/jidc.5998

Santos-Sanz, S., Sierra-Moros, M. J., Oliva-Iñiguez, L., Sanchez-Gómez, A., Suarez-Rodriguez, B., Simón-Soria, F., et al. (2014). [Possible introduction and autochthonous transmission of dengue virus in Spain]. *Rev. Esp. Salud Publica* 88, 555–567. doi: 10.4321/S1135-572720140005 00002

Sasmono, R. T., Wahid, I., Trimarsanto, H., Yohan, B., Wahyuni, S., Hertanto, M., et al. (2015). Genomic analysis and growth characteristic of dengue viruses from Makassar, Indonesia. *Infect. Genet. Evol.* 32, 165–177. doi: 10.1016/j.meegid.2015.03.006

Tajima, S., Nukui, Y., Ito, M., Takasaki, T., and Kurane, I. (2006). Nineteen nucleotides in the variable region of 3' non-translated region are dispensable for the replication of dengue type 1 virus *in vitro*. *Virus Res.* 116, 38–44. doi: 10.1016/j.virusres.2005.08.015

Tajima, S., Nukui, Y., Takasaki, T., and Kurane, I. (2007). Characterization of the variable region in the 3' non-translated region of dengue type 1 virus. *J. Gen. Virol.* 88, 2214–2222. doi: 10.1099/vir.0.82661-0

Vashist, S., Anantpadma, M., Sharma, H., and Vrati, S. (2009). La protein binds the predicted loop structures in the 3' non-coding region of Japanese encephalitis virus genome: role in virus replication. *J. Gen. Virol.* 90, 1343–1352. doi: 10.1099/vir.0.010850-0

Wang, X., Ma, D., Huang, X., Li, L., Li, D., Zhao, Y., et al. (2017). Complete genome analysis of dengue virus type 3 isolated from the 2013 dengue outbreak in Yunnan, China. *Virus Res.* 238, 164–170. doi: 10.1016/j.virusres.2017.06.015

Wei, Y., Jiang, T., Li, X., Zhao, H., Liu, Z., Deng, Y., et al. (2008). [Effects of RNA elements within 3'untranslated region on dengue virus translation]. *Wei Sheng Wu Xue Bao* 48, 583–588. doi: 10.3321/j.issn:0001-6209.2008.05.004

Xiong, Y., and Chen, Q. (2014). [Epidemiology of dengue fever in China since 1978]. *Nan Fang Yi Ke Da Xue Xue Bao* 34, 1822–1825. doi: 10.3969/j.issn.1673-4254.2014.12.24

Ye, Q., Li, X. F., Zhao, H., Li, S. H., Deng, Y. Q., Cao, R. Y., et al. (2012). A single nucleotide mutation in NS2A of Japanese encephalitis-live vaccine virus

(SA14-14-2) ablates NS1' formation and contributes to attenuation. *J. Gen. Virol.* 93, 1959–1964. doi: 10.1099/vir.0.043844-0

Yuan, L., Huang, X. Y., Liu, Z. Y., Zhang, F., Zhu, X. L., Yu, J. Y., et al. (2017). A single mutation in the prM protein of Zika virus contributes to fetal microcephaly. *Science* 358, 933–936. doi: 10.1126/science.aam7120

Zhang, F. C., Zhao, H., Li, L. H., Jiang, T., Hong, W. X., Wang, J., et al. (2014). Severe dengue outbreak in Yunnan, China, 2013. *Int. J. Infect. Dis.* 27, 4–6. doi: 10.1016/j.ijid.2014.03.1392

Zhang, H. L., Fu, S. H., Deng, Z., Yuan, J., Jiang, H. Y., Li, M. H., et al. (2013). [An outbreak of imported dengue fever from Myanmar to the border of China, with its viral molecular epidemiological features]. *Zhonghua Liu Xing Bing Xue Za Zhi* 34, 428–432. doi: 10.3760/cma.j.issn.02546450.2013.05.004

Zhao, Y., Li, L., Ma, D., Luo, J., Ma, Z., Wang, X., et al. (2016). Molecular characterization and viral origin of the 2015 dengue outbreak in Xishuangbanna, Yunnan, China. *Sci. Rep.* 6:34444. doi: 10.1038/srep34444

Conflict of Interest Statement: The authors declare that the research was conducted in the absence of any commercial or financial relationships that could be construed as a potential conflict of interest.

frontiers in Cellular and Infection Microbiology

ORIGINAL RESEARCH
published: 27 June 2018
doi: 10.3389/fcimb.2018.00219

Molecular Characterization of Dengue Virus Serotype 2 Cosmospolitan Genotype From 2015 Dengue Outbreak in Yunnan, China

Liming Jiang[1,2,3], Dehong Ma[4], Chao Ye[1,2,3,5], Lihua Li[4], Xiaoman Li[6], Jiajia Yang[1,2,3], Yujiao Zhao[1,2,3], Juemin Xi[1,2,3], Xiaodan Wang[1,2,3], Junying Chen[1,2,3], Yue Pan[1,2,3], Xiyun Shan[4] and Qiangming Sun[1,2,3]**

[1] Institute of Medical Biology, Chinese Academy of Medical Sciences and Peking Union Medical College, Kunming, China, [2] Yunnan Key Laboratory of Vaccine Research and Development on Severe Infectious Diseases, Kunming, China, [3] Yunnan Key Laboratory of Vector-borne Infectious Disease, Kunming, China, [4] Xishuangbanna Dai Autonomous Prefecture People's Hospital, Xishuangbanna, China, [5] School of Basic Medicine, Kunming Medical University, Kunming, China, [6] The Affiliated Children's Hospital of Kunming Medical University, Kunming, China

In 2015, a dengue outbreak with 1,067 reported cases occurred in Xishuangbanna, a city in China that borders Burma and Laos. To characterize the virus, the complete genome sequence was obtained and phylogenetic, mutation, substitution and recombinant analyses were performed. DENV-NS1 positive serum samples were collected from dengue fever patients, and complete genome sequences were obtained through RT-qPCR from these serum samples. Phylogenetic trees were then constructed by maximum likelihood phylogeny test (MEGA7.0), followed by analysis of nucleotide mutation and amino acid substitution. The recombination events among DENVs were also analyzed by RDP4 package. The diversity analysis of secondary structure for translated viral proteins was also performed. The complete genome sequences of four amplified viruses (YNXJ10, YNXJ12, YNXJ13, and YNXJ16) were 10,742, 10,742, 10,741, and 10,734 nucleotides in length, and phylogenetic analysis classified the viruses as cosmopolitan genotype of DENV-2. All viruses were close to DENV Singapore 2013 (KX380828.1) and the DENV China 2013 (KF479233.1). In comparison to DENV-2SS (M29095), the total numbers of base substitutions were 712 nt (YNXJ10), 809 nt (YNXJ12), 772 nt (YNXJ13), and 841 nt (YNXJ16), resulting in 109, 171, 130, and 180 amino acid substitutions in translated regions, respectively. In addition, compared with KX380828.1, there were 44, 105, 64, and 116 amino acid substitutions in translated regions, respectively. The highest mutation rate occurred in the prM region, and the lowest mutation rate occurred in the NS4B region. Most of the recombination events occurred in the prM, E and NS2B/3 regions, which corresponded with the mutation frequency of the related portion. Secondary structure prediction within the 3,391 amino acids of DENV structural proteins showed there were 7 new possible nucleotide-binding sites and 6 lost sites compared to DENV-2SS. In addition, 41 distinct amino acid

OPEN ACCESS

Edited by:
Rachel L. Roper, The Brody School of Medicine at East Carolina University, United States

Reviewed by:
Tatsuo Shioda, Osaka University, Japan
Erna Geessien Kroon, Universidade Federal de Minas Gerais, Brazil

***Correspondence:**
Qiangming Sun
qsun@imbcams.com.cn
Xiyun Shan
sgtrhh@126.com

Received: 28 December 2017
Accepted: 08 June 2018
Published: 27 June 2018

Citation:
Jiang L, Ma D, Ye C, Li L, Li X, Yang J, Zhao Y, Xi J, Wang X, Chen J, Pan Y, Shan X and Sun Q (2018) Molecular Characterization of Dengue Virus Serotype 2 Cosmospolitan Genotype From 2015 Dengue Outbreak in Yunnan, China. Front. Cell. Infect. Microbiol. 8:219. doi: 10.3389/fcimb.2018.00219

changes were found in the helix regions, although the distribution of the exposed and buried regions changed only slightly. Our findings may help to understand the intrinsic geographical relatedness of DENV-2 and contributes to the understanding of viral evolution and its impact on the epidemic potential and pathogenicity of DENV.

Keywords: dengue virus, genome, characterization, phylogenetic analysis, recombinant analysis

INTRODUCTION

Dengue virus (DENV) belongs to the Flavivirus genus and is transmitted by *Aedes aegypti* and *Ae. Albopictus* mosquitoes, found in tropical and subtropical regions of world (Bhatt et al., 2013). DENV annually infects approximately 50 million people in more than 100 countries (maybe mention here that DENV can be lethal due to hemorrhagic fever or cite number of deaths—or the lack of effective vaccine or problem with antibody-dependent enhancement due to serotypes) (San Martín et al., 2010). The WHO declared that along with climate change, economic integration and migration have contributed to the expanded geographical range of DENV over the past decade (WHO, 2015).

There are four serotypes (DENV-1/2/3/4) that are closely related but are nonetheless antigenically and genetically distinct. Each DENV serotype is further subdivided into several phylogenetically distinct genotypes (Weaver and Vasilakis, 2009). The serotypes were identified by the difference of antigenicity and the genotypes were identified by the phylogenetic tree of DENV gene sequences. The genome of DENV is a linear, non-segmented, positive-sense strand of RNA of approximately 10.6–11 kb, and the MW is 4.2×10^6 (Dash et al., 2015), and the full-length polyprotein which is processed by viral and host proteases into seven non-structural proteins (NS1, NS2A, NS2B, NS3, NS4A, NS4B, and NS5) and three structural proteins (capsid, premembrane, and envelope) (Holmes and Twiddy, 2003). The 3' UTR lacks a poly real (A) tail; they have A non-coding regions in 5′ end and 3′ end (Markoff, 2003). The four DENV serotypes share 65–70% sequence homology and are further clustered into different genotypes on account of high mutation rates (Holmes and Twiddy, 2003; Anoop et al., 2012). Each of the four serotypes of DENV (DEVN 1–4) can cause a spectrum of illness in human from mild dengue fever (DF) aggravate to severe life-threatening dengue shock syndrome (DSS) and dengue hemorrhagic fever (DHF) (Rodenhuis-Zybert et al., 2010).

Xishuangbanna (N22°0′42.00″, E100°47′45.68″) is located in the southernmost prefecture of Yunnan Province and is situated along a tropical rainforest area where dengue fever is endemic. A population of more than 1 million and the long summer without winter. Imported cases of DENV infection sporadically occur in bordering regions of Yunnan Province, such as Dehong and Xishuangbanna (Wang et al., 2015). The first outbreak of dengue fever in Yunnan was reported in 2008, with 56 confirmed cases (MOH, 2008). After the initial outbreak, larger epidemics have been regularly reported in Xishuangbannan. For instance, 1,538 infection cases were reported in 2013, 1,067 infection cases were reported in 2015, and 1,184 infected patients were detected by November 2017, indicating that dengue fever remains an epidemiological threat in Yunnan (Zhang et al., 2014; Wang et al., 2015, 2016; Yang et al., 2015; Zhao et al., 2016). A previous study by Zhao et al. found that the DENV-2 epidemic of Xishuangbanna in 2015 was most similar to the Indian and Sri Lankan epidemics that occurred in 2001 and 2004, respectively (Zhao et al., 2016).

In 2015, the first case of dengue fever in Xishuangbanna was reported on July 13th and the epidemic continued to 15th of November, with more than 1,000 confirmed cases. So far, detailed genomic characterization and identification of molecular recombination events during this DENV-2 outbreak have not been completed. In this article, we report for the first time the complete genomic sequences and comprehensive genetic analyses of four DENV-2 isolates from the 2015 outbreak in Yunnan, China. These findings supplement our understanding of flavivirus genetics and endemic transmission of DENV originating from the border areas of China, Laos, Burma, and Vietnam.

MATERIALS AND METHODS

Ethics Statement

Ethical approval was obtained from the Institutional Ethics Committee (Institute of Medical Biology, Chinese Academy of Medical Sciences, and Peking Union Medical College). The study protocol was in accordance with the Declaration of Helsinki for Human Research of 1974 (last modified in 2000). Written informed consent was received from each patient before sample collection.

Samples

During the dengue outbreak in the Xishuangbannan, Yunnan Province in 2015, the serum samples were collected from DENV-NS1 positive human patients at Xishuangbanna Dai Autonomous Prefecture People's Hospital (XDAPPH). A total of 852 DENV-NS1 positive serum samples were obtained. Sera of four patients were randomly selected for complete genomic analysis of DENV. The four patients ranged in age from 23 to 58 years old, without record of traveling abroad, and developed symptoms of fever, with fatigue and body rash.

ELISA Test

DENV IgG/IgM was detected in each sample using Dengue Virus IgG/IgM ELISA kit (Neobioscience Technology Co., Ltd., China). The assay was performed according to the operation manual.

Virus RNA Extraction, RT-PCR, and Genomic Sequencing

Serum samples were separated from collected blood. Viral RNA was extracted from 150 μL of collected serum using the RNA mini kit (Qiagen, Hilden, Germany) and eluted in 50 μL of nuclease-free water. The extracted RNA was used for RT-qPCR amplification, and genomic sequencing was carried out as previously described (Drosten et al., 2002). The One-step PrimeScriptTM RT-qPCR kit (TaKaRa Co., Ltd. Dalian, China) was used to amplify two overlapping fragments in the virus gene by RT-qPCR with the following protocol: initial reverse transcription at 42°C for 45 min; 35 cycles of denaturation at 94°C for 30 s, annealing at 55°C for 30 s, elongation at 72°C for 1 min and a final elongation step at 72°C for 5 min. Then, the PCR products were purified and sequenced by Sangon Biotech after identification with agarose gel electrophoresis (AGE).

The complete viral genomic sequences were sequenced in 22 fragments. The primer pairs were selected from Primer-BLAST in NCBI to amplify the DENV-2 genome based on the standard of M29095 (Irie et al., 1989). All primers were synthesized and purified through Sangon Biotech (Shanghai, China). A total of 22 overlapping amplifications spanning the complete genomic region were amplified using 44 primers (**Table 1**). The amplification of various genomic fragments was implemented following the standard methods (Wang et al., 2015). The specific PCR products were purified using the gel extraction kit (Qiagen, Germany) followed by double pass sequencing (Sangon Biotech, Shanghai, China). The 5′ 22 nucleotides and 3′ 23 nucleotides were obtained from the NCBI database.

TABLE 1 | Primers used for the complete genomic characterization of DENV-2.

Primer name	Sequence 5′-3′	Position	Length
DV2-1-F	AGTTGTTAGTCTACGTGGACCG	1–22	656
DV2-1-R	GTGGACGTAGAGTTGCACCA	637–656	
DV2-2-F	ACCCTCATGGCCATAGACCT	541–560	557
DV2-2-R	GGCAGGTTGTTTGGCTTCTG	1079–1098	
DV2-3-F	GGGGTTTCAGGAGGAAGCTG	976–995	767
DV2-3-R	TTCTGTAGCCCCTGTGAGTG	1724–1743	
DV2-4-F	CCCACGCCAAGAAACAGGAT	1664–1683	538
DV2-4-R	AAATCCCAGGCTGTGTCACC	2182–2202	
DV2-5-F	AACCGGGACAACTGAAGCTC	2084–2103	457
DV2-5-R	TGAAGGGGATTCTGGTTGGA	2522–2541	
DV2-6-F	GGTGCAGGCTGATAGTGGTT	2412–2431	595
DV2-6-R	CATGGACGGCTCTGTTGTCT	2988–3007	
DV2-7-F	GCCCTGAAACAGCAGAATGC	2831–2850	735
DV2-7-R	TTCGTTCCTACTCGGGTCCT	3547–3566	
DV2-8-F	TCAACTCCTTGGTCACAGCC	3458–3477	528
DV2-8-R	GTGCAACTCACCTTCCATGC	3967–3986	
DV2-9-F	CTTTCCCAAAGCACCTTGCC	3808–3827	683
DV2-9-R	TGCTGCTGCCGTAATTGGTA	4472–4491	
DV2-10-F	AGGAAGCAGCCCAATTCTGT	4335–4354	565
DV2-10-R	ATACAGCGCCTATGGTTCCG	4881–4900	
DV2-11-F	ATCCCAGAGCTGTCCAAACG	4835–4854	743
DV2-11-R	CCGTGACCCATTCATGTCCT	5559–5578	
DV2-12-F	GGTGAAGCAGCCGGGATTTT	5440–5459	590
DV2-12-R	TCCTTCGGGTGTGTTGATGT	6011–6030	
DV2-13-F	CAGCGCAAAGAAGAGGGAGA	5882–5901	681
DV2-13-R	GCTGCCAGGAGTGTCAGTAG	6544–6563	
DV2-14-F	CTGCATACGGCTGAGGTAGG	6466–6485	693
DV2-14-R	GAAGAGCTGCTGTGAGGGTT	7140–7159	
DV2-15-F	ACAGCCATTGCTAACCAAGC	7021–7042	729
DV2-15-R	TTGCTGATCCTCGTGACACA	7750–7731	
DV2-16-F	TGCTGTGTCACGAGGATCAG	7728–7747	491
DV2-16-R	TCATGCGTGGAGTTTCGTGA	8200–8219	
DV2-17-F	CCCACGATAGAAGCAGGACG	8209–8048	346
DV2-17-R	GTCAGCAGTCTGACCACTCC	8536–8555	
DV2-18-F	CCACCCATACAAAACGTGGG	8460–8479	623
DV2-18-R	CTCAGGGAGTTCCCTCTGGA	9064–9083	
DV2-19-F	GGAGCTGGTTGACAGGGAAA	8865–8884	631
DV2-19-R	CAGCGATTTCTTCTGTGGCG	9477–9496	
DV2-20-F	AAGACCAAAGAGGCAGTGGG	9356–9375	578
DV2-20-R	GAACCCAATGTGACGGGACT	9915–9934	
DV2-21-F	ATGTACTTCCACAGACGCGA	9862–9881	510
DV2-21-R	TTTAACGTCCTTGGACGGGG	10353–10372	
DV2-22-F	TGCGGCTCATTGATTGGGTT	10108–10127	615
DV2-22-R	AGAACCTGTTGATTCAACAGCA	10701–10723	

Genomic Characterization and Phylogenetic Analysis

The 22 sequences were assembled using DNASTAR version 7.0. The assembled nucleotide sequences and translated amino acid sequences were analyzed by BioEdit. Phylogenetic analysis, based on the complete genomes, was conducted using the Molecular Evolutionary Genetics Analysis (MEGA) software version 7.0 (maximum likelihood phylogeny test) and gamma-distributed rates among sites with 1,000 bootstrap replicates.

The reference DENV-2 complete viral genome sequences used to construct the distinct phylogenetic branches were obtained from the GenBank sequence database under the following country and accession numbers: China (KC131142.1, EU359009.1, KF479233.1, JX470186.1); Philippines (KU517847.1, KU509276.1); Australia (KX372564.1, AY037116.1); Singapore (JN851127.1, KX380828.1); Indonesia Jakarta (Y858035.2); Malaysia Johor Bahru (KU666945.1); China Taiwan (DQ645552.1); Indonesia (GQ398258.1); Burkina Faso (EU056810.1); India Hyderabad (JX475906.1); Djibouti or Ethiopia (LC121816.1); Saudi Arabia (KJ830750.1); Sri Lanka (GQ252676.1); India (DQ448231.2); Papua New Guinea (KM204118.1); standard (M29095, KU725663.1); USA (JF730054.1, KM587709.1, EU687243.1); Thailand (FJ810410.1, GQ868542.1); Viet Nam (FJ461305.1, JX649148.1); Peru Puerto Maldonado (KC294201.1); Venezuela Aragua (GQ868541.1); Puerto Rico (GQ398314.1); Haiti (KY415992.1); Brazil (KP188555.1); Guadeloupe (EU920850.1); Colombia Guaviare (FJ182012.1); Venezuela HQ332190.1); Venezuela Aragua (FJ639822.1); Mexico (KJ189370.1); Nicaragua Managua (EU482680.1); South Korea (KP406804.1); Tonga (HM582115.1).

Recombination Analysis

Recombination and molecular evolution analysis was conducted with RDP4.56 package (Martin et al., 2010). The reference viral sequences used in the recombination analysis were obtained from the GenBank sequence database based on phylogenetic trees or geographically close viral sequences under the following accession numbers: KX380828.1-2013-Singapore; KF479233.1-2013-China; JX475906.1-2009-India, Hyderabad; JN851127.1-2004-Singapore; KX372564.1-2015-Australia; KP188555.1-2013-Brazil; EU687243.1-2004-USA, Puerto Rico.

Secondary Structure Analysis of Complete Genome

PredictProtein (https://www.predictprotein.org/) was used to calculate the differences in the secondary structure between the structural and non-structural proteins of the DENV-2SS and 2015 Xishuangbanna epidemic viruses. The amino acid composition and potential RNA, DNA, nucleotide and protein binding sites were analyzed. The potential helical structure was also evaluated.

RESULTS

Laboratory Diagnosis

All 4 patients had typical dengue-like symptoms, including headache, fever, joint pain, myalgia, vascular leakage, pleural effusion, vomiting and nausea. Laboratory investigations of the patients revealed low platelet counts ($<100 * 10^9$/L) and elevated liver enzyme levels (>100 U/L) (including alanine amino transferase and aspartate amino transferase). Further analysis showed that patients' sera were positive for anti-dengue IgM antibodies but tested negative for anti-dengue IgG antibodies, indicating an acute primary dengue infection. After a week of hospitalization, the four patients recovered and then were discharged.

Nucleotide Sequence Analysis of the YNXJ10, YNXJ12, YNXJ13, and YNXJ16 Sequences

RT-PCR amplification generated 22 specific amplicons, which were gel purified and sequenced. After editing and aligning the sequences of overlapping fragments, the complete genome sequences of the newly obtained viruses (named YNXJ10, YNXJ12, YNXJ13, and YNXJ16) were determined. The complete genome sequences of YNXJ10 and YNXJ12 were 10,742 nucleotides (nt) in length, with the ORF located between nucleotides 100–10,275. The length of YNXJ13 and YNXJ16 were 10,741 and 10,734 nt, respectively, with the ORF located between nucleotides 97–10,272 and 90–10,265, respectively.

The nucleotide composition of the four viruses were as follows: YNXJ10 (33.03% A, 25.41% G, 21.05% U, and 20.51% C), YNXJ12 (32.88% A, 25.48% G, 21.03% U, and 20.61% C), YNXJ13 (33.01% A, 25.40% G, 21.13% U, and 20.45% C), YNXJ16 (33.35% A, 25.72% G, 20.90% U, and 20.03% C). In comparison, the nucleotide composition of the DENV-2SS (M29095) virus was 33.09% A, 25.36% G, 20.88% U, and 20.66% C. The A+G content in YNXJ10, YNXJ12, YNXJ13, and YNXJ16 was similar to that of DENV-2 standard virus M29095 (58.45%). The complete genomic sequences of these four viruses were deposited into the NCBI GenBank database (https://www.ncbi.nlm.nih.gov/nuccore): KY937185, KY937187, KY937188, and KY937189.

Genome Phylogenetic Analysis of the YNXJ10, YNXJ12, YNXJ13, and YNXJ16 Sequences

Genome phylogenetic analysis of YNXJ10, YNXJ12, YNXJ13, and YNXJ16 were performed by aligning these viruses against 43 other representative DENV-2 viruses of diverse geographical origins retrieved from GenBank. The result indicated that the YNXJ10, YNXJ12, YNXJ13, and YNXJ16 viruses clustered in the cosmopolitan genotype close to DENV-2 KX380828.1-2013-Singapore and KF479233.1-2013-China. Not surprisingly, the closely related DENV-2 viruses from the 2015 epidemic, Philippines-2015 (KU517847.1) and Australia-2015 (KX372564.1), were from geographically near locations, and both of them belonged to the Asian genotype. Meanwhile, according to the phylogenetic analysis, the causative DENV-2 of the 2015 dengue outbreak in Yunnan most likely originated from the Singapore-2013(KX380828.1) virus, not from the Philippines-2015 (KU517847.1) or the Australia-2015 (KX372564.1) viruses (**Figure 1**).

Base Substitution and Amino Acid Mutation Analysis of the YNXJ10, YNXJ12, YNXJ13, and YNXJ16 Coding Sequences (CDS)

The Blastx-translated nucleotide sequence identity showed that YNXJ10, YNXJ12, YNXJ13, and YNXJ16 were highly matched, with an identity of 97 ∼ 98%. However, the identity with the standard viruses DENV-2SS (m29095) was 91 ∼92%.

The total number of amino acids in YNXJ10, YNXJ12, YNXJ13, and YNXJ16 was 3,392. As shown in **Table 1**, compared to standard viruses DENV-2SS (GenBank ID: M29095), the total numbers of base substitutions in YNXJ10, YNXJ12, YNXJ13, and YNXJ16 were 712, 809, 772, and 841 nt, respectively. The highest mutation rate was located at the coding region of structural protein prM, whereas the lowest mutation rate was found within the coding region of the non-structural protein NS4B.

The numbers of non-synonymous substitutions in YNXJ10, YNXJ12, YNXJ13, and YNXJ16 viruses were 327, 316, 383, and 301 nt, corresponding to rates of 44, 39, 49, and 36% of all the mutations, respectively.

Amino Acid Mutations in Structural Protein Regions

In the structural protein regions of the four viruses, the nucleotide sequence coding for C-prM/M-E was 2,322 nt in length and codes for a 774 amino acid sequence. The lengths of the capsid, premembrane, and envelope amino acid sequences in the four viruses were 113, 166, and 495, respectively. Compared to the DENV-2 standard virus M29095, the total numbers of

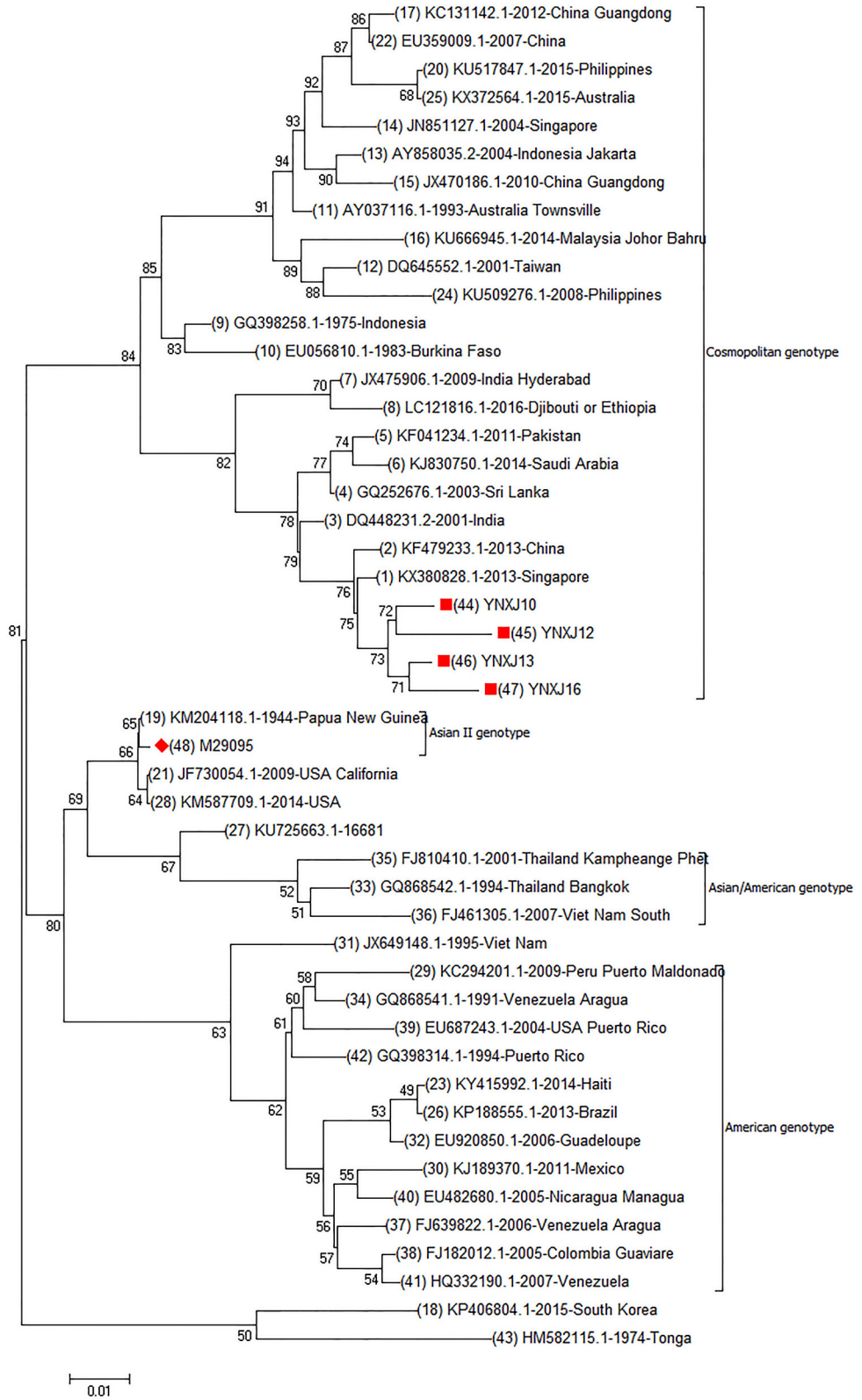

FIGURE 1 | Complete genomic phylogenetic analysis of YNXJ10, YNXJ12, YNXJ13, and YNXJ16. Study sequences are labeled in the red circle. The DENV-2 standard M29095 are labeled with red diamond. Others are representative of DENV-2 from diverse geographical origins retrieved from GenBank. Phylogenetic analysis, based on the complete genomes, was conducted using the MEGA software version 7.0 (maximum likelihood phylogeny test) and gamma-distributed rates among sites with 1,000 bootstrap replicates.

base substitution mutations in the C-prM-E region were 171 (YNXJ10), 148 (YNXJ12), 205 (YNXJ13), and 241 (YNXJ16), and the numbers of non-synonymous substitutions were 41 (YNXJ10), 26 (YNXJ12), 58 (YNXJ13), and 99 (YNXJ16). Consequently, the rate of non-synonymous mutations in the structural protein regions of the C-prM-E proteins were 5.30, 3.36, 7.50, and 11.50%, respectively (**Table 2**).

Compared with M29095, three non-synonymous mutations were observed in the sequences encoding the β-sheet (196:T → A; 262:H → Y; 266:A → V), and 6 non-synonymous mutations were observed in the sequences encoding the coil (351:D → A; 406:K → E; 409:V → I; 421:I → V; 429:H → N; 444:I→ V; 499:P → S), compared with M29095. The detected mutations are summarized in **Figure 2**.

TABLE 2 | Amino acid substitutions in the translated regions.

		C	prM	E	NS1	NS2A	NS2B	NS3	NS4A	NS4B	NS5	Total
YNXJ10 vs. M29095	Base substitution	20	49	102	69	54	29	142	61	18	168	712
	Base substitution rate	5.90	9.84	6.87	6.53	8.26	7.44	7.66	7.11	5.36	6.21	6.70
	AA substitutions	2	14	25	7	9	5	16	7	0	24	109
	AA substitution rate	1.77	8.43	5.05	1.99	4.13	3.85	2.59	2.45	0	2.66	3.21
YNXJ12 vs. M29095	Base substitution	20	33	95	71	54	32	179	99	18	208	809
	Base substitution rate	5.90	6.63	6.40	6.72	8.26	8.21	9.65	11.54	5.36	7.69	7.95
	AA substitutions	2	6	18	7	9	7	44	39	0	39	171
	AA substitution rate	1.77	3.61	3.63	1.99	4.13	5.38	7.12	13.64	0	4.32	5.04
YNXJ13 vs. M29095	Base substitution	21	94	90	76	52	22	138	69	18	192	772
	Base substitution rate	6.19	18.88	6.06	7.20	7.95	5.64	7.44	8.04	5.36	7.10	7.59
	AA substitutions	2	38	18	10	9	1	15	8	0	29	130
	AA substitution rate	1.77	22.90	3.63	2.84	4.13	0.77	2.43	2.80	0	3.22	3.83
YNXJ16 vs. M29095	Base substitution	51	62	128	75	54	22	175	68	18	188	841
	Base substitution rate	15.04	12.45	8.62	7.10	8.26	5.64	9.44	7.93	5.36	6.95	8.26
	AA substitutions	24	23	42	9	9	1	36	8	0	28	180
	AA substitution rate	21.2	13.86	8.48	2.56	4.13	0.77	5.83	2.80	0	3.10	5.31

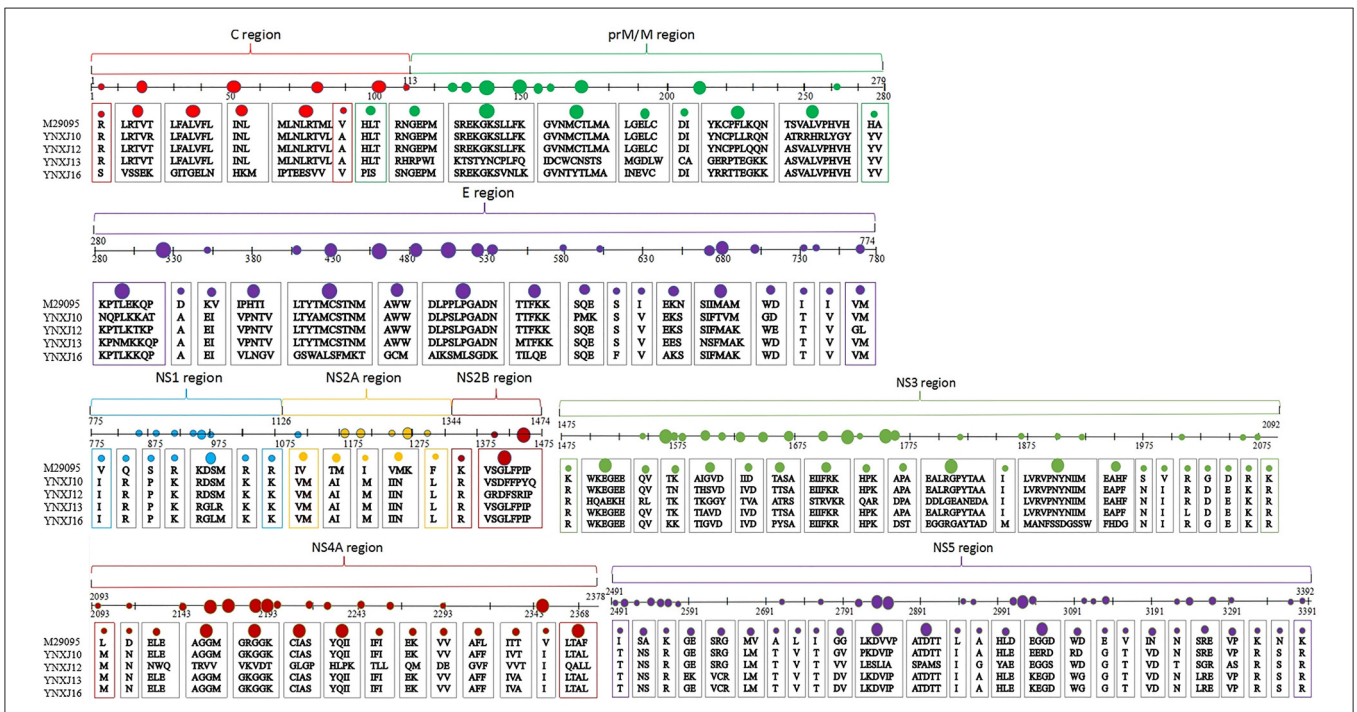

FIGURE 2 | Amino acid substitutions in YNXJ10, YNXJ12, YNXJ13, and YNXJ16 compared to the DEN2SS M29095. The first line is M29095, and the second to fifth lines are YNXJ10, YNXJ12, YNXJ13, and YNXJ16, respectively. The labeled numbers represent the amino acid position.

As **Figure 2** indicates, within Domain II of the E protein, a T to C substitution at position 1606 changes the amino acid S (Serine) to P (Proline) (amino acid position 536), which changes the polarity. Meanwhile, a G to A substitution at position 1612 was observed, and this mutation converted the negatively-charged amino acid E (Glutamic acid) to a positively-charged K (Lysine) (amino acid position 538).

Amino Acid Mutations in Non-structural Protein Regions

Within the non-structural protein region, the length of the NS1-NS2A-NS2B-NS3-NS4A-NS4B-NS5 sequence of the four viruses was 7,854 nt. Compared with M29095, there were 69–76 single nucleotide changes identified in the NS1 region, including 7–10 non-synonymous substitutions (**Figure 2**). The base substitution T2710C modified the non-polar amino acid I (Isoleucine) to polar T (Threonine). At amino acid position 1266, K (Lysine) changed to N (Asparagine), which converted a basic amino acid to an uncharged amino acid in the coil.

Compared with M29095, there were 76–86 base mutations found in the NS2A-NS2B region, and 10–16 were non-synonymous substitutions; the total number of base substitution mutations in the NS3 region was 138–179, and the number of non-synonymous substitutions was 16–44; (**Figure 2**). There were 7 and 39 amino acid substitutions in NS4A and NS4B, respectively. For NS5, the total number of base substitutions was 168-208, and there were 24–29 non-synonymous substitutions found in this region, with a substitution rate of 2.66 ∼ 4.32% (**Figure 2**). In addition, compared with KX380828.1, there were 44, 105, and 64 amino acid substitutions in the translated regions of YNXJ10, YNXJ12, and YNXJ13, respectively (**Figure 3**).

Recombination Events of DENV-2 Genome

The predictive complete genomic mutation map was performed in comparison with the closely related viruses, Singapore 2013 (KX380828.1), China 2013 (KF479233.1), and India 2009 (JX475906.1). Some recombination events may have occurred between the four viruses from Xishuangbanna and the closely related viruses, KX380828.1-2013-Singapore and KF479233.1-2013-China. There were many suspected recombination mutation areas in the complete genome. The suspected recombination mutations of the YNXJ10 virus might related to YNXJ16, while the suspected recombination mutations of YNXJ13 virus might related to KX380828. Meanwhile, the prediction results showed that the most likely recombination events were located at the structural genes prM and E, and no recombination events were observed in the non-structural region of 2K and NS4B (**Figure 4**).

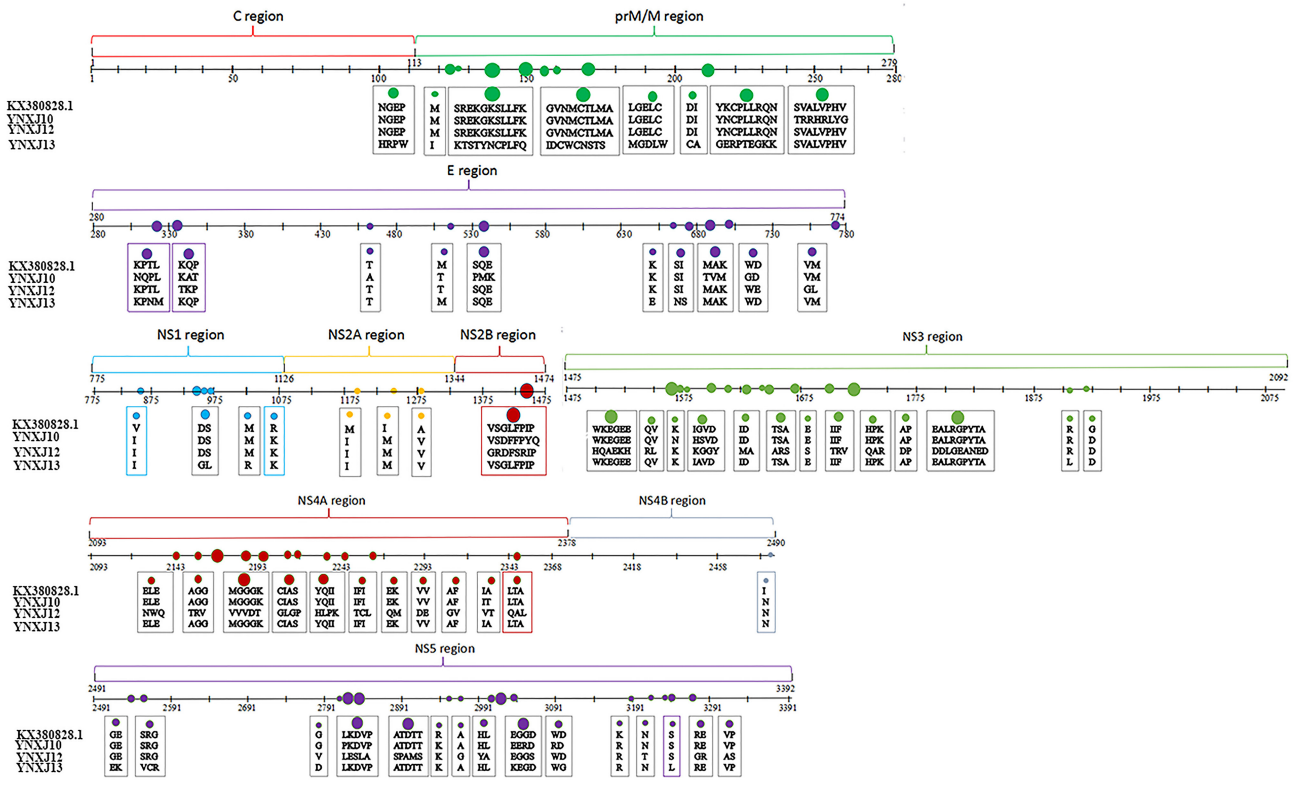

FIGURE 3 | Amino acid substitutions of YNXJ10, YNXJ12, and YNXJ13 compared to the closely-related Singapore in 2013 (KX380828.1). The first line is KX380828.1, and the second to fourth lines are YNXJ10, YNXJ12, YNXJ13, respectively. The labeled numbers represent the amino acid position.

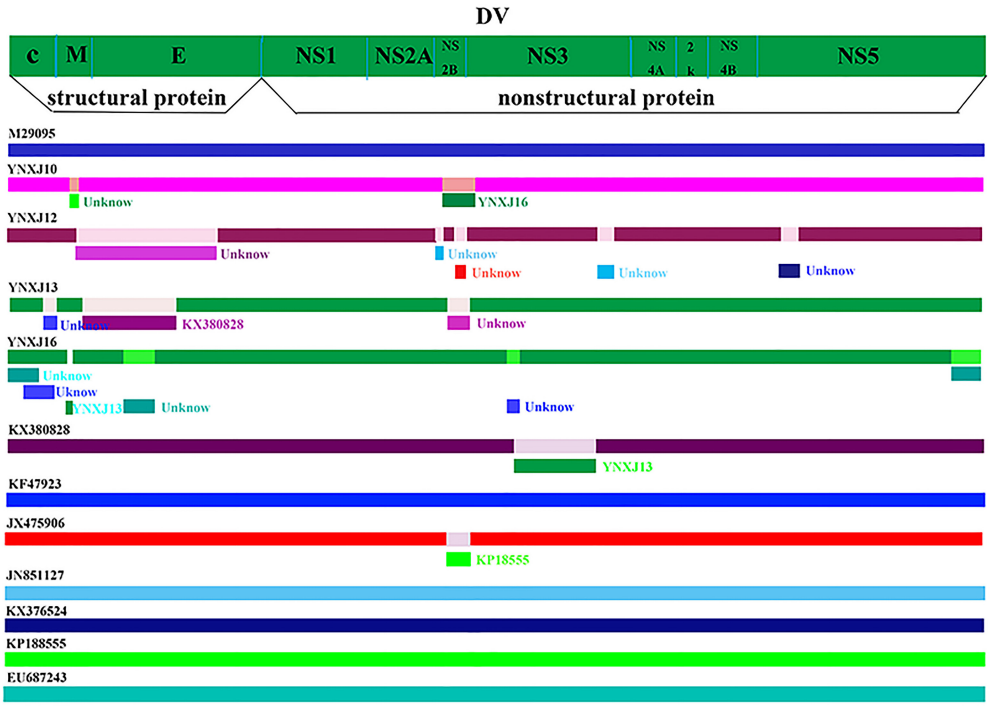

FIGURE 4 | Recombination events in DENV-2. Schematic representation indicates the predictive recombination events among M29095, YNXJ10, YNXJ12, YNXJ13, YNXJ16, KX380828.1, KF479233, JX475906, JN851127, KX372564, KP188555, and EU687243, and analyzed by RDP package. Continuous lines indicate no recombination possibility.

Possible Secondary Structures in Structural and Non-structural Protein Regions

The possible secondary structure of structural and non-structural proteins of YNXJ10, YNXJ12, YNXJ13, and YNXJ16 were then compared with that of M29095 (DEN2SS). Of the 3,391 total amino acids that code for the YNXJ structural and non-structural proteins, there are 10 amino acids that may participate in nucleotide binding. Seven possible nucleotide-binding sites (including 4, 10, 11, 13, 22, 67, and 82) were present only in YNXJ10, YNXJ12, YNXJ13, and YNXJ16, whereas the other three sites (6, 9, and 25) were lost, compared with M29095.

Forty-one changes at possible protein binding sites were observed among the 3,391 amino acids that form YNXJ structural and non-structural proteins. Of these, 24 possible protein binding sites (including 1, 4,94, 97, 98, 142, 158, 183, 236, 408, 663, 972, 1,156, 1,265, 1,582, 1,631, 1,935, 2,068, 2,084, 2,108, 2,377, 2,760, 2,863, and 2,880) were observed in YNXJ10, YNXJ12, YNXJ13, and YNXJ16, whereas sites 20, 26, 27, 28, 262, 429, 876, 1,131, 1,268, 1,587, 1,627, 1,915, 2,069, 2,080, 2,097, 2,269, and 2,862 were lost, compared with M29095.

Approximately 41 distinct nucleotide mutations were observed in the helix regions, whereas only a few mutations were found in the buried and exposed regions. Moreover, there were 13 nucleotide mutations observed in the disordered region of YNXJ10, YNXJ12, YNXJ13, and YNXJ16 (**Figure 5**). Of these, 8 mutations (13, 15, 17, 201, 877, 880, 1,487, and 2,909) occurred in YNXJ10, YNXJ12, YNXJ13, and YNXJ16, while 5 mutations (including 358, 2,954, 3,382, 3,383, and 3,384) existed only in M29095.

DISCUSSION

The occurrence of dengue fever has increased remarkably in China in recent decades due to urbanization, globalization, climate change, migration and other factors (Murray et al., 2013; Chen and Liu, 2015; Guzman and Harris, 2015). The epidemic area, Xishuangbanna, Yunnan is located in southwestern China where dengue fever has been prevalent since 2008 (MOH, 2008). Since then, epidemics have been regularly reported in Xishuangbanna, Yunnan. A serious outbreak of DENV-3 occurred in 2013, with 1,538 infected individuals (Zhang et al., 2014; Wang et al., 2015, 2016; Yang et al., 2015). In 2015, Xishuangbanna experienced a large DENV-2 outbreak, which was the largest dengue epidemic in the past few years. Although the cause of this outbreak is not clear, it is coincident with the increasing global trend (Qin and Shi, 2014; Zhao et al., 2016). In recent years, the incidence of dengue fever in China's neighboring countries, such as Indonesia, Myanmar, Singapore and Malaysia, has been higher than in previous years (Dash et al., 2013; Ng et al., 2013). Xishuangbanna has close contact with Laos, Thailand and Myanmar. Furthermore, Xishuangbanna is a tourist destination

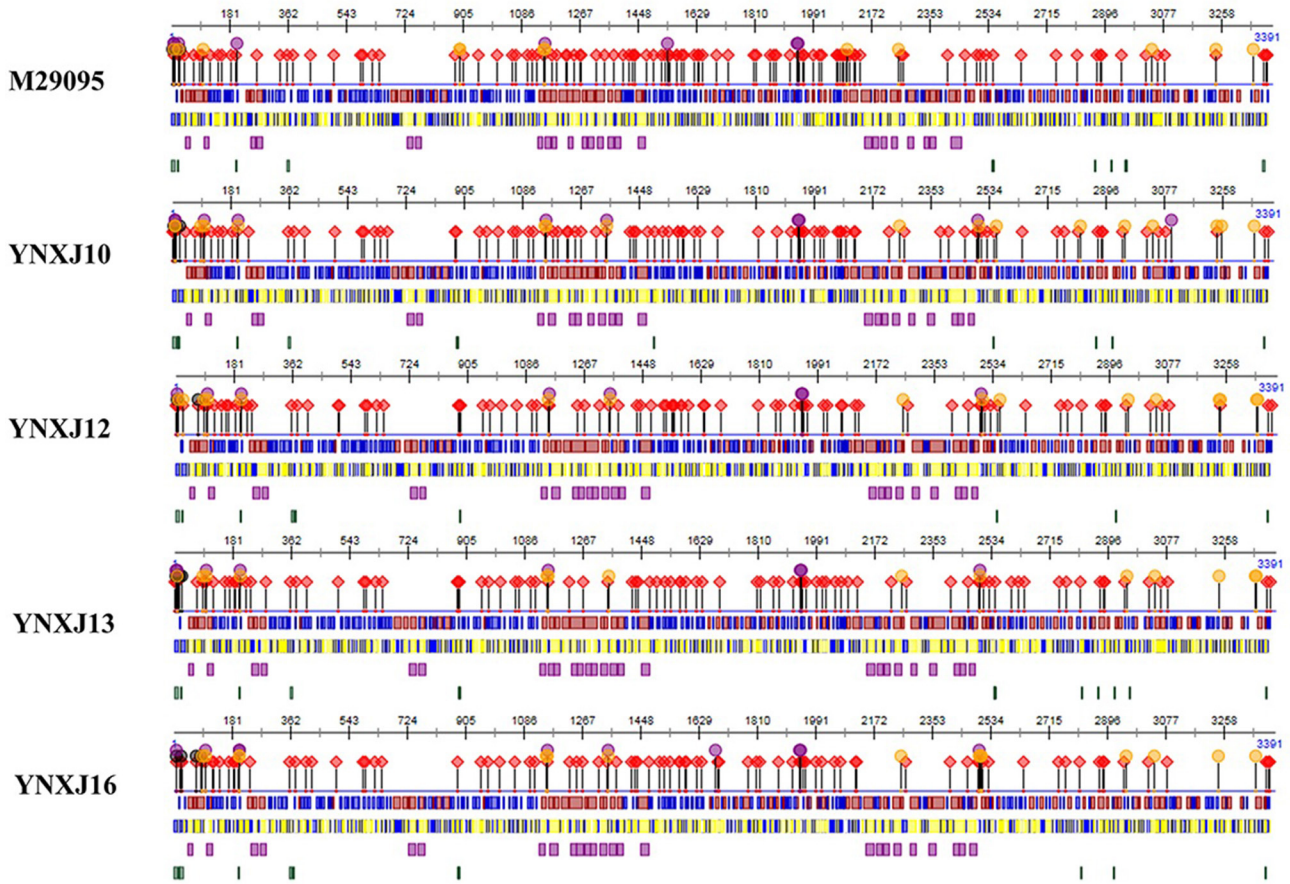

FIGURE 5 | Secondary structure prediction of the structural and non-structural proteins for DEN2SS M29095 and YNXJ10, YNXJ12, YNXJ13, and YNXJ16. The purple dots denote the RNA-binding region, the black dots denote the nucleotide-binding region, the red rhombuses denote the protein-binding region, and the yellow dots denote the DNA-binding region. Red and blue in the first line represent the strand and helix regions, respectively. Yellow and blue in the second line represent the buried and exposed regions, respectively. Purple in the third line indicates the helical transmembrane regions, and green in the fourth line represents the disordered regions. The first map is M29095, and the second, third, fourth, and fifth maps are YNXJ10, YNXJ12, YNXJ13, and YNXJ16.

and attracts more than 14 million tourists from around the world annually, resulting in an increased risk of DENV epidemic (Lowe et al., 2014).

The molecular characterization of DENV-2 at the genomic level is very important to understand the spread of dengue fever in Xishuangbanna. In this article, we were interested in extending previous studies and elucidating the genetic relationship between circulating DENV-2 viruses in southwest China and other parts of the world. Phylogenetic analysis and sequence alignment of the full-length genomes of YNXJ10, YNXJ12, YNXJ13, and YNXJ16 showed a close relationship with KX380828.1-2013-Singapore and KF479233.1-2013-China that are clustered in the Asian genotype.

Comparing the four Xishuangbanna DENV-2 sequences to KX380828.1-2013-Singapore and KF479233.1-2013-China, the greatest number of mutations occurred in the structural protein gene prM, while no mutation was observed in the non-structural gene NS4B. More mutations occurred in structural genes than in non-structural genes, indicating that structural genes are more variable while the non-structural genes are more stable under selective pressure. During host-pathogen interaction, the structural protein is located in the envelope region that interacts with host cell surface, which is under more selective pressure; however, the non-structural protein is located in the interior of the virion, which allows for minimal adaption from the host. This phenomenon coincided with the mutation patterns of YNXJ10, YNXJ12, YNXJ13, and YNXJ16.

The emergence of recombinant viruses could have a great impact on epidemiological and clinical outcomes. Interestingly, recombination events were observed between YNXJ13 and the KX380828.1-2013-Singapore. According to our prediction of possible recombination events, most recombination events were predicted to occur in the structural gene prM/E and non-structural gene NS2B/NS3. NS2B/NS3 helps the virus escape from the host immune system by cutting antiviral protein STING. As a protease, NS2B/NS3 also plays an essential role during flaviviral polyprotein processing. Thus, amino acid substitution in both prM/E and NS2B/NS3 proteins may greatly affect the efficiency of viral replication.

In summary, we report the first complete genome sequences of DENV-2 from Xishuangbanna, Yunnan, China. There were extensive outbreaks of dengue virus of different serotypes and genotypes in surrounding areas, such as Singapore, Taiwan, Guangdong, Vietnam, Burma, and Laos, in 2015. Hence, the origin of the Xishuangbanna epidemic is difficult to pinpoint with certainty. This study could help identify the role of geography and human migratory patterns that ultimately act in concert with intrinsic viral adaptive capabilities to result in large-scale outbreaks, and could offer further insight into DENV-2 pathogenicity, infectivity, and vaccine development.

AUTHOR CONTRIBUTIONS

LJ, CY, JY, and XL: acquisition and analysis of data; drafting of the manuscript; DM, XS, and LL: providing blood samples and experimental requirement; YZ, JX, XW, JC, and YP: material or technical support; QS and XS: study concept and design; critical revision of the manuscript; study supervision; obtained funding. All authors read and approved the final manuscript.

FUNDING

This research was supported by the Foundation of the CAMS Initiative for Innovative Medicine (CAMS-I2M) (grant no. 2017-I2M-2-006), the National Twelfth Five Year major new drug discovery technology major projects (grant no. 2012ZX09104-302), the Natural Science Foundation of Yunnan Province (2012FB188 and 2016FA029), the Jointly Supported Foundation of the National Project in Yunnan Province (2013GA018), the foundation of Kunming science and technology innovation team, and the National Natural Science Foundation of China (81171946).

ACKNOWLEDGMENTS

We would like to thank Dr. Jesse Hwang of Yale University, School of Medicine, Internal Medicine/Infectious Diseases, and Dr. Penghua Wang of Department of Microbiology and Immunology, School of Medicine, New York Medical College, for proofreading and reviewing our manuscript.

REFERENCES

Anoop, M., Mathew, A. J., Jayakumar, B., Issac, A., Nair, S., Abraham, R., et al. (2012). Complete genome sequencing and evolutionary analysis of dengue virus serotype 1 isolates from an outbreak in Kerala, South India. *Virus Genes*. 45, 1–13. doi: 10.1007/s11262-012-0756-3

Bhatt, S., Gething, P. W., Brady, O. J., Messina, J. P., Farlow, A. W., Moyes, C. L., et al. (2013). The global distribution and burden of dengue. *Nature*. 496, 504–507. doi: 10.1038/nature12060

Chen, B., and Liu, Q. (2015). Dengue fever in China. *Lancet*. 385,1621–1622. doi: 10.1016/S0140-6736(15)60793-0

Dash, P. K., Sharma, S., Soni, M., Agarwal, A., Parida, M., and Rao, P. V. L. (2013). Complete genome sequencing and evolutionary analysis of Indian isolates of dengue 2 virus. *Biochem. Biophys. Res. Commun*. 436, 478–485. doi: 10.1016/j.bbrc.2013.05.130

Dash, P. K., Sharma, S., Soni, M., Agarwal, A., Sahni, A. K., Parida, M., et al. (2015). Complete genome sequencing and evolutionary phylogeography analysis of Indian isolates of Dengue virus type 1. *Virus Res*. 195, 124–134. doi: 10.1016/j.virusres.2014.08.018

Drosten, C., Göttig, S., Schilling, S., Asper, M., Panning, M., Schmitz, H., et al. (2002). Rapid detection and quantification of RNA of Ebola and Marburg viruses, Lassa virus, Crimean-Congo hemorrhagic fever virus, Rift Valley fever virus, dengue virus, and yellow fever virus by real-time reverse transcription-PCR. *J Clin Microbiol*. 40, 2323–2330. doi: 10.1128/JCM.40.7.2323-2330.2002

Guzman, M. G., and Harris, E. (2015). Dengue. *Lancet*., 385, 453–465. doi: 10.1016/S0140-6736(14)60572-9

Holmes, E., and Twiddy, S. (2003). The origin, emergence and evolutionary genetics of dengue virus. *Infect. Genet. Evol*. 3, 19–28. doi: 10.1016/S1567-1348(03)00004-2

Irie, K., Mohan, P. M., Sasaguri, Y., Putnak, R., and Padmanabhan, R. (1989). Sequence analysis of cloned dengue virus type 2 genome (New Guinea-C strain). *Gene* 75, 197–211.

Lowe, R., Barcellos, C., Coelho, C. A., Bailey, T. C., Coelho, G. E., Graham, R., et al. (2014). Dengue outlook for the World Cup in Brazil: an early warning model framework driven by real-time seasonal climate forecasts. *Lancet Infect Dis*. 14, 619–626. doi: 10.1016/S1473-3099(14)70781-9

Markoff, L. (2003). 5'- and 3'-noncoding regions in flavivirus RNA. *Adv. Virus Res*. 59, 177–228. doi: 10.1016/S0065-3527(03)59006-6

Martin, D. P., Lemey, P., Lott, M., Moulton, V., Posada, D., Lefeuvre, P., et al. (2010). RDP3: a flexible and fast computer program for analyzing recombination. *Bioinformatics* 26, 2462–2463. doi: 10.1093/bioinformatics/btq467

MOH (2008). *State Ministry of Public Heath in October 2008, Public Health Reports*. Available online at: http://www.moh.gov.cn/publicfiles/business/htmlfiles/zwgkzt/pyq/index.htm (Accessed November 16, 2008).

Murray, N. E., Quam, M. B., and Wilder-Smith, A. (2013). Epidemiology of dengue: past, present and future prospects. *Clin Epidemiol*. 5, 299–309. doi: 10.2147/CLEP.S34440

Ng, L. C., Chem, Y. K., Koo, C., Mudin, R. N., Amin, F. M., Lee, K. S., et al. (2013). 2013 dengue outbreaks in Singapore and Malaysia caused by different viral strains. *Am J Trop Med Hyg*. 92, 1550–1555. doi: 10.4269/ajtmh.14-0588

Qin, C., and Shi, P. (2014). Dengue in China: not a passing problem. *Sci China Life Sci*. 57, 1230–1231. doi: 10.1007/s11427-014-4783-2

Rodenhuis-Zybert, I. A., Wilschut, J., and Smit, J. M. (2010). Dengue virus life cycle: viral and host factors modulating infectivity. *Cell. Mol. Life Sci*. 67, 2773–2786. doi: 10.1007/s00018-010-0357-z

San Martín, J. L., Brathwaite, O., Zambrano, B., Solorzano, J. O., Bouckenooghe, A., Dayan, G. H., et al. (2010). The epidemiology of dengue in the Americas over the last three decades: a worrisome reality. *Am. J. Trop. Med. Hyg*. 82, 128–135.

Wang, B., Li, Y., Feng, Y., Zhou, H., Liang, Y., Dai, J., et al. (2015). Phylogenetic analysis of dengue virus reveals the high relatedness between imported and local strains during the 2013 dengue outbreak in Yunnan, China: a retrospective analysis. *BMC Infect Dis*. 21:142. doi: 10.1186/s12879-015-0908-x

Wang, B., Yang, H., Feng, Y., Zhou, H., Dai, J., Hu, Y., et al. (2016). The distinct distribution and phylogenetic characteristics of dengue virus serotypes/genotypes during the 2013 outbreak in Yunnan, China: phylogenetic characteristics of 2013 dengue outbreak in Yunnan, China. *Infect Genet Evol*. 37, 1–7. doi: 10.1016/j.meegid.2015.10.022

Weaver, S. C., and Vasilakis, N. (2009). Molecular evolution of dengue viruses: contributions of phylogenetics to understanding the history and epidemiology of the preeminent arboviral disease. *Infect. Genet. Evol*. 9, 523–540. doi: 10.1016/j.meegid.2009.02.003

WHO. (2015). COP21: *A Defining Moment for Human Health, Media Centre*. Available online at: http://www.who.int/mediacentre/commentaries/cop21-health/en/ (Accessed December 4, 2015).

Yang, M. D., Jiang, J. Y., Guo, X.F., Wu, C., and Zhou, H. N. (2015). Investigation and analysis of dengue fever pidemic in Yunnan province during 2009–2014. *Chin. J. Pathogen Biol.* 10, 738–742.

Zhang, F. C., Zhao, H., Li, L. H., Jiang, T., Hong, W. X., Wang, J., et al. (2014). Severe dengue outbreak in Yunnan, China. *Int. J. Infect. Dis.* 27, 4–6. doi: 10.1016/j.ijid.2014.03.1392

Zhao, Y., Li, L., Ma, D., Luo, J.,Ma, Z., Wang, X., et al. (2016). Molecular characterization and viral origin of the 2015 dengue outbreak in Xishuangbanna, Yunnan, China. *Sci. Rep.* 6, 1–8. doi: 10.1038/srep34444

Conflict of Interest Statement: The authors declare that the research was conducted in the absence of any commercial or financial relationships that could be construed as a potential conflict of interest.

frontiers in Cellular and Infection Microbiology

ORIGINAL RESEARCH
published: 04 July 2018
doi: 10.3389/fcimb.2018.00216

Epidemiological Characterization of the 2017 Dengue Outbreak in Zhejiang, China and Molecular Characterization of the Viruses

Hao Yan[1†], Zheyuan Ding[2†], Juying Yan[1], Wenwu Yao[1], Junhang Pan[1], Zhangnv Yang[1], Xiuyu Lou[1], Haiyan Mao[1], Junfen Lin[2], Jimin Sun[3], Juan Hou[3], Haocheng Wu[2], Chen Wu[2] and Yanjun Zhang[1]*

[1] Department of Microbiology, Zhejiang Provincial Center for Disease Control and Prevention, Hangzhou, China, [2] Department of Public Health Surveillance and Advisory, Zhejiang Provincial Center for Disease Control and Prevention, Hangzhou, China, [3] Department of Communicable Disease Control and Prevention, Zhejiang Provincial Center for Disease Control and Prevention, Hangzhou, China

OPEN ACCESS

Edited by:
Qiangming Sun,
Institute of Medical Biology (CAMS), China

Reviewed by:
Penghua Wang,
University of Connecticut Health Center, United States
Chunxia Jing,
Jinan University, China
Erna Geessien Kroon,
Universidade Federal de Minas Gerais, Brazil

***Correspondence:**
Yanjun Zhang
yjzhang@cdc.zj.cn

[†]These authors have contributed equally to this work.

Received: 09 January 2018
Accepted: 07 June 2018
Published: 04 July 2018

Citation:
Yan H, Ding Z, Yan J, Yao W, Pan J, Yang Z, Lou X, Mao H, Lin J, Sun J, Hou J, Wu H, Wu C and Zhang Y (2018) Epidemiological Characterization of the 2017 Dengue Outbreak in Zhejiang, China and Molecular Characterization of the Viruses. Front. Cell. Infect. Microbiol. 8:216. doi: 10.3389/fcimb.2018.00216

Dengue, a mosquito-borne disease caused by the dengue virus (DV), has been recognized as a global public health threat. In 2017, an unexpected dengue outbreak occurred in Zhejiang, China. To clarify and characterize the causative agent of this outbreak, data on dengue fever cases were collected from the China Information System for Disease Control and Prevention in Zhejiang province for subsequent epidemiological analysis. A total of 1,229 cases were reported, including 1,149 indigenous and 80 imported cases. Most indigenous cases (1,128 cases) were in Hangzhou. The epidemic peak occurred in late August and early September, and the incidence rate of elderly people (4.34 per 100,000) was relatively high. Imported cases were reported all year round, and most were from South-East Asia and Western Pacific regions. Young people and men accounted for a large fraction of the cases. Acute phase serums of patients were collected for virus isolation. And 35 isolates (including 25 DV-2, 8 DV-1, 1 DV-3, and 1 DV-4) were obtained after inoculation and culture in mosquito C6/36 cells. The E genes of the 35 new DV isolates and the complete genome of a DV-2 isolate (Zhejiang/HZ33/2017), and the E gene of a DV-2 isolate from *Ae. albopictus* (Zhejiang/Aedes-1/2017) were determined. Phylogenetic analyses were performed using the neighbor-joining method with the Tajima-Nei model. Phylogenetically, DVs of all four serotypes with multiple genotypes (mainly including 21 Cosmopolitan genotype DV-2, 4 Asian I genotype DV-2, 6 genotype I DV-1, and 2 genotype V DV-1) were present in the indigenous and imported cases in Zhejiang during the same period. Most of the isolates probably originated from South-East Asia and Western Pacific countries. The imported cases, high density of mosquito vector, and missed diagnosis might contribute to the 2017 outbreak in Zhejiang.

Keywords: dengue fever, dengue virus, molecular characterization, E gene, phylogenetic analysis, epidemiological analysis, Zhejiang

INTRODUCTION

Dengue is a mosquito-borne viral infection causing a severe flu-like illness and, sometimes causing a potentially lethal complication called severe dengue (previously known as dengue hemorrhagic fever). The vast distribution of mosquito vectors, which is fueled by frequent human migration, and a lack of adequate listed vaccines and effective drugs have resulted in a dramatic increase in dengue virus (DV) infections, which have undergone 30-fold growth over the past 50 years (Li et al., 2017). One recent estimate has indicated 390 million dengue infections per year, of which 96 million manifest clinically (Bhatt et al., 2013). Another study on the prevalence of dengue has estimated that 3.9 billion people in 128 countries are at risk of infection with DV (Brady et al., 2012). DV is a single-stranded, positive-sense RNA virus which belong to the genus *Flavivirus*, family *Flaviviridae.* Its genome is approximately 10,700 bp, comprising a single open reading frame that encodes three structural proteins (C, capsid; prM/M, precursor of membrane; and E, envelope) and seven non-structural proteins (NS1, NS2a, NS2b, NS3, NS4a, NS4b, and NS5) (Kuhn et al., 2002). DV can be grouped into four distinct serotypes (DV-1, DV-2, DV-3, and DV-4), each of which can be sub-classified into several genotypes on the basis of E gene sequences (Li et al., 2017).

Most countries in Asia have reported epidemic dengue outbreaks, including Myanmar, Laos, Thailand, Nepal, Malaysia, Indonesia, Cambodia, the Philippines, Vietnam, Japan, and Pakistan (Jarman et al., 2008; Holmes et al., 2009; Vu et al., 2010; Dubot-Pérès et al., 2013; Akram and Idrees, 2016; Ngwe Tun et al., 2016; Tajima et al., 2017). China has seen an increase in dengue fever (DF) cases in recent years. Since the first reported dengue outbreak in 1978, outbreaks have been reported in many provinces of mainland China, including Hainan, Guangxi, Guangdong, Yunnan, Fujian, and Zhejiang (Chen and Liu, 2015; Sun et al., 2017). Moreover, all four DV serotypes have been identified and found to be prevalent in China.

Zhejiang province, which has a typical subtropical climate, lies along the southeast coast of China. The topographic features in this province are complex, including plains, hills, and mountain lands, thus creating ideal conditions for the growth of mosquitoes (Guo et al., 2014). Zhejiang has a population of about 56.57 million. *Ae. albopictus* is the only vector for DV transmission in Zhejiang. In 2004, a DF outbreak caused by an indigenous patient who had traveled from Thailand occurred in Cixi, a city in the northeast of Zhejiang, and 83 cases were reported (Xu et al., 2007). A larger epidemic occurred in 2009, and there were 196 cases in Yiwu (Sun et al., 2011). In recent years, sporadic imported cases of DF have been reported almost annually in Zhejiang Province.

In 2017, an unexpected large dengue epidemic occurred, and a total of 1229 DF cases (93.8% emerging in Hangzhou) but no deaths were reported in Zhejiang, China. The DV cases in Zhejiang Province were mainly DV serotype 2, with a small fraction of DV serotype 1, 3, and 4. To analyze the molecular evolution of the virus, a phylogenetic tree can be constructed by using specific regions of the DV genome, such as the full-length sequence, E, or E/NS1 (Huang et al., 2012; Wang et al., 2016). In this study, we analyzed the phylogenetic, molecular, and epidemiological characteristics of DV outbreaks, investigated the origin of the 36 new dengue isolates and reported the complete genome sequence of a DV-2 isolate (Zhejiang/HZ33/2017) isolated from the 2017 outbreak in Zhejiang.

MATERIALS AND METHODS

Data Sources

DF case data for the year 2017 were acquired from the National Notifiable Infectious Disease Reporting Information System (NNIDRIS) at the China Information System for Disease Control and Prevention in Zhejiang province. In China, DF is classified as a class-B notifiable infectious disease. Cases of DF must be reported to NNIDRIS within 24 h after diagnosis. Dengue cases were diagnosed according to the criteria for DF from the Chinese Ministry of Health. Information on each dengue case included demographic characteristics, laboratory confirmation, onset data, diagnosis data, and whether the case was imported or indigenous. An imported dengue case was defined as an infected person whose whereabouts could be traced to an origin in a dengue-endemic area outside Zhejiang Province within 15 days of the onset data; otherwise, cases were defined as indigenous. Characteristics of dengue cases were described by age, sex, occupation composition, and temporal and spatial distribution. Incidence was calculated as the number of cases divided by the population size during the study period. Temporal and spatial analyses of indigenous and imported cases were performed in Zhejiang Province, and spatiotemporal analysis of indigenous cases was performed in 13 districts of Hangzhou. Statistical analyses were performed by using ArcGIS 10.3 (ESRI, Redlands, CA, USA) and R statistical software, version 3.2.2 (R Development Core Team 2015).

Vector Monitoring

The mosquitoes were collected in sweeping nets at various communities located in the main urban area of Hangzhou during the 2017 dengue outbreak. The pooled mosquitoes were then stored at −80°C until virus detection. DV nucleotide detection, serotype identification and E gene amplification used the methods that mentioned below. Breteau index (BI, number of positive containers per 100 houses) was used to record *Ae. albopictus* infestation levels. Vector surveillance continued until BI was less than 5 according to dengue guidelines for diagnosis, treatment, prevention and control of the World Health Organization.

Sample Collection and Laboratory Diagnosis

A total of 90 serum samples of patients were obtained from the municipal Centers for Disease Control and Prevention (CDC) of Zhejiang. DV nucleotide detection and serotype identification were performed according to diagnostic criteria for DF (WS 216–2008) of the Ministry of Health of China.

TABLE 1 | Demographic characteristics of dengue cases in Zhejiang Province, 2017.

	Indigenous cases		Imported cases	
	Number	**Incidence rate/10^5**	**N**	**Incidence rate/10^5**
Total	1,149	2.07	80	0.14
Sex				
Male	573	2.00	53	0.19
Female	576	2.11	27	0.10
Age (median, IQR)	51,35–63		35,27.5–50.5	
<20	48	0.45	1	0.01
20~	302	1.66	49	0.27
40~	399	2.22	23	0.13
60~	348	4.47	7	0.09
80~	52	3.63	0	0.00
Occupation		(Constituent ratio %)		
Retiree	346	30.11	5	6.25
Commercial service people	159	13.84	15	18.75
Household/Unemployed person	150	13.05	3	3.75
Industrial worker	139	12.10	14	17.5
Cadres	130	11.31	13	16.25
Farmer	50	4.35	15	18.75
Other	175	15.23	15	18.75

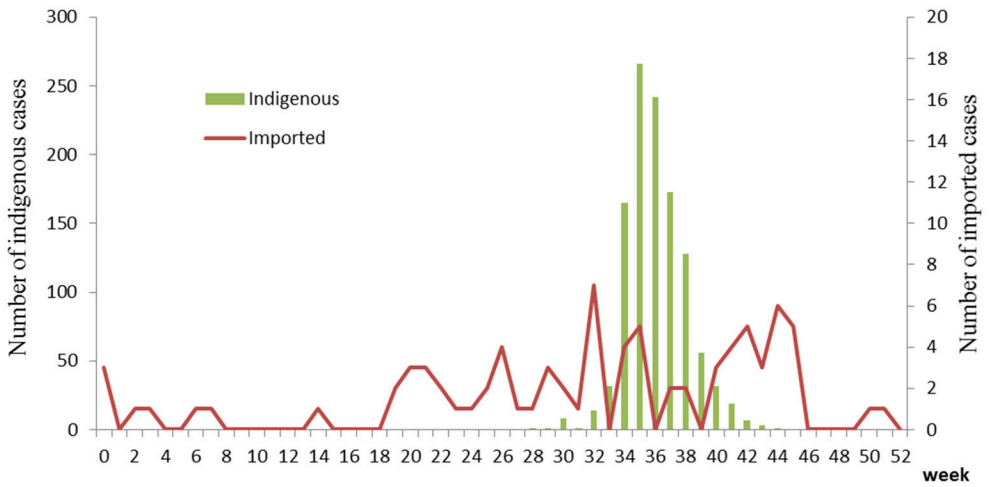

FIGURE 1 | Temporal distribution of dengue cases in Zhejiang, China, 2017.

Virus Isolation

Patients' positive acute phase serums (collected within 1–5 days of illness onset) were inoculated in *Ae. albopictus* mosquito C6/36 cells, which were a gift from the National Institute for Viral Disease Control and Prevention. The C6/36 cell line was cultured in minimum essential medium (MEM) (Gibco, USA) supplemented with 2% fetal bovine serum (Gibco, USA) at 28°C in 5% CO_2. When complete cytopathic effects (CPE) were observed, culture supernatant was collected and stored at −80°C until use.

RNA Extraction and Genome Sequencing

Viral RNA was extracted with a RNeasy Mini Kit (Qiagen, Germany) according to the manufacturer's instructions. Complete genome sequencing of the DV-2 isolate from an indigenous case in Hangzhou (Zhejiang/HZ33/2017) was performed as previously described (Zhao et al., 2014). The E genes of the other 35 DVs were amplified with the following primers: DV1-E-F, 5′CAAGAACCGAAACRTGGATGTC3′ and DV1-E-R, 5′GGCTGATCGAATTCCACACAC3′; DV2-E-F, 5′AACATGGATGTCATCAGAAGG3′ and DV2-E-R, 5′CCA ATCTTGTTACTGAGCGG3′; DV3-E-F, 5′GCCCTATTTCTT

GCCCATTACA3′ and DV3-E-R, 5′CCGCACACTCCATTC TCCCAA3′ (Aquino et al., 2006); DV4-E/777F, 5′GCTTGG AAACATGCTCAGAG3′, DV4-E/1766R, 5′ACATGTGGTTTC CATCACCG3′, DV4-E/1639F, 5′TGGTGACATTCAAGGTTC CTC3′, and DV4-E/2509R, 5′ACTGTTCTGTCCAAGTGTGC3′ (Cao-Lormeau et al., 2011). Reverse transcription-polymerase chain reaction (RT-PCR) was carried out in one step with the following protocol: initial reverse transcription at 50°C for 30 min; denaturation at 94°C for 2 min; 40 cycles of denaturation at 94°C for 30 s, annealing at 53°C for 30 s, and extension at 72 °C for 2 min; and a final extension step at 72 °C for 10 min. Agarose gel electrophoresis (1.5%) was used to analyze the PCR products, which were then sequenced by a commercial facility (Tsingke Biotechnology Ltd, Hangzhou, China).

Sequence Alignment and Phylogenetic Analysis

The sequence was spliced in SEQMAN from the LaserGene package (DNASTAR Inc., Madison, WI). The nucleotide sequences were aligned using the Clustal W multiple sequence alignment program. DV reference sequences were downloaded from the GenBank database. The phylogenetic analysis based on full genome and E gene sequences was carried out by using the neighbor-joining method with the Tajima-Nei model in MEGA version 6.06 (http://www.megasoftware.net/). Bootstrap values ≥70%, calculated from 1,000 replicates, are shown at the tree branches. DV genotype was analyzed by including related reference sequences with known genotypes in the phylogenetic tree.

Ethics Statement

This study was approved by the Institutional Ethical Committee of Zhejiang Provincial Center for Disease Control and Prevention. Written informed consent was obtained from each participant.

RESULTS

Epidemiological Characteristics

Indigenous Cases

Since July 2017, a dengue outbreak has attacked Zhejiang Province, China. The index case was a 28-year-old man with fever, headache, fatigue, rash, myalgia, and arthralgia began on August 14 and diagnosed on August 22. A total of 1,149 indigenous cases were reported, including 962 confirmed cases and 187 clinically diagnosed cases. There were 573 infected men and 576 infected women (0.99:1 ratio), and the incidence rate was 2.00 and 2.11 per 100,000, respectively. The median age was 51 (IQR: 35–63). The incidence rate of elderly people was relatively high, and retirees accounted for nearly one third of all cases (**Table 1**).

The first case began on July 15. The number of cases increased markedly from 34th week, reached a peak in 35–36th week, and then began to decrease (**Figure 1**). The highest daily number of cases was 53 on August 28. There were 21 cases living outside of Hangzhou, which were distributed among the six prefecture-level cities Taizhou, Jiaxing, Jinhua, Wenzhou, Huzhou and Quzhou, which had 11, 4, 3, 1, 1, and 1 cases, respectively. The remaining 1,128 cases were in Hangzhou, the provincial capital of Zhejiang. All counties except for Tonglu and Lin'an in Hangzhou reported indigenous dengue cases. Three main urban areas of Hangzhou (Gongshu, Xiacheng,

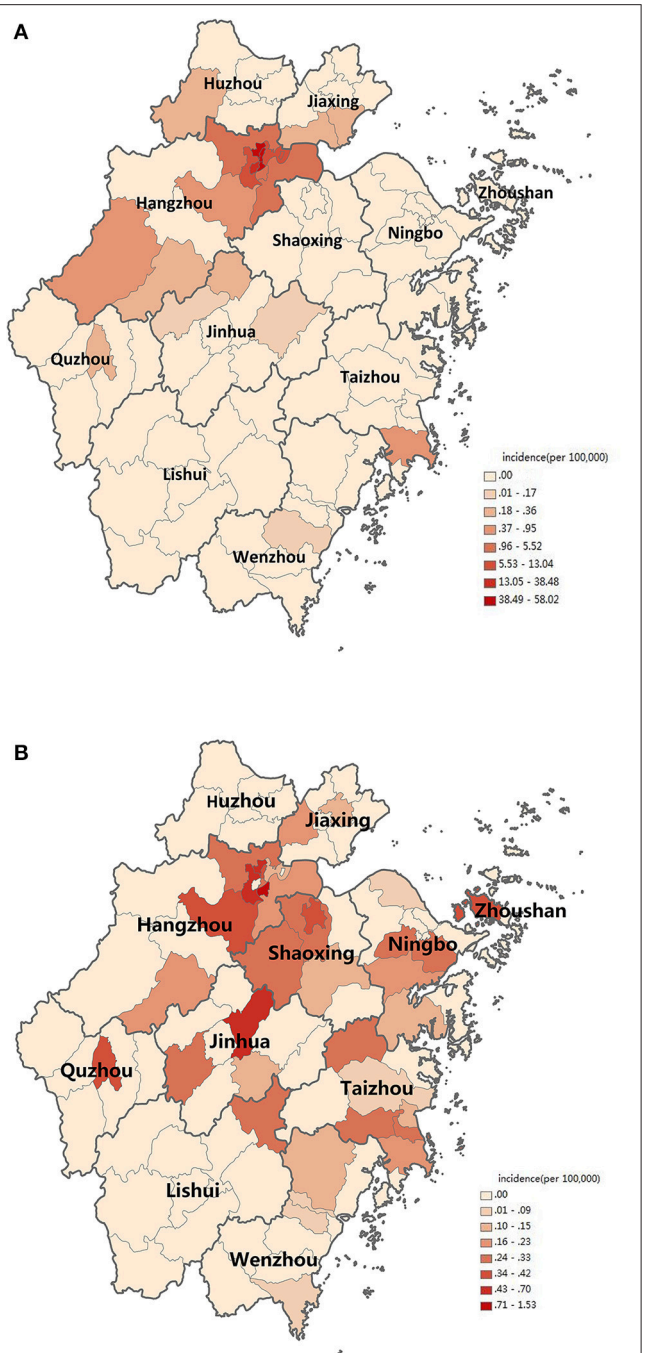

FIGURE 2 | Distribution of dengue cases in Zhejiang, China, 2017. **(A)** Distribution of indigenous dengue cases. **(B)** Distribution of imported dengue cases. Incidence is marked on the map according to counties in Zhejiang Province.

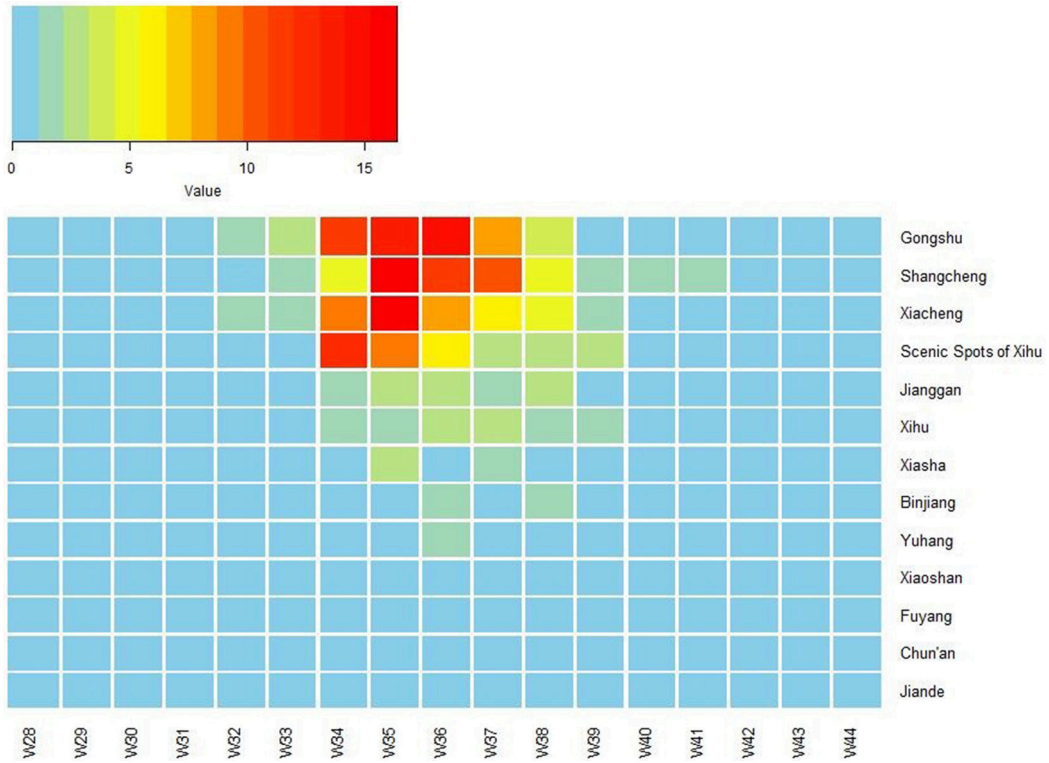

FIGURE 3 | Heat map of incidence of imported dengue cases by 13 counties of Hangzhou, Zhejiang Province, China, 2017. The X-axis lists week number in 2017, and the Y-axis lists the name of 13 counties of Hangzhou. W, week.

and Shangcheng) were the most hard-hit areas, consisting of more than 70% cases. The epidemic radiated out from these areas but was limited in Hangzhou and its surrounding regions (**Figure 2A**). Spatiotemporal analysis showed that the epidemic started in Gongshu and Xiacheng district, followed by neighboring districts (Shangcheng, Jianggan, and Xihu), and then Yuhang, Xiaoshan, and Xiasha (Hangzhou Economic and Technological Development Area). The epidemic was most severe in Gongshu, Xiacheng, and Shangcheng during 34th to 37th week (**Figure 3**).

Imported Cases

A total of 80 imported dengue cases were reported in Zhejiang Province during the study period, including 53 men and 27 women (1.96:1 ratio). The median age was 35 (IQR: 27.5–50.5), and the incidences in the age groups of 20–39 years old were relatively high. Farmer, commercial service people, industrial worker and cadres accounted for most cases (**Table 1**).

Imported cases were reported year round. Around 32–35th and 42–45th week, the case number increased slightly (**Figure 1**). Most cases distributed in the north region of Zhejiang Province (**Figure 2B**). Most cases were imported from South-East Asia (42 cases) and Western Pacific (27 cases) regions, in which the top countries was Thailand (20 cases) and Vietnam (11 cases), respectively (**Table 2**).

TABLE 2 | Distribution of countries of origin for imported dengue cases.

Original country	Number of cases
South-East Asia Region	42
Thailand	20
Myanmar	7
India	6
Sri Lanka	5
Indonesia	2
Maldives	1
Bangladesh	1
Western Pacific Region	27
Viet Nam	11
Cambodia	5
Philippines	5
Laos	3
Malaysia	3
African Region	7
Tanzania	2
Cote d'Ivoire	2
Angola	1
Ethiopia	1
Mauritius	1
Other Provinces in China	4
Total	80

TABLE 3 | Serotype and genotype identification and amplification of the E gene of dengue cases in Zhejiang, China, 2017.

Prefecture	Indigenous	Imported	Total
Hangzhou	6	0	6
	II(6 with 6 Cosmopolitan genotype)[a]		II(6)
Taizhou	4	4	8
	I(4 with 2 genotype I and 2 genotype V)	I(1 with 1 genotype I) II(3 with 2 Cosmopolitan genotype and 1 Asian I genotype)	I(5) II(3)
Jiaxing	1	1	2
	II(1 with 1 Cosmopolitan genotype)	I(1 with 1 genotype I)	I(1) II(1)
Jinhua	3	3	6
	II(3 with 3 Cosmopolitan genotype)	II(2 with 2 Cosmopolitan genotype) III(1 with 1 genotype III)	II(5) III(1)
Huzhou	1	0	1
	II(1 with 1 Cosmopolitan genotype)		II(1)
Shaoxing	1	8	9
	II(1 with 1 Cosmopolitan genotype)	I(2 with 2 genotype I) II(6 with 3 Cosmopolitan genotype and 3 Asian I genotype)	I(2) II(7)
Yiwu	0	1	1
		II(1 with 1 Cosmopolitan genotype)	II(1)
Zhoushan	0	2	2
		II(1 with 1 Cosmopolitan genotype) IV(1 with 1 genotype I)	II(1) IV(1)

[a] *I, II, III, and IV is the 4 distinct serotypes: DV-1, DV-2, DV-3, and DV-4, respectively; the number in the bracket is the number of DV serotype and genotype.*

Entomologic Investigation

A total of 136 mosquitoes were collected in a community in Shangcheng district of Hangzhou, of which 52 were identified based on morphology as *Ae. albopictus*, whereas 84 were identified as *Culex*. They were divided into one pool respectively. The *Culex* pool was negative for DV genome, while the *Ae. albopictus* pool was positive for DV-2. The BIs of the main urban area of Hangzhou were extremely high in the first statistics in 35th week (Gongshu 16, Xiacheng 27, Xihu 40.33, and Shangcheng 23.30). With the process of mosquito eradication, the BIs decreased rapidly and were all less than 5 in 37th week (Gongshu 0, Xiacheng 2.6, Xihu 4.53, and Shangcheng 2.3).

Laboratory Diagnosis, Virus Isolation, and Genome Sequencing

Eighty-one of the 90 collected serum samples were DV RNA positive, including 55 indigenous cases and 26 imported cases. Serotype identification results indicated the presence of all four serotypes DVs in Zhejiang Province in 2017: 68 DV-2 cases (50 indigenous and 18 imported), 10 DV-1 cases (5 indigenous and 5 imported), 2 DV-3 imported cases, and one DV-4 imported case. Among 43 randomly-selected acute phase serums that were positive for DV RNA, 35 DV isolates were successfully obtained after inoculation and culture in C6/36 cells. Routine RT-PCR was performed with virus culture and the supernatant of the pooled *Ae. albopictus* mosquitoes homogenates to amplify the whole genome and E gene. The complete genome sequences of DV-2 isolate Zhejiang/HZ33/2017 and the E gene of 35 additional isolates were obtained and submitted to the NCBI GenBank database (GenBank accession numbers: MH010595-MH010630).

Phylogenetic Analysis

Phylogenetic analysis was performed based on the sequences obtained, including reference sequences from the NCBI GenBank database. This analysis indicated that DVs of all four serotypes were present in indigenous and/or imported cases in Zhejiang Province, 2017 (**Table 3**).

The complete genome sequences of isolate Zhejiang/HZ33/2017 and sequences from representative isolates of different countries were chosen to construct a phylogenetic tree, and sequences of the DV-1 strain Hawaii, DV-3 strain H87, and DV-4 strain H241 were used as outgroups. The phylogenetic reconstruction classified all the DV-2 isolates into five genotypes, and Zhejiang/HZ33/2017 was identified as the Cosmopolitan genotype and was closely related to viruses from Malaysia and Singapore (**Figure 4**). In recent years, the sequences of DV that have been uploaded mostly contain the E gene but fewer full-length genome. To further clarify the origin of Zhejiang/HZ33/2017, the 26 DV-2 isolates (including Zhejiang/HZ33/2017 and Zhejiang/Aedes-1/2017) generated from the E gene were aligned with reference isolates of various genotypes (**Figure 5**). The results showed that 22 isolates clustered into DV-2 Cosmopolitan genotype, in which all 12 isolates (Zhejiang/HZ33/2017, Zhejiang/HZ49/2017, Zhejiang/HZ73/2017, Zhejiang/HZ98/2017, Zhejiang/HZ111/2017, Zhejiang/HZ138/2017, Zhejiang/17-03/2017, Zhejiang/17-04/2017, Zhejiang/17-14/2017, Zhejiang/17-18/2017, Zhejiang/17-38/2017, and Zhejiang/17-47/2017) from indigenous cases, 4 isolates (Zhejiang/17-08/2017, Zhejiang/17-32/2017, Zhejiang/17-39/2017, and Zhejiang/17-40/2017) from imported cases, and Zhejiang/Aedes-1/2017 formed a tight subclade. The other 4 isolates from imported cases belonged to DV-2 Asian I genotype.

The phylogenetic tree based on E gene categorized all DV-1 isolates into five genotypes and revealed that DV-1 from Zhejiang Province had a different genotype (**Figure 6**). Two pairs

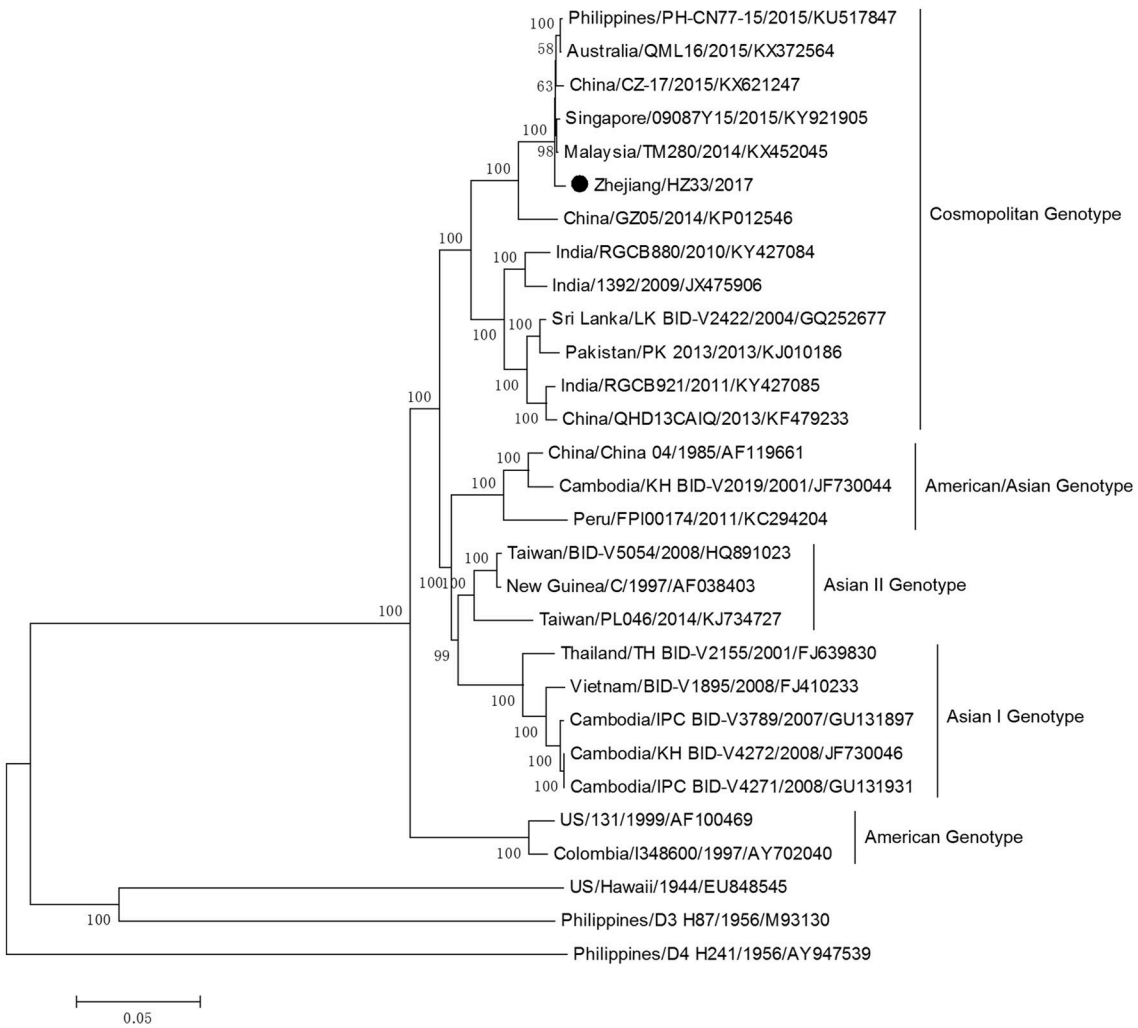

FIGURE 4 | Phylogenetic tree constructed from full-length DV sequences from different countries. Zhejiang/HZ33/2017 isolated in this study is labeled with a black circle. DV-1 strain Hawaii, DV-3 strain H87 and DV-4 strain H241 were used as outgroups.

of isolates from 4 indigenous cases in Taizhou city (located in the southeast of Zhejiang) belonged to DV-1 genotypes I and V, respectively. The first two isolates, Zhejiang/17-35/2017 and Zhejiang/17-37/2017, were closely related to viruses from Yunnan and Zhejiang, China (2013). The second two isolates, Zhejiang/17-44/2017 and Zhejiang/17-45/2017, clustered with virus from Thailand (2013).

DV-3 and DV-4 isolated from DF cases in Zhejiang in 2017 were all imported. Phylogenetic analysis indicated that the DV-3 isolate Zhejiang/17-16/2017 belonged to genotype III, clustering closely with virus from Africa (2013) (**Figure 7**). The isolate Zhejiang/17-42/2017 was identified as D-4 genotype I, closest relative to the isolates from India and Sri Lanka (**Figure 8**).

DISCUSSION

DF was clearly reported in the coastal provinces of China in the early twentieth century; and the first DF outbreak was identified in Guangdong province in 1978. Since the 1990s, dengue epidemics have spread gradually from Guangdong, Hainan, and Guangxi provinces in the southern coastal regions to the relatively northern and western regions including Fujian, Zhejiang, and Yunnan provinces. (Wu et al., 2010; Li et al., 2017). Since then, sporadic cases of DF have been reported almost every year in Zhejiang Province, and outbreaks occurred in the years 2004 and 2009 (Xu et al., 2007; Sun et al., 2011). This study was conducted to molecular and epidemiological characterize and phylogenetic analyze isolates from Zhejiang Province, in 2017. This local dengue outbreak was the largest and most severe in Zhejiang Province in the past 10 years. There are four possible reasons that may explain this outbreak. First, rapid development of globalization has caused global spread of DF worldwide, and the incidence of this disease has increased markedly both globally (Bhatt et al., 2013; Guzman and Harris, 2015) and in China (Ren et al., 2015). In Zhejiang Province, increasing tourism, trade, and investments with dengue-epidemic countries has led to high

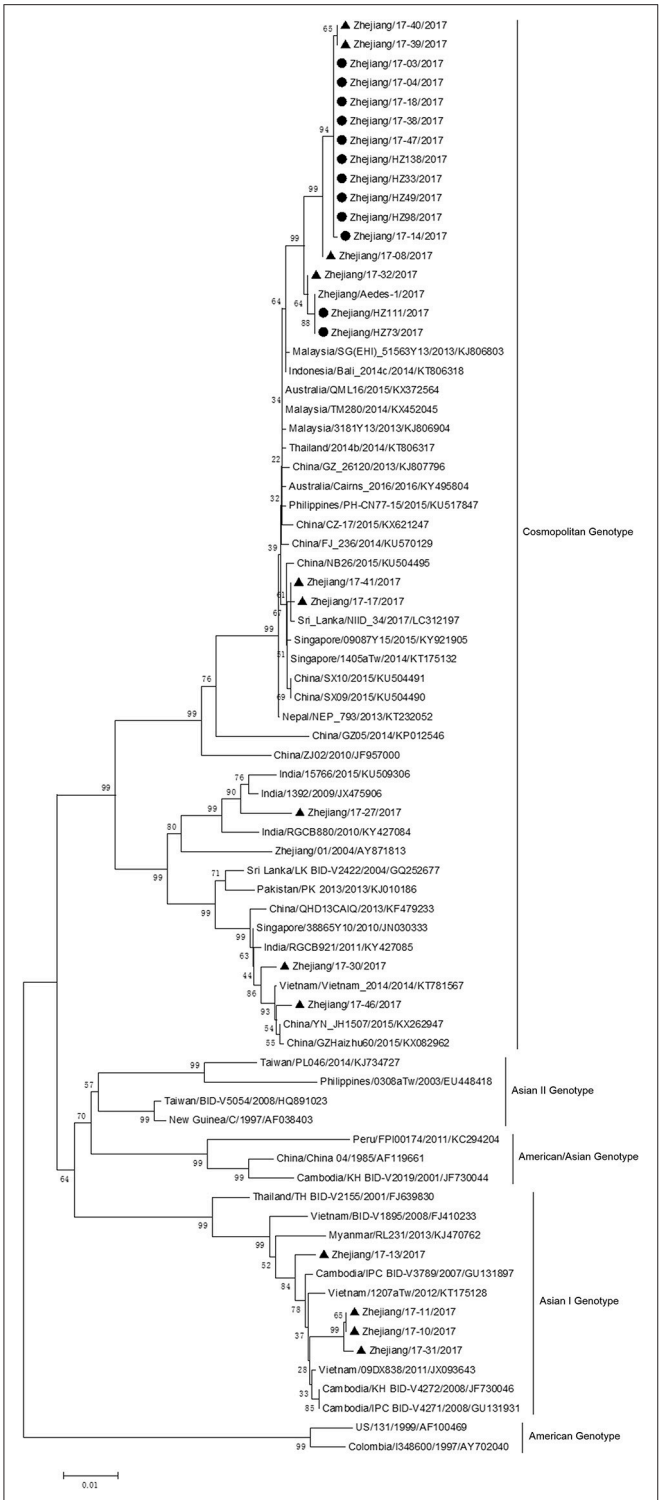

FIGURE 5 | Phylogenetic analysis of DV-2 sequences based on the E gene. The phylogenetic tree was generated in MEGA version 6.06 using the neighbor-joining method with 1,000 bootstrap replicates. Isolates from indigenous cases are labeled with black circles, and isolates from imported cases are labeled with black triangles.

population mobility, which in turn has increased the risk of disease spread. Second, weather factors such as temperature and rainfall in summer-autumn season in Zhejiang are suitable for the survival and breeding of mosquito vectors. Third, dengue is not an epidemic disease in Zhejiang Province, so susceptibility in the population is high. Fourth, the rate of asymptomatic dengue infection is high (Wang et al., 2015), but the clinical diagnostic capacity is insufficient (Ding et al., 2018), so rapid and accurate diagnosis has been limited to a certain extent. Delay of diagnosis of imported dengue cases may increase the risk of transmission and local spread of dengue.

Elderly people had higher incidence than younger people in this outbreak, a finding consistent with those from studies in other areas of China, such as Guangdong (Xiao et al., 2016) and Taiwan (Lin et al., 2012), which have experienced local dengue epidemic outbreaks. This observation might be attributed to more time spent outdoors and a higher likelihood of existing chronic diseases in elderly people and retirees (Xiao et al., 2016). No significant difference in incidence between sexes was found, since both men and women were susceptible to DV. This outbreak first occurred in Gongshu district, an urban area in Hangzhou that has a high population density and mobility, and then spread to the neighboring districts and then the outskirts, thus indicating that the epidemic distribution spread over time. The most serious duration of the epidemic was in late August and early September, when the density of mosquitoes was high in Zhejiang Province (Wu et al., 2015). In the 35th week, high BIs were observed in the main urban area of Hangzhou, which was consistent with the peak reported. Because of the latent phase of dengue, the decline in new cases is lagging behind when the BIs reduce to less than 5 in 37th week. Once new foci were founded, anti-mosquito measures were carried out immediately by community health departments. As a result, only 136 mosquitoes were captured and only one positive *Ae. albopictus* pool was determined. And the virus infection situation in local mosquito vectors was still unclear.

Compared with indigenous cases, imported cases were mainly young people, and there were more men than women. The purposes of overseas travel were mainly tourism, then trade and labor export (Ding et al., 2018). Most of the countries of origin for these cases were in South-East Asia and Western Pacific, possibly because of the highly developed tourism industries in these regions, especially in Thailand and Vietnam. Cases were reported year round, thus leading to persistent risks of virus transmission. When weather conditions are suitable, and the density of mosquito vectors reaches a high level, local epidemics are prone to outbreak.

The phylogenetic tree of DV-2 based on full-length sequences indicated that Zhejiang/HZ33/2017 probably originated from Guangdong or a Southeast Asian country (**Figure 4**). The E protein of DV encoded by the E gene is responsible for cell receptor binding, which is the main target of neutralizing antibodies and vaccine development (Whitehead et al., 2007; Webster et al., 2009). In recent years, most

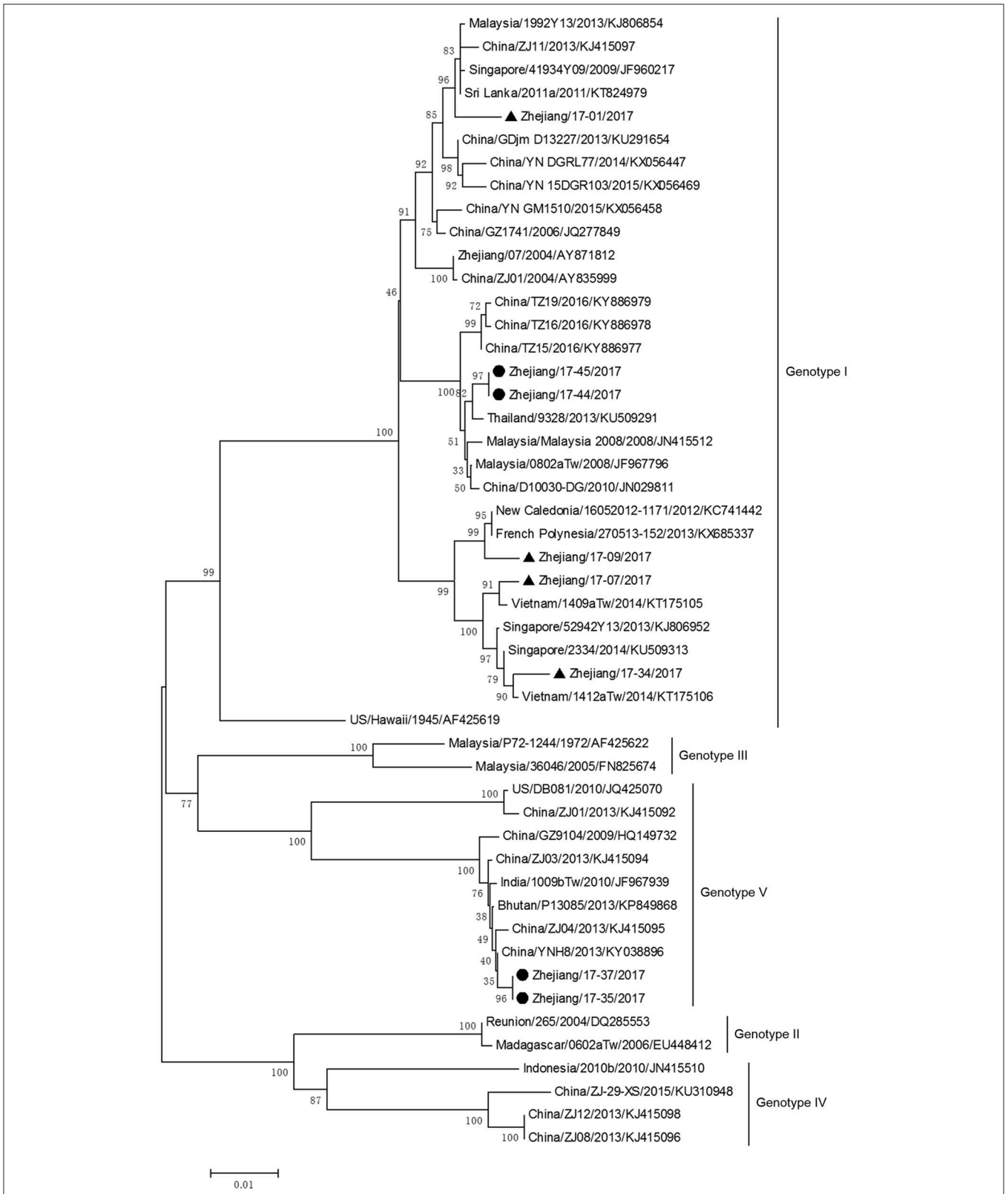

FIGURE 6 | Phylogenetic analysis of DV-1 sequences based on the E gene. The phylogenetic tree was generated in MEGA version 6.06 using the neighbor-joining method with 1,000 bootstrap replicates. Isolates from indigenous cases are labeled with black circles, and isolates from imported cases are labeled with black triangles.

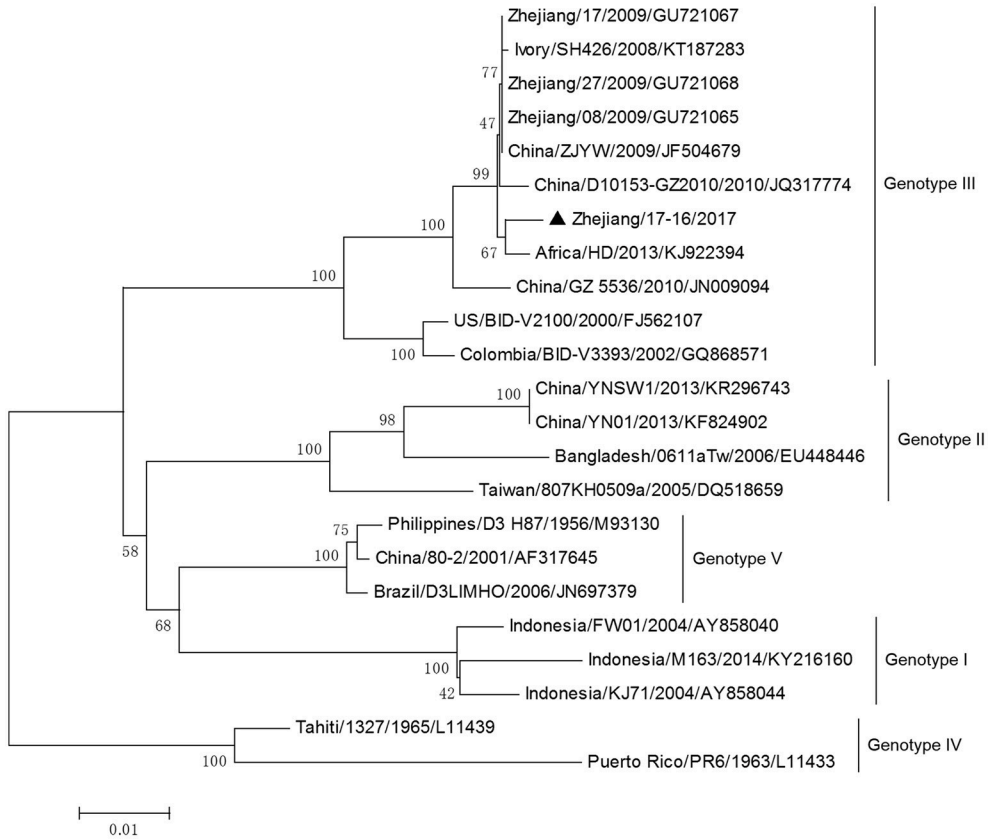

FIGURE 7 | Phylogenetic analysis of DV-3 sequences based on the E gene. The phylogenetic tree was generated in MEGA version 6.06 using the neighbor-joining method with 1,000 bootstrap replicates. Isolates from imported cases are labeled with a black triangle.

DV sequences in GenBank were from the E gene only. To further determine the origin of Zhejiang/HZ33/2017 and the rest of the 25 new DV-2 isolates, a phylogenetic analysis based on the E gene was conducted (**Figure 5**). We found that the 26 new DV-2 isolates from Zhejiang belonged to Cosmopolitan genotype and Asian I genotype. All 12 isolates (Zhejiang/HZ33/2017, Zhejiang/HZ49/2017, Zhejiang/HZ73/2017, Zhejiang/HZ98/2017, Zhejiang/HZ111/2017, Zhejiang/HZ138/2017, Zhejiang/17-03/2017, Zhejiang/17-04/2017, Zhejiang/17-14/2017, Zhejiang/17-18/2017, Zhejiang/17-38/2017, and Zhejiang/17-47/2017) from indigenous cases, the Zhejiang/Aedes-1/2017, and 4 isolates (Zhejiang/17-40/2017, Zhejiang/17-39/2017, Zhejiang/17-08/2017, and Zhejiang/17-32/2017) from imported cases were clustered in the same subclade. We confirmed that the 6 indigenous cases (17-03, 17-04, 17-18, 17-38, 17-47, and 17-14) were imported from Hangzhou to other cities in Zhejiang. According to epidemiological data, 17-32, 17-08, 17-39, and 17-40 were imported from Malaysia and Thailand, so we speculated that HZ33, HZ49, HZ73, HZ98, HZ111, HZ138, and Aedes-1 were most likely originated from Malaysia or Thailand, rather than from Guangdong. Another 9 isolates (Zhejiang/17-41/2017, Zhejiang/17-17/2017, Zhejiang/17-27/2017, Zhejiang/17-30/2017, Zhejiang/17-46/2017, Zhejiang/17-13/2017, Zhejiang/17-11/2017, Zhejiang/17-10/2017, and Zhejiang/17-31/2017) from imported cases probably originated from South-East Asia or Western Pacific countries such as Sri Lanka, India, Vietnam, and Cambodia.

The rest of the 10 new isolates (8 DV-1, one DV-3, and one DV-4) were also analyzed based on their E gene sequences, respectively. Four DV-1 isolates from indigenous cases in Taizhou were located in two clusters belonging to genotypes I and V (**Figure 6**). Case 17-37 was a neighbor of 17–35, whose husband had returned from India before she became ill. The phylogenetic analysis showed that Zhejiang/17-35/2017 and Zhejiang/17-37/2017 were closely related to isolates from Yunnan and Zhejiang (KY038896 and KJ415095), but we further found that YNH8 (2013) originated from India, and ZJ04 (2013) was imported from Myanmar. After combining with epidemiological data, we supposed that Zhejiang/17-35/2017 and Zhejiang/17-37/2017 were likely originated from India. Zhejiang/17-44/2017 and Zhejiang/17-45/2017 (epidemiological information of the cases were limited) belonged to DV-1 genotype I and probably originated from Thailand. These four DV-1 isolates from indigenous cases had a certain phylogenetic distance to the viruses outbreak in Cixi, Zhejiang, 2004 (AY871812 and AY835999). The phylogenetic reconstruction indicated that the other 4 isolates (Zhejiang/17-01/2017, Zhejiang/17-09/2017, Zhejiang/17-07/2017, and Zhejiang/17-34/2017) from imported cases were likely originated from India, Vietnam, and

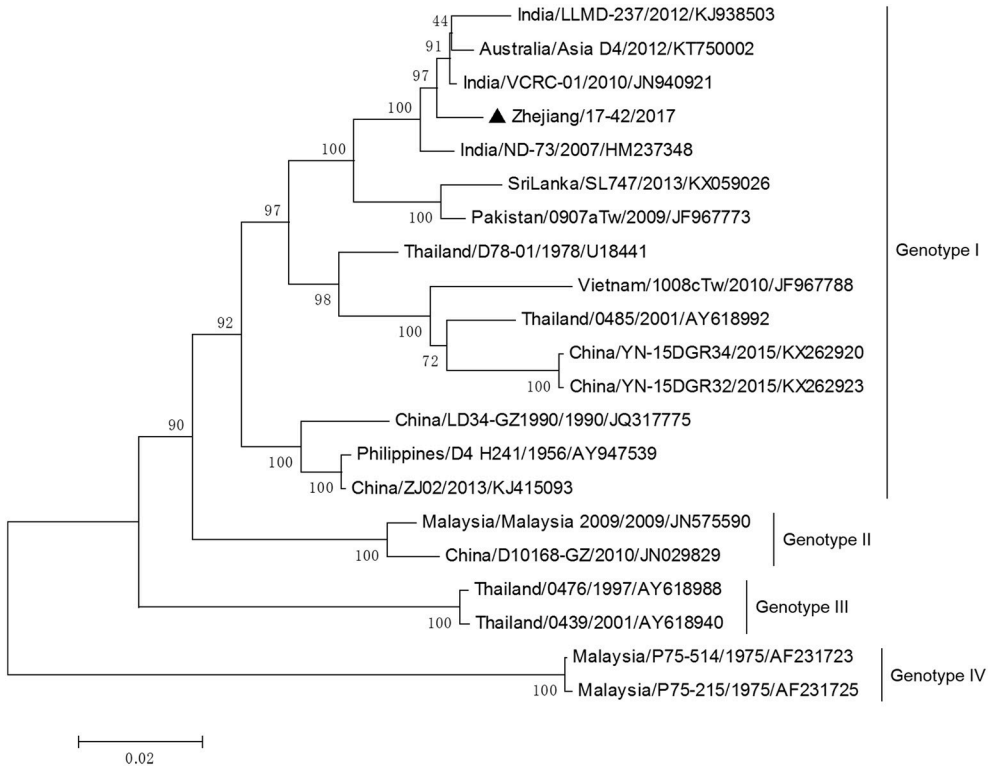

FIGURE 8 | Phylogenetic analysis of DV-4 sequences based on the E gene. The phylogenetic tree was generated in MEGA version 6.06 using the neighbor-joining method with 1,000 bootstrap replicates. Isolates from imported cases are labeled with a black triangle.

Cambodia. The phylogenetic tree revealed that Zhejiang/17-16/2017, which was imported from Nigeria, had a close link with virus from Africa (2013). Moreover, Zhejiang/17-42/2017, which was imported from India, was closely related to the isolates from India and Sri Lanka, thus suggesting that they were most likely originated from those corresponding countries (**Figures 7**, **8**).

This was a large outbreak with 1,229 cases, including 1,153 cases (1,128 indigenous and 25 imported) in Hangzhou, the provincial capital of Zhejiang. DV-2 was the dominant serotype epidemic in Zhejiang; however, all four serotypes emerged during the same period. Although Zhejiang does not belong to the endemic area of dengue, there are vector mosquitoes and environmental conditions supporting DV transmission in some regions of Zhejiang. There is always a risk of local outbreak caused by imported cases, such as the DV-1 and DV-3 outbreaks in 2004 and 2009, respectively. There are imported dengue cases in Hangzhou every year that do not cause a large scale endemic transmission every time. Hence, why was there a dengue outbreak in 2017? We inferred some probable reasons that may have led to this unexpected large outbreak. First, for Hangzhou residents, some South-East Asia and Western Pacific countries, including Thailand, Myanmar, Sri Lanka, Vietnam, Malaysia, are popular tourist destinations. Second, Hangzhou is a beautiful and economically advanced city in China that experiences high population mobility every year, as notably occurred after the Group 20 Summit in 2016. Third, long periods of high temperature and abundant precipitation in the summer and fall of 2017 in Hangzhou probably led to more frequent mosquito activity and facilitated mosquito breeding (Yang et al., 2009; Sarfraz et al., 2014). Fourth, DV infection often causes severe flu-like clinical symptoms that are easily misdiagnosed by inexperienced clinicians, thus leading to the occurrence of secondary cases or even the outbreak of dengue.

In our study, it was found that DVs of all four serotypes have been identified in Zhejiang Province. During 2017, the DV-2 Cosmopolitan genotype and DV-1 genotypes I and V were verified in indigenous cases. Multiple isolates of each serotype were present, and this may have increased patients' risk of dengue hemorrhagic fever and dengue shock syndrome, and threatened patients' lives (Morens, 1994; Gubler, 2011). Fortunately, DV-3 and DV-4 were detected only in sporadic imported cases. The present study reported the complete genome sequence of a clinical DV-2 isolate and investigated the origin of the 36 new DV isolates during this outbreak in Zhejiang Province. However, extensive virological studies and comprehensive epidemiological investigation are warranted in the future.

Our results indicated that imported DF patients from South-East Asia and Western Pacific countries were probably the primary cause of the DF epidemics in Zhejiang Province. Widely distributed of *Ae. albopictus* in urban areas increase the risk of indigenous dengue transmission and indigenous DF epidemics in Zhejiang Province. Because no effective vaccines and drugs

are available for dengue, prevention and control measures should be strengthened. Determining the origin of the 2017 isolates from Zhejiang Province might provide information that could lead to more effective control measures. Efforts should be made in improving the capabilities of clinicians to diagnose this disease, improving and disseminating proper preventive measures in high-risk populations, surveillance of imported cases, strengthening vector control, and prevention and control of local epidemics.

AUTHOR CONTRIBUTIONS

YZ designed and supervised the experiments. HY, JY, WY, JP, and XL carried out the experiments. HY, ZD, JY, JP, JS, HW, and CW analyzed the data. HY and ZD wrote the paper. JY, HY, JH, and HM performed sample collections. ZY, HM, and JL provided helpful suggestions about the study. All authors read and approved the final manuscript.

ACKNOWLEDGMENTS

The authors would like to thank staff members from Center for Disease Control and Prevention in 12 prefectures of Zhejiang, China, and all individuals who contributed to this research. Dr Yan Wang provided helpful feedback on an earlier version of the paper.

This study was supported by the Major Science and Technology Special Projects of Zhejiang, China (2013C03045-1), the Key Disciplinary of Health and Family Planning Commission of Zhejiang Province (CX-9), the Monitor Technology Platform of Infectious Diseases of the State Major Science and Technology Special Projects during the 12th and 13th 5-year plan of China (2012ZX10004-210 and 2017ZX10103008-002), the Zhejiang Provincial Program for the Cultivation of High-level Innovative Health Talents, and the Zhejiang Provincial Medical Science and Technology Platform Project (2017RC018).

REFERENCES

Akram, M., and Idrees, M. (2016). Complete genome sequencing and comparative analysis of three dengue virus type 2 Pakistani isolates. *Virusdisease* 27, 27–33. doi: 10.1007/s13337-015-0279-3

Aquino, V. H., Anatriello, E., Gonçalves, P. F., DA Silva, E. V., Vasconcelos, P. F., Vieira, D. S., et al. (2006). Molecular epidemiology of dengue type 3 virus in Brazil and Paraguay, 2002-2004. *Am. J. Trop. Med. Hyg.* 75, 710–715.

Bhatt, S., Gething, P. W., Brady, O. J., Messina, J. P., Farlow, A. W., Moyes, C. L., et al. (2013). The global distribution and burden of dengue. *Nature* 496, 504–507. doi: 10.1038/nature12060

Brady, O. J., Gething, P. W., Bhatt, S., Messina, J. P., Brownstein, J. S., Hoen, A. G., et al. (2012). Refining the global spatial limits of dengue virus transmission by evidence-based consensus. *PLoS Negl. Trop. Dis.* 6:e1760. doi: 10.1371/journal.pntd.0001760

Cao-Lormeau, V. M., Roche, C., Aubry, M., Teissier, A., Lastere, S., Daudens, E., et al. (2011). Recent emergence of dengue virus serotype 4 in French Polynesia results from multiple introductions from other South Pacific Islands. *PLoS ONE* 6:e29555. doi: 10.1371/journal.pone.0029555

Chen, B., and Liu, Q. (2015). Dengue fever in China. *Lancet* 385, 1621–1622. doi: 10.1016/S0140-6736(15)60793-0

Ding, Z., Wu, C., Wu, H., Lu, Q., and Lin, J. (2018). The epidemiology of imported acute infectious diseases in Zhejiang Province, China, 2011-2016: analysis of surveillance data. *Am. J. Trop. Med. Hyg*. 98, 913–919. doi: 10.4269/ajtmh.17-0284

Dubot-Pérès, A., Vongphrachanh, P., Denny, J., Phetsouvanh, R., Linthavong, S., Sengkeopraseuth, B., et al. (2013). An epidemic of dengue-1 in a remote village in rural Laos. *PLoS Negl. Trop. Dis.* 7:e2360. doi: 10.1371/journal.pntd.0002360

Gubler, D. J. (2011). Dengue, urbanization and globalization: the unholy trinity of the 21(st) century. *Trop. Med. Health*. 39, 3–11. doi: 10.2149/tmh.2011-S05

Guo, S., Ling, F., Hou, J., Wang, J., Fu, G., and Gong, Z. (2014). Mosquito surveillance revealed lagged effects of mosquito abundance on mosquito-borne disease transmission: a retrospective study in Zhejiang, China. *PLoS ONE* 9:e112975. doi: 10.1371/journal.pone.0112975

Guzman, M. G., and Harris, E. (2015). Dengue. *Lancet* 385, 453–465. doi: 10.1016/S0140-6736(14)60572-9

Holmes, E. C., Tio, P. H., Perera, D., Muhi, J., and Cardosa, J. (2009). Importation and co-circulation of multiple serotypes of dengue virus in Sarawak, Malaysia. *Virus Res.* 143, 1–5. doi: 10.1016/j.virusres.2009.02.020

Huang, J. H., Su, C. L., Yang, C. F., Liao, T. L., Hsu, T. C., Chang, S. F., et al. (2012). Molecular characterization and phylogenetic analysis of dengue viruses imported into Taiwan during 2008-2010. *Am. J. Trop. Med. Hyg.* 87, 349–358. doi: 10.4269/ajtmh.2012.11-0666

Jarman, R. G., Holmes, E. C., Rodpradit, P., Klungthong, C., Gibbons, R. V., Nisalak, A., et al. (2008). Microevolution of Dengue viruses circulating among primary school children in Kamphaeng Phet, Thailand. *J. Virol.* 82, 5494–5500. doi: 10.1128/JVI.02728-07

Kuhn, R. J., Zhang, W., Rossmann, M. G., Pletnev, S. V., Corver, J., Lenches, E., et al. (2002). Structure of dengue virus: implications for flavivirus organization, maturation, and fusion. *Cell* 108, 717–725 doi: 10.1016/S0092-8674(02)00660-8

Li, G., Pan, P., He, Q., Kong, X., Wu, K., Zhang, W., et al. (2017). Molecular epidemiology demonstrates that imported and local strains circulated during the 2014 dengue outbreak in Guangzhou, China. *Virol. Sin.* 32, 63–72. doi: 10.1007/s12250-016-3872-8

Lin, C. H., Schioler, K. L., Jepsen, M. R., Ho, C. K., Li, S. H., and Konradsen, F. (2012). Dengue outbreaks in high-income area, Kaohsiung City, Taiwan, 2003-2009. *Emerging Infect. Dis.* 18, 1603–1611. doi: 10.3201/eid1810.111929

Morens, D. M. (1994). Antibody-dependent enhancement of infection and the pathogenesis of viral disease. *Clin. Infect. Dis.* 19, 500–512 doi: 10.1093/clinids/19.3.500

Ngwe Tun, M. M., Kyaw, A. K., Makki, N., Muthugala, R., Nabeshima, T., Inoue, S., et al. (2016). Characterization of the 2013 dengue epidemic in Myanmar with dengue virus 1 as the dominant serotype. *Infect. Genet. Evol.* 43, 31–37. doi: 10.1016/j.meegid.2016.04.025

Ren, H., Ning, W., Lu, L., Zhuang, D., and Liu, Q. (2015). Characterization of dengue epidemics in mainland China over the past decade. *J. Infect. Dev. Ctries.* 9, 970–976. doi: 10.3855/jidc.5998

Sarfraz, M. S., Tripathi, N. K., Faruque, F. S., Bajwa, U. I., Kitamoto, A., and Souris, M. (2014). Mapping urban and peri-urban breeding habitats of Aedes mosquitoes using a fuzzy analytical hierarchical process based on climatic and physical parameters. *Geospat. Health* 8, S685–S697. doi: 10.4081/gh.2014.297

Sun, J., Lin, J., Yan, J., Fan, W., Lu, L., Lv, H., et al. (2011). Dengue virus serotype 3 subtype III, Zhejiang Province, China. *Emerg. Infect. Dis.* 17, 321–323. doi: 10.3201/eid1702.100396

Sun, J., Lu, L., Wu, H., Yang, J., Xu, L., Sang, S., et al. (2017). Epidemiological trends of dengue in mainland China, 2005-2015. *Int. J. Infect. Dis.* 57, 86–91. doi: 10.1016/j.ijid.2017.02.007

Tajima, S., Nakayama, E., Kotaki, A., Moi, M. L., Ikeda, M., Yagasaki, K., et al. (2017). Whole genome sequencing-based molecular epidemiologic analysis of autochthonous dengue virus type 1 strains circulating in Japan in 2014. *Jpn. J. Infect. Dis.* 70, 45–49. doi: 10.7883/yoken.JJID.2016.086

Vu, T. T., Holmes, E. C., Duong, V., Nguyen, T. Q., Tran, T. H., Quail, M., et al. (2010). Emergence of the Asian 1 genotype of dengue virus serotype 2 in viet nam: *in vivo* fitness advantage and lineage replacement in South-East Asia. *PLoS Negl. Trop. Dis.* 4:e757. doi: doi: 10.1371/journal.pntd.0000757

Wang, P., Wang, H., Yu, J., Xie, Q., Yao, Z., Qin, Z., et al. (2016). Molecular characterization and phylogenetic analysis of dengue virus type 1 in Guangdong in 2014. *Springerplus* 5:1942 doi: 10.1186/s40064-016-3604-4

Wang, T., Wang, M., Shu, B., Chen, X. Q., Luo, L., Wang, J. Y., et al. (2015). Evaluation of inapparent dengue infections during an outbreak in Southern China. *PLoS Negl. Trop. Dis.* 9:e0003677. doi: 10.1371/journal.pntd.0003677

Webster, D. P., Farrar, J., and Rowland-Jones, S. (2009). Progress towards a dengue vaccine. *Lancet Infect. Dis.* 9, 678–687. doi: 10.1016/S1473-3099(09)70254-3

Whitehead, S. S., Blaney, J. E., Durbin, A. P., and Murphy, B. R. (2007). Prospects for a dengue virus vaccine. *Nat. Rev. Microbiol.* 5, 518–528 doi: 10.1038/nrmicro1690

Wu, J. Y., Lun, Z. R., James, A. A., and Chen, X. G. (2010). Dengue Fever in mainland China. *Am. J. Trop. Med. Hyg.* 83, 664–671. doi: 10.4269/ajtmh.2010.09-0755

Wu, Y., Lin, F., and Gong, Z. (2015). Surveillance for mosquito density and species in Zhejiang, 2011-2013. *Dis. Surveill.* 30, 497–500.

Xiao, J. P., He, J. F., Deng, A. P., Lin, H. L., Song, T., Peng, Z. Q., et al. (2016). Characterizing a large outbreak of dengue fever in Guangdong Province, China. *Infect Dis Poverty*. 5:44. doi: 10.1186/s40249-016-0131-z

Xu, G., Dong, H., Shi, N., Liu, S., Zhou, A., Cheng, Z., et al. (2007). An outbreak of dengue virus serotype 1 infection in Cixi, Ningbo, People's Republic of China, 2004, associated with a traveler from Thailand and high density of *Aedes albopictus*. *Am. J. Trop. Med. Hyg.* 76, 1182–1188

Yang, T., Lu, L., Fu, G., Zhong, S., Ding, G., Xu, R., et al. (2009). Epidemiology and vector efficiency during a dengue fever outbreak in Cixi, Zhejiang Province, China. *J. Vector Ecol.* 34, 148–154. doi: 10.1111/j.1948-7134.2009.00018.x

Zhao, H., Zhao, L., Jiang, T., Li, X., Fan, H., Hong, W., et al. (2014). Isolation and characterization of dengue virus serotype 2 from the large dengue outbreak in Guangdong, China in 2014. *Sci. China Life Sci.* 57, 1149–1155. doi: 10.1007/s11427-014-4782-3

Conflict of Interest Statement: The authors declare that the research was conducted in the absence of any commercial or financial relationships that could be construed as a potential conflict of interest.

Advantages of publishing in Frontiers

OPEN ACCESS
Articles are free to read for greatest visibility and readership

FAST PUBLICATION
Around 90 days from submission to decision

HIGH QUALITY PEER-REVIEW
Rigorous, collaborative, and constructive peer-review

TRANSPARENT PEER-REVIEW
Editors and reviewers acknowledged by name on published articles

Frontiers
Avenue du Tribunal-Fédéral 34
1005 Lausanne | Switzerland

Visit us: www.frontiersin.org
Contact us: info@frontiersin.org | +41 21 510 17 00

REPRODUCIBILITY OF RESEARCH
Support open data and methods to enhance research reproducibility

DIGITAL PUBLISHING
Articles designed for optimal readership across devices

FOLLOW US
@frontiersin

IMPACT METRICS
Advanced article metrics track visibility across digital media

EXTENSIVE PROMOTION
Marketing and promotion of impactful research

LOOP RESEARCH NETWORK
Our network increases your article's readership